MIOCENE DEEP-SEA BENTHIC FORAMINIFERA FROM ODP SITES 752, 1139 AND 1168 (SOUTHERN INDIAN OCEAN)

by

DANA NOORY RIDHA

A thesis submitted to

the University of Birmingham

for the degree of

DOCTOR OF PHILOSOPHY

School of Geography, Earth and
Environmental Sciences
University of Birmingham

October 2019

UNIVERSITY OF
BIRMINGHAM

University of Birmingham Research Archive

e-theses repository

This unpublished thesis/dissertation is copyright of the author and/or third parties. The intellectual property rights of the author or third parties in respect of this work are as defined by The Copyright Designs and Patents Act 1988 or as modified by any successor legislation.

Any use made of information contained in this thesis/dissertation must be in accordance with that legislation and must be properly acknowledged. Further distribution or reproduction in any format is prohibited without the permission of the copyright holder.

Abstract

Miocene deep-sea benthic foraminifera from ODP Sites 752A (Broken Ridge), 1168A (Western Tasmanian Margin) and 1139A (Kerguelen Plateau) in the southern Indian Ocean, have been studied for their stratigraphic distribution, diversity, abundance and test-size changes during periods of global climate shifts. All sites yielded similar taxa though the exact assemblage composition varied at each site. No major faunal extinctions were noted with many taxa ranging through. Site 752A had a major foraminiferal assemblage shift at ~13 Ma. While those from 1168A and 1139A recorded a significant drop in the Shannon diversity index at about 14 Ma. These events may relate to the expansion of the East Antarctic Ice Sheet during this period of marked global cooling, indicating an impact in deep-sea ecosystems. *Nuttalides umbonifera* and *Sphaeriodina bulloides* are the most abundant species of the early to the mid-Miocene interval at these sites, with the former known to favour highly oligotrophic conditions. *Abdetodentrix pseudothalmani* and *Trifarina angulosa* had their peak abundance during the mid-late Miocene in association with global cooling. Test size variability measured in five separate taxa (*Abdetodentrix pseudothalmani, Cibicidoides mundulus, Globocassidulina subglobosa*, *Nuttalides umbonifera* and *Sphaeroidina bulloides*) demonstrated rapid size increase at around 12 Ma in all Sites. Studies of benthic foraminiferal stable isotopes $\delta^{18}O$ and $\delta^{13}C$ at all sites accords well with global published records for this interval. All sites demonstrated increasing $\delta^{13}C$ values from the late early Miocene to mid-Miocene, coinciding with the early to mid-Miocene Monterey carbon isotope excursion. Mid-late Miocene $\delta^{18}O$ values reflect global cooling during the expansion of the East Antarctic Ice Sheet (14-12 Ma).

Acknowledgements

I want to express my sincere gratitude to my sponsor, HCED (The Higher Committee for Education Development in Iraq). The completion of this study could not have been possible without them. I want to thank my supervisors Ian Boomer, and Kirsty Edgar, for the patient guidance, encouragement, and their very kind support. Special thanks to the International Ocean Discovery Program (IODP) for providing samples and data.

My special thanks to my wife, Esra Ali for her generous support and my children for their patience during the completion of my thesis. I cannot forget to thank my family and friends for all the support in these very intense academic years.

In addition, I would like to express my gratitude to my friends Mehdi Mahmud and Marcelo Mota for their kindly help.

Table of Contents

Chapter One 1

Introduction and Background 1

1.1 Miocene palaeoclimates & tectonics 1

1.2 Miocene palaeoceanography 6

1.2.1 Indian Ocean Miocene palaeoceanography 6

1.2.2 Southern Ocean Miocene palaeoceanography 10

1.3 Miocene deep-sea benthic foraminifera 13

1.3.1 Previous studies in the Indian and the Southern oceans 16

1.3.2 Deep-sea benthic foraminifera of the Indian Ocean and the Southern oceans 20

1.4 Aims and Objectives 23

Chapter Two 25

Site Descriptions and Methodologies 25

2.1 752A – Broken Ridge 25

2.1.1 Site & Core Description 26

2.1.2 Age-depth model & palaeodepth reconstruction 27

2.1.3 Benthic Foraminifera 30

2.2 Hole 1168A – Western Tasmania margin 37

2.2.1 Site & Core Description 38

2.2.2 Age depth-Model & Palaeodepth 40

2.2.3 Benthic Foraminifera 44

2.3 1139A – Skiff Bank (Kerguelen Plateau) 50

2.3.1 Site & Core Description 50

2.3.2 Age depth-Model & Palaeodepth 53

2.3.3 Benthic Foraminifera 60

2.4 Methodologies 61

2.4.1 Sample preparations 61

2.4.2 Dendrogram, diversity and rarefaction curves 61

2.4.3 Benthic foraminifera accumulation rate 62

2.4.4 Correlation Coefficient and significant value: 63

2.4.5 Test sizes 63

2.4.6 Carbonate Mass Accumulation Rates: 64

Chapter Three 65

Latest Oligocene to earliest Pliocene deep-sea benthic foraminifera from ODP Sites 752, 1168 and 1139 southern Indian Ocean. 65

3.1 Introduction 66

3.2 Materials and Methods 69

3.3 Foraminiferal Assemblages 71

3.4 Taxonomy *[Note, on acceptance, all figured specimens will be given Museum Numbers, Lapworth Museum of Geology, University of Birmingham]* 74

Class FORAMINIFEREA J. J. Lee, 1990 74

Order BULIMINIDA Fursenko, 1958 74

Superfamily **BOLIVINACEA** Glaessner, 1937 74

Family **BOLIVINIDAE** Glaessner, 1937 74

Genus *Bolivina* d'Orbigny, 1839c 74

Genus *Bolivinellina* Saidova, 1975 82

Superfamily **BOLIVINITACEA** Cushman, 1927 84

Family **BOLIVINITIDAE** Cushman, 1927 84

Genus *Abditodentrix* Patterson, 1985 84

Superfamily **BULIMINACEA** Jones in Griffith and Henfrey, 1875 85

Family **BULIMINIDAE** Jones, 1875 85

Genus *Bulimina* d'Orbigny, 1826 85

Family **Turrilinidae** Cushman, 1927 90

Subfamily **Turrilininae** Cushman, 1927 90

Genus *Eubuliminella* Revets, 1993 90

Superfamily **CASSIDULINACEA** d'Orbigny, 1839a 91

Family **CASSIDULINIDAE** d'Orbigny, 1839a 91

Subfamily **CASSIDULININAE** d'Orbigny, 1839a 91

Genus *Globocassidulina* Voloshinova, 1960 91

Genus *Paracassidulina* Nomura, 1983b 92

Subfamily **EHRENBERGININAE** Cushman, 1927 93

Genus *Ehrenbergina* Reuss, 1850 93

Genus *Burseolina* Seguenza, 1880 96

Superfamily **PLEUROSTOMELIACEA** Reuss, 1860 98

Family **PLEUROSTOMELLIDAE** Reuss, 1860 98

Subfamily **PLEUROSTOMELLINAE** Reuss, 1860 98

Genus *Pleurostomella* Reuss, 1860 98

Superfamily **STILOSTOMELLACEA** Finlay, 1947 99

Family **STILOSTOMELLIDAE** Finlay, 1947 99

Genus *Orthomorphina* Stainforth, 1952 99

Genus *Siphonodosaria* Silvestri, 1924 101

Genus *Stilostomella* Guppy, 1894 103

Genus *Strictocostella* Patterson, 1987 104

Family **UVIGERINIDAE** Haeckel, 1894 107

Subfamily **ANGULOGERININAE** Galloway, 1933 107

Genus *Trifarina* Cushman, 1923 107

Subfamily **UVIGERININAE** Haeckel, 1894 109

Genus *Siphouvigerina* Parr, 1950 109
Genus *Uvigerina* d'Orbigny, 1826 112

Order LAGENIDA Lankester, 1885 114
Superfamily NODOSARIACEA Ehrenberg, 1838 114
Family VAGINULINIDAE Reuss, 1862 114
Subfamily LENTICULININAE Chapman, Parr, and Collins, 1934 114
Genus *Lenticulina* Lamarck, 1804 114
Subfamily MARGINULININAE Wedekind, 1937 115
Genus *Amphicoryna* Schlumberger, in Milne-Edwards, 1881 115

Order ROTALIIDA Lankester, 1885 116
Superfamily ASTERIGERINACEA d'Orbigny, 1839a 116
Family EPISTOMARIIDAE Hofker, 1954 116
Subfamily NUTTALLIDINAE Saidova, 1981 116
Genus *Nuttallides* Finlay, 1939 116
Superfamily CHILOSTOMELLACEA Brady, 1881 118
Family GAVELINELLIDAE Hofker, 1956a 118
Subfamily GAVELINELLINAE Hofker, 1956a 118
Genus *Gyroidinoides* Brotzen, 1942 118
Family ORIDORSALIDAE Loeblich and Tappan, 1984 122
Genus *Oridorsalis* Andersen, 1961 122
Genus *Osangularia* Brotzen, 1940 123
Superfamily DISCORBACEA Ehrenberg, 1838 124
Family ROSALINIDAE Reiss, 1963 124
Genus *Gavelinopsis* Hofker, 1951a 124
Family SPHAEROIDINIDAE Cushman, 1927 125
Genus *Sphaeroidina* d'Orbigny, 1826 125
Superfamily DISCORBINELLACEA Sigal in Piveteau, 1952 127
Family DISCORBINELLIDAE Sigal in Piveteau, 1952 127
Subfamily DISCORBINELLINAE Sigal in Piveteau, 1952 127
Genus *Laticarinina* Galloway and Wissler, 1927 127
Family PSEUDOPARRELLIDAE Voloshinova, 1952 128
Subfamily PSEUDOPARRELLINAE Voloshinova, 1952 128
Genus *Epistominella* Husezima and Maruhasi, 1944 128
Superfamily NONIONACEA Schultze, 1854 131
Family NONIONIDAE Schultze, 1854 131
Subfamily ASTRONONIONINAE Saidova, 1981 131
Genus *Astrononion* Cushman & Edwards, 1937 131
Subfamily PULLENIINAE Schwager, 1877 132
Genus *Melonis* de Montfort, 1808 132
Geuns *Pullenia* Parker & Jones, 1862 in Carpenter et al., 1862 134
Superfamily PLANORBULINACEA Schwager, 1877 136

Family **CIBICIDIDAE** Cushman, 1927 136
Subfamily **CIBICIDINAE** Cushman, 1927 136
Genus *Cibicidoides* Saidova, 1975 136
Family **PLANULINIDAE** Bermúdez, 1952 139
Genus *Planulina* d'Orbigny, 1826 139
Order TEXTULARIIDA Lankester, 1885 142
Superfamily **TEXTULARIACEA** Ehrenberg, 1838 142
Family **EGGERELLIDAE** Cushman, 1937b 142
Subfamily **EGGERELLINAE** Cushman, 1937b 142
Genus *Eggerella* Cushman, 1933a 142
3.5 Summary 143
Author contributions 144
Competing Interests 144
Acknowledgements 144
Chapter Four 145
Foraminifera: Results and Discussion 145
4.1 Introduction: 145
4.2 Results: 146
4.2.1 ODP Site 752 Hole A: 146
4.2.1.1 Cluster analysis: 146
4.2.1.2 Diversity: 149
4.2.1.3 Benthic Foraminifera Accumulation Rate (BFAR): 149
4.2.1.4 Rarefaction curves: 151
4.2.1.5 Faunal composition: 153
4.2.2 ODP Site, 1168 Hole A: 156
4.2.2.1 Cluster analysis: 156
4.2.2.2 Diversity: 158
4.2.2.3 Benthic Foraminifera Accumulation Rate: 158
4.2.2.4 Rarefaction curves: 159
4.2.2.5 Faunal composition: 159
4.2.3 ODP Site, 1139 Hole A: 163
4.2.3.1 Cluster analysis: 163
4.2.3.2 Diversity: 165
4.2.3.3 Benthic Foraminifera Accumulation Rate (BFAR): 166
4.2.3.4 Rarefaction curves: 166
4.2.3.5 Faunal composition: 170
4.3 Discussion: 173
4.3.1 ODP Site 752 Hole A: 173

4.3.1.1 Cluster analysis: 173
4.3.1.2 Diversity: 174
4.3.1.3 Benthic Foraminifera Accumulation Rate (BFAR): 175
4.3.1.4 Faunal composition: 177
4.3.2 ODP Site 1168 Hole A: 177
4.3.2.1 Cluster analysis: 177
4.3.2.2 Diversity: 178
4.3.2.3 Benthic Foraminifera Accumulation Rate (BFAR): 179
4.3.2.4 Faunal composition: 180
4.3.3 ODP Site 1139 Hole A: 180
4.3.3.1 Cluster analysis: 180
4.3.3.2 Diversity: 182
4.3.3.3 Benthic Foraminifera Accumulation Rate (BFAR): 182
4.3.3.4 Faunal composition: 183
4.3.4 Species diversity and abundance comparison: 183
4.3.4.1 Species diversity comparison at three studied Sites (752A, 1168A and 1139A): 183
4.3.4.2 Most abundant taxa comparison between the studied Sites (752A, 1168A and 1139A) and other Miocene localities around the world: 186
Chapter Five 196
Test sizes, Carbonate crash and Biogenic blooms 196
5.1 Test sizes: 196
5.1.1 Introduction: 196
5.1.2 Results: 197
5.1.3 Discussion: 201
5.2 Carbonate crash and Biogenic blooms: 204
5.2.1 Introduction: 204
5.2.2 Results: 205
5.2.2.1 ODP Site 752 Hole A: 205
5.2.2.2 ODP Site 1168 Hole A: 206
5.2.2.3 ODP Site 1139 Hole A: 207
5.2.3 Discussion: 208
5.2.3.1 ODP Site 752 Hole A: 208
5.2.3.2 ODP Site 1168 Hole A: 209
5.2.3.3 ODP Site 1139 Hole A: 209
Chapter Six 210
Stable Isotopes 210
6.1 Introduction 210
6.1.1 Background 210
6.1.2 Aim of study 212

6.2 Methodology 212
6.3 Results: 215
6.3.1 Site 752 Hole A 215
6.3.2 Site 1168 Hole A 216
6.3.3 Site 1139 Hole A 216
6.4 Discussion: 218
6.4.1 Site 752 Hole A 218
6.4.2 Site 1168 Hole A 222
6.4.3 Site 1139 Hole A 225
6.4.4 Stable isotope comparison 226
Chapter Seven 230
Summary and Conclusions 230
Recommendation and Future work 237
References 239
Appendices 256
Appendix A: Benthic foraminifera species checklist at ODP Site 752 Hole A. 256
Appendix B: Benthic foraminifera species checklist at ODP Site 1168 Hole A. 266
Appendix C: Benthic foraminifera species checklist at ODP Site 1139 Hole A. 278
Appendix D: The most abundance species of each clusters at the studied Sites 752A, 1168A and 1139A. 286
Appendix E: Diversity indices and age (Ma) of thirty samples at the Hole 752A. Diversities are calculated by past software (PAST 3.25) (Hammer et al., 2001). 288
Appendix F: The data used for calculating Benthic Foraminifera Accumulation Rate (BFAR) and MAR $_{carbonate}$ at the Site 752 Hole A, the Dry Bulk Density and $CaCO_3$ % data derived from the Initial Report (Shipboard Scientific Party, 1989a). 289
Appendix G: Diversity indices and age (Ma) of forty-two samples at the Hole 1168A. Diversities have calculated by past software (PAST 3.25) (Hammer et al., 2001). 290
Appendix H: The data used for calculating Benthic Foraminifera Accumulation Rate (BFAR) and MAR $_{carbonate}$ at the Site 1168 Hole A. The Dry Bulk Density and $CaCO_3$ % data derived from the Initial Report (Shipboard Scientific Party, 2001a). 291
Appendix I: Diversity indices and age (Ma) of twenty-five samples at the Hole 1139A. Diversities calculated by past software (PAST 3.25) (Hammer et al., 2001). 293
Appendix J: The data used for calculating Benthic Foraminifera Accumulation Rate (BFAR) and MAR $_{carbonate}$ at the Site 1139 Hole A. The Dry Bulk Density and $CaCO_3$ % data derived from the Initial Report (Shipboard Scientific Party, 2000). 294
Appendix K: 1) Correlation coefficient (R-value) and Statistically significant value (P-value) calculated from 13 species in each Hole (752A, 1168A & 1139A) and diversity (Shannon_H). 295

2) Correlation coefficient for 5 species at the study Holes (752A, 1168A & 1139A) calculated from maximum size values and relative abundance of each species. 295

Appendix L: The size (μm) and the number of specimens of *Abditodentrix pseudothalmanni* at ODP Sites 752, 1139 &1168. The mean values and standard deviations have calculated for different sizes at each sample. 296

Appendix M: The size (μm) and the number of specimens of *Globocassidulina subglobosa* at ODP Sites 752, 1139 &1168. The mean values and standard deviations have calculated for different sizes at each sample. 298

Appendix N: The size (μm) and the number of specimens of *Cibicidoides mundulus* at ODP Sites 752, 1139 &1168. The mean values and standard deviations have calculated for different sizes at each sample. 300

Appendix O: The size (μm) and the number of specimens of *Nuttalides umbonifera* at ODP Sites 752, 1139 &1168. The mean values and standard deviations have calculated for different sizes at each sample. 302

Appendix P: The size (μm) and the number of specimens of *Sphaeroidina bulloides* at ODP Sites 752, 1139 &1168. The mean values and standard deviations have calculated for different sizes at each sample. 304

Appendix Q: Carbon and Oxygen Isotope data for benthic foraminifera species standardised to *Cibicidoides mundulus* at 752A. The bold values at the bottom are the mean difference (offset) between *C. mundulus* and both *C. wuellerstorfi* and *Planulina costata*. 306

Appendix R: Carbon Isotope data for benthic foraminifera species (standardised benthic foraminifera Isotope) at 1168A. The bold values at the bottom are the mean difference (offset) between *C. mundulus* and six different species..... 307

Appendix S: Oxygen Isotope data for benthic foraminifera species (standardised benthic foraminifera Isotope) at 1168A. The bold values at the bottom are the mean difference (offset) between *C. mundulus* and six different species..... 308

Appendix T: Carbon and Oxygen Isotope data for benthic foraminifera species (standardised benthic foraminifera Isotope) at 1139A. The bold values at the bottom are the mean difference (offset) between *C. mundulus* and *Epistominella exigua*. 309

Appendix U: Age and isotope values of Site 754A. The age is determined based on the first and last occurrence of nine nannofossil species (Appx U (1)) which provided by Shipboard Scientific Party (1989b) and revised by ATNTS2012 in GTS2012 (Hilgen et al., 2012) (Appx U(3)). Oxygen and carbon data of 754A provided by Rea et al. (1991) and the data conducted on *Cibicidoides* sp. (Appx U (2))..... 310

Appendix V: The age model and isotope values of 1170A. Chronozones and nannofossil ages have provided by (Stickley et al., 2004) (Appx V (1)) and revised by ATNTS2012 in GTS2012 (Hilgen et al., 2012) (Appx V (3)). The isotope values have supplied by Ennyu and Arthur (2004a) (Appx V (2))..... 311

Appendix W: The isotope values and chronozones of the Site 747 Hole A have provided by Wright and Miller (1992), and the Chronozone C6cn2 has provided by Berggren (1992). The age has revised by ATNTS2012 in GTS2012 (Hilgen et al., 2012) (Appx W (1,2)). The isotope values for 747A measured for *Cibicidoides* spp. (Wright and Miller, 1992) (Appx W (3)). 313

Appendix X: The sea surface temperature (SST) of the Miocene at 1168A by using alkenones as SST biomarkers. The temperature values have provided by Knee-Robinson (2018). 315

List of Figures

Figure 1. 1: Global deep-sea oxygen isotope records based on compiled data for more than 40 DSDP, ODP sites (36) and climatic events. Most of the data are from analysing long-ranging benthic foraminifera, Cibicidoides and Nuttalides (after Zachos et al., 2001). 8

Figure 1. 2: The location map of the Hole 752A (ODP) with the black dot, the arrow showing different oceanic currents affecting this hole. SJC = South Java Current, LC = Leeuwin Current, SEC = South Equatorial Current, WAC = West Australian Current. From (Singh et al., 2012) (after Wijffels et al., 1996). 11

Figure 2. 1: Location map of the ODP studied Site 752 Hole A on the Broken Ridge. The contour lines represent the predicted bathymetry in metres (after Ingle et al., 2003)..... 28

Figure 2. 2: Summary diagram of ODP Site 752 Hole A on the Broken Ridge, showing the recovery, age, nannofossil zones, magnetic polarity, lithology and water depth (After Shipboard Scientific Party, 1989a). 31

Figure 2. 3: Age-Depth model created from the original data (Shipboard Scientific Party, 1989a) using calcareous nannofossils bioevents and revised by ATNTS2012 in GTS2012. 32

Figure 2. 4: Neogene stratigraphic subdivision, geomagnetic polarity, and standard zonation of planktonic foraminifera and calcareous nannofossils (After (Hilgen et al., 2012)). 33

Figure 2. 5: Age-Depth plot and the rate of sedimentation (Site 752 Hole A). The black line represents the age-depth plot, while the red line represents the rate of sedimentation. The yellow boxes show the intervals of sedimentation rate changes. 35

Figure 2. 6: Offshore Tasmanian region. Showing seafloor topography and topographic feature from 42°S to 44°S. Solid circle = ODP Site 1168 Hole A. Colour tones in scale bar are representing different bathymetry (after Shipboard Scientific Party, 2001a). 42

Figure 2. 7: Lithology and recovery of the Site 1168 Hole A, western Tasmanian margin, from depth 65-488 mbsf. The age is revised by ATNTS2012 in GTS2012 (Hilgen et al., 2012). Calcareous nannofossil zones follow (Hilgen et al., 2012), (after Shipboard Scientific Party, 2001a). 43

Figure 2. 8: Age-Depth model for Hole 1168A created from Stickley et al. (2004) using calcareous nannofossils bioevents, planktonic foraminifera and geomagnetic polarity datum and revised by ATNTS2012 in GTS2012 (Hilgen et al., 2012). 47

Figure 2. 9: Age-Depth plot and the rate of sedimentation (Site 1168 Hole A). The black line is the age-depth plot, while the red line is the sedimentation rate. The yellow boxes show the rapid change in the rate of sedimentation in two different range of times. 49

Figure 2. 10: Location map of the studied area, the contour line is predicted bathymetry in meters below the seafloor. The solid circle is the position of the studied site at Skiff Bank in Kerguelen Plateau (after Ingle et al., 2003)..... 54

Figure 2. 11: Stratigraphic section of the Hole 1139A showing core recovery, lithology, lithologic units and ages of units revised by ATNTS2012 in GTS2012 (Hilgen et al., 2012), with nannofossil zones (after Shipboard Scientific Party, 2000)..... 55

Figure 2. 12: Age-Depth model created from the original data using calcareous nannofossils and planktonic foraminifera bioevents and revised by ATNTS2012 in GTS2012 (Hilgen et al., 2012)..... 57

Figure 2. 13: Age-Depth plot and rate of sedimentation (Site 1139 Hole A). The black line is the age-depth plot, while the orange line indicates the sedimentation rate. The yellow boxes indicate two periods of change in the sedimentation rate. The upper box shows the steep change, while the lower box shows the highest rate of sedimentation. 60

Figure 3. 1: Location map of the study area. Studied sites are marked as stars (752, 1168 and 1139), additional sites referred to in the text are located by dots (after Weatherall et al., 2015). Sites 752, 754 & 756 (Leg 121), Site 1168 (Leg 189), Site 1139 (Leg 183), sites 705-716 (Leg 115) and DSDP Site 236 (Leg 24)..... 69

Figure 3. 2: Range chart of fifty-two most abundant benthic foraminifera species encountered at Ocean Drilling Program (ODP) Holes 752A, 1139A and 1168A. 73

Figure 3. 3: SEM Images 79

Figure 3. 4: SEM Images 94

Figure 3. 5: SEM Images 111

Figure 3. 6: SEM Images 120

Figure 3. 7: SEM Images 130

Figure 3. 8: SEM Images 141

Figure 4. 1: Constrained cluster diagram of samples in the late Oligocene and Neogene (Miocene & early Pliocene) at the Site 752 Hole A, exhibiting the presence of six major cluster groups..... 147

Figure 4. 2: Diversity indices, dominance, species richness and evenness at the Site 752 Hole A, the shaded area are six clusters formed from samples with similar composition, separated from each other in the places where diversity changed. 150

Figure 4. 3: Benthic Foraminifera Accumulation Rate (BFAR) and High productivity taxa relative abundance versus age at Hole 752A. The red arrow points to an increasing trend of BFAR values..... 152

Figure 4. 4: Rarefaction curve of the thirty samples at the Site 752 Hole A. The numbers on each curve represent the Age (Ma). The vertical axis is species diversity, and the horizontal axis is the number of collected specimens. 153

Figure 4. 5: Species relative abundance, diversity (Shannon_H) and Benthic Foraminifera accumulation Rate (BFAR) versus age at Site 752 Hole A..... 155

Figure 4. 6: Constrained Cluster diagram of samples in the late Oligocene and Neogene (Miocene and early Pliocene) at the Site 1168 Hole A, exhibiting the presence of six major cluster groups. 157

Figure 4. 7: Diversity indices, dominance, species richness and evenness at the Site 1168 Hole A, the shaded area are six clusters formed from samples with similar composition. 160

Figure 4. 8: Benthic Foraminifera Accumulation Rate (BFAR) and High productivity taxa versus age at the Hole 1168A. The x-axis of BFAR is a logarithmic scale. 161

Figure 4. 9: Rarefaction curve of the forty-two samples at the Site 1168 Hole A. The numbers on each curve represent the Age (Ma). The vertical axis is species diversity, and the horizontal axis is the number of collected specimens. 162

Figure 4. 10: Species relative abundance, diversity (Shannon_H) and Benthic Foraminifera accumulation Rate (BFAR) versus age at Site 1168 Hole A. The red curve is Cibicidoides wuellerstorfi (smooth type). 164

Figure 4. 11: Cluster diagram of samples in the late Oligocene and Miocene (early & early late Miocene) at the Site 1139 Hole A, exhibiting the presence of five major cluster groups. 167

Figure 4. 12: Diversity indices, dominance, species richness and evenness at the Site 1139 Hole A, the shaded area are five clusters formed from samples with similar composition. 168

Figure 4. 13: Benthic Foraminifera Accumulation Rate (BFAR) and High productivity taxa versus age at the Hole 1139A. The x-axis of BFAR is a logarithmic scale. 169

Figure 4. 14: Rarefaction curve of the twenty-five samples at the Site 1139 Hole A. The numbers on each curve represent the Age (Ma). The vertical axis is species diversity (richness), and the horizontal axis is the number of collected specimens. 170

Figure 4. 15: Species relative abundance, diversity (Shannon_H) and Benthic Foraminifera accumulation Rate (BFAR) versus age at Site 1139 Hole A. The red curve is Cibicidoides wuellerstorfi (smooth type). 172

Figure 4. 16: Diversity versus age of studied Sites 752A, 1168A and 1139A. The red arrows pointed to the periods of glaciation and inter-glaciation. The shaded areas are Miocene cooling and warming events. 188

Figure 4. 17: Comparing between four most abundant species at the study sites 752A, 1168A and 1139A plotted versus age. The shaded areas with the red arrows point to global climatic events. 192

Figure 4. 18: Comparing between four most abundant species at the study Sites 752A, 1168A and 1139A plotted versus age. The shaded area with the red arrows pointing to the global events. 195

Figure 5. 1: Size and relative abundance of Abdetodentrix pseudothalmani at the studied Sites versus age. The solid line in the size graph is the mean size, and the empty circles are representing the smallest and largest test. The horizontal lines in size graphs are standard deviation (STDV)..... 198

Figure 5. 2: Size and relative abundance of Globocassidulina subglobosa at the studied Sites versus age. The solid line in the size graph is the mean size, and the empty circles are representing the smallest and largest test. The horizontal lines in size graphs are standard deviation (STDV). 199

Figure 5. 3: Size and relative abundance of Cibicidoides mundulus at the studied Sites versus age. The solid line in the size graph is the mean size, and the empty circles are representing the smallest and largest test. The horizontal lines in size graphs are standard deviation (STDV). 200

Figure 5. 4: Size and relative abundance of Nuttalides umbonifera at the studied Sites versus age. The solid line in the size graph is the mean size, and the empty circles are representing the smallest and largest test. The horizontal lines in size graphs are standard deviation (STDV). 201

Figure 5. 5: Size and relative abundance of Sphaeroidina bulloides at the studied Sites versus age. The solid line in the size graph is the mean size, and the empty circles are representing the smallest and largest test. The horizontal lines in size graphs are standard deviation (STDV). 203

Figure 5. 6: Carbonate content (%), carbonate mass accumulation rates (MAR $_{carbonate}$), benthic foraminiferal abundance, diversity and isotope values plotted versus age at the studied Site 752 Hole A. 206

Figure 5. 7: Carbonate content (%), carbonate mass accumulation rates (MAR $_{carbonate}$), benthic foraminiferal abundance, diversity and isotope values plotted versus age at the studied Site 1168 Hole A. 207

Figure 5. 8: Carbonate content (%), carbonate mass accumulation rates (MAR $_{carbonate}$), benthic foraminiferal abundance, diversity and isotope values plotted versus age at the studied Site 1139 Hole A. 208

Figure 6. 1: Oxygen ($\delta^{18}O$) and Carbone ($\delta^{13}C$) Stable isotope records for the ODP Holes 752A and 754A. The isotope values corrected to Cibicidoides mundulus for 752A while, the values at 754A conducted on Cibicidoides sp. Oxygen and carbon data of 754A provided by Rea et al. (1991)..... 217

Figure 6. 2: Oxygen ($\delta^{18}O$) and carbon ($\delta^{13}C$) stable isotope records for the ODP Holes 1168A and 1170A. Most of the isotope values corrected to Cibicidoides mundulus for 1168A while the values at 1170A are for Cibicidoides mundulus (A). The oxygen and carbon curves from the interval between ~ 20.5 to ~24 Ma at 1168A (B) provided by Pfuhl et al. (2004), and the age is after Cande and Kent (1992, 1995). 219

Figure 6. 3: Oxygen ($\delta^{18}O$) and carbon ($\delta^{13}C$) stable isotope records for the ODP Holes 1139A and 747A. Most of the isotope values corrected to *Cibicidoides mundulus* for 1139A while the values at 747A are for *Cibicidoides* spp. The green line represents *Sphaeroidina bulloides* at 1139A. 220

Figure 6. 4: Oxygen ($\delta^{18}O$) and carbon ($\delta^{13}C$) stable isotope records for the ODP Holes 752A, 1168A and 1139A compared with global isotopic records (Cramer et al., 2009). Both Climatic and bio- events have shown. The ranges of the important species at all sites have shown in the right. 228

Figure 6. 5: Sea surface temperature and oxygen isotope at 1168A. The temperature (SST) data are provided by Knee-Robinson (2018). 229

List of Tables

Table 1. 1: Miocene deep-sea benthic foraminifera species with their microhabitats, environmental preferences, water masses and period of greatest dominance at the current study Sites (752A, 1168A and 1139A). Bolivinids (in general) include all Bolivinid species. 14

Table 2. 1: Lithologic units at the Site 752 Hole A (After Shipboard Scientific Party, 1989a)..... 28

Table 2. 2: Age-Depth model depending on the range of abundant calcareous nannofossil species. .. 32

Table 2. 3: Age-Depth data of the current study of both original and revised ages after ATNTS2012 in GTS2012, with the rate of the deposition calculated from revised ages. 34

Table 2. 4: Benthic foraminifera species and their palaeodepths (bathymetry). Species bathymetry in bold represents the most abundant and indicative species for late Oligocene to early Miocene. Palaeodepth interpretations of the most abundant species follow Van Morkhoven et al. (1986) and Holbourn et al. (2013). 36

Table 2. 5: Age-Depth model data for Hole 1168A based on the ranges of calcareous nannofossil species, planktonic foraminifera and geomagnetic polarity datum. 45

Table 2. 6: Age-Depth data for Hole 1168A with revised ages after ATNTS2012 in GTS2012, with the rate of the deposition of each depth calculated from revised age and paleodepth depending on benthic foraminifera assemblages (Shipboard Scientific Party, 2001a). 48

Table 2. 7: Depths and ages of calcareous nannofossils to find the chronology of Site 1139, established by Shipboard scientific Party, (2000) in Reusch (2002). 56

Table 2. 8: Established age-depth of Site 1139A using planktic foraminifera (F) (Shipboard Scientific Party, 2000) and nannofossil datums (N) (Persico et al., 2003) and revised using ATNTS2012 in GTS2012 (Hilgen et al., 2012). 56

Table 2. 9: Age-Depth data of the current study revised ages after ATNTS2012 in GTS2012, with the rate of the sedimentation of each depth calculated from revised age and paleodepth depending on benthic foraminifera assemblages from the current study and Reusch (2002). 59

LIST OF ABBREVIATIONS AND SYMBOLS

AADW	Antarctic Deep Water
AAIW	Antarctic Intermediate Water
ACC	Antarctic Circumpolar Current
AIS	Antarctic Ice Sheet
APC	Advanced Hydraulic Piston Corer
ATNTS	Astronomically Tuned Neogene Time Scale
BF	Number of Benthic Foraminifera
BFAR	Benthic Foraminifera Accumulation Rates
C5Cn, C5En	Geomagnetic Polarity Datum
CC	Core Catcher
CCD	Calcium Carbonate Compensation Depth
CM	Carbon Maxima
CN2	Calcareous Nannofossil biozone 2
CP	Paleocene Calcareous Nannofossil biozone
D	Dominance
DBD	Dry Bulk Density
DSDP	Deep-Sea Drilling Project
E	Equitability
EAIS	East Antarctic Ice Sheet
ENSO	El Niño-Southern Oscillation
FO	First Occurrence
GTS	Geologic Time Scale
GXM XTL3101	Binocular Stereoscopic Microscope type
H	Shannon Diversity Index (Information Function)
H_2O_2	Hydrogen Peroxide
IAEA	International Atomic Energy Agency
IDW	Indian Deep Water
IODP	Integrated Ocean Drilling Program
ITF	Indonesian Throughflow
ka	kilo annum (thousand years)
LC	Leeuwin Current
LO	Last Occurrence
LSR	Linear Sedimentation Rate
Ma	Mega-annum (a million years)
mbsf	meter below sea floor
Mi-1	Miocene Oxygen Isotope Excursion Event
MMCO	Mid-Miocene Climatic Optimum
MMCT	Mid- Miocene Climatic Transition
NADW	North Atlantic Deep Water
NBS-18	Carbonatite (isotope standards)

NBS-19	TS-Limestone (isotope standards)
NCW	Northern Component Water
NH1	Neogene Hiatus event 1
NHG	North Hemisphere major Glaciation
NKP	Northern Kerguelen Plateau
NN	Nannofossil zone
ODP	Oceanic Drilling Program
OMZ	Oxygen Minimum Zone
S	Species Diversity
SCW	Southern Component Water
SEC	South Equatorial Current
SEM	Scanning Electron Microscope
SJC	South Java Current
SST	Sea Surface Temperature
STDV	Standard Deviation
STR	South Tasmanian Rise
TISW	Tethyan Indian Saline Water
TOW	Tethyan Outflow water
UPGMA	Unweighted Pair-Group Average
VPDB	Vienna Pee Dee Belemnite
WAC	West Australian Current
WAIS	West Antarctic Ice Sheet
WoRMS	World Register of Marine Species
XCB	Extended Core Barrel
$\delta^{13}C$	Delta-13 C (stable carbon isotope)
$\delta^{18}O$	Delta-18 O (stable oxygen isotope)
µl	microliter
µm	micrometre

Chapter One

Introduction and Background

1.1 Miocene palaeoclimates & tectonics

The Neogene (Miocene & Pliocene, approximately 23-2.5 Ma) divided into an early Neogene warm climate interval and late Neogene cool interval. The Miocene marked by different stages of climatic transition (Flower and Kennett, 1993). The early Miocene has been characterised as a warm interval in contrast to the early and mid-Oligocene with significant cooling beginning after permanent emplacement of the East Antarctic Ice Sheet (EAIS) during the mid-Miocene (Shackleton and Kennett, 1975).

The later part of the early Miocene from (~ 16 Ma) represents the warm stage ended with the early mid-Miocene cooling stage~ 14.8 to 12.9 Ma, and this reflects climatic changes that result in the major growth of EAIS (East Antarctic Ice Sheet). The mid-Miocene cooling interval coincided with increased development of Antarctic Deep Water (AADW) and major growth of the EAIS (Flower and Kennett, 1993). Badger et al. (2013) suggested that the development of the East Antarctica Ice Sheet happened at about 14 Ma. This development followed by positive carbon isotope excursion (carbon maximum 6 (CM6)), because of increased organic carbon burial and depleting of carbon dioxide in the atmosphere.

The Miocene was a time of major ocean-atmospheric change. The first establishment of the Antarctic ice sheet was during the early Oligocene, in response to circumpolar oceanic current then developed during the middle Miocene (Ramstein et al., 1997).

Banerjee et al. (2017) used planktonic and benthic foraminifera carbon and oxygen isotope as a proxy to show palaeoceanographic changes in the Northern Indian Ocean (ODP Site 758) during the Miocene. They reported the global warmth period at ~17–14 Ma which coexisted to increase of organic carbon deposition (Monterey excursion), this period followed by the cold event of EAIS at ~14–12 Ma and initiation of Indian Summer Monsoon (ISM) with the waning of Antarctica Ice sheet (12.3–10.4 Ma).

At the time of Antarctic Ice Sheet expansion (14.7 to 12.7 Ma) and global cooling low summer insolation over Antarctica coexisted with decreasing atmospheric carbon dioxide levels from the northwest and southeast subtropical Pacific Ocean (Holbourn et al., 2005).

During the study of West Pacific Ocean (Ocean Drilling Program Site 1146) Holbourn et al. (2013) observed from the $\delta^{18}O$ curve that the continuous deep water cooling and glaciation episodes following the end of the Mid-Miocene Climatic Optimum especially after ~ 13 Ma until 9 Ma except of short warming episode at about 10.8‑10.7Ma at peak insolation during eccentricity maxima (100 and 400 kyr).

The rapid expansion of the East Antarctic Ice Sheet (EAIS) at 13.8 Ma is accompanied by a sea-level fall of ~60 m (Miller et al., 2005, Lear et al., 2015). The mid-Miocene is an interval of high

$\delta^{13}C$ values linked to the so-called “Monterey Carbon Excursion” (17.5-13 Ma); Vincent et al., 1985, Holbourn et al., 2007), characterized by several distinct $\delta^{13}C$ maxima (Carbon Maxima or CM events; Woodruff and Savin, 1991) that were accompanied by organic carbon removal in marine (Compton et al., 1990, Vincent et al., 1985) or terrestrial realms (Diester-Haass et al., 2006). Greenop et al. (2014) suggested that two intervals of Antarctic ice sheet retreating occurred during the Mid Miocene Climatic Optimum when recording high CO2 and orbital obliquity variability.

The sea surface temperature SST at Site 608 in the North Atlantic Ocean from the Oligocene/ Miocene boundary to the middle Miocene Climatic Optimum (23.03 to 14.5 Ma) was nearly 15 °C warmer than modern temperature. While during the Middle Miocene Climatic Transition (MMCT, 14.5 to 12.5 Ma), SSTs decreased by ~6 °C. This decreasing continued until 9 Ma. The cooling of SST coincided with a *p*CO2 decrease from an average of ~430 ppm in MCO to ~305 ppm after the MMCT (Super et al., 2018).

During the 6 Ma of the mid-Miocene, a substantial increase in oceanic $\delta^{18}O$ was recorded (Zachos et al., 2008) reflecting the increase in global ice volume as a consequence of global cooling. During this interval, the EAIS is considered to be a major ice sheet (Westerhold et al., 2005).

The stable isotope records (marine) at ~14 Ma shows a significant growth of the ice sheet on Antarctica (Flower and Kennett, 1995). The development of the oceanic front in the Tasmania and New Zealand sectors of the Southern Ocean coincides with the continuing cooling trend by the middle/late Miocene (Exon et al., 2001).

The interval of the peak warmth during the MMCO has a minor impact on benthic foraminifera accumulation rates, number of specimens and assemblage composition during the study of the late early to middle Miocene benthic foraminiferal assemblages in eastern equatorial Pacific Sites U1337 and U1338. While during the major cooling, a significant change of the assemblage composition has recorded which indicated by increasing organic flux to the sea floor, surface productivity increasing and intensification of the equatorial upwelling (Kochhann et al., 2017). During around 13.8 Ma the bottom water temperature decreased by ~ 2 °C at both Sites U1338 and 1146, this decrease coincided with the increasing of $\delta^{18}O_{sw}$ by 0.9–1.0 ‰ (Kochhann et al., 2017).

The equatorial ocean gateway (The Indonesian Throughflow) transfers heat from the Pacific into the Indian Ocean. West Pacific Warm Pool fluctuations are related to variability in the Indonesian Throughflow which acts as a control on inter-annual climate variation such as the SE Asian monsoon and the El Niño-Southern Oscillation (ENSO) (Hall et al., 2011).

Indonesian Gateway restriction starting, and termination of deep-water flow, from the Early Miocene, seems to have coincided with major global climate system perturbations which include rapid warming during the Late Oligocene followed by short term glaciation or pulse

glaciation and coincided with positive carbon isotopic excursion in the earliest Miocene (Zachos et al., 2001).

The rapid change in tectonics, topography and land/sea distributions is a complicated history of the Indian-Pacific Ocean gateway during the Neogene (Hall, 1998). As the closure of the deep-water connection happened, mountains rose, increasing area of the land and shelf areas and the formation of the new deep basins. This closure accompanied by number of changes such as high mountains rose first in Borneo and later elsewhere in Indonesia. The erosion and rainfall also may have been changed. Oceanic circulation would have been affected by geologically controlled passages changes and modifications. Through the gateway, there was passing from warm South Pacific to colder North Pacific waters. The climate changed from drier to wetter. These tropical gateway changes had a similar impact to changes in other oceanic gateways and the rise of Tibet for the global climate system (Hall et al., 2011).

Tasmanian Gateway was rapidly deepening and widened during the early Oligocene and brought cooler, open ocean conditions (Exon et al., 2001). The relatively shallow Tasmanian Gateway is one of the few places in the mid to high latitudes were fairly completed (McGonigal, 2007).

The tectonic separation between Australia and Antarctica is a key for the Antarctic Circumpolar Current (ACC) development during the Cenozoic (Kennett et al., 1975). The Kerguelen Plateau is situated 1000 km north of the Antarctic continent in the Southern Ocean.

It is tectonically active and geographically connected to the South Pole since its formation at 110 Ma (Mutter and Cande, 1983).

Mutter and Cande (1983) have described in detail the separating mechanism of the Broken Ridge and the Kerguelen Plateau, which started around 100 Ma this similar to the total fit of Antarctica and Australia. Mutter and Cande (1983) noted several horsts and grabens are trending N-S and NW-SE at the eastern side of the Kerguelen Plateau these clarify the mechanism of the separation of the Broken Ridge and the Kerguelen Plateau.

Sea surface temperature variations may have caused changes of the surface hydrography at the Kerguelen Plateau; these also may have been driven by obliquity and long-term eccentricity.Iit is suggesting that the astronomical forcing played a key role in the evolution of Southern Ocean dynamics during the Middle Miocene (Verducci et al., 2009). According to Verducci et al. (2009), the intense cooling phase identification was derived from a detailed study of the climatic and hydrographic changes that occurred in the region especially in ODP Hole 747A (Kerguelen Plateau, southern Indian Ocean) during the Middle Miocene Climatic Transition (the Middle Miocene Shift).

1.2 Miocene palaeoceanography

1.2.1 Indian Ocean Miocene palaeoceanography

The connectivity of the Pacific and the Indian Ocean is by transporting water through the Indonesian seaway (Indonesian throughflow (ITF)) from the North Pacific (Gordon and Fine,

1996). The movement of surface and thermocline components of the ITF towards the Indian Ocean was unobstructed by topography, while below the thermocline many sills separating the Indonesian seas prevented throughflow. The link between the Indian Ocean and Indonesian sea was recorded in the Timor vicinity (Gordon et al., 2003).

According to Fieux et al. (1996), cooler, more saline and highly oxygenated water was observed in the Timor passage below 1500 m. According to Van Aken et al. (1988), the sill which will block the passage between the Indian Ocean and Indonesian sea were observed at the depth 1450m. Before the Miocene, the open connection existed between the Pacific and Indian oceans (Martin and Scher, 2006). According to the Martin and Scher (2006) during their study at 757 (Ninetyeast Ridge) from 40 to 10 Ma, it was observed (based on Nd isotope) that the waters at this site were derived from the Southern Ocean and are intermediate to deep waters, although a true Antarctic Circumpolar Current did not exist throughout this entire interval.

Nishimura and Suparka (1997) believed that the deep-sea connection between the Pacific and Indian Oceans closed in the latest Miocene at ~6 Ma. The restriction of the Indonesian seaway was finally observed in the early Pliocene 4-3 Ma which led to separation in the thermocline water source between the South Pacific to the North Pacific Ocean (Cane and Molnar, 2001). The final closure of the deep-sea connection between the Pacific and Indian oceans may have affected the deep-sea biota and changed the thermohaline circulation of the eastern Indian Ocean (Singh and Gupta, 2010).

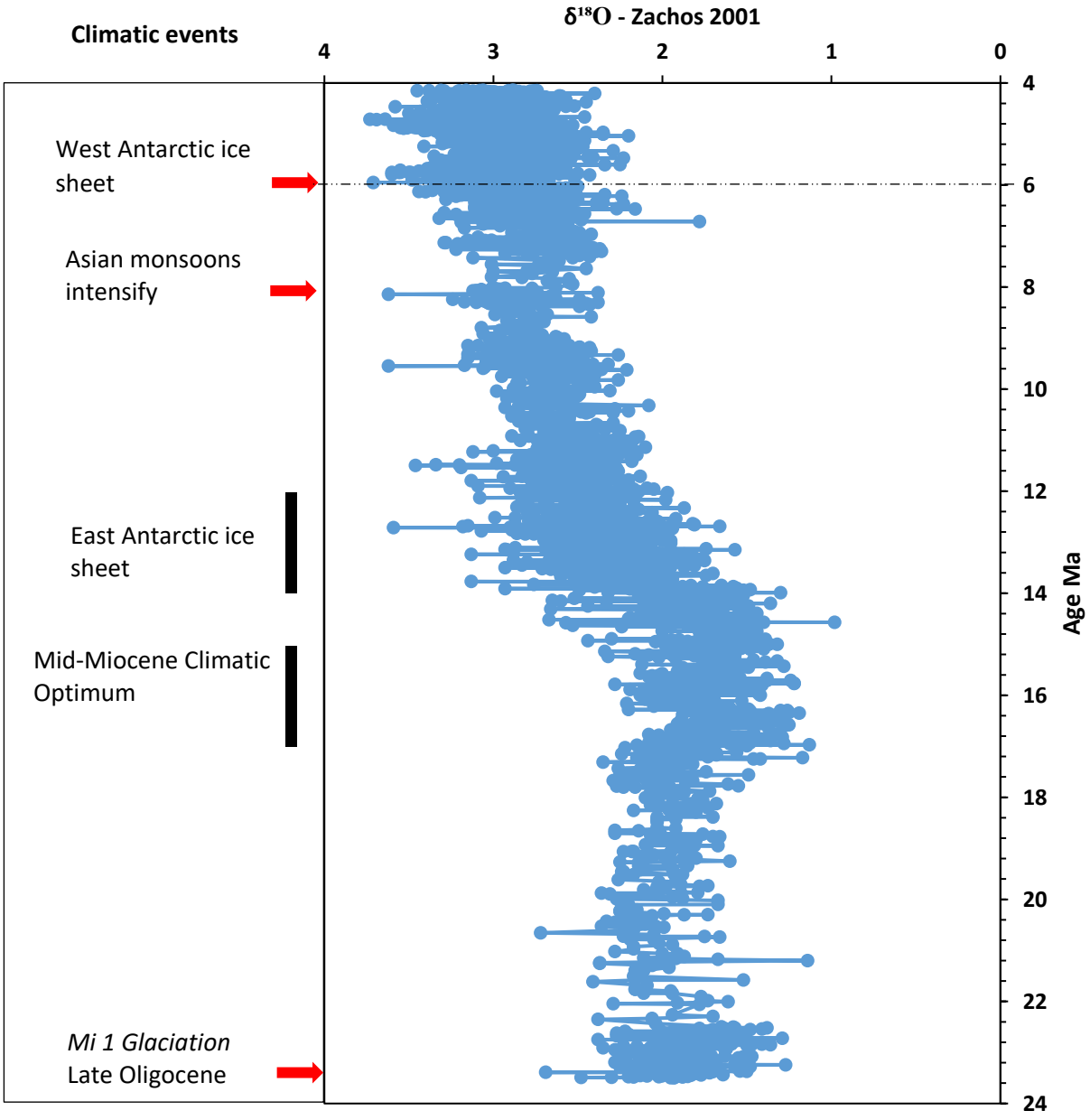


Figure 1. 1: Global deep-sea oxygen isotope records based on compiled data for more than 40 DSDP, ODP sites (36) and climatic events. Most of the data are from analysing long-ranging benthic foraminifera, Cibicidoides and Nuttalides (after Zachos et al., 2001).

Tethyan Indian Saline Water (TISW) upwelled in the Antarctic region throughout the early Miocene; meridional heat transported by this deep water source (TISW) may have prevented large scale formation of the EAIS, this had continued until the middle Miocene ~14 Ma (Woodruff and Savin, 1989). The TISW was competing against cold, Southern Component Water (SCW) during the early to early middle Miocene. The termination of TISW was due to the collision of Africa with Eurasia, where the eastern Mediterranean and Paratethys seas became separated from the northern Indian Ocean and the flow of warm and saline water decreased (Hsu and Bernoulli, 1978), especially during early middle Miocene when major growth of the EAIS was recorded (Flower and Kennett, 1993).

Through studying twelve sites in the ODP leg 115 from the north-central Indian Ocean, Boersma (1990) noticed that benthic foraminifer index faunas characterise the late Oligocene to late Pliocene vertical water-mass stratification along depth traverses. Benthic foraminifera fauna indicates well-oxygenated, deep bottom water conditions during most of this time, at all depths except under the southern Indian upwelling and in the Pliocene in the southern Arabian Sea. These well-oxygenated bottom waters considered to have been more fertile than Antarctic Intermediate Water (AAIW) that covers intermediate depths in the low to middle latitude Mascarene and Central Indian basins (Boersma, 1990).

Singh et al. (2012) clarify in detail the mechanism of the movements of the surface winds and currents at Hole 752A on the Broken Ridge (south-eastern Indian Ocean) (Figure 1.2), and the West Wind Drift, the South Equatorial Current and the Subtropical Convergence, which largely control the surface water circulation at that area. Other currents such as the Leeuwin Current

and South Indian Current are other components of the surface circulation off the coast of Western Australia located near Hole 752A. This hole has been mainly under the impact of the southern component deep water during the entire Neogene, and its present water depth has remained the same with an extremely low sedimentation rate of <0.61 cm ka^{-1} (Peirce et al., 1989).

1.2.2 Southern Ocean Miocene palaeoceanography

According to Huang et al. (2017), mixed layer deepening in the southwest Ross Sea and the southeast Weddell Sea during the MMCT suggested that upward movement of more saline deep waters and their partial mixing with shallow surface water along the Antarctic continental margin might have provided higher densities needed for the production of the AABW. Huang et al. (2017) inferred that the decrease of atmospheric CO_2 level from 450 ppm to 278 ppm had little effect on the distribution of deep-water formation.

According to Mackensen (1992) from his study of some ODP Sites (747, Central Kerguelen Plateau; 748 and 751, Southern Kerguelen Plateau) Miocene, bottom-water circulation stayed the same until late mid-Miocene. Mackensen (1992) also noted that the early late Miocene shows the retreating of carbonate-corrosive, deeper abyssal regions occupied by newly formed bottom-water masses from the Kerguelen Plateau, and shallow bathyal regions occupied by an aged water mass, such as NADW (North Atlantic Deep Water).

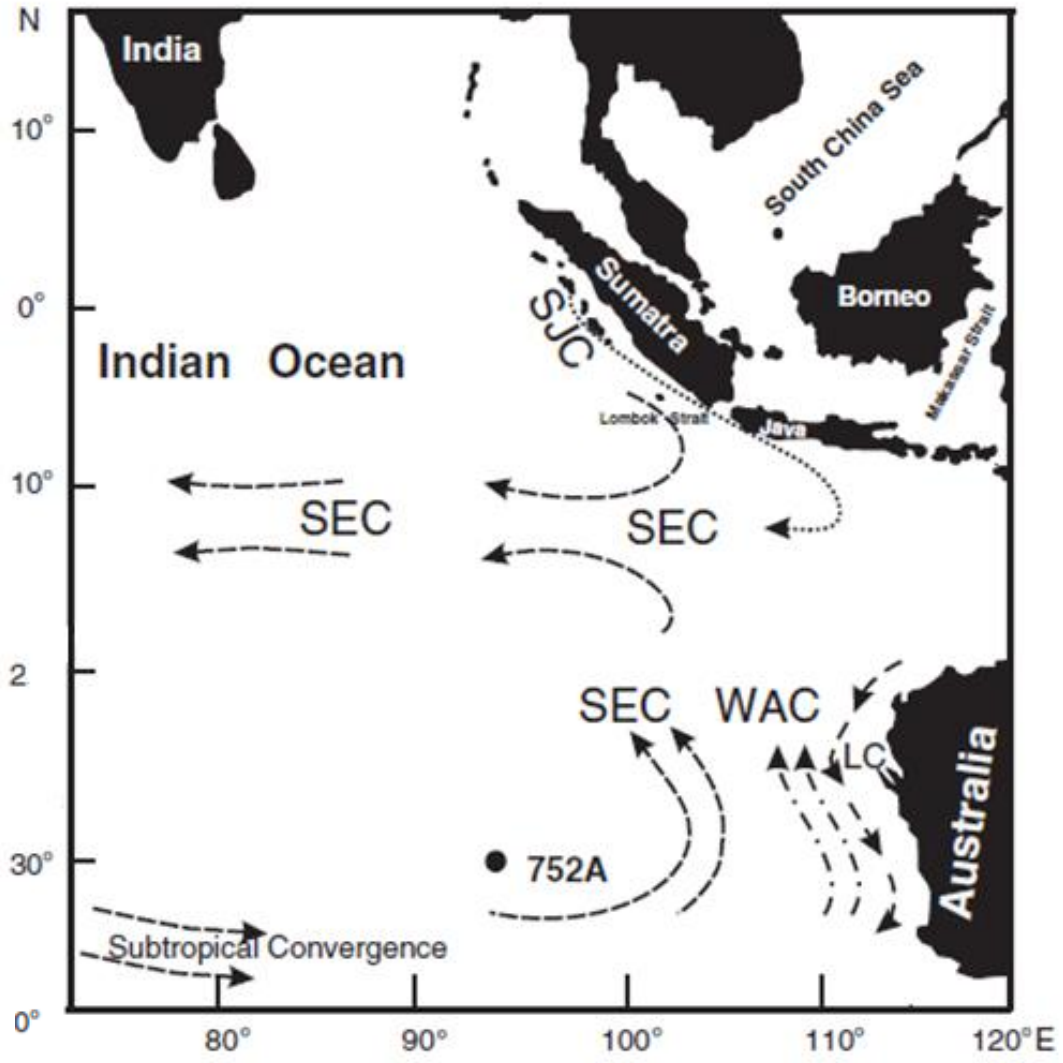


Figure 1. 2: The location map of the Hole 752A (ODP) with the black dot, the arrow showing different oceanic currents affecting this hole. SJC = South Java Current, LC = Leeuwin Current, SEC = South Equatorial Current, WAC = West Australian Current. From (Singh et al., 2012) (after Wijffels et al., 1996).

The opening of the Drake Passage in the early Neogene coincided with the continuous opening of the Tasmanian Seaway. In the early Neogene, the Antarctic Circumpolar Current (ACC) highly separated Antarctica from lower latitudes warm water influences (Exon et al., 2001). The northern regularly movement of the Tasmanian region happened during ~ 15 Ma, at the

time when EAIS (East Antarctic Ice sheet) expanded and the deposition of the pelagic carbonates in deep water at an average of 1-2 $cm.ka^{-1}$ was also observed (Exon et al., 2001). The late Miocene ice-sheet expansion after 5 Ma affected in Australia and caused high aridity and dust accumulation in some sequences had also observed (Exon et al., 2001).

McGonigal (2007) tried to reconstruct the palaeoceanographic conditions in the Tasmanian Gateway during the Miocene by using calcareous nannofossil assemblage data, with age models, geochemical and sedimentological data during his study of different sites (1168, 1170, 1171 and 1172). During the Miocene in the Tasmanian region when Australia and Antarctica continued to separate, the complete development of both ACC (Antarctic Circumpolar Current) and oceanic fronts in the Southern Ocean happened and the ice volume on Antarctica waxed and waned (McGonigal, 2007).

Woodruff and Savin (1989) suggested that the TISW flowed from the northern Indian Ocean to Antarctic region and operated as a significant factor in transporting meridional heat which connected high- and low-latitude climates in early Miocene time. Deepwater circulation from 11 to 5 Ma was similar to modern circulation. When NADW flowed southward to the Antarctic circumpolar region, it became entrained in that water, and become an important constituent of Antarctica deep water (Woodruff and Savin, 1989, Wright et al., 1992). According to Bialik et al. 2019, the water mass exchange between the Mediterranean Sea and the Indian Ocean via the Mesopotamian Seaway has reduced by ~90% in a first step at ca. 20 Ma during the initiation of South Asian Monsoon (SAM). The final closure of the seaway coexisted with the sea-level drop caused by permanent glaciation initiation of Antarctica at around 13.8 Ma.

1.3 Miocene deep-sea benthic foraminifera

Benthic foraminifera are one of the important constituents of deep-sea environments; they can thrive at different depths and habitats above the carbonate compensation depth and all latitudes from tropics to poles. They have very good fossilisation potential. To understand more about the nature and distribution of the water masses, studying benthic foraminifera will be a good proxy for determining bottom water conditions in the geologic past (Singh and Gupta, 2010).

Several studies were emphasised the sensitivity of the benthic foraminifera to the different factors such as nutrients, the oxygen level of the bottom water and pore water oxygenation (Corliss, 1985, Gooday, 1988). Below are listed a number of common, widespread taxa that are known to have associations with particular water-masses and/or environmental conditions (See Table 1.1).

Smooth walled bolivinids were previously mentioned by Smart and Ramsay (1995) and Ramsay et. al. (1998) lately changed to genus *Streptochilus* by Smart and Thomas (2006, 2007).

Smart and Thomas (2006) stated that the abundant early Miocene (18.9–17.2 Ma) small biserial foraminifera in the eastern Atlantic and western Indian Oceans which previously assigned to genus *Bolivina* were planktic (genus *Streptochilus*) depending on isotopic composition, apertural morphology and sedimentation rate. Smart and Thomas (2007) recognised three different species of *Streptochilus* in the eastern Atlantic and western Indian Oceans which previously assigned to genus *Bolivina*.

Species	Micro-habitats	Environmental preferences	References	Period of greatest Dominance (current study)
Abdetodentrix peudothalmanni	Infauna	Low oxygen conditions.	(Hayward et al., 2002)	The mid-late Miocene (752A, 1168A), early and mid- Miocene at 1139A.
Astrononion umbilicatulum	Infauna	High organic flux, low temperature.	(Gooday, 1994)	The mid- Miocene at 752A and earliest Miocene and mid to late Miocene at 1168A and earliest Miocene at 1139A.
Globocassidulina subglobosa	Shallow infauna	High oxygen, high temperature and strongly pulsed food. Associated with AABW in the south-eastern Indian Ocean.	(Corliss, 1979a, Singh and Gupta, 2004, Singh et al., 2012)	The earliest Miocene and mid-Miocene at all Sites.
Cibicidoides mundulus	Epifauna	High primary productivity.	(Mackensen, 1992)	The early and the late Miocene at 752A, the earliest Miocene and the mid- Miocene at 1168 and the early Miocene at 1139A.
Epistominella exigua	Epifauna	Oxygenated conditions. highly productivity and prefer cooler water.	(Poag and Low, 1984, Kurihara and Kennett, 1992,Thomas et al., 1995)	The mid-late Miocene at 752A & 1139A and the early Miocene at 1168A.
Nuttalides umbonifera	Epifauna	High oxygen, low temperature, low food, and low productivity. Associated with AABW in the Indian Ocean and NADW in the Atlantic and Southern oceans.	(Bremer and Lohmann, 1982, Corliss, 1983, Loubere and Fariduddin, 1999, Gooday, 2003, Singh et al., 2012)	The early and mid - Miocene at 752A, the mid and the late Miocene at 1168A and the mid-Miocene at 1139A.
Siphonodosaria lepidula	Infauna	Moderately low oxygen and high organic carbon.	(Boersma, 1990)	The early Miocene in the current Sites (752A, 1168A and 1168A).
Trifarina angulosa	Infauna	Prefer cold and strong bottom water currents.	(Mackensen, 1992)	During the late Miocene at 752A and 1168A, the mid-Miocene (~15Ma) at 1139A.
Cibicidoides wuellerstorfi	Epifauna	Low organic carbon, strong bottom currents, oligotrophic condition, and high seasonal food. Associated with AABW in the Indian Ocean and NADW in the Atlantic and Southern oceans.	(Corliss, 1983, Linke and Lutze, 1993, Gupta, 1997, Loubere and Fariduddin ,1999, Gooday, 2003)	The mid to the late Miocene at 752A, the early and the late Miocene at 1168A, the late early Miocene and the mid-Miocene at 1139A.

Table 1. 1: Miocene deep-sea benthic foraminifera species with their microhabitats, environmental preferences, water masses and period of greatest dominance at the current study Sites (752A, 1168A and 1139A). Bolivinids (in general) include all Bolivinid species.

Species	Micro-habitats	Environmental preferences	References	Period of greatest Dominance (current study)
Ehrenbergina carinata	Infauna	High temperature, high nutrient, and low oxygen environment.	(Gupta and Satapathy, 2000, Gupta et al., 2006)	The latest Miocene at 752A, the early to late Miocene at 1168A.
Smooth walled Bolivinids	Infauna	Low oxygen conditions. Associated with NCW, TOW in Atlantic and Indian oceans.	(Corliss and Fois, 1990, Corliss, 1991, Smart and Ramsay, 1995, Ramsay et al., 1998)	*Bolivina dilatata* dominated in the early Miocene at 1168A, the earliest Miocene at 1139A. The other smooth Bolivinids (*Bolivina* sp.3 and *B* . sp.9) were dominant in the late Oligocene and the early Miocene at 752A and 1139A, the early and the late Miocene at 1168A.
Bolivinids (in general)	Infauna	High organic flux, and high primary productivity.	(Poag and Low, 1984, Boersma and Mikkelsen, 1990, Gupta, 1994)	The late Oligocene, the Miocene, and the early Pliocene at all studied Sites.
Oridorsalis umbonatus	Infauna	Well-oxygenated water, low organic condition. Associated with AABW in the Indian Ocean.	(Mackensen et al., 1985, Gupta, 1994)	The mid- Miocene at 752A, the early Miocene to the early Pliocene at 1168A, the early to the mid- Miocene at 1139A.
Cibicidoides bradyi	epifauna	Low oxygenated conditions.	(Gupta and Thomas, 1999)	The mid- Miocene at 752A, the early to the mid- Miocene at 1168A and the early Miocene at 1139A.
Osangularia culter	Infauna	Low oxygenated conditions.	(Gupta and Thomas, 1999)	The early to the mid- Miocene at 752A and 1139A, and the mid- Miocene at 1168A.
Uvigerinids	Infauna	High organic flux, cool water and highly productivity.	(Boersma, 1986, Gooday, 1994, Gupta et al., 2001b, Gupta et al., 2004, Thomas et al., 1995)	The early and the late Miocene at 752A, the early Miocene at 1139A and the late Miocene at 1168A.
Melonis barleeanus	Infauna	High organic flux, cool water.	(Gooday, 1994)	The mid- Miocene to the early Pliocene at 752A, the late Oligocene to the early Pliocene at 1168A and the late Oligocene to the mid- Miocene at 1139A.

Table 1. 1: Continued

1.3.1 Previous studies in the Indian and the Southern oceans

There are many reports and studies from the ODP, IODP and DSDP sites which have published, and these provide useful resources. Woodruff and Savin (1989) collected faunal, carbon and oxygen isotope data from all around the world to investigate the evolution of Miocene thermohaline circulation, through three periods, approximately early, middle, and late Miocene times.

Boersma and Mikkelsen (1990) studied the primary productivity and the development of a mid-depth oxygen minimum in the Central Equatorial Indian Ocean between ~ 17 and 10 Ma. Data from benthic foraminifera, siliceous fossils, and stable isotopes demonstrated the enhancement of organic carbon oxidation in the sediments, and high primary productivity in the southern Indian upwelling zone during the Miocene at the ODP Site 714. It has been observed that with increasing diatom productivity index, the *Thalassionema* group, elevated diatom and uvigerinid abundances, and bolivinid diversity resulting in enhanced primary productivity and oxygen minimum.

Schroder-Adams (1991) studied Middle Eocene to Holocene benthic foraminifers from sites 736, 738, and 744 (Kerguelen Plateau). Significant faunal changes were observed in the middle Eocene, late Eocene/early Oligocene, middle Miocene, and late Miocene. Gradual species replacement was observed for the benthic assemblages at those sites.

Smart and Ramsay (1995) presented a summary of published stable isotope and benthic foraminiferal assemblages record between 24 and 8 Ma in the Atlantic and Indian oceans. A

low oxygenated intermediate to deep-water mass was identified which was restricted to North West Indian, Atlantic and the Tethys (Mediterranean) oceans. Highly abundant smooth-walled bolivinids occurred coevally (19.5-16.5 Ma) in these oceans. Smart and Ramsay (1995) interpreted the southward flow of North Component Water (NCW) produced in the Atlantic Ocean between 20 and 16 Ma, via Tethys, to the intermediate and deep-water flow into the northern Indian Ocean.

Gupta and Satapathy (2000) studied thirty-one samples of latest Miocene-Pleistocene from the Deep-Sea Drilling Project (DSDP) Site 236. They did the multivariate analysis of the abyssal benthic foraminifera, west-central Indian Ocean (Eastern Somali Basin). The result shows significant changes of deep ocean environments during the Neogene, which affect the distribution of the benthic foraminifera (Woodruff and Savin, 1989). Gupta and Satapathy (2000) suggested that benthic foraminifera distribution was controlled by the amount of food supply and rate of the bottom water oxygenation.

Gupta et al. (2004) believed that the intensification of the Indian monsoon system (10-8 Ma) originated from the uplift of the Himalayas and Tibetan Plateau. This intensification caused major changes in fauna and flora on land as well as in the Indian Ocean. The monsoon increased productivity and upwelling. These changes observed during the study of benthic foraminifera isotope data of the eastern and south-eastern Oceanic Drilling Program Sites (752, 757 and 758 (Leg 121) and Deep-Sea Drilling Project (DSDP) Sites 214 and 216 (Leg 22).

Singh and Gupta (2010) studied deep-sea benthic foraminifera from 194 samples from Ocean Drilling Program (ODP) Hole 757A, located on the Ninetyeast Ridge, the south-eastern Indian Ocean below the equatorial divergence zone. Singh and Gupta (2010) noticed that benthic foraminifera assemblages showed significant changes at Hole 757B since the late Oligocene. The well-oxygenated, oligotrophic species including *Cibicides cicatricosus*, *C. pseudoungerianus* and *Oridorsalis umbonatus* were dominant during the late Oligocene to the early Miocene. These species began to decrease when Site 757 moved northward towards the influence of the Indonesian Throughflow (ITF) subsurface water masses from the Pacific Ocean. In the early Eocene (~50 Ma) Hole 757B (1500 m water depth) is located at 45° S. Across the Oligocene-Miocene boundary (~23.5 Ma) 757B was located at 29° S in a temperate region near the subtropical convergence zone at a water depth of 1500 m. At ~5 Ma this site shifted to 21° S at ~10 Ma and 18°30' S (Peirce et al., 1989).

Singh et al. (2012) measured different diversity parameters of Neogene deep-sea benthic foraminifera of the ODP Hole 752A. The value of all diversity parameters declined between 25 to 23 Ma and after that increased with peak values at ~13.5 Ma. This Site is also studied in the current project since no detailed assemblage data has been published. According to Singh et al. (2012), the late Oligocene to earliest Miocene was an environmentally unstable interval at Hole 752A, which was dominated by species typical for low organic carbon, well-oxygenated and carbon corrosive conditions. The highest diversity parameters coincided with the early Middle Miocene Climatic Optimum.

Greenop et al. (2014) studied Miocene sediments from Ocean Drilling Program (ODP) Hole 761B in the Indian Ocean. They reported two intervals of Antarctic ice sheet retreating during MMCO when recording high CO2 and orbital obliquity variability.

Banerjee et al. (2017) recorded many climatic events in the Northeast Indian Ocean at ODP Site 758, such as MMCO (17–15 Ma), Monterey excursion (17–14 Ma), EAIS formation (13.8 Ma), summer monsoon initiation (12.3–10.4 Ma), and recording cooling event during 10.2–9.6 Ma .

Huang et al. (2017) stated that the Weddell Sea is the main location of the formation of bottom water and, also, an important component of global ocean circulation. Despite CO_2 concentrations fluctuations during the middle Miocene, the Weddell Sea shows enhanced Antarctic Bottom Water (AABW) formation and gyre transportation during this time.

Lubbers et al. (2019) reported the range between 13.5 to 8.2 Ma as an interval of declination of carbonate percentages and carbonate accumulation rates at International Ocean Discovery Program Site U1443 (Ninetyeast Ridge, Indian Ocean). Marked decrease in carbonate accumulation rates together with decrease carbonate percentages were reported after ~13.2 Ma. This continued until ~8.7 Ma, which coincides with the middle to late Miocene carbonate crash (Lubbers et al., 2019).

1.3.2 Deep-sea benthic foraminifera of the Indian Ocean and the Southern oceans

Benthic foraminifera have been studied in different localities in the Indian and Southern Oceans. The distribution and abundance of benthic foraminifera may have been affected by different water masses in different water depths, as well as the salinity, water temperature and the rate of organic matter input.

Nomura (1991) studied benthic foraminifera assemblages at sites 754 (Broken Ridge) and 756 (Ninetyeast Ridge), eastern Indian Ocean, and linked them with palaeoceanographic changes. Nomura (1991) observed that the major faunal changes were the increasing abundance of *Cibicidoides wuellerstorfi* and the decline of the *Burseolina* cf. *pacifica*- *Cibicidoides mundulus* assemblages at ~13 Ma at the Site 754. These changes coincided with diversity decreasing. The *Gavelinopsis lobatulus*- *Uvigerina proboscidea* assemblage increased in the earliest Pliocene ~5 Ma at Site 754.

According to Singh and Gupta (2010) at Hole 757B *Cibicides cicatricosus* and *Cibicides pseudoungerianus* disappeared, whereas *Stilostomella lepidula* showed a decrease in abundance in the early late Miocene during ~12-10 Ma, coinciding with a major decline in the population of *Oridorsalis umbonatus*. A major decrease in the abundance of *Stilosomella lepidula* occurred between 12-11 Ma which coincided with a major gradual increase of *Nuttalides umbonifera*. *Stilostomella lepidula* is a cosmopolitan taxon which prefer complicated ecological systems and its distribution still not clear (Singh and Gupta, 2010). According to Johnson et al. (2011) during the study of the two ODP sites of the subtropical Pacific Ocean (ODP Sites 1146, South China Sea; ODP Site 1237, southeast Pacific) they believe

that the relative abundance of elongate group taxa has not changed during the cooling period of the middle Miocene Climate Transition. They suppose that the environmental changes associated with the mid-Miocene global cooling did not affect the elongated group.

Nomura (1991) also observed decreasing *Cibicidoides mundulus- Epistominella umbonifera* assemblages at the Site 756 during the late early Miocene (~17.1 Ma), also the development of the *Uvigerina proboscidea* assemblage was earlier than the same assemblage at Site 754, which developed at around 7.3 Ma. According to Nomura (1991), faunal change may be related to palaeoceanographic changes. While the timing of the assemblage changes was not simultaneous at sites 754 and 756, these sites are located at different water depths. The deeper Site (756) may have a connection to the deeper water upwelling, while Site 754 is located at the centre of the flat crest of Broken Ridge which may be far from direct water upwelling.

On the Southern Kerguelen Plateau especially at sites, 744 and 738 *Epistominella exigua* dominates the bathyal to abyssal sediments during the late Miocene to Holocene. This species is considered a high productivity species associated with increased upwelling near the Antarctic convergence (Schroder-Adams, 1991).

Mackensen (1992) believed that the high productivity environments favoured the *Uvigerina hispidocostata* assemblages on the southern Kerguelen Plateau in the early Miocene. In the latest Miocene at Site 751 *Epistominella exigua* was a dominant species associated with the

Antarctic polar frontal zone and indicating the position of this site below the highly productive surface water masses (Mackensen, 1992).

Ramsay et al. (1998) believed that *Nuttalides umbonifera* and smooth-walled bolivinids abundances simultaneously increased in Atlantic, Mediterranean Sea and Indian Ocean sites between 19.5 and 16.5 Ma. According to Mackensen et al. (1990), *Nuttalides umbonifera* is typical of the middle Miocene interval on the Maud Rise and southern Kerguelen Plateau. The highest relative abundance of the smooth-walled bolivinids was seen at the Indian Ocean Site 237 however they are absent at Site 710, while no smooth-walled bolivinids were seen at the eastern Indian Ocean Sites 216 and 758 (Ramsay et al., 1998, Smart and Ramsay, 1995).

Ramsay et al. (1998) observed the different distribution of bolivinids in different water depths. The shallow to intermediate sites were characterised by coarse-walled bolivinids (Site 707), while in the intermediate to deep water sites (237,709) the smooth-walled bolivinids were observed. The smooth-walled bolivinides lately changed to three different species of *Streptochilus* (planktonic foraminifera) by Smart and Thomas (2007). *Nuttalides umbonifera* recorded their highest abundant in a deep-water site (710).

On the flat western side of the East Tasman Plateau at Site 1172 the benthic foraminifera assemblages were mainly dominated by *Cibicidoides mundulus*, and *Cibicidoides wuellerstorfi* in the uppermost Oligocene through lowermost upper Pliocene. *Melonis barleeanum* is dominated the Early Neogene, but it has much minor role than at sites 1168 and 1170 (Shipboard Scientific Party, 2001c).

During the early Miocene at Site 1171 in the East Tasman Plateau, the lower bathyal to abyssal water depths (~1500–2500 m) is characterised by the presence of *Cibicidoides mundulus* and *Nuttalides umbonifera*. In the Middle Miocene when the deposition of the sediments was in upper abyssal depths (~2000 –3000 m) *Epistominella exigua* dominated (Shipboard Scientific Party, 2001b). The percentage of *Nuttalides umbonifera* and *Epistominella exigua* increased at the DSDP sites 709 and 710 during around 14- 13 Ma. These species have peak abundance at the deepest Site 710 during about 11- 9 Ma (Smart et al., 2007).

1.4 Aims and Objectives

The current study focuses on the benthic foraminifera assemblage abundance and diversity fluctuations at three different localities (ODP holes 752A, 1139A and 1168A) in the Southern Indian Ocean during the Miocene. The main objective of this study is to interpret benthic foraminifera data assemblages to reconstruct palaeoceanography of the Broken Ridge (752A), Tasmanian Gateway (1168A) and Kerguelen Plateau (1139A) during the Miocene epoch. The assemblages will be investigated using additional quantitative techniques (clustering), diversity indices, calculating the Benthic Foraminifera Accumulation Rates (BFAR), and examine the foraminiferal test sizes, carbonate crash, biogenic blooms and also stable isotope analyses will be used to help reconstruct the environmental controls on the assemblage changes.

Major palaeoceanographic and paleoclimatic changes in this region during the Miocene represent a key of the global climatic evolution during the Miocene (Flower and Kennett, 1993). According to Flower and Kennett (1993) and Woodruff (1985), benthic foraminiferal

assemblages start to change in the late early Miocene, and this continues into the mid-Miocene in the Pacific and Atlantic. It is likely that physicochemical variations in the bottom water masses, such as changes in deep-water nutrients level and corrosivity related to surface water productivity, and deep water temperature fluctuations during the Miocene strongly affected the distribution of individual benthic foraminifera species during this time (Flower and Kennett, 1993).

Woodruff and Savin (1989) believed that global thermohaline circulation strongly affected by warm saline water influx to the Indian Ocean during the early Miocene. Tethyan Indian Saline Water (TISW) flowing in the northern Indian Ocean finally disappeared at around 14 Ma. The diminishing of the TSIW and formation of the North Atlantic Deep Water (NADW) before 14.5 Ma may have affected the abundance and distribution of benthic fauna in a different part of the world. The current study tries to understand the impact of different water masses and climate changes from the south-eastern Indian Ocean and the Southern Oceans on small sized (> 63 µm) benthic foraminifera assemblages during the Miocene Epoch.

Chapter Two

Site Descriptions and Methodologies

2.1 752A – Broken Ridge

Broken Ridge is 3500 m above the surrounding seafloor in the south-eastern Indian Ocean; it is an elongated plateau-like feature (Figure 2.1). Shallow water (<1,500m) sediments have accumulated on Broken Ridge since the mid-Cretaceous. These sediments record both the geological and oceanographic history of the mid-latitudes of the Indian Ocean (Rea et al., 1990).

Tectonically the Broken Ridge originated from the northern flank of the Kerguelen-Broken Ridge Plateau, this separated from the main part during the Eocene (Rea et al., 1990). Uplift of the Broken Ridge occurred at about 60 Ma by flexure that occurred in response to intra-plateau rifting. Seafloor spreading began after the rifting between both parts of the old plateau at the Southeast Indian Ocean Ridge around 42 Ma (Houtz et al., 1977, Rea et al., 1990).

According to Rea et al. (1990), the palaeoceanographic and paleoclimate history of the Broken Ridge was the main objective of ODP Leg 121 Drilling. As the position of the Broken Ridge is always above the calcium carbonate compensation depth (CCD), it allowed the deposition of fossiliferous calcareous sedimentary units. The upper Paleogene chalk and Neogene calcareous oozes are separated by an angular unconformity associated with Eocene rifting

from underlying, northerly dipping Cretaceous and lower Paleogene tuffs and limestone (Rea et al., 1990).

Four ODP sites (752, 753, 754 and 755) were drilled, located along a 21.2-km north-south transect, Extending across the shallow platform of Broken Ridge (1,100 m). The sedimentary record of these sites contains important evidence of volcanic activity, high biological productivity during Palaeocene and Miocene, Cretaceous-Paleogene boundary events at high southern latitudes, Eocene uplifting and erosion, sea-level change of the Oligocene and finally current winnowing of the Neogene (Rea et al., 1990).

2.1.1 Site & Core Description

Ocean Drilling Program (ODP) Site 752 (proposed Site BR-2) is near the crest of Broken Ridge, about 16 km north of the main southward-facing escarpment (Shipboard Scientific Party, 1989a) (Figure 2.1). Hole 752A is situated at a water depth of 1086.3 m (30°53.475'S, 93°34.652'E). The current study covered an interval of 79.7 m which includes latest Oligocene, the whole Miocene, and a part of the early Pliocene.

The advanced hydraulic piston corer (APC) and extended core barrel (XCB) systems were used to core 752A. The extended core barrel (XCB) system sheared off at 308 m below seafloor (mbsf) when it penetrated a very hard chert layer. The average core recovery was 70.6% (Shipboard Scientific Party, 1989a).

The recovery at this site is 436 m of Pleistocene through upper Maastrichtian sediments for both holes (752A and 752B). Two lithologic units were identified. The current hole (752A) is part of Unit-1, 112.9 m of foraminifer and nannofossil ooze of Pleistocene to late Eocene age; Unit II comprises a complete, 322.7-m-thick, chalk sequence of early Eocene to late Maastrichtian age (Table 2.1) (Shipboard Scientific Party, 1989a).

The recovery of Unit I is from 121-752A-1H to 121-752A-12X (0-112.9 mbsf), the upper part is composed mainly of foraminiferal ooze which represents nearly the top 45 m. The lower part of the succession is composed mainly of nannofossil-foraminifera or foraminifera-nannofossil ooze. The sediment colour ranges from alternations of white (10YR 8/2) to pale brown (10YR 8/3) in the first core, changed to the stark white, which is whiter than (10YR 8/1) through Core 121-752A-5H at 45 mbsf and grades down into a dark yellow-brown (7.5YR 7/6) in Cores 121-752A-9H through 121-752A-11H. Some shell fragments are found, including few cm diameters of bivalve shell which been observed in cores 121-752A-9H and 121-752A-10H (Shipboard Scientific Party, 1989a) (Figure 2.2).

2.1.2 Age-depth model & palaeodepth reconstruction

The age of the sediments in the current study was determined based on the first (FO) and last occurrence (LO) of seven nannofossil species. Recovery in the Cenozoic section is very good at 752A. Calcareous nannofossils within foraminifera and nannofossil oozes are abundant, with good preservation in Pliocene-Pleistocene sediments and moderate to poor in Miocene sections (Shipboard Scientific Party, 1989a).

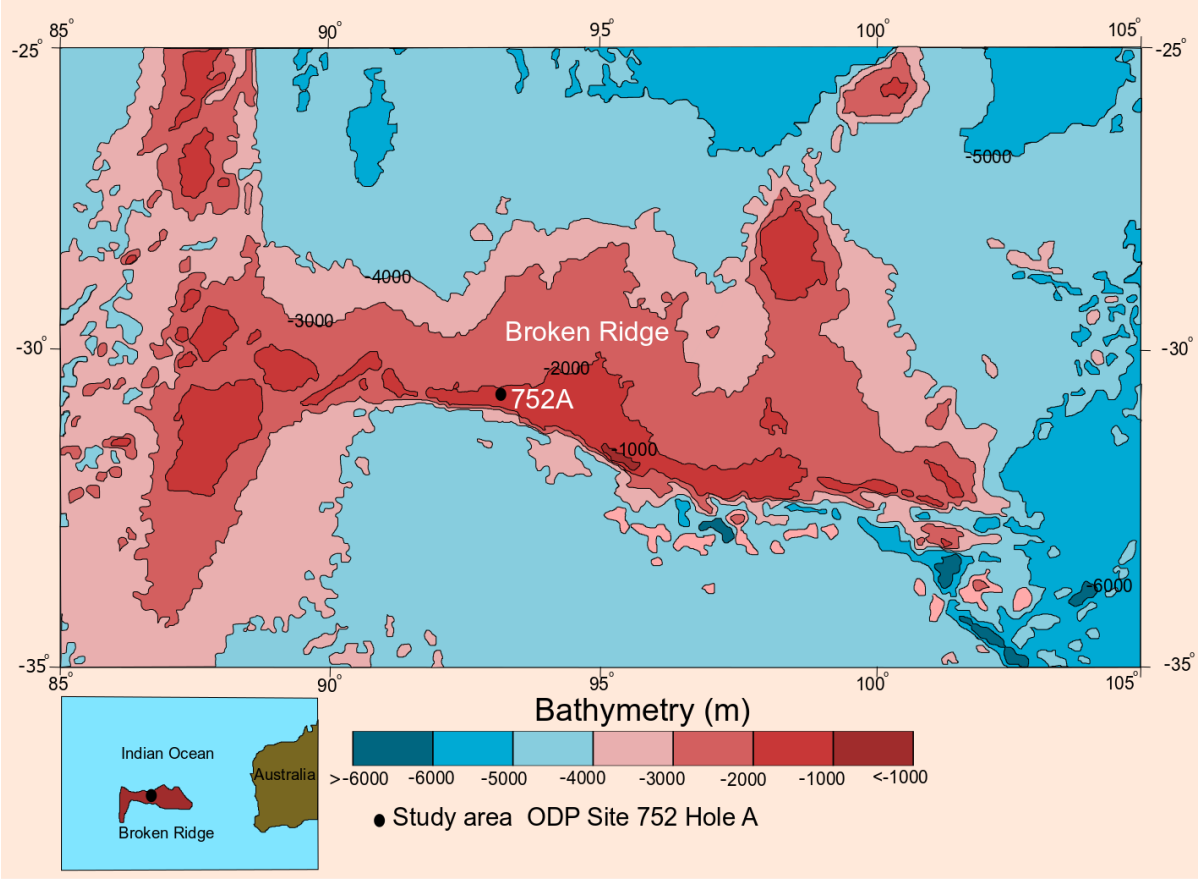


Figure 2. 1: Location map of the ODP studied Site 752 Hole A on the Broken Ridge. The contour lines represent the predicted bathymetry in metres (after Ingle et al., 2003).

Unit	Core Interval	Depth (mbsf)	Lithology	Age
I	1H-12X	0.00-112.90	Foraminifera/ nannofossil ooze	Pleistocene to late Eocene
IIA	13X-22X	112.90-209.80	Nannofossil/ calcareous chalk	Early Eocene to late Paleocene
IIB	23X-31X	209.80-288.70	Siliceous chalk	Late to mid Paleocene
IIC	32X-34X	288.70-317.60	Indurated chalk	Mid Paleocene to late Maastrichtian

Table 2. 1: Lithologic units at the Site 752 Hole A (After Shipboard Scientific Party, 1989a).

The zonation scheme of Okada and Bukry (1980) (Figure 2.2) was used by the Shipboard Scientific Party (1989a) to date the upper Neogene, but some problems were seen in middle and lower Miocene sediments due to poor preservation of the nannofossil assemblages and the strong overgrowth of the discoasters. At least two zones have been used and comparisons made between zonal assignments of the Miocene from the Broken Ridge to the Ninetyeast Ridge (ODP Site 756) to give a better precision (Shipboard Scientific Party, 1989a).

It has been noted that the Okada and Bukry (1980) Zone CN2 is missing in the lower Miocene section, which may be related to the presence of a hiatus (Shipboard Scientific Party, 1989a). The current study age-depth model was calculated depending on the calcareous nannofossils data used by Shipboard Scientific Party (1989a) as shown in Table 2.2, and the ages were revised by using ATNTS2012 in GTS2012 (Hilgen et al., 2012). The range of the index calcareous nannofossil and planktonic foraminifera species is shown in Figure 2.4 with their zones.

The age-depth model is plotted in Figure 2.3, and the age-depth relationship is determined for the current study based on the trend line equations which appear in the graphs (Figure 2.3). The sedimentation rates fluctuated from about 1 cm ka^{-1} in the Neogene to 3-4 cm ka^{-1} in the Paleogene-Maastrichtian (Shipboard Scientific Party, 1989a), while by using the same age model been created by them it has been observed that average sedimentation rate of current study Hole (752A) in Neogene and late Oligocene is 0.413 cm ka^{-1} (Table 2.3). The current study average rate of deposition is 0.44 cm ka^{-1}. The calculated age has been plotted versus depth and rate of sedimentation (Figure 2.5). It has been observed that the rate of the deposition is

changed in two different times, the first change is around 5.61 Ma and the second change is around 13.56 Ma.

The palaeodepth reconstruction is based on the 29 most abundant species from the late Oligocene to early Pliocene (Table 2.4). Bathymetric terminology in this study follows Van Morkhoven et al. (1986): inner shelf = 0–50 m, mid-shelf = 50–100 m, outer shelf = 100–200 m, upper bathyal = 200–600 m, mid bathyal = 600–1000 m, lower bathyal = 1000–2000 m, abyssal = 2000–6000 m. Palaeodepth interpretations of the most abundant species at 752A follows Van Morkhoven et al. (1986) and Holbourn et al. (2013). For *Uvigerina peregrina* and *Gavelinopsis lobatulus* Van Marle (1988) is used, and for *Ehrenbergina carinata* Eade (1967) is used.

According to Shipboard Scientific Party (1989a) the early Miocene to the late Pliocene interval, core 9H to 1H, the water depth is middle-lower bathyal. The palaeodepth of the late Oligocene to the early Miocene interval studied (core 10H) is upper bathyal based on the palaeodepth of the most abundant species such as *Planulina costa* and costate uvigerinids; these species are indicators of middle to upper bathyal depths.

2.1.3 Benthic Foraminifera

The late Oligocene and Neogene Benthic foraminifera are very well preserved. Pliocene-Pleistocene faunas are characterized by *Cibicidoides kullenbergi, Stilostomella lepidula, Planulina wuellerstorfi, Globocassidulina subglobosa, Gyroidina orbicularis, Pullenia bulloides, Oridorsalis umbonatus,* and nodosariid and dentalinid taxa (Shipboard Scientific Party, 1989a).

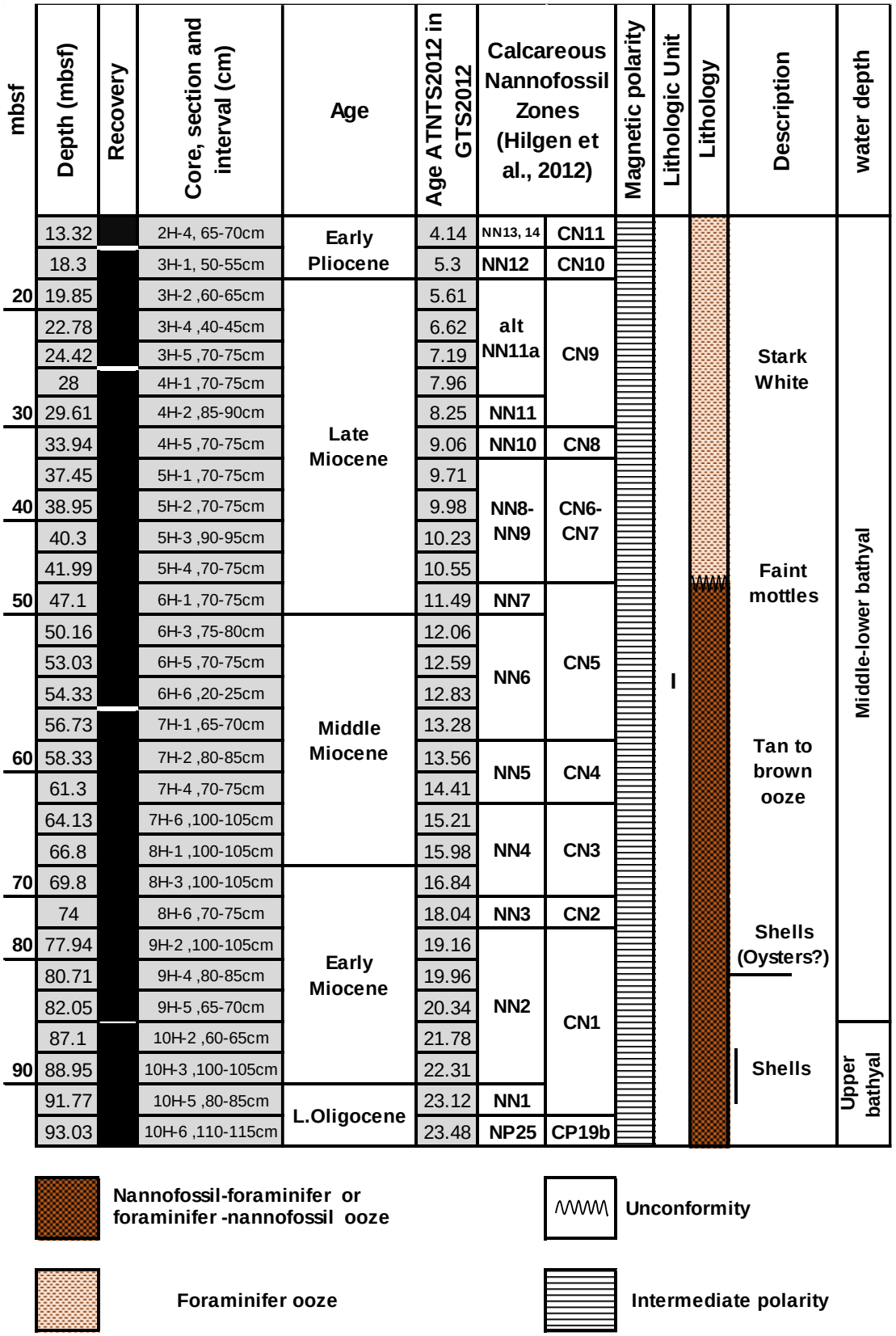


Figure 2. 2: Summary diagram of ODP Site 752 Hole A on the Broken Ridge, showing the recovery, age, nannofossil zones, magnetic polarity, lithology and water depth (After Shipboard Scientific Party, 1989a).

Species (Events)	Age (Ma) Original Data (Shipboard Scientific Party, 1989a)	Age (Ma) ATNTS2012 in GTS2012	Depth (mbsf)
LO *Discoaster brouweri*	1.90	1.93	4.30
LO *Reticulofenestra pseudoumbilica*	3.40	3.70	10.30
FO *Ceratolithus acutus*	5.00	5.35	19.10
FO *Amaurolithus primus*	6.40	7.42	25.10
LO *Sphenolithus heteromorphus*	14.30	13.53	58.10
FO *Sphenolithus heteromorphus*	17.10	17.71	73.10
LO *Reticulofenestra bisecta*	23.70	23.13	91.70

Table 2. 2: Age-Depth model depending on the range of abundant calcareous nannofossil species.

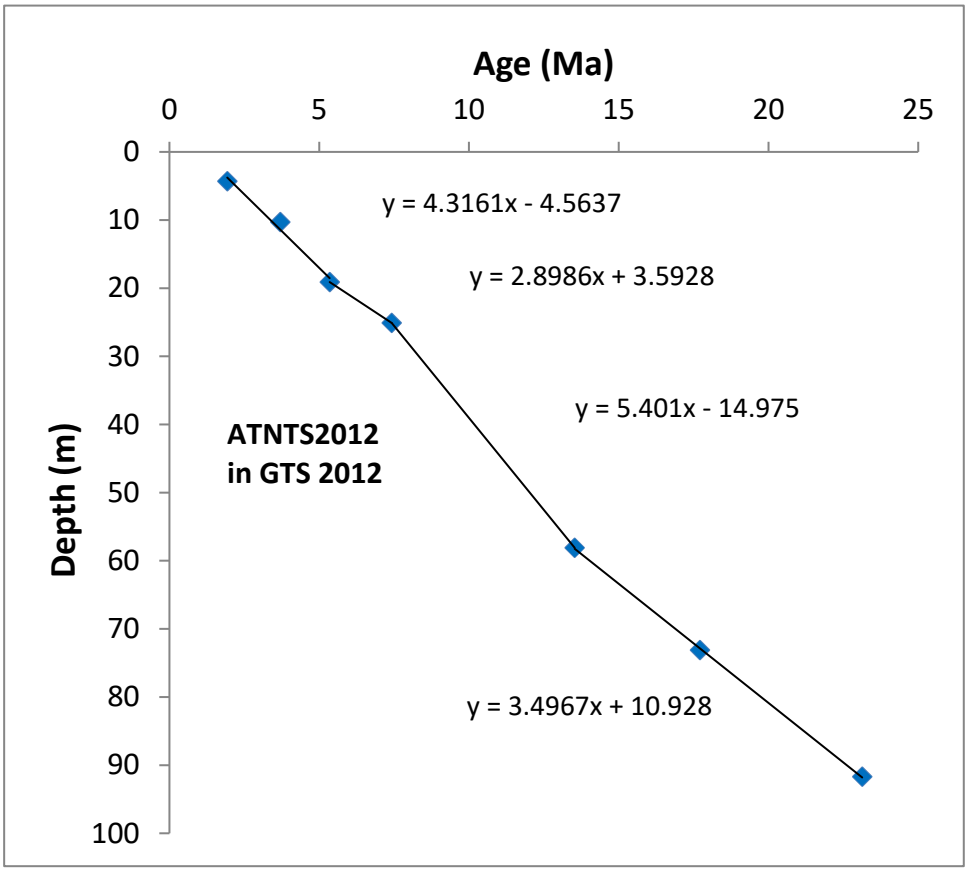


Figure 2. 3: Age-Depth model created from the original data (Shipboard Scientific Party, 1989a) using calcareous nannofossils bioevents and revised by ATNTS2012 in GTS2012.

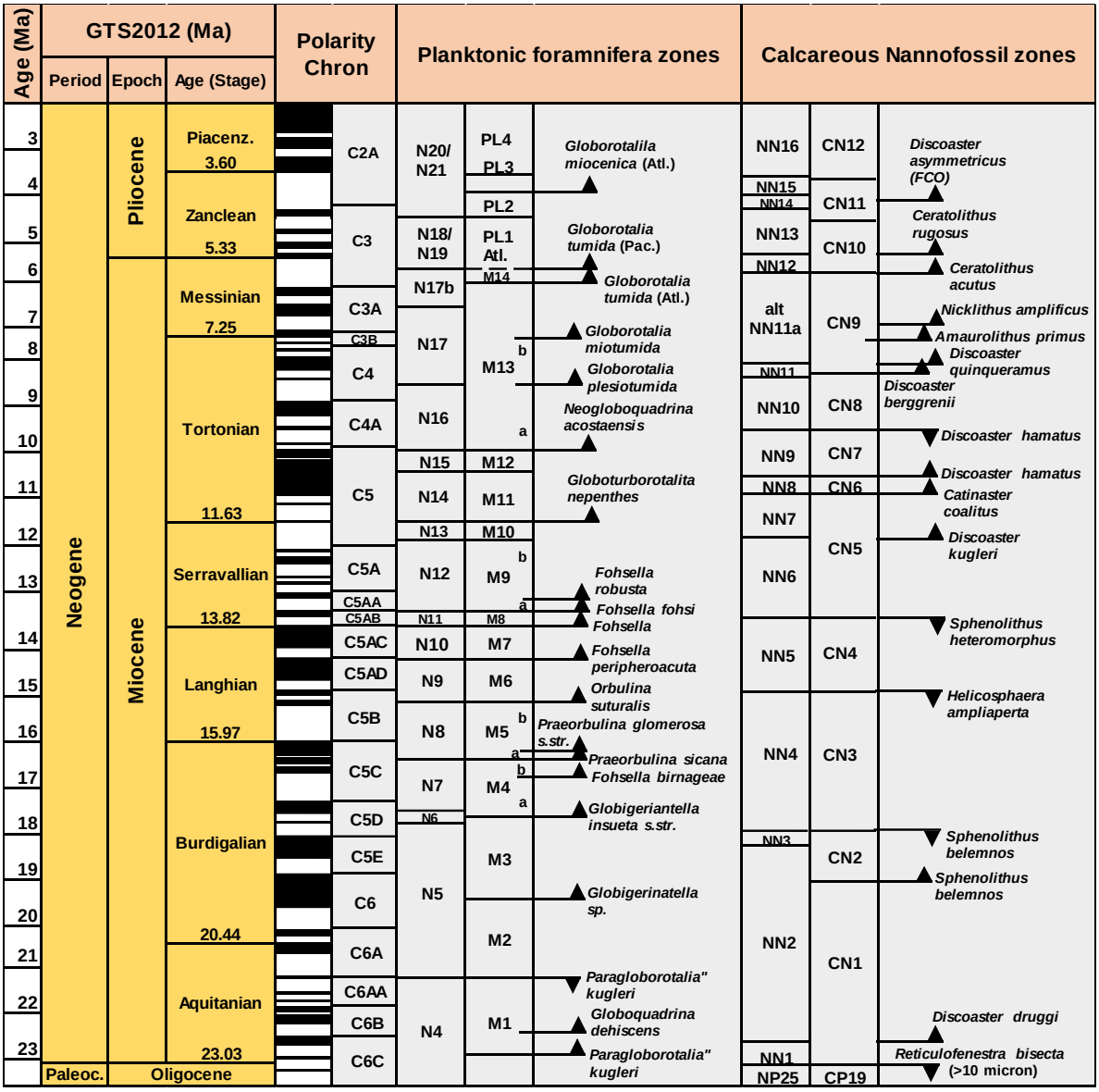


Figure 2. 4: Neogene stratigraphic subdivision, geomagnetic polarity, and standard zonation of planktonic foraminifera and calcareous nannofossils (After (Hilgen et al., 2012)).

Depth	Original Data (Ma) (Shipboard Scientific Party, 1989a)	rate of sedimentation cm ka^{-1}	ATNTS2012 in GTS 2012	rate of Sedimentation cm ka^{-1}
13.32	3.95	0.49	4.14	0.43
18.30	4.96	0.49	5.30	0.50
19.85	5.27	0.49	5.61	0.29
22.78	5.87	0.49	6.62	0.29
24.42	6.20	0.40	7.19	0.46
28.00	7.09	0.42	7.96	0.54
29.61	7.48	0.42	8.25	0.54
33.94	8.52	0.42	9.06	0.54
37.45	9.36	0.42	9.71	0.54
38.95	9.72	0.42	9.98	0.54
40.30	10.04	0.42	10.23	0.54
41.99	10.44	0.42	10.55	0.54
47.10	11.67	0.42	11.49	0.54
50.16	12.40	0.42	12.06	0.54
53.03	13.09	0.42	12.59	0.54
54.33	13.40	0.42	12.83	0.54
56.73	13.97	0.42	13.28	0.57
58.33	14.36	0.55	13.56	0.35
61.30	14.90	0.54	14.41	0.35
64.13	15.43	0.54	15.21	0.35
66.80	15.92	0.54	15.98	0.35
69.80	16.48	0.54	16.84	0.35
74.00	17.27	0.25	18.04	0.35
77.94	18.82	0.28	19.16	0.35
80.71	19.80	0.28	19.96	0.35
82.05	20.28	0.28	20.34	0.35
87.10	22.07	0.28	21.78	0.35
88.95	22.72	0.28	22.31	0.35
91.77	23.72	0.28	23.12	0.35
93.03	24.17	0.38	23.48	0.40

Table 2. 3: Age-Depth data of the current study of both original and revised ages after ATNTS2012 in GTS2012, with the rate of the deposition calculated from revised ages.

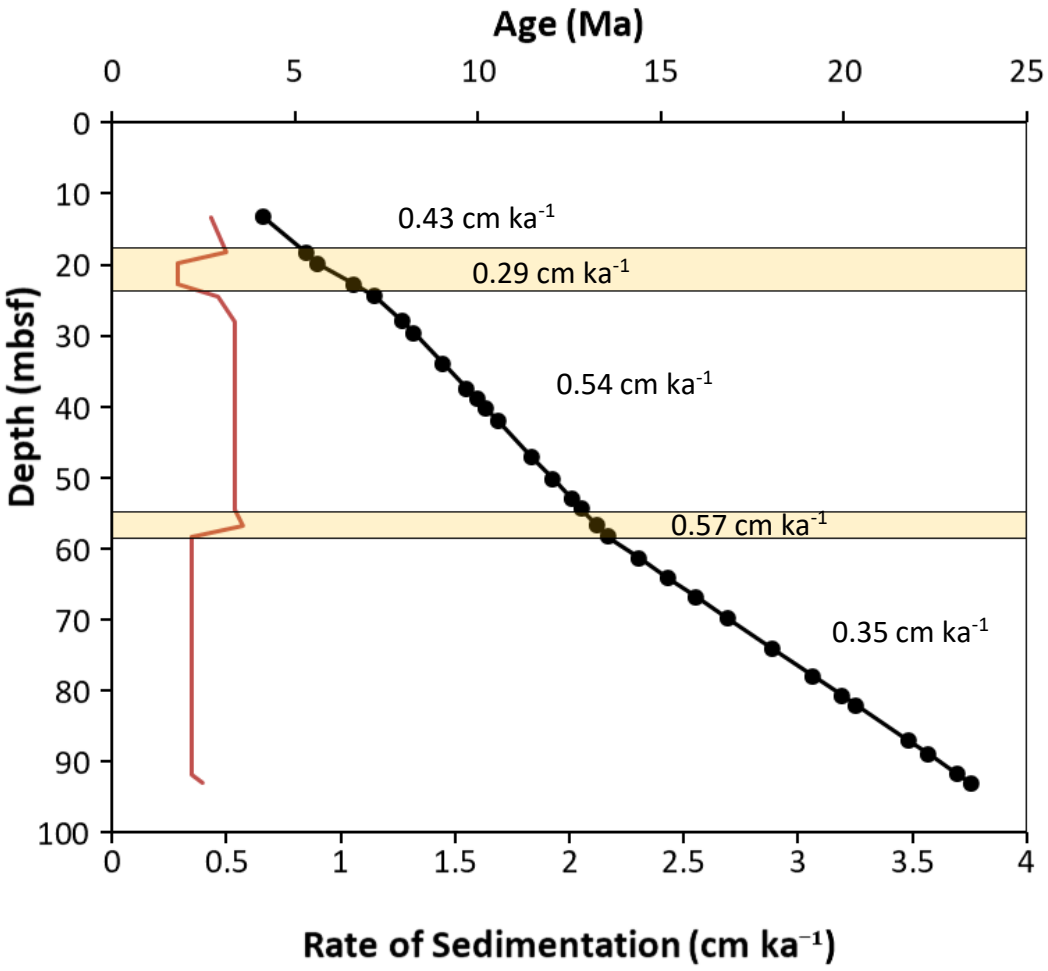


Figure 2. 5: Age-Depth plot and the rate of sedimentation (Site 752 Hole A). The black line represents the age-depth plot, while the red line represents the rate of sedimentation. The yellow boxes show the intervals of sedimentation rate changes.

Early Miocene faunas almost similar to the late Miocene fauna, because *Cibicidoides* and Stilostomillids appear as a common species in early Miocene. Species like *Lenticulina* have been found in Sample 121-752A-9H-CC, which have been associated and co-occurred with Globocassidulinids. These faunas are good indicators of the lower-middle bathyal environment. In the early Miocene *Martinottiella scabra* (agglutinated taxon) is also recorded (Shipboard Scientific Party, 1989a).

Benthic foraminifera species	Bathymetry
Amphicoryna scalaris	neritic to bathyal
Bolivina huneri	**bathyal to abyssal**
Bulimina truncana	middle to lower bathyal
Cibicidoides bradyi	bathyal to abyssal
Cibicidoides mundulus	bathyal to abyssal
Eggerella bradyi	bathyal to abyssal
Globocassidulina subglobosa	bathyal to abyssal
Gyroidinoides soldanii	bathyal
Nuttalides umbonifera	lower bathyal to abyssal
Oridorsalis umbonatus	Lower neritic to abyssal
Osangularia culter	middle to lower bathyal
Pullenia bulloides	bathyal to abyssal
Pullenia quinqueloba	neritic to abyssal
Siphonodosaria lepidula	**bathyal**
Sphaeroidina bulloides	**middle and upper bathyal**
Stilostomella subspinosa	bathyal to abyssal
Trifarina angulosa	Lower neritic to upper bathyal
Bulimina striata	upper to middle bathyal
Laticarinina pauperata	bathyal to abyssal
Uvigerina peregrina	**middle bathyal**
Cibicidoides wuellerstorfi	lower bathyal to abyssal
Planulina costata	**middle and upper bathyal depth**
Uvigerina auberiana	neritic to abyssal
Trifarina bradyi	Lower neritic to bathyal
Melonis barleeanus	bathyal
Epistominella exigua	lower bathyal to abyssal
Gavelinopsis lobatulus	middle bathyal
Siphouvigerina hispida	Upper middle bathyal
Ehrenbergina carinata	lower bathyal to abyssal

Table 2. 4: Benthic foraminifera species and their palaeodepths (bathymetry). Species bathymetry in bold represents the most abundant and indicative species for late Oligocene to early Miocene. Palaeodepth interpretations of the most abundant species follow Van Morkhoven et al. (1986) and Holbourn et al. (2013).

Late Miocene faunas are dominated by *Ehrenbergina carinata*, *Cibicidoides kullenbergi*, *Stilostomella lepidula*, *Planulina wuellerstorfi*, *Oridorsalis umbonatus*, *Pullenia bulloides*, and *Gyroidina soldanii*.

Many of the taxa in the current study have a long stratigraphical range except for species such as *Bolivina huneri* which appears only in the early Miocene. *Uvigerina peregrina* and *Planulina costata* range from the early to mid-Miocene. *Trifarina angulosa* is abundant in the mid-Miocene, and species such as *Melonis barleeanus*, *Epistominella exigua*, and *Gavelinopsis lobatulus* range from the mid-Miocene to early Pliocene. *Siphouvigerina hispida* ranges from the mid-Miocene to early late Miocene, and *Ehrenbergina carinata* from late Miocene to Pliocene.

2.2 Hole 1168A – Western Tasmania margin

The present western Tasmania margin as part of the east Gondwana supercontinent, until the separation of Australia from Antarctica during the Late Cretaceous through early Cenozoic. The early separation was from the Cretaceous through the middle Eocene, formed the Australo-Antarctic Gulf. This separation was associated with the northwest direction movement of the western Tasmania margin. The separation was also followed by a north-south movement that had less effect on the margin on the location of the studied site (Shipboard Scientific Party, 2001a). In the late Palaeocene/early Eocene the western terrane rifted away from Antarctica and underwent strong deformation as the Antarctic plate moved southward away from the Australian plate.

The Tasman Fracture Zone transform margin was shaped by shear motion, which continued until the early Miocene (chron 6B, 23 Ma) when the Southeast Indian Ridge axis cleared from the western edge of the South Tasman Rise (Rollet, 1997).

The present continental shelf around Tasmania is mostly non-depositional. The continental slope west of Tasmania slopes is at ~4°, from 200 to 4000 m. The continental rise situated at 4000– 4500 m, and the abyssal plain is generally 4500–5000 m deep. The slope is underlain by continental basement, shallow-marine sandstone and siltstone. The mudstone of Upper Cretaceous and Paleogene are widespread in the deep water west of Tasmania, underlying Oligocene to Holocene pelagic carbonates. The seismic interpretation shows that the basement is overlain by several kilometres of sediments (Shipboard Scientific Party, 2001a).

2.2.1 Site & Core Description

Oceanic Drilling Program (ODP) Hole 1168A is located in middle bathyal in water depth (2463 m) situated in the 4° slope of the western Tasmanian margin (70 km from the coast) in a 25 km-wide strike-slip basin between up-thrown northwest-trending ridges of Cretaceous rocks (Figure 2.6). The site was separated initially from the Pacific Ocean by the Tasman land bridge which was located at the eastern end of the restricted Australo-Antarctic Gulf.

The site lies north of the oceanographic Subtropical Front, 80 km southeast of Deep-Sea Drilling Project (DSDP) Site 282, is located in deeper water and on a structural high. Hole 1168A reached 883.5 mbsf with 98% recovery (Shipboard Scientific Party, 2001a).

Two advanced hydraulic piston corer/extended core barrel corer (APC/XCB) holes and the third hole with just the APC were used at Site 1168 (Shipboard Scientific Party, 2001a). The lithology of the hole varies, from the surface until a depth of 260 mbsf (Core 189-1168A-28X). It is dominated by calcareous biogenic components (nannofossils and foraminifers) of the mid-Miocene and younger (Lithostratigraphic Unit I), these are succeeded by 400 m of nannofossil siltstone, clayey chalk, and sandstone of early Miocene and Oligocene age (Unit II) and then 220 m of shallow-marine carbonaceous mudstone and sandstone (Units III–V) of the late Eocene. When the first appearance of siliciclastic clay-sized particles was observed they appear to associate with siliciclastic silty particles below 530 mbsf (Core 189-1168A-56X; (Shipboard Scientific Party, 2001a) (Figure 2.7).

Lithostratigraphic Unit I (0–260 mbsf) is subdivided into two subunits. The first subunit IA started from 0 (zero) to 45 mbsf, and the second subunit IB continues to 260 mbsf. The lithology of subunit IA is light greenish-grey foraminifer-bearing nannofossil ooze with minor calcareous turbidite sands and subunit IB is a white nannofossil ooze. Carbonate content in this unit has an average of 90 wt%, little alteration is seen in the calcareous microfossils, benthic foraminifera is present throughout the successions, dinoflagellates cysts are absent only in the mid-Miocene, and are common in the late Miocene. The age of Unit I based on microfossils is early mid-Miocene to Pleistocene. The average sedimentation rate is 1.65 cm ka^{-1}. The depositional setting of Unit I is middle bathyal with well-oxygenated bottom water (Shipboard Scientific Party, 2001a).

Lithostratigraphic Unit II (260–660 mbsf) consists of three subunits, and subunit IIA is 260 to 410 mbsf, Subunit IIB from 410 to 540 mbsf, and Subunit IIC from 540 to 660 mbsf. These three subunits are olive-grey become darker and more silty and clayey downward. The preservation of the calcareous microfossils is good with little alteration, they are abundant in the Miocene and moderately preserved in late Oligocene. Dinoflagellates and benthic foraminifers are common, radiolarians are uncommon, and diatoms are rarely recorded. The sedimentation rate is higher than the previous unit (Unit I), with an average sedimentation rate of 4.3 cm ka^{-1} through the Miocene and late Oligocene. The water depth is bathyal, and the bottom water oxygenation is variable. Subunit IIA is mainly clay-bearing nannofossil chalk and nannofossil claystone and average carbonate content of 40 wt%. Subunit IIB consists of nannofossil-bearing claystone and nannofossil claystone with an average carbonate content of 30 wt%. Subunit IIC consists of silty nannofossil chalk to nannofossil siltstone. Average carbonate content is 40 wt% (Shipboard Scientific Party, 2001a).

2.2.2 Age depth-Model & Palaeodepth

The age of the sediments in the current study have been determined based on the first (FO) and last occurrence (LO) of eleven nannofossil species, twelve planktonic foraminifera species and twenty seven geomagnetic polarity datums calculated by Stickley et al. (2004) and revised by ATNTS2012 in GTS2012 (Hilgen et al., 2012) (Table 2.5). An age-depth model was previously provided by Shipboard Scientific Party (2001a) where they calculated the boundaries of the Miocene depending on calcareous and siliceous microfossils. According to Stickley et al. (2004), the calculated age model gives linear sedimentation rate from the early Miocene of ~2 cm ka^{-1} decreasing onward from middle Miocene to a ~1.6 cm ka^{-1}.

McGonigal (2007) used the calcareous nannofossils to determine the age and placing the Miocene boundaries for the Site 1168 Hole A. According to McGonigal (2007), The Miocene was limited between samples 189-1168A-10H-2, 15 cm, and 47X-4, 68 cm and the Oligocene/Miocene boundary (CN1a/CP19) are placed at 439.94 mbsf between Samples 189-1168A-47X-4, 40 cm, and 47X-4, 68 cm.

The current study age models have been established depending on calcareous nannofossils, planktonic foraminifera and geomagnetic polarity datums from Stickley et al. (2004) these been revised by ATNTS2012 in GTS2012 (Hilgen et al., 2012) (Table 2.5).

The age-depth model is plotted in Figure 2.8, and the age-depth relationship is determined for the current study based on the trendline equations which appear in the graph (Figure 2.8).

The average rate of sedimentation for the Hole 1168A is 1.82 cm ka^{-1} (Table 2.6). The rate of the sedimentation is higher in two different intervals, first at around 9.6-10.3 Ma (5.67 cm ka^{-1}) and again at around 21.84-23.03 (6.68 cm ka^{-1}) (Figure 2.9).

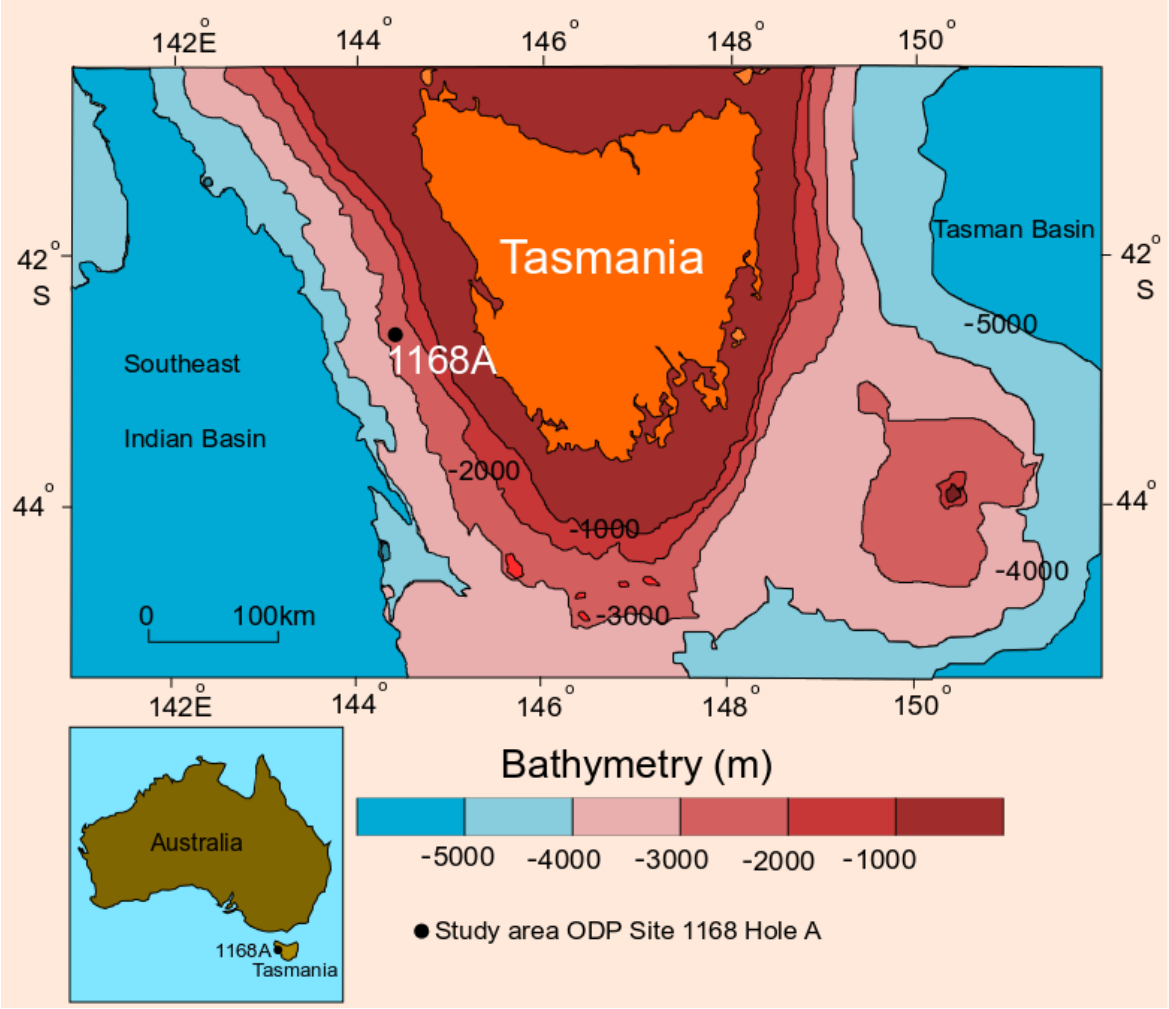


Figure 2. 6: Offshore Tasmanian region. Showing seafloor topography and topographic feature from 42°S to 44°S. Solid circle = ODP Site 1168 Hole A. Colour tones in scale bar are representing different bathymetry (after Shipboard Scientific Party, 2001a).

According to Gupta et al. (2004) due to increasing the Antarctic ice sheet volume at around 10- 8 Ma, the wind system strengthened, which increased the oceanic productivity. Paul et al. (2000) supposed that a large and short glacial maximum recorded at 22.95 and 21.1 Ma.

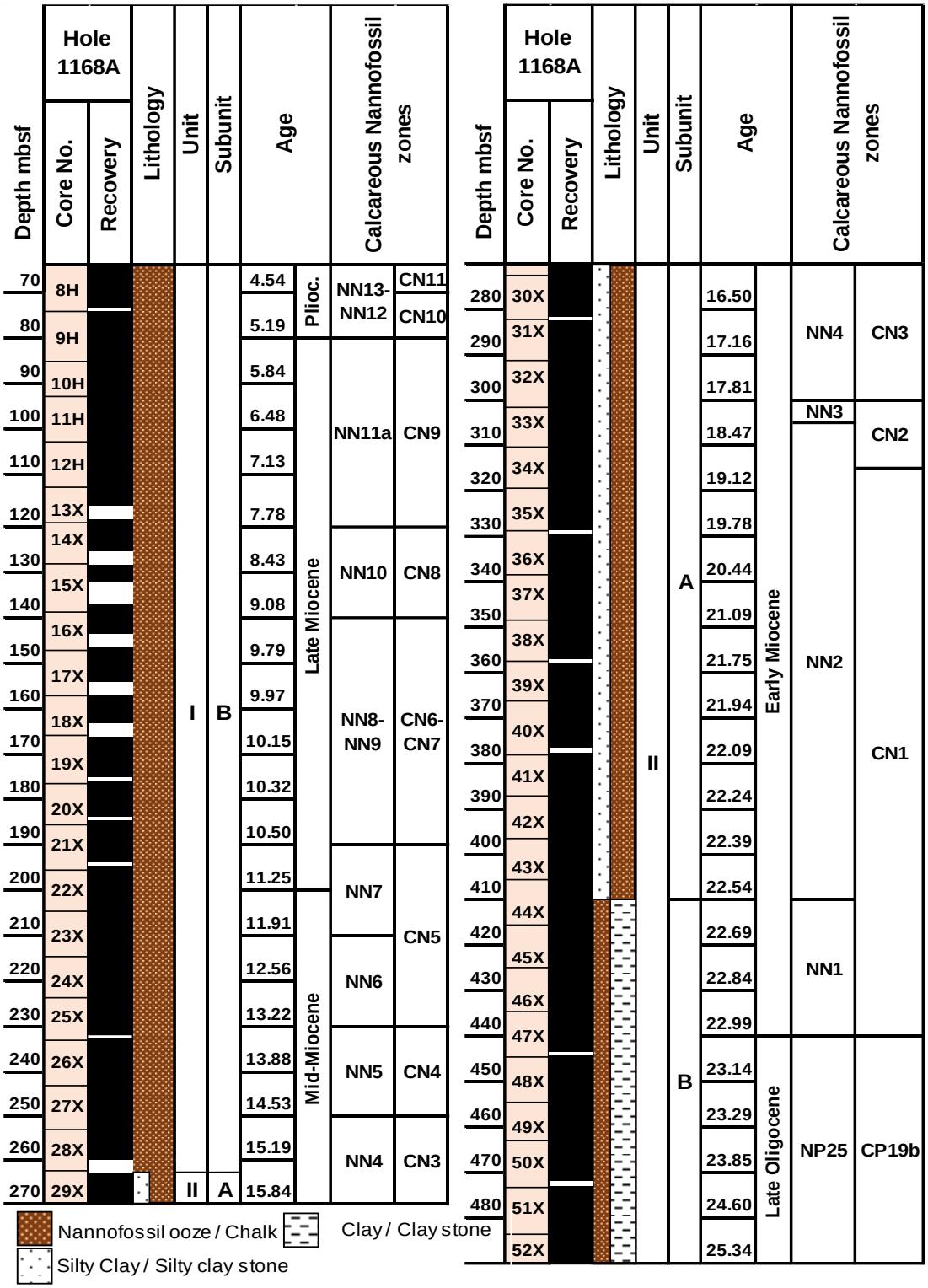


Figure 2. 7: Lithology and recovery of the Site 1168 Hole A, western Tasmanian margin, from depth 65- 488 mbsf. The age is revised by ATNTS2012 in GTS2012 (Hilgen et al., 2012). Calcareous nannofossil zones follow (Hilgen et al., 2012), (after Shipboard Scientific Party, 2001a).

2.2.3 Benthic Foraminifera

Late Oligocene has an abundant fauna with *Dentalina*, *Cibicidoides* spp., and siliceous agglutinated foraminifera representing well-oxygenated assemblages and gives bathyal (~400–2000 m) depth to the Late Oligocene sediments (Shipboard Scientific Party, 2001a). The Neogene benthic foraminifera assemblages are abundant, diverse and well preserved, characteristic of open marine settings , for instance *Valvulina pennatula* in late early Miocene to early mid-Miocene, *Cibicidoides wuellerstorfi* (~280–50 mbsf) in the late early Miocene to Pliocene, *Cibicidoides mundulus* in Miocene and early Pliocene and *Sigmoilopsis schlumbergeri* and *Melonis barleeanus* (Table 2.6) in the late Miocene and upward (Shipboard Scientific Party, 2001a).

The Neogene bathymetry is lower bathyal/upper abyssal (~1000–2500 m) according to previously mentioned abundant benthic foraminifera assemblages (Shipboard Scientific Party, 2001a). The oxygen level increase from very poorly oxygenated to well-oxygenated, which coincided with the paleodepth increases from Eocene to Neogene. Based on the benthic foraminifera assemblages the paleodepth is neritic to upper bathyal (~100–200 m) in the upper Eocene, and it deepens to lower bathyal/upper abyssal (~1000–2500 m) in the Neogene (Table 2.6) (Shipboard Scientific Party, 2001a).

Age	Age (Ma) Stickley et al. (2004)	Events	ATNTS2012 in GTS 2012	Mean Depth (m)	Depth errors(m)
Pliocene	4.70	(FO) *Globorotalia crassaformis* (F)	4.31	76.12	1.50
	5.23	(LO) *Triquetrorhabdulus rugosus (Orthorhabdus rugosus)* (N)	5.28	84.21	0.75
Miocene	7.40	(FO) *Amaurolithus primus* (N)	7.42	110.71	0.75
	7.80	(LO) *Minylitha convallis* (N)	8.68	129.01	0.75
	5.80	(LO) *Globoquadrina dehiscens* (F)	5.92	130.42	1.50
	7.80	(FO) *Globorotalia cibaoensis* (F)	9.45	132.39	0.47
	8.10	(FO)*Globorotalia juanai* (F)	9.69	140.02	1.50
	9.40	(FO) *Minylitha convallis* (N)	9.76	152.70	0.75
	11.40	(LO) *Paragloborotalia mayeri* (F)	10.47	188.02	1.50
	11.90	(LO)*Cyclicargolithus floridanus* (N)	12.12	197.81	0.75
	12.70	(LO) *Calcidiscus premacintyrei* (N)	11.24	221.51	0.75
	14.00	(LO) *Globorotalia peripheroronda* (F)	13.80	224.60	0.42
	13.20	(LCO) *Cyclicargolithus floridanus* (N)	13.28	236.21	0.75
	13.52	(LO) *Sphenolithus heteromorphus* (N)	13.53	242.21	0.75
	15.10	(FO) *Orbulina suturalis* (F)	15.10	255.27	1.46
	16.30	(FO) *Praeorbulina curva* (F)	16.28	264.91	1.50
	16.29	Onset C5Cn.1n (M)	16.27	272.20	0.00
	16.33	Termination C5Cn.2n (M)	16.30	276.70	0.00
	16.49	Onset C5Cn.2n (M)	16.47	279.00	0.00
	16.56	Termination C5Cn.3n (M)	16.54	282.10	0.00
	16.73	Onset C5Cn.3n (M)	16.72	287.40	0.00
	17.30	(LO) *Catapsydrax dissimilis* (F)	17.54	288.54	2.93
	17.28	Termination C5Dn (M)	17.24	292.20	0.00
	18.20	(FO) *Sphenolithus heteromorphus* (N)	17.71	293.81	0.75
	17.62	Onset C5Dn (M)	17.53	296.50	0.00
	18.30	(LO) *Sphenolithus belemnos* (N)	17.95	299.56	0.50
	18.28	Termination C5En (M)	18.06	307.00	0.00
	18.50	(FO) *Globorotalia praescitula* (F)	18.26	307.17	2.66

Table 2. 5: Age-Depth model data for Hole 1168A based on the ranges of calcareous nannofossil species, planktonic foraminifera and geomagnetic polarity datum.

Age	Age (Ma) Stickley et al. (2004)	Events	ATNTS2012 in GTS 2012	Mean Depth (m)	Depth errors (m)
Miocene	19.20	(FO) *Sphenolithus belemnos* (N)	19.03	313.91	0.75
	18.78	Onset C5En (M)	18.52	315.00	0.00
	19.05	Termination C6n (M)	18.75	321.20	0.00
	20.13	Onset C6n (M)	19.72	334.60	0.00
	20.52	Termination C6An.1n (M)	20.04	339.50	0.00
	21.40	(LO) *Tenuitella munda* (F)	20.78	341.11	1.50
	20.73	Onset C6An.1n (M)	20.21	341.50	0.00
	21.00	Termination C6An.2n (M)	20.44	343.70	0.00
	21.32	Onset C6An.2n (M)	20.71	346.70	0.00
	21.77	Termination C6AAn (M)	21.08	349.80	0.00
	21.86	Onset C6AAn (M)	21.16	351.10	0.00
	22.15	Termination C6AAr.1n (M)	21.40	351.80	0.00
	22.25	Onset C6AAr.1n (M)	21.48	353.50	0.00
	22.46	Termination C6AAr.2n (M)	21.66	358.40	0.00
	22.49	Onset C6AAr.2n (M)	21.69	359.00	0.00
	22.59	Termination C6Bn.1n (M)	21.77	359.90	0.00
	22.75	Onset C6Bn.1n (M)	21.94	366.00	0.00
	22.80	Termination C6Bn.2n (M)	21.99	371.30	0.00
	23.07	Onset C6Bn.2n (M)	22.27	386.20	0.00
	23.20	(FO) *Globoquadrina dehiscens* (F)	22.50	409.48	1.83
Oligocene	24.12	Onset C6Cn.3n?	23.30	462.60	0.00
	24.73	Termination C7n.1n?	24.00	472.00	0.00

Table 2. 5: Continued

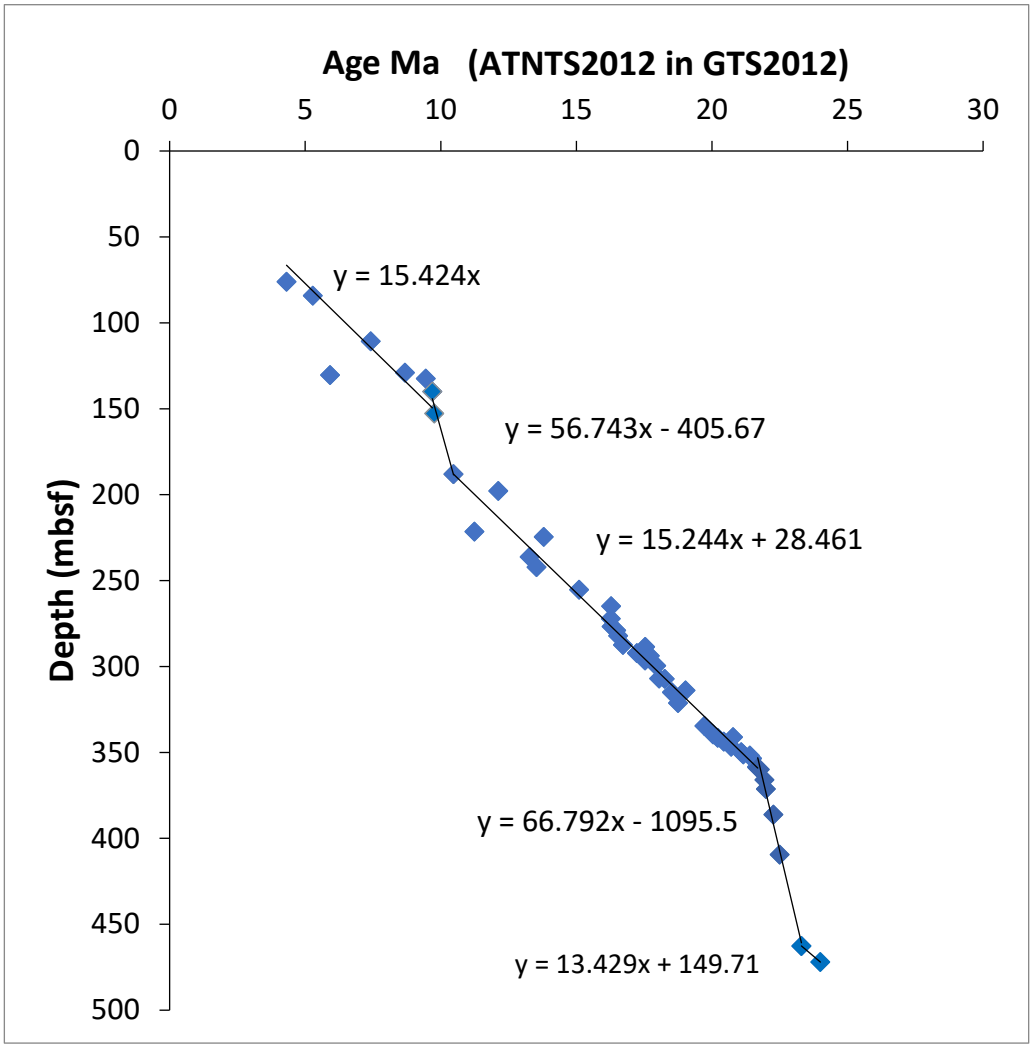


Figure 2. 8: Age-Depth model for Hole 1168A created from Stickley et al. (2004) using calcareous nannofossils bioevents, planktonic foraminifera and geomagnetic polarity datum and revised by ATNTS2012 in GTS2012 (Hilgen et al., 2012).

Depth (m.)	Age (Ma) ATNTS2012 in GTS2012	Rate of Sedimentation cm Ka^{-1}	Paleodepth (Shipboard Scientific Party, 2001a)	Benthic foraminifera assemblages
65.30	4.23	1.54	lower bathyal to upper abyssal (~1000–2500 m)	*Sigmoilopsis schlumbergeri* *C. mundulus* + C. wuellerstorfi *Melonis barleeanus*
77.31	5.01	1.54		
85.60	5.55	1.54		
99.70	6.46	1.54		*Cibicidoides mundulus* — *C. wuellerstorfi*
103.05	6.68	1.54		
112.20	7.27	1.54		
123.45	8.00	1.54		
130.36	8.45	0.84		
140.20	9.62	5.67		
151.30	9.82	5.67		
163.70	10.03	5.67		
171.70	10.18	5.67		
180.10	10.32	5.67		
186.70	10.44	1.67		
197.35	11.08	1.52		
208.74	11.83	1.52		
222.67	12.74	1.52		
226.11	12.97	1.52		
230.64	13.26	1.52		
236.03	13.62	1.52		
242.05	14.01	1.52		
248.63	14.44	1.52		
256.67	14.97	1.52		*Vulvulina pennatula*
265.06	15.52	1.52		
276.06	16.24	1.52		
288.66	17.07	1.52		
296.70	17.60	1.52		
304.60	18.12	1.52		
310.95	18.53	1.52		
320.25	19.14	1.52		
337.33	20.26	1.52		*Cibicidoides mundulus* (well oxygenated)
347.05	20.90	1.52		
352.00	21.22	1.86		
363.55	21.85	6.68		
369.99	21.94	6.68		
383.97	22.15	6.68		
390.60	22.25	6.68		
423.72	22.75	6.68		
442.85	23.03	6.68		
457.62	23.25	2.05	bathyal (~400–2000 m)	
470.22	23.87	1.34		
488.10	25.20	1.34		

(Average= 1.82)

Table 2. 6: Age-Depth data for Hole 1168A with revised ages after ATNTS2012 in GTS2012, with the rate of the deposition of each depth calculated from revised age and paleodepth depending on benthic foraminifera assemblages (Shipboard Scientific Party, 2001a).

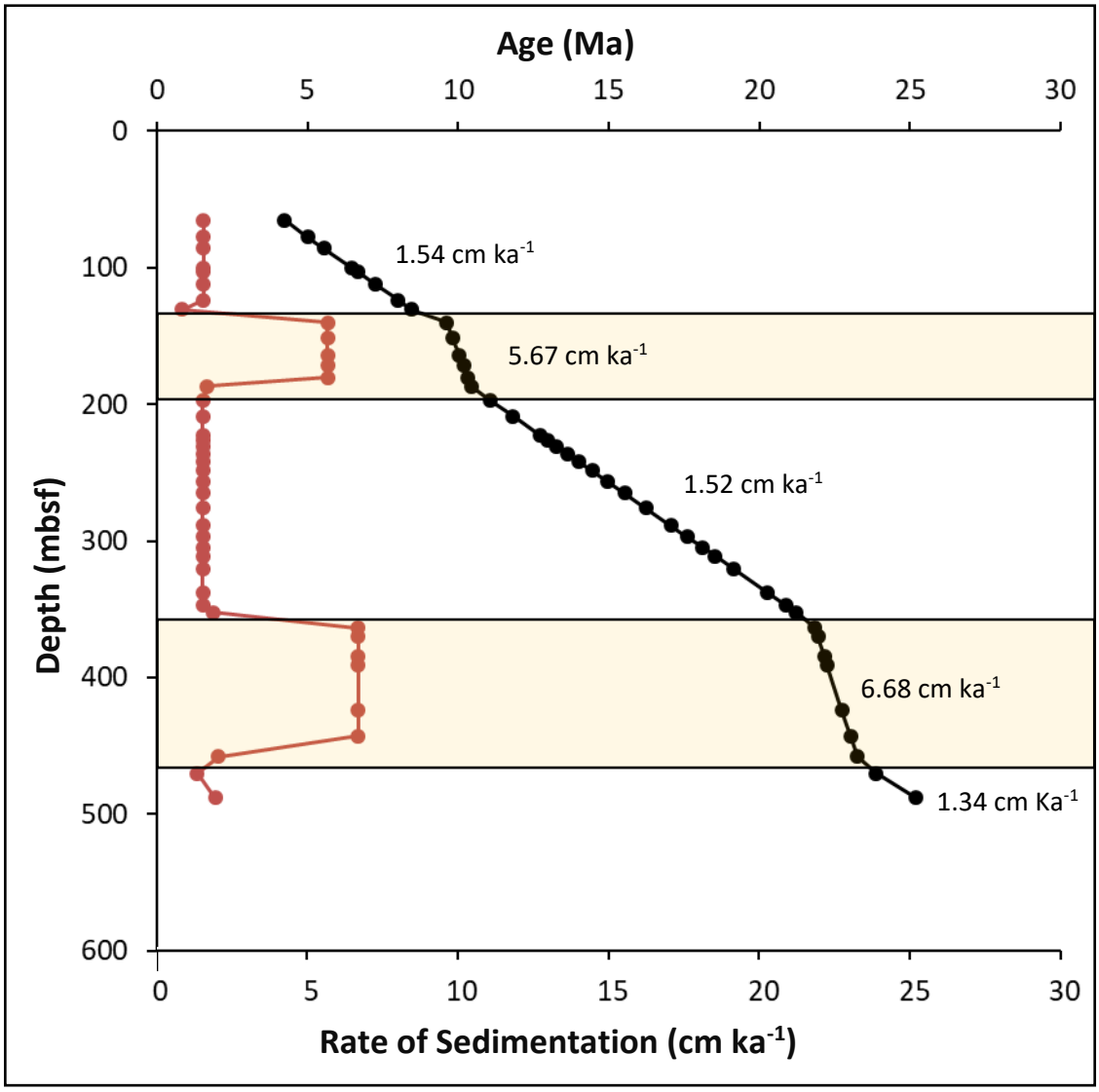


Figure 2. 9: Age-Depth plot and the rate of sedimentation (Site 1168 Hole A). The black line is the age-depth plot, while the red line is the sedimentation rate. The yellow boxes show the rapid change in the rate of sedimentation in two different range of times.

2.3 1139A – Skiff Bank (Kerguelen Plateau)

Site 1139 is situated on the Skiff Bank (Leclaire Rise), ~350 km west-southwest of Kerguelen Archipelago at a water depth of 1415 m (Figure 2.10) (Shipboard Scientific Party, 2000). Skiff Bank is close to the northern Kerguelen Plateau (NKP), and it also has a similar structure and bathymetrically continuous with (NKP) (Schlich et al., 1998). Duncan and Storey (1992) suggested that Skiff Bank is the current site of the Kerguelen hot spot, but a thick sedimentary cover (hundreds of meters) in the Skiff Bank dispute against the idea that it could be entirely formed during the Holocene volcanism. The age of the Skiff Bank's igneous crust and its relation with northern Kerguelen Plateau (NKP) have not yet been fully established, however the northern Kerguelen Plateau (NKP) is believed to be Cenozoic, forming around ~40 Ma when the Southern Indian Ridge separated the Broken Ridge and Kerguelen Plateau (Shipboard Scientific Party, 2000).

2.3.1 Site & Core Description

The current study covered nearly 168m of latest Oligocene and early to mid-Miocene and early late Miocene. Rotary coring continued at the Hole 1139A to a depth of 694.2 mbsf. From the lower 233 m of the hole altered volcaniclastic rocks, basalts, and few beds of sedimentary were recovered. The upper part of the hole (above the igneous basement) consist of ~383 m calcareous claystone and chalk, and at the top and bottom, they are intercalated with thin intervals of calcareous ooze and calcareous chalk. These sediments overlie thin sandy packstones (<10m) and ~ 77m of grainstone. Five sedimentary lithologic units were covered

in the upper part (0-461.7m) of the hole (1139A) (Shipboard Scientific Party, 2000) and only two of the units are covered in the current study (late Oligocene and early late Miocene).

The first unit (Unit I) covers 47.5 m between 1R-1, 0 cm, to 5R-CC, 25 cm (early Pleistocene-early Miocene). The top three cores of the unit are composed of calcareous ooze; they are soupy and were highly disturbed during drilling, which makes an accurate determination of the thickness and stratigraphic limits between beds difficult. Based on the abundance of diatoms, Unit I has divided into two subunits (Figure 2.11). The major gap between early Pleistocene to middle Miocene is marked by the lithology changes between cores 1139A-2R and 3R.

Subunit 1A (1R-1, 0 cm- 2R-CC, 19 cm; 0–19.00 mbsf) is composed of light grey foraminifer- and diatom-bearing nannofossil ooze (middle-early Pleistocene). Thin beds of disturbed white foraminifer-bearing nannofossil ooze (1R-3, 48–95 cm; 2R-1, 28–53 cm; 2R-1, 98–136 cm; and 2R-2, 47–85 cm) are part of the Subunit 1A. The carbonate content ranged from 64 to 75 wt%. Small pebbles and basaltic sand grains were found scattered in this subunit. The base of the Subunit IA is marked by a major gap (Shipboard Scientific Party, 2000).

Subunit IB (3R-1, 0 cm, to 5R-CC, 25 cm; 19.00–47.50 mbsf) is composed of foraminifer-bearing nannofossil ooze (middle-early Miocene), downward colour gradation of this subunit has changed from white to very light grey to dark brown and light greenish-grey. The lower part is gradational. The Core 3R is mainly composed of foraminifera-bearing, diatom bearing nannofossil ooze. Both sponge spicules and clay minerals are present in Core 5R. The

carbonate content of the subunit ranged from 74 to 83 wt%. A few basalt pebbles and other volcanic clasts have been seen in Section 3R-1, traces of glauconite and burrows have been seen distributed through the Cores 4R and 5R (Shipboard Scientific Party, 2000).

Unit II (6R-1, 0 cm, to 40R-5, 92 cm: 47.50-380.72 mbsf) ranged from late Oligocene to middle Miocene. This unit is comprising most of the sedimentary section (333m), composed of interbedded grey to greenish-grey nannofossil bearing clay and claystone and nannofossil-bearing ooze and chalk. In the upper part of the unit (47.5–170 mbsf, Cores 6R through 18R) the colour ranges are from dark greenish-grey to greenish-grey. In the lower part, the colour is grey interbedded with the light grey of several thin intervals (170–380.72 mbsf, Cores 18R through 40R). The sediments become gradually indurated with depth, and it became very hard by 100–110 mbsf (Cores 11R and 12R), and they classified as claystone and chalk.

Most of the sedimentary intervals between 8R-1, 0 cm to 10R-CC, 19 cm (66.5–95.1 mbsf) are composed of diatom bearing, nannofossil-bearing clay and ooze. The sediments of Unit II are highly burrowed, traces like *Zoophycos* and *Chondrites* have been seen in the sediments. The average carbonate content in this unit is 44 wt%, and it fluctuates in the succession, reflecting that the sediments are nannofossil clay or claystone with interbeds of nannofossil ooze or chalk, nannofossil-bearing clay or claystone, and rare claystone. Carbonate rich intervals are seen above Core 9R (<70mbsf), between 18R and 25R (160–230 mbsf), and below Core 36R (>340 mbsf) (Shipboard Scientific Party, 2000).

2.3.2 Age depth-Model & Palaeodepth

Age determination is based on the calcareous nannofossil ranges and magnetostratigraphy (Shipboard Scientific Party, 2000) (Table 2.7). An age model has been established using planktic foraminifera (Shipboard Scientific Party, 2000) and calcareous nannofossil datums (Persico et al., 2003) these are also compared with (Reusch, 2002) (Table 2.7) and ages revised using ATNTS2012 in GTS2012 (Hilgen et al., 2012) (Table 2.8).

The age model for the current study has been established depending on calcareous nannofossils, planktonic foraminifera these been revised by ATNTS2012 in GTS2012 (Hilgen et al., 2012) (Table 2.9).

The age-depth model is plotted in Figure 2.12, and the age-depth relationship is determined for the current study based on the trendline equations which appear in the graphs (Figure 2.12).

The average rate of sedimentation at the Site 1139 Hole A is 2.58 cm ka^{-1} (Table 2.9). The rate of sedimentation from 19.30 to 33.75 (mbsf) is 0.30 cm ka^{-1} and from the depth 48.21 until 145.25 (mbsf) the rate increases very rapidly with to a high rate of sedimentation (2.32 cm ka^{-1}), while the highest rate of sedimentation (7.06 cm ka^{-1}) is recorded from 156.71 to 186.6 (mbsf) (Figure 2.13). The derivation of terrigenous clastic deposits and high pelagic input from the exposed volcanic edifice In the Skiff Bank had affected the high sedimentation rates at 1139A (Shipboard Scientific Party, 2000).

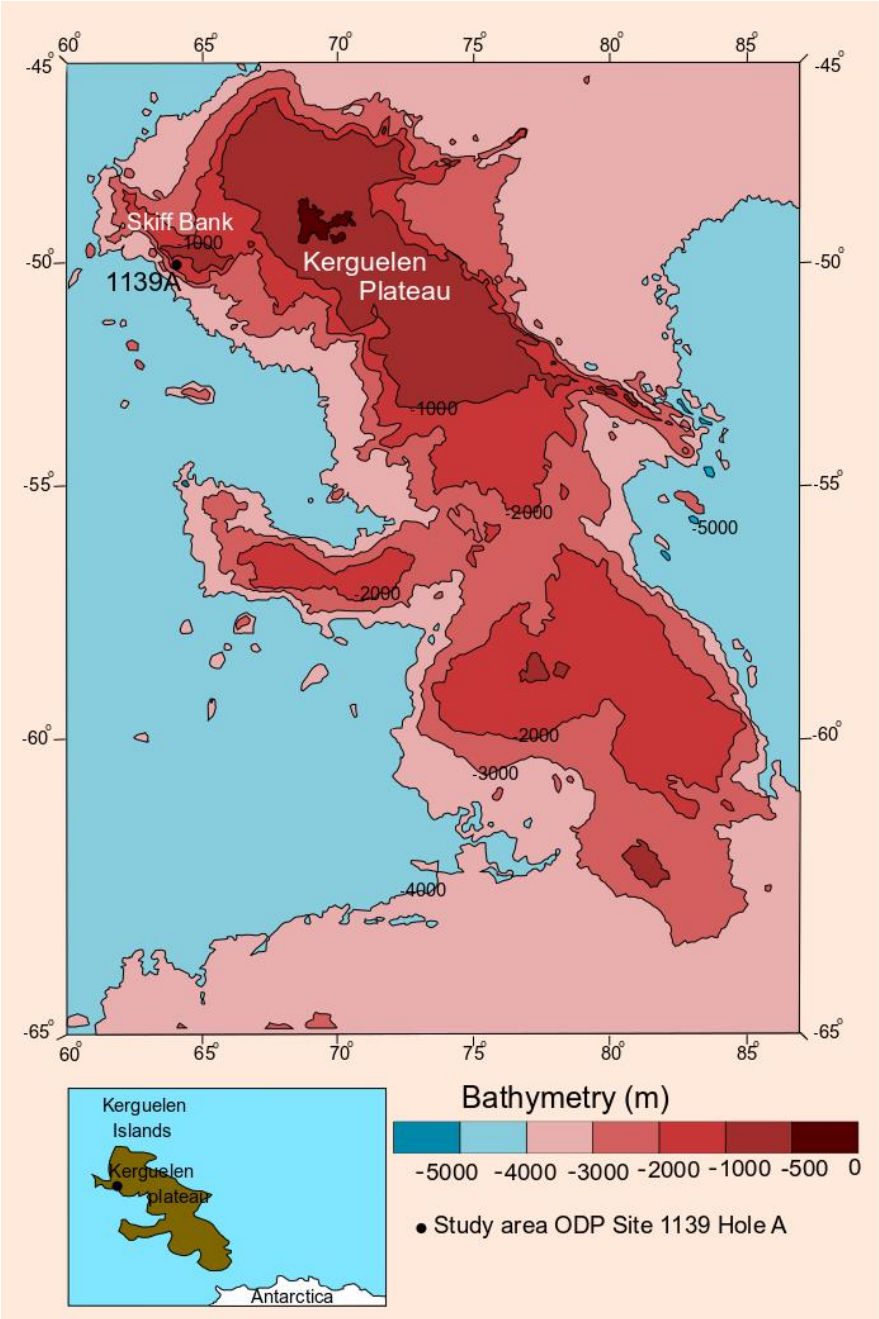


Figure 2. 10: Location map of the studied area, the contour line is predicted bathymetry in meters below the seafloor. The solid circle is the position of the studied site at Skiff Bank in Kerguelen Plateau (after Ingle et al., 2003).

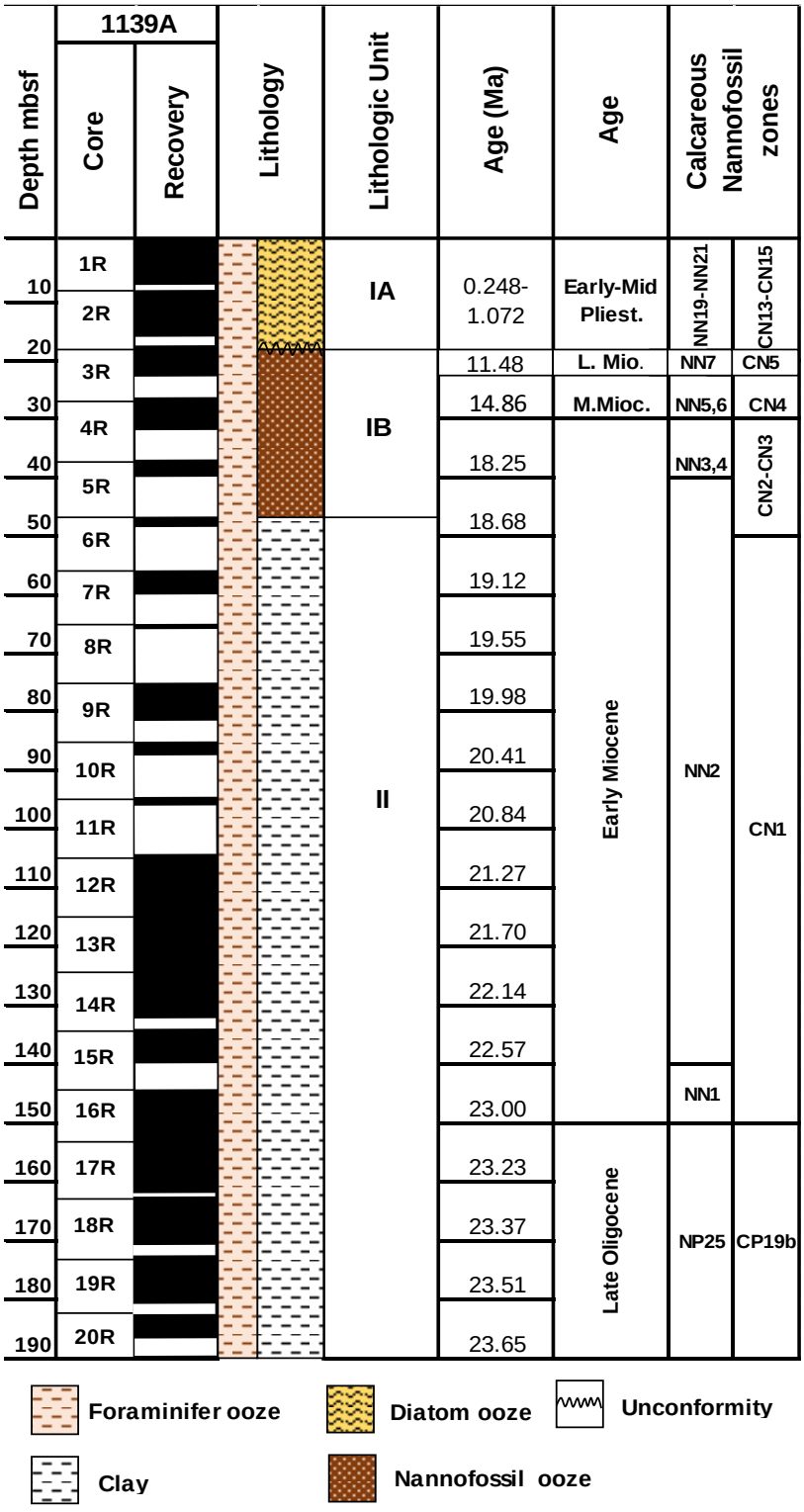


Figure 2. 11: Stratigraphic section of the Hole 1139A showing core recovery, lithology, lithologic units and ages of units revised by ATNTS2012 in GTS2012 (Hilgen et al., 2012), with nannofossil zones (after Shipboard Scientific Party, 2000).

Core	Datum	Type	Age (Ma)	Depth (mbsf)	Age
3R-CC	CN5a/CN3	Nannofossil	15.00-16.00	24.00	early middle Miocene
8R-CC	CN2-CN1	Nannofossil			mid-early Miocene
19R-CC	LO *Reticulofenestra bisecta*	Nannofossil	24.00	179.75	latest Oligocene
21R-CC	LO *Zygrhablithus bijugatus*	Nannofossil	26.20	200.25	late Oligocene

Table 2. 7: Depths and ages of calcareous nannofossils to find the chronology of Site 1139, established by Shipboard scientific Party, (2000) in Reusch (2002).

Events	Age ATNTS2012 in (GTS 2012) (Ma)	Depth (mbsf)
T *Cyclicargolithus floridanus* (N)	12.12	15.93
T *Cocolithus miopelagicus* (N)	10.62	19.25
T *Globoconella praescitula* (F)	13.73	24.38
B *Calcidiscus macintyrei* (N)	13.36	32.50
B *Globoconella miozea* (F)	16.70	34.77
B *Globoconella praescitula* (F)	18.26	40.16
T *Reticulofenestra bisecta* (N)	23.13	153.05
T *Zygrablithus bijugatus* (N)	23.76	197.55

Table 2. 8: Established age-depth of Site 1139A using planktic foraminifera (F) (Shipboard Scientific Party, 2000) and nannofossil datums (N) (Persico et al., 2003) and revised using ATNTS2012 in GTS2012 (Hilgen et al., 2012).

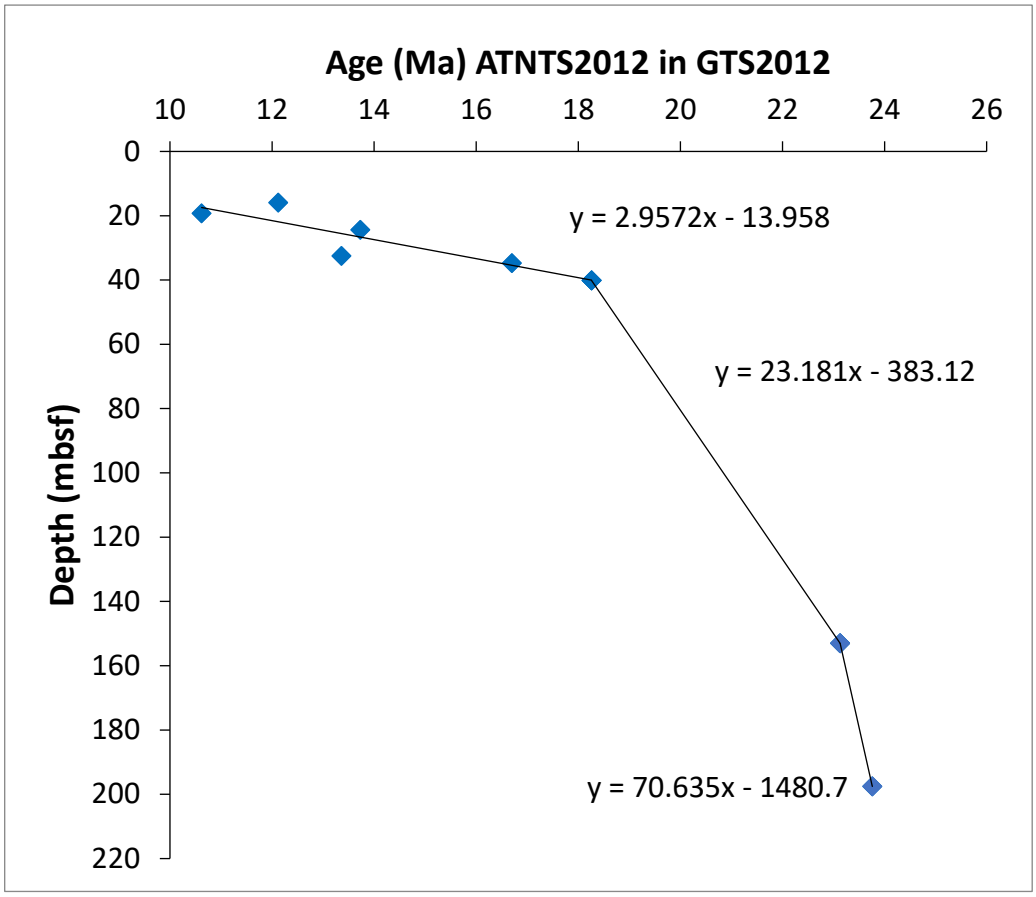


Figure 2. 12: Age-Depth model created from the original data using calcareous nannofossils and planktonic foraminifera bioevents and revised by ATNTS2012 in GTS2012 (Hilgen et al., 2012).

Palaeobathymetry at Site 1139 is determined depending on benthic foraminifera abundance in Oligocene, which is sparse and low and found in different depths at the current Site (Reusch, 2002). Oligocene benthic foraminifera species are two groups each indicate a different bathymetry. According to Reusch (2002) the bathyal (200-2000 m) to upper abyssal (2000-3000 m) species are *Astrononion pusillum, Bulimina macilenta, Cibicidoides bradyi, Cibicidoides dickersoni, Cibicidoides eocaenus, Laticarinina pauperata, Melonis barleeanum, Nonion havanense, Osangularia mexicana, Planunlina renzi,* and *Sphaeroidina bulloides*, while

the most common bathyal (200-2000 m) species are *Planulina costata, Planulina renzi, Rectuvigerina multicostata, Uvigerina mexicana,* and *Uvigerina spinulosa. Cibicidoides praemundulus and Laticarinina pauperata* are most abundant at >1000 m, and they are recorded throughout the current Oligocene samples. From these data Reusch (2002) established the paleobathymetry of the Oligocene at Site 1139 Hole A, which is estimated at 1000-2000 m due to the sparse benthic foraminifera, and the fact that assemblages of the current Site are similar to those identified from latest Eocene-Oligocene at the sites 747 and 748 (Mackensen and Berggren, 1992, Reusch, 2002). The water depth of Site 747 is 1695 mbsf, and Site 748 is 1287.5 mbsf which are close to a water depth of the current Site (1139A). According to Schlich and Wise Jr (1989), the paleodepth of Site 747 is lower bathyal to upper abyssal for the Oligocene and early Miocene.

High abundance of many species during early Miocene to early late Miocene such as *Cibicidoides mundulus*, *Cibicidoides wuellerstorfi*, *Globocassidulina subglobosa*, *Cibicidoides bradyi*, *Nuttalides umbonifera*, *Epistominella exigua*, *Oridorsalis umbonatus*, indicate bathyal to abyssal depths and species like *Sphaeroidina bulloides*, *Gavelinopsis lobatulus* and *Uvigerina peregrina* are indicative of middle to upper bathyal depths (Table 2.4). The paleodepth of the current study during early to early late Miocene may be of middle to lower bathyal depending on the species mentioned above. The bathymetry of the Site 1139 Hole A is, therefore, bathyal from the late Oligocene to mid-Miocene (Shipboard Scientific Party, 2000).

Depth (m.)	Age (Ma) ATNTS2012 in GTS2012	Rate of Sedimentation cm ka^{-1}	Paleodepth	Common Benthic foraminifera assemblages
19.30	11.25	0.30	Middle to lower bathyal	*Cibicidoides mundulus*, *Cibicidoides wuellerstorfi*, *Globocassidulina subglobosa*, *Cibicidoides bradyi*, *Nuttalides umbonifera*, *Epistominella exigua, Oridorsalis umbonatus*, *Sphaeroidina bulloides*, *Gavelinopsis lobatulus*, *Uvigerina peregrina*
21.50	11.99	0.30		
23.82	12.78	0.30		
28.90	14.49	0.30		
31.05	15.22	0.30		
33.75	16.13	0.30		
39.21	17.98	1.43		
48.21	18.61	2.32		
58.11	19.03	2.32		
60.45	19.14	2.32		
66.95	19.42	2.32		
80.39	20.00	2.32		
87.45	20.30	2.32		
95.45	20.65	2.32		
106.91	21.14	2.32		
111.60	21.34	2.32		
121.20	21.76	2.32		
129.15	22.10	2.32		
135.95	22.39	2.32		
138.41	22.50	2.32		
145.25	22.79	2.95		
156.71	23.18	7.06	Lower bathyal	*Astrononion pusillum, Cibicidoides bradyi, Planulina costata, Planulina renzi*
163.46	23.28	7.06		
174.21	23.43	7.06		
186.60	23.60	7.06		

(Average=2.58)

Table 2. 9: Age-Depth data of the current study revised ages after ATNTS2012 in GTS2012, with the rate of the sedimentation of each depth calculated from revised age and paleodepth depending on benthic foraminifera assemblages from the current study and Reusch (2002).

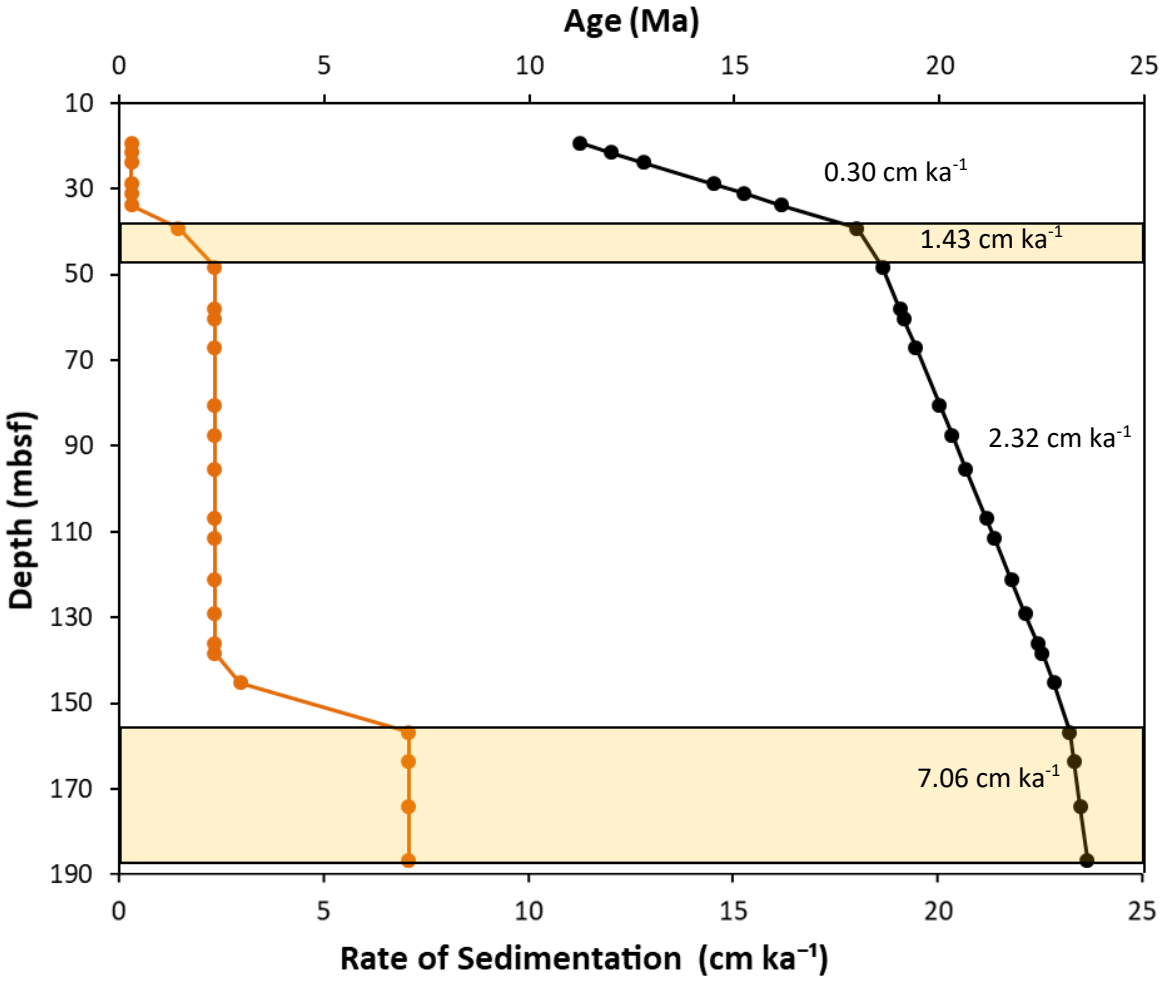


Figure 2. 13: Age-Depth plot and rate of sedimentation (Site 1139 Hole A). The black line is the age-depth plot, while the orange line indicates the sedimentation rate. The yellow boxes indicate two periods of change in the sedimentation rate. The upper box shows the steep change, while the lower box shows the highest rate of sedimentation.

2.3.3 Benthic Foraminifera

Benthic foraminifera have not been mentioned in the initial report even though there are many highly abundant species, especially in late early Miocene and early to mid-Miocene intervals. The Oligocene assemblages were of low abundance; some species were used to determine the paleo-depth which have been previously mentioned (Reusch, 2002).

2.4 Methodologies

2.4.1 Sample preparations

Ninety-seven (97) samples from the latest Oligocene, Miocene and early Pliocene were processed by using > 63 µm sieve. The core samples were firstly dried in the oven at 40 C °, and then all the samples were weighed (dry weight) and processed to get a size of > 63 µm. The dry samples were soaked in distilled water then washed (> 63 µm) to disaggregate and dried in the oven at 40 C °.

Thirteen (13) samples at 1168A and sixteen (16) samples at 1139A were disaggregated by using a freeze-thaw method, especially those samples which were hard to disaggregate by water. Twenty (20) samples at 1168A and seventeen (17) samples at 1139A were disaggregated (1168A) by using diluted hydrogen peroxide (H_2O_2) then all samples were washed by using > 63 µm sieve and dried. The dried samples were split by a splitter to get different fractions (see Appendices F, H & J). For each sample, one fraction or more were used to pick an aliquot of 300 to more than 300 benthic foraminifera specimens. During the picking of thirty samples (30) at 752A, 268 species were identified and from picking forty-two (42) samples at 1168A, 331 species were identified, while during the picking of twenty-five (25) samples at 1139A, 224 species were identified.

2.4.2 Dendrogram, diversity and rarefaction curves

All data of ninety-seven (97) samples of the studied sites (752A, 1168A and 1139A) were examined using PAST software (PAST 3.25) to plot diversity, dendrogram and rarefaction

curves (Hammer et al., 2001). The dendrogram was made by using the Bray-Curtis similarity index, Unweighted Pair-Group Average (UPGMA), stratigraphically constrained (Figures 4.1, 4.6 & 4.11).

2.4.3 Benthic foraminifera accumulation rate

Benthic foraminifera accumulation rate is expressed as number of specimens /cm^2 per ka.; this is useful for sea-floor organic flux estimation (Herguera and Berger, 1991) and was calculated as follows:

BFAR (number of specimens/ cm^2 per ka) = BF * LSR * DBD
BF= number of benthic foraminifera per gram of dry sediment.
LSR= linear sedimentation rate (cm ka^{-1}).
DBD= dry bulk density of sediment (g/cm^3).

The dry bulk density of the Site 752A (See Appendix F) was calculated from the Initial Reports (Shipboard Scientific Party, 1989a). The calculation of some intervals was stopped due to an error from the range between 65-110 mbsf (Shipboard Scientific Party, 1989a). These uncalculated intervals are recalculated depending on the DBD average values of shallower intervals than 65 mbsf and deeper ranges below 110 mbsf.

The dry bulk density at 1168A was calculated from the Initial Reports (Shipboard Scientific Party, 2001a) (See Appendix H). The dry bulk density was calculated for most samples based on the values of the same cores and sections in the initial report. While the dry bulk density of the eighteen samples between 17X-3 to 52X-4 were calculated depending on the mean

value of the nearest sections to these samples, for instance, the density of the sample 17X-3 is calculated by taking the mean density value of 17X-2 and 17X-4 in the initial report.

Dry bulk density of the Site 1139A (See Appendix J) was calculated from the initial report (Shipboard Scientific Party, 2000). Dry bulk density (DBD) for the 3R-1, 3R-2 and 20R-4 calculated from the mean value of the nearest sections to these samples.

2.4.4 Correlation Coefficient and significant value:

Correlation coefficient and significant values are calculated using Microsoft excel 2016. Correlation coefficient directly calculated using the insert function, while significant values determined from data analysis through using regression analysis tool.

2.4.5 Test sizes

Five different species are used to examine the change of the test size during the late Oligocene and the Neogene at the Sites 752A, 1168A and 1139A (Figures 5.1- 5.5). The selected species are representing the most abundant species at the study sites. The test sizes have measured by taking the maximum diameter of each specimen under a stereoscopic microscope (GXM XTL3101) in the University of Birmingham, Geology Department. The specimens magnified to the limit where each grid of the objective lens give 25 µm that is why the difference between each size is 25 µm (See Appendices L- P).

2.4.6 Carbonate Mass Accumulation Rates:

Carbonate mass accumulation rates ($MAR_{carbonate}$; g cm^{-2} ka^{-1}) are calculated based on carbonate content (%), linear sedimentation rate (LSR; cm ka^{-1}) and dry bulk densities (DBD). To calculate $MAR_{carbonate}$ firstly $MAR_{bulk\ sediments}$ (g cm^{-2} ka^{-1}) should be calculated by using the following equation:

$MAR_{bulk\ sediments} = LSR * DBD$

Then the following equation will use to calculate $MAR_{carbonate}$:

$MAR_{carbonate} = (CaCO_3\%/100) * MAR_{bulk\ sediments}$

Carbonate content (%) derived from the initial reports at all studied Sites (752A, 1168A and 1139A). In some intervals, the carbonate content (%) of closest depths to the current study samples is used.

Chapter Three

This chapter has done by the contribution of Ian Boomer and Kirsty Edgar in abstract, introduction and systematic descriptions

Latest Oligocene to earliest Pliocene deep-sea benthic foraminifera from ODP Sites 752, 1168 and 1139 southern Indian Ocean.

Dana Ridha[1], Ian Boomer[1] & Kirsty Edgar[1]
[1]Earth Sciences, GEES, University of Birmingham, Edgbaston, B15 2TT, UK

Correspondence to: Ian Boomer (i.boomer@bham.ac.uk)

Abstract. Deep-sea benthic foraminifera provide important markers of environmental conditions in the deep-ocean basins where their assemblage composition and test chemistry are influenced by ambient physical and chemical conditions in bottom-water masses. However, all foraminiferal studies must be underpinned by robust taxonomic approaches. Although many parts of the world's oceans have been examined, over a range of geological timescales, the Neogene benthic foraminifera from the southern Indian Ocean has only been recorded from a few isolated sites. In this study, we have examined 97 samples from Neogene sediments recovered from three ODP Sites in the southern Indian Ocean (752, Broken Ridge; 1139, Kerguelen Plateau; 1168, West Tasmania) that cover a range of palaeolatitudes and water depths to examine the impact of known global climatic shifts on the deep oceans in this region. More than 200 species of benthic foraminifera were recorded at each site and, despite their geographic and bathymetric separation, the most abundant taxa were similar at all three sites. Many of these species range-through from late Oligocene to early Pliocene demonstrating relatively little faunal turnover of the most abundant taxa during the key palaeoclimatic shifts of the Miocene. We illustrate and document the occurrence of the 52

most-abundant species (i.e. those with >1% abundance) encountered across the three study sites.

3.1 Introduction

The Neogene (Miocene & Pliocene, 23.03-2.58 Ma) can be informally subdivided into an early warm interval and late cool interval (Flower and Kennett, 1993). Superimposed on this long-term cooling is the Mid-Miocene climatic optimum (MMCO) between ~15-17 Ma, marking the warmest interval of the Neogene (Zachos et al., 2001). Cooling following the MMCO culminated at ~13-14 Ma in major growth of the East Antarctic Ice Sheet (EAIS). Further cooling coincided with increasing intensification of Antarctic deep-water formation and growth of the AIS and Greenland Ice Sheet (Flower and Kennett, 1993, 1994, 1995).

Profound palaeoclimatic and palaeoceanographic changes in the Neogene drove progressive and significant turnover of deep-sea benthic foraminiferal communities from the so-called Transitional fauna characterising the late Oligocene-early Miocene to the late Neogene fauna of the late Miocene, and finally the establishment of recognisably modern assemblages in the mid-Pleistocene (Jones, 1994, Kaiho, 1994). The first major transitional interval occurred in the early-middle Miocene, between ~13-17 Ma (Kaiho, 1994), spanning the onset of the MMCO and subsequent East Antarctic Ice Sheet growth, and associated changes in water mass character and upwelling intensity (Woodruff, 1985). Further changes in species abundance occur ~8-10 Ma, in the late Miocene. Finally, the last global extinction of benthic foraminifera (~20% of deep-sea genera) occurred in the late Pliocene-mid Pleistocene (Hayward et al., 2012) and is variously attributed to increasing ocean productivity and intensification of low

oxygen zones, and changes in the food type and supply, due to the expansion of the Antarctic and later Northern Hemisphere ice sheets and global cooling (Hermoyian and Owen, 2001, Gupta et al., 2004, Smart et al., 2007).

Superimposed on this long-term global pattern of benthic foraminifera assemblage change are distinct basinal and latitudinal differences in the timing of certain events. For instance, the global decline in deep-sea benthic foraminifera species abundance and richness occurs much earlier (late Oligocene-Miocene) in the Southern Ocean, than in the Indian Ocean (late Miocene; Hayward et al., 2012). However, responses in the Indian Ocean remain relatively poorly constrained. The present study aims to expand our understanding of the spatial and temporal distribution of the most abundant benthic foraminifera from the deep-sea Miocene sediments of this region.

Previous records of Miocene benthic foraminifera from the central and southern Indian Ocean are largely single-site reports with a focus on palaeoceanographical interpretations though some provide a useful illustration for comparison with the present study. Boersma (1990) reported benthic foraminifera from twelve ODP sites from Leg 115 across the central Indian Ocean, where quantitative studies of the benthic foraminifera indicated faunal separation at intermediate, deep, and abyssal water depths from the late Oligocene onwards and hence the development of a more strongly vertically stratified ocean. Nomura (1991) systematically described the most abundant Oligocene to Pleistocene benthic foraminifera species and assemblage changes at ODP Sites 754 (Broken Ridge) and 756 (Ninetyeast Ridge) in the eastern

Indian Ocean, linking them with palaeoceanographic changes and noting, for example, a major faunal change at ~13 Ma.

There have been two studies focussing on the Kerguelen Plateau. Schroder-Adams (1991) investigated middle Eocene to Holocene benthic foraminifera from Sites 736, 738, and 744 on the Kerguelen Plateau (Figure 1), describing and illustrating many species. Significant faunal changes (and species replacements) were noted in the middle Eocene, late Eocene/early Oligocene, middle Miocene and late Miocene. Mackensen (1992) quantitatively studied benthic foraminiferal assemblages from the lower Miocene through to upper Pleistocene interval from ODP Site 747 (Central Kerguelen Plateau) and Sites 748 and 751 (Southern Kerguelen Plateau).

Gupta and Satapathy (2000) studied abyssal benthic foraminifera from thirty-one samples of the latest Miocene to Pleistocene from Deep Sea Drilling Project (DSDP) Site 236, north of the Mascarene Plateau. This study investigated the link between benthic foraminifera distribution, productivity and deep-ocean thermohaline circulation in the west-central Indian Ocean during that period.

The main aim of this work is to provide a taxonomic and stratigraphic reference for the most common Miocene benthic foraminifera encountered in the southern Indian Ocean, supported by scanning electron microphotograph (SEM) images. The study deals with foraminifera encountered in ODP Holes 752A, 1139A and 1168A, all in the southern part of the Indian Ocean (Figure 1). Of these, the latter two have not previously been investigated for benthic

foraminiferal assemblages, and whilst Neogene benthic foraminifera assemblages have been used for palaeoceanographic reconstructions in Hole 752A (Singh et al., 2012), no systematic species description or reference images were provided.

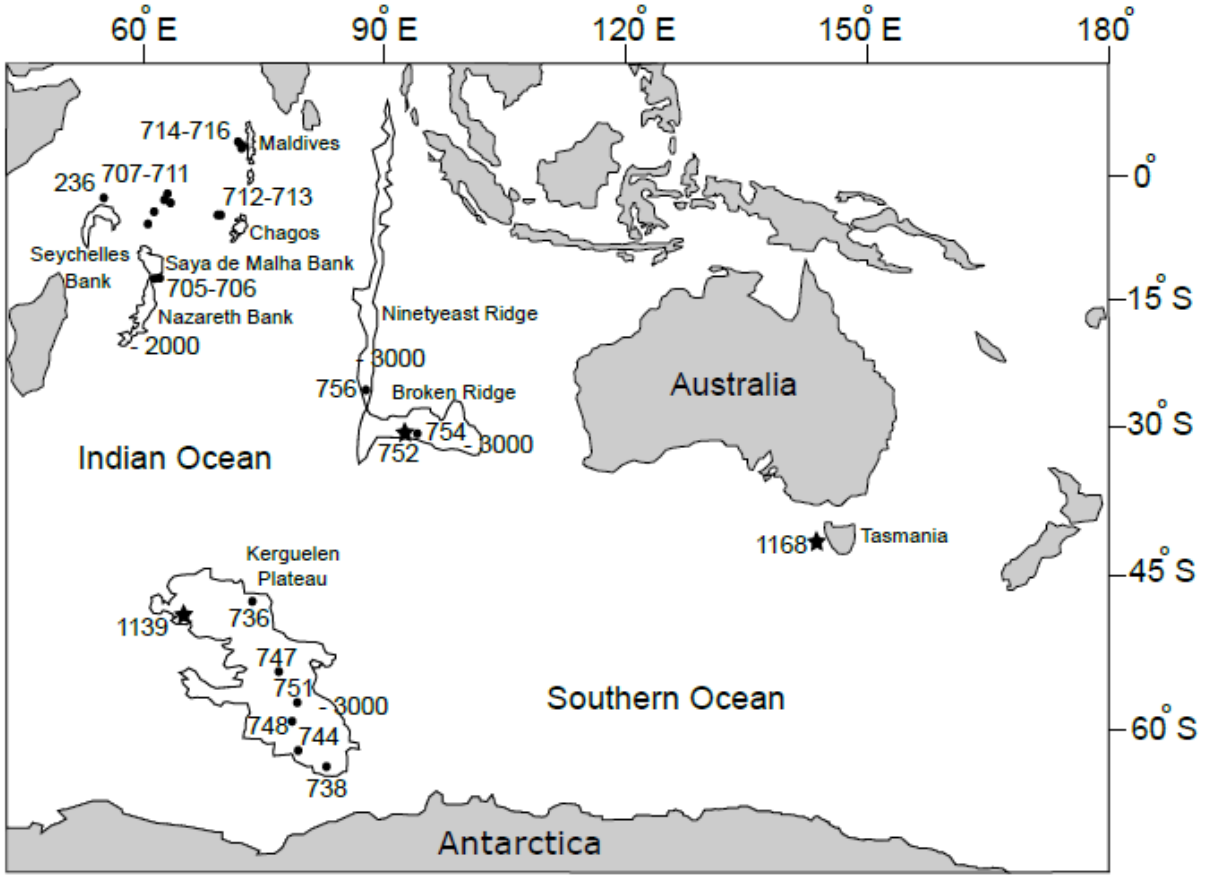


Figure 3. 1: Location map of the study area. Studied sites are marked as stars (752, 1168 and 1139), additional sites referred to in the text are located by dots (after Weatherall et al., 2015). Sites 752, 754 & 756 (Leg 121), Site 1168 (Leg 189), Site 1139 (Leg 183), sites 705-716 (Leg 115) and DSDP Site 236 (Leg 24).

3.2 Materials and Methods

ODP Site 752 is situated on the Broken Ridge in the south-eastern Indian Ocean (30°53.475'' S, 93°34.652'' E; Fig. 1) at a water depth of 1086 m (Shipboard Scientific Party, 1989a). The

current study covered a 79.7 m interval of sediments from Hole 752A, which includes latest Oligocene through early Pliocene, the average core recovery is 70.6 %, composed mainly of foraminifera and nannofossil ooze. An age model for Hole 752A was developed using the calcareous nannofossil datums from the initial report (Shipboard Scientific Party, 1989a), with revised ages from Astronomically Tuned Neogene Time Scale (ATNT2012) in GTS2012 (Hilgen et al., 2012).

ODP Site 1139 is located west of Kerguelen Island (50°11'20''S, 63°55'40''E; Fig. 1) at a water depth of 1415 m (Shipboard Scientific Party, 2000). The late Oligocene to the earliest, late Miocene interval was sampled from Hole 1139A comprising 167.3 m with an average core recovery of 62 %. The sediments are foraminifera-bearing nannofossil ooze, nannofossil-bearing clay and claystone and nannofossil-bearing ooze and chalk. An age model has been established using planktic foraminifera (Shipboard Scientific Party, 2000) and calcareous nannofossil datums (Persico et al., 2003) with ages revised using ATNT2012 in GTS2012 (Hilgen et al., 2012).

ODP Site 1168 is situated at a middle bathyal water depth (2463 m) on the western margin of Tasmania (42°38'40"S, 144°25'30"E; Fig. 1) (Shipboard Scientific Party, 2001a). The sedimentary interval studied in Hole 1168A covers 422.8 m with an average recovery of 98%. This interval covers the latest Oligocene through to early Pliocene, which is mainly composed of nannofossil ooze, silty clay and claystone. The age model for Hole 1168A uses planktic foraminifera, calcareous nannofossils and geomagnetic polarity datums calculated by Stickley et al. (2004) with revised ages from ATNT2012 in GTS2012 (Hilgen et al., 2012).

In total, 97 samples were selected from the study sites (30, 25 and 42 samples at ODP Sites 752, 1139 and 1168, respectively). Sediment samples were processed by first disaggregating them in water and then wet sieving at 63 µm. Samples were then dried overnight in an oven at 40^{o}C, the dry >63 µm sieve size fraction was then split until an aliquot of >300 benthic foraminifer specimens was achieved and subsequently picked clean of all benthic foraminifer. The 52 most- abundant species encountered (of more than 500 species provisionally determined across all three sites) were selected for this work as they represent ~79% of the total benthic foraminifera specimens found across all sites. Scanning electron microscope images of representative (uncoated) specimens of each selected species were taken on a Phenom Desktop SEM at the University of Birmingham. The total size range of specimens observed within the study was also recorded by measuring the longest axis of the specimens using a reticle on a stereo-microscope.

3.3 Foraminiferal Assemblages

In the current study, the generic and suprageneric classification of the foraminifera follows Loeblich and Tappan (1987, 1994). The classification of Loeblich and Tappan (1994) is broadly the same as that of Loeblich and Tappan (1987) with some modification of high-level categories as given in Loeblich and Tappan (1992). Specifically, the elevation of the foraminifera to a higher taxonomic rank by Lee (1990) to Class Foraminiferea was accepted by Loeblich and Tappan (1992) and Kaminski (2004). The key sources for species identification are Wright (1978), Hayward (2002), Hayward et al. (2012) and Holbourn et al. (2013). Descriptions are based on existing literature with additional observations from this study.

Benthic foraminifer assemblages are relatively well preserved (albeit recrystallized) with specimens largely complete and surficial details preserved. Assemblages are diverse with more than 200 species identified in total in each site (500 within the entire study) and are dominated by calcareous benthic foraminifera. This diversity is higher than previously documented in the Indian Ocean (e.g. Boersma, 1990; Nomura, 1991; Schroder-Adams, 1991 and Mackensen, 1992).The previously mentioned workers did not use the smaller fractions (>63 µm) except Boersma (1990), while the current study results recorded higher diversity. This may be due to including smaller fractions. The 52 selected species described here are assigned to 33 different genera and are subdivided into four orders, 14 superfamilies, 20 families and 16 subfamilies. Four recorded species are left in open nomenclature, two each from *Bolivina* and *Gyroidinoides*. All taxa described are calcareous hyaline forms with the exception of one agglutinated species. Representatives of the Buliminida (31 species) constitute the majority of those recorded, especially in ODP Hole 752A, but they are also both abundant and diverse in Holes 1139A and 1168A. Species of the Rotaliida are the next most important components of the benthic foraminifer assemblages.

Discussion of the stratigraphic range of each species at the individual study sites is included in the taxonomic section and shown in Figure 2. Many species occur throughout the studied interval, and many of the most abundant occur at all sites, with just a few exceptions. Notably, there appear to be environmentally cued distributions, for example, *Bolivina huneri* only occurs in the early Miocene of Hole 752A, and the mid- to late Miocene of Hole 1168A, not occurring at all at Hole 1139A. It is clear that, although there is a faunal similarity between the three sites, in terms of species occurrence, the faunal composition at each site differs through

the studied interval and each site responds differently to climatic events through the Miocene. A full discussion of the assemblage data and palaeoceanographic implications are deferred to a later contribution.

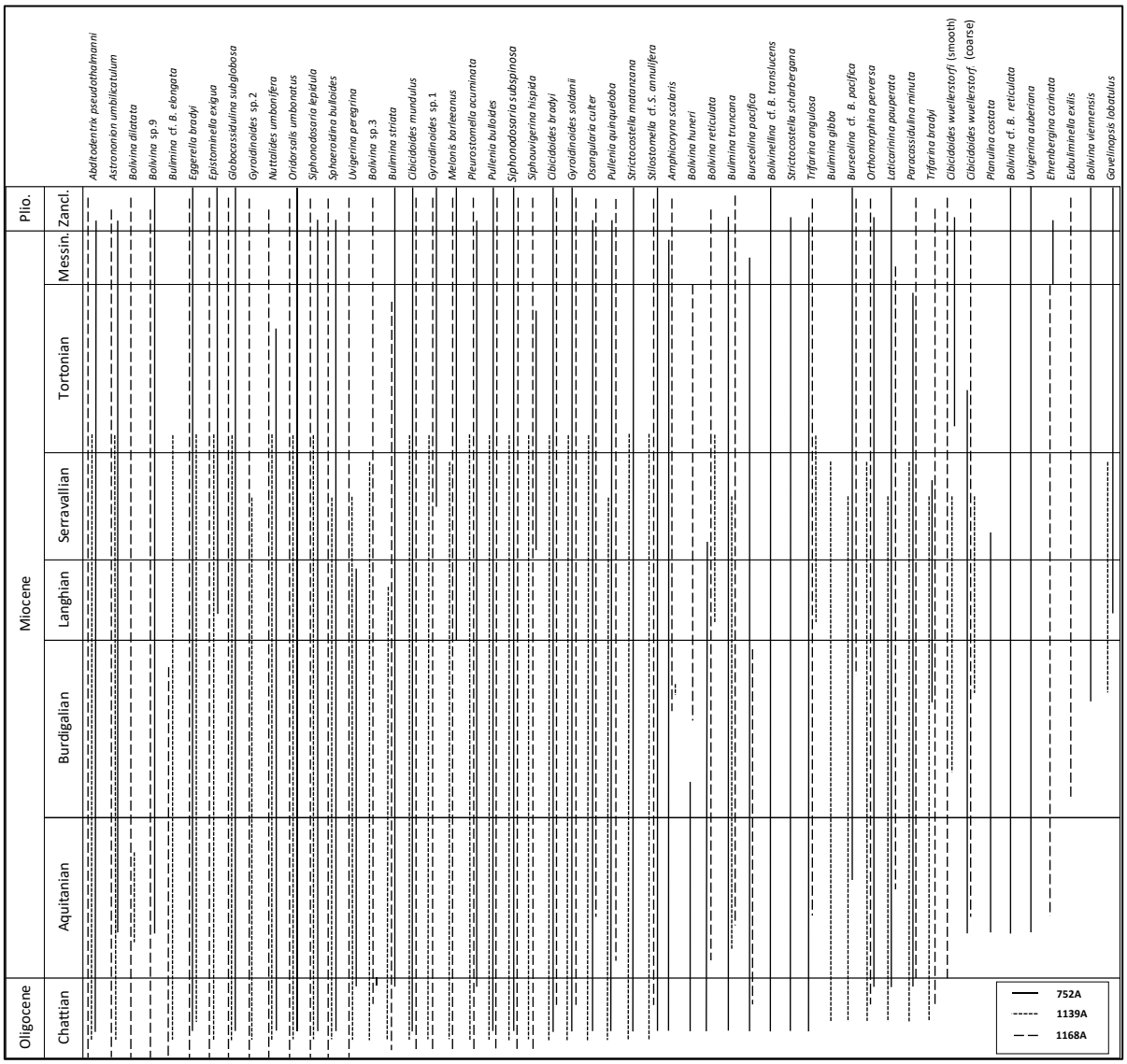


Figure 3. 2: Range chart of fifty-two most abundant benthic foraminifera species encountered at Ocean Drilling Program (ODP) Holes 752A, 1139A and 1168A.

3.4 Taxonomy *[Note, on acceptance, all figured specimens will be given Museum Numbers, Lapworth Museum of Geology, University of Birmingham]*

Class **FORAMINIFEREA** J. J. Lee, 1990

Order **BULIMINIDA** Fursenko, 1958

Superfamily **BOLIVINACEA** Glaessner, 1937

Family **BOLIVINIDAE** Glaessner, 1937

Genus *Bolivina* d'Orbigny, 1839c

Bolivina dilatata Reuss 1850

Figure 3.3, 1a-b

1850 *Bolivina dilatata* Reuss: p. 381, pl. 48, fig. 15a-c.

1949 *Bolivina subspathulata* Boomgaart, p.112, pl.12, fig. 4.

2016 *Bolivina dilatata* Reuss; Lei and Li, p. 202, pl. 2, figs. a-h.

Description: The test is biserial elongate, has perforated hyaline wall; the shape of the chambers is triangular to trapezoidal. The sutures are depressed. The aperture is a slit-like to arcuate opening with a thin tooth plate in the middle. The aperture location is terminal.

Dimensions: The species length ranges from 125-250 µm in the current study.

Stratigraphic range: This species is recorded in the Aquitanian of 1139 and late Oligocene (Chattian) to early Pliocene (Zanclean) at 1168. This species is not recorded at 752 consistent with earlier studies (Nomura, 1995).

Remarks: This is considered a cosmopolitan species (Lei and Li, 2016) but to the best of our knowledge this is the first time it has been recorded in the Indian Ocean. This species is also accepted as *Bolivina dilatata* (Hayward et al. 2020) in the World Register of Marine Species (WoRMS).

Bolivina huneri Howe, 1939

Figure 3.3, 2a-b

1939 *Bolivina huneri* Howe: p. 66, pl. 9, figs. 3, 4.

1983 *Bolivina huneri* Howe; Tjalsma and Lohmann, p. 23, pl. 11, fig. 5.

1987 *Bolivina huneri* Howe; Miller and Katz, p. 124, pl. 1, figs. 7a-b.

2013 *Bolivina huneri* Howe; Holbourn et al., p. 68, figs. 1-3.

Description: Very densely ornamented biserial species, with a tapered test. The test surface has reticulate ornamentation largely obscuring sutures with the exception of the final chamber. The inflated chambers are elongated. The aperture is situated at the base of the last chamber and is arcuate with wide aperture view and tooth plate.

Dimensions: The species length ranges from 175-250 μm in the current study.

Stratigraphic range: This species is recorded from the Chattian through early Burdigalian of 752. At 1168 the species is confined to the Miocene and ranges from Burdigalian to Tortonian, the species is not recorded at 1139. These ranges fall within the middle Eocene-late Miocene (Tortonian) range determined by Holbourn et al. (2013).

Remarks: The distribution is cosmopolitan (Holbourn et al., 2013) and it has previously been recorded on the Kerguelen Plateau, southern Indian Ocean at ODP sites 748 and 751 (Mackensen, 1992) and 736, 738 and 744 (Schroder-Adams, 1991).

Bolivina reticulata Hantken, 1875

Figure 3.3, 3a-b

1875 *Bolivina reticulata* Hantken: p. 65, pl. 15, fig. 6.

1978 *Bolivina reticulata* Hantken; Wright, p. 711, pl. 2, figs. 8-10.

Description: Broad biserial test with wide, slightly inflated, elongate chambers, characteristically covered by narrow anastomosing ribs. The test is slightly perforated and has a narrow keel around the periphery. Depressed and limbate sutures are observed. The aperture is sub-rounded, located at the base of the last chamber with an internal tooth plate. The species is characterised by its sub-rounded shape in a side view and slightly compressed in cross-section.

Dimensions: The species length ranged from 150-375 µm in the current study.

Stratigraphic range: The species is recorded at 752 from the Chattian to Serravallian, from the Miocene and Early Pliocene (Zanclean) at 1168 and Langhian-Tortonian at 1139.

Remarks: This species is recorded in the Mediterranean (Wright, 1978) and South Atlantic Ocean (Tjalsma, 1983). This species has a highly variable morphology both in terms of test shape and ornamentation (Wright, 1978). This species is included by some authors as a junior synonym of *Latibolivina subreticulata* (Parr) by Loeblich and Tappan (1994) and Holbourn et

al. (2013) and is primarily recorded from the tropical Indian and Pacific Oceans (Holbourn et al., 2013). Thus, this species likely has a global distribution.

Bolivina sp.3

Figure 3.3, 4a-c

Description: The test is biserial, elongate with a smooth surface. Some specimens are highly perforated. The chambers are elongate to trapezoid in shape. The sutures are slightly depressed. The aperture is sub-rounded and located at the base of the last chamber.

Dimensions: The species length ranged from 150-250 µm in the current study.

Stratigraphic range: The species is only observed in the late Oligocene (Chattian) of 752. At 1139 it occurs between the Chattian and Serravallian. At 1168 the species ranges throughout the Miocene and into the early Pliocene (Zanclean).

Remarks: This species differs from *Bolivina dilatata* (Reuss, 1850), by having a longer test relative to its width (2.5x long as wide rather than 2:1), the sutures are extremely shallow. The current species is similar to the *Bolivina* cf. *dilatata maxima* (p. 148, fig. 7, pl. k) recorded in the Central Paratethys (Peryt, 2013) but the latter has more depressed sutures. The current species differs from *Bolivina spathulata* (Williamson, 1858), which has a sharp edge in the apertural view, whereas specimens here have a subrounded edge in apertural view. Also, specimens from the China Seas (Lei and Li, 2016) have an anastomosing imperforate costae ornamentation and are much larger ~550 µm (2x longer than those observed here). This species is so far only been recorded in the southern Indian Ocean (current study).

Bolivina cf. *reticulata* Hantken, 1875

Figure 3.3, 5a-b

cf 1875 *Bolivina reticulata* Hantken: p. 65, pl. 15, fig. 6.

cf 1978 *Bolivina reticulata* Hantken; Wright, p. 711, pl. 2, figs. 8-10.

cf 2013 *Latibolivina subreticulata* (Parr); Holbourn et al., p. 327, figs. 1-4.

Description: The test is biserial, with hyaline wall composition. The chamber shape is elongate to a trapezoid. The suture is depressed and limbate. The ornamentation is of anastomosing ribs. The aperture is basal, rounded with a tooth plate.

Dimensions: The species length ranges from 125-375 μm in the current study.

Stratigraphic range: The species is only observed at 752 through the Miocene and early Pliocene (Zanclean). This species is highly abundant in the mid-late Miocene.

Remarks: This species is similar to *Bolivina reticulata* (Hantken, 1875), but *B. reticulata* has a broader (particularly towards the base) and relatively more elongate test, with a more compressed periphery in apertural view. According to Wright (1978), *Bolivina reticulata* varies in shape from an elongate form with limbate sutures to specimens with little ornamentation. This species is also similar to *Bolivina viennensis* (Marks, 1951) reported in Polish Carpathian Foredeep Basin (Central Paratethys) by Peryt (2013). This form is so far only recorded in the Indian Ocean.

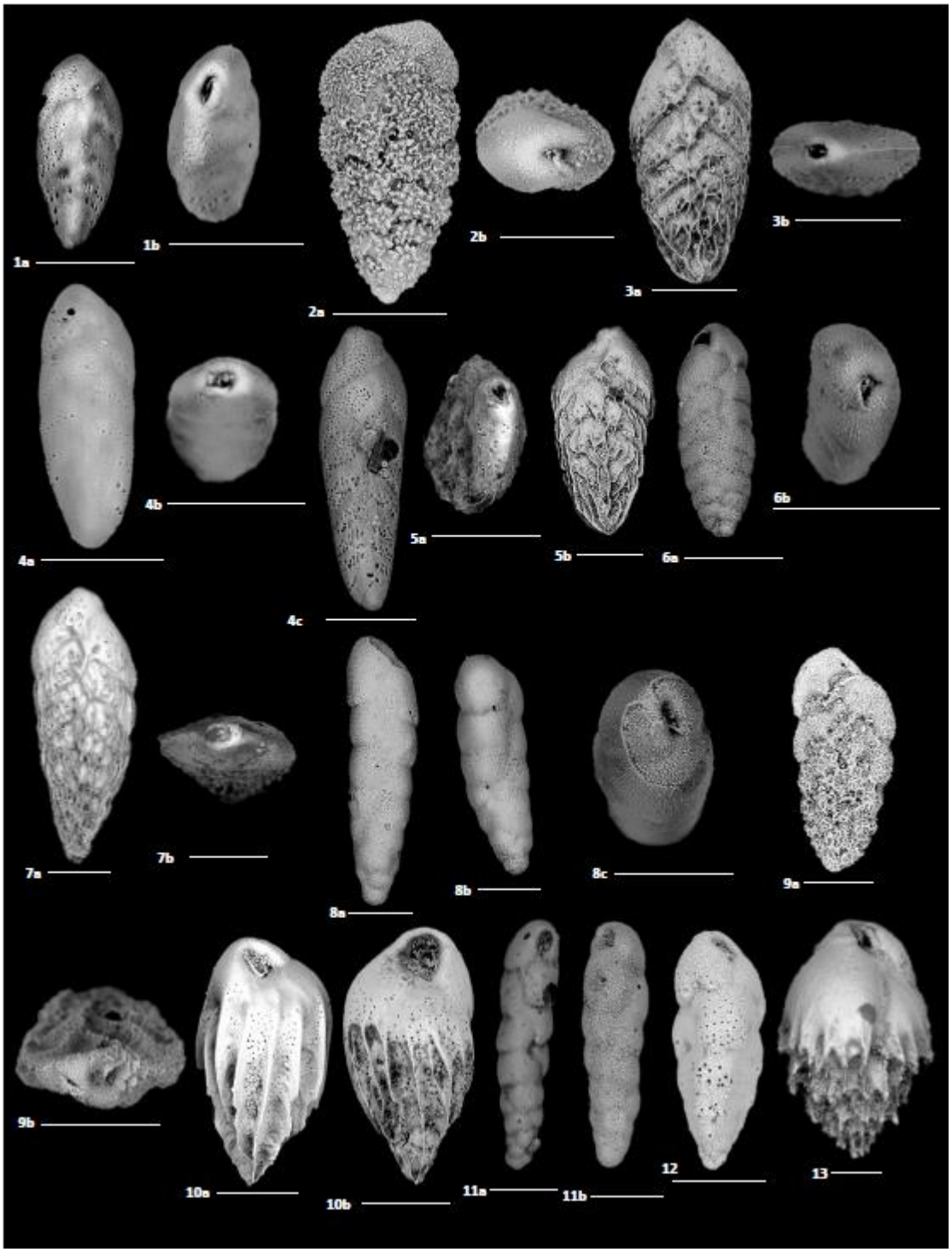


Figure 3. 3:

(Scale bar = 100 µm)

1a-b. *Bolivina dilatata*, 1168A, 37X-6, 75-79cm: 1a. side view; 1b. apertural view.

2a-b. *Bolivina huneri*, 752A, 10H-5, 77-81cm. 2a. side view; 2b. apertural view.

3a-b. *Bolivina reticulata*, 1168A, 15X-2, 76-80cm: 3a. side view; 3b. apertural view.

4a-b. *Bolivina* sp.3, 1168A, 4a-b. 26X-2, 73-77cm: 4a. side view; 4b. apertural view. 4c. 37X-6, 75-79cm: side view.

5a-b. *Bolivina* cf. *reticulata,* 752A, 5a. 5H-1, 65-70cm: apertural view. 5b. 3H-5, 62-67cm: side view.

6a-b. *Bolivina* sp.9, 752A, 9H-2, 104-109cm: 6a. side view; 6b. apertural view.

7a-b. *Bolivina viennensis*, 752A, 5H-1, 65-70cm: 7a. side view; 7b. apertural view.

8a-c. *Bolivinellina* cf. *B. translucens*, 752A, 3H-1, 50-55cm: 8a-b. side view; 8c. apertural view.

9a-b. *Abditodentrix pseudothalmanni*, 1139A, 19R-2, 60.5-64.5cm: 9a. side view; 9b. apertural view.

10a-b. *Bulimina truncana*, 10a. 752A, 9H-5, 65-70cm: lateral view. 10b. 1168A, 37X-6, 75-79cm: apertural side view.

11a-b. *Bulimina* cf. *B. elongata*, 11a. 1168A, 23X-3, 74-78cm: apertural side view. 11b. 1139A, 18R-1, 96-100cm: apertural side view.

12. *Bulimina gibba*, 1139A, 19R-2, 60.5-64.5cm: lateral view.

13. *Bulimina striata*, 752A, 5H-1, 65-70cm: apertural side view.

Bolivina sp.9

Figure 3.3, 6a-b

Description: The test is finely perforated, smooth, and elongate, with a hyaline wall composition. Chambers are abroad, trapezoid, biserial arranged, with a depressed suture between chambers. Aperture is loop-shaped, basal position. The test length is nearly three times longer than the width. The test is tapered at both ends.

Dimensions: The species length ranges from 125-250 μm in the current study.

Stratigraphic range: The species occurs through the Miocene and into the early Pliocene (Zanclean) at 752. The species is very abundant in the early Burdigalian at 752. Only very few specimens have been recorded at 1168, mainly in the Chattian and between the Burdigalian to Serravallian with a very few records in the early Pliocene (Zanclean). This species is not recorded at 1139.

Remarks: This species is similar to *Bolivinellina pseudopunctata* (Alve and Murray, 2001) recorded in intertidal environments from southern England (*Ibid*. pl. 2, figs 7-9). The current species has a wider loop-shaped aperture with the last slightly irregular chamber. While *B. pseudopunctata* has a narrower, slightly compressed aperture, and the shape of the chambers are consistently trapezoidal. This species differs from *Bolivina spathulata* (Williamson, 1858) by having a big and rounded (loop-shaped) aperture on the apertural face rather than a small and narrow loop-shaped aperture. Also, *Bolivina spathulata* specimens from the China Seas (Lei and Li, 2016) have an anastomosing imperforate costae ornamentation, not been observed in the current study.

Bolivina viennensis Marks, 1951

Figure 3.3, 7a-b

1951 *Bolivina viennensis* Marks: p. 60, pl. 7, fig.1.

1991 *Brizalina albatrossi* (Cushman); Nomura, p.53, pl. 1, fig. 3.

2005 *Bolivina viennensis* Marks; Popescu and Crihan, p.380, pl. 1, figs. 14-16.

2008 *Bolivina viennensis* Marks; Baldi and Hohenegger, p. 2, pl. 3, fig. a.

Description: The test is biserial, elongated. Chambers elongated to trapezoid; sutures depressed. Surface ornamentation reticulate showing an anastomosing pattern. Aperture rounded, terminal. Normal pores are relatively few and concentrated near the margin of the chambers.

Dimensions: The species length ranges from 175-575 µm in the current study.

Stratigraphic range: This species is only present at 752 and ranges from the Burdigalian to Messinian, re-appearing in the early Pliocene (Zanclean).

Remarks: This species is similar to *Bolivina* cf. *reticulata*, but the length of *Bolivina viennensis* is nearly three times longer than the width, and the test has a sharp end near the proloculus, while *Bolivina* cf. *reticulata* is shorter and is sub-rounded near the proloculus. This species is recorded as *Bolivina viennensis* in the southern Vienna Basin (Austria) (Baldi and Hohenegger, 2008), and in Romania (Popescu and Crihan, 2005). Similar specimens are recorded as *Brizalina albatrossi* in the Eastern Indian Ocean at Site 754 in the Broken Ridge (Nomura, 1991).

Genus *Bolivinellina* Saidova, 1975

Bolivinellina cf. *B. translucens* (Phleger & Parker, 1951)

Figure 3.3, 8a-c

cf. 1951 *Bolivina translucens* Phleger & Parker: p. 15, pl. 7, figs. 13, 14.

cf. 1987 *Bolivinellina translucens* (Phleger & Parker); Loeblich and Tappan: pl. 547, figs. 6, 7.

cf. 1999 *Bolivina translucens* (Phleger & Parker); Ohkushi et al., p. 139, pl. 2, figs. 11, 12.

Description: Test elongate, triserial to biserial, narrow, oval in section. Chambers narrow and moderately inflated, sutures depressed and oblique. Wall calcareous, hyaline and smooth, a few pores apparent near the sutures. Aperture basal slit to loop-shaped with a tooth plate at the base of the aperture. Test nearly 3-4 times longer than wide.

Dimensions: The species length ranges from 175-475 µm in this study.

Stratigraphic range: The species is only found at Site 752 where it is distributed throughout the succession, with the greatest abundance in the late Miocene (Messinian) and early Pliocene (Zanclean).

Remarks: The chambers appear triserially arranged in the initial part of the test, with inflated chambers which become less inflated later towards the aperture. *Bolivinellina translucens* is widely distributed in the Gulf of Mexico (Phleger and Parker, 1951) and, more locally, has been recorded along the central West Coast of India (Mazumder et al., 2003) and throughout the Indian Ocean (current study).

Superfamily **BOLIVINITACEA** Cushman, 1927

Family **BOLIVINITIDAE** Cushman, 1927

Genus *Abditodentrix* Patterson, 1985

Abditodentrix pseudothalmanni (Boltovskoy & Guissani de Kahn, 1981)

Figure 3.3, 9a-b

1981 *Bolivinita pseudothalmanni* Boltovskoy & Guissani de Kahn: p.44-46, pl. 1, figs. 1–5.

1985 *Abditodentrix asketocomptella* Patterson, p.139, pl. 1, figs. 1-9.

1987 *Abditodentrix pseudothalmanni* (Boltovskoy & Guissani de Kahn); Loeblich and Tappan, p. 503, pl. 554, figs. 1-5.

cf. 1991 *Brizalina thalmanni* (Renz, 1948), Nomura, p. 53, pl. 1, fig. 4.

Description: Test elongate, biserial and saggitate. The test is flattened in the side view with a distinctive truncate margin giving it a rectangular appearance in section. Chambers are elongated to a trapezoid. The sutures are depressed. Aperture is in a basal position, elliptical in shape with tooth plate infolded on one side. The surface is densely covered with elevated reticulate ornamentation.

Dimensions: The species length ranges from 100-425 µm in this study.

Stratigraphic range: Occurs in the late Oligocene (Chattian) in all studies sites, ranging into the early late Miocene (early Tortonian) in 1139 and the early Pliocene (Zanclean) at 752 and 1168.

Remarks: Most of the observed specimens are highly compressed in cross-section and densely ornamented in the initial portion, near the proloculus, with simple reticulation or no

ornamentation near the aperture. This species is recorded in the southwest Pacific Ocean (Hayward et al., 2002) and the southwest Atlantic Ocean (Loeblich & Tappan, 1987). It is recorded as *Brizalina* cf. *thalmanni* in the eastern Indian Ocean (Nomura, 1991).

Superfamily **BULIMINACEA** Jones in Griffith and Henfrey, 1875

Family BULIMINIDAE Jones, 1875

Genus *Bulimina* d'Orbigny, 1826

Bulimina truncana Gümbel, 1868

Figure 3.3, 10a-b

1868 *Bulimina truncana* Gümbel: p. 727, pl.2, figs. 77a, b.

1884 *Bulimina rostrata* Brady: p. 408, pl. 5, figs. 14, 15.

1927 *Bulimina alazanensis* Cushman: p. 161, pl. 25, fig. 4

1940 *Bulimina bremneri* Finlay: p.455, pl.64, figs. 84-86.

1991 *Bulimina alazanensis* Cushman: Schroder-Adams, p.624, pl. 1, fig. 5.

1991 *Bulimina truncana* Gümbel: Hermalin, p. 65, pl. 1, figs. 10, 16.

2002 *Bulimina truncana* Gümbel: Hayward et al., Plate 1, figs. 9, 10.

Description: Test tri-serial, elongate, sub-triangular in cross section, tapered in outline. Rounded to sub-rounded in the apertural end and pointed in the apical end. The chambers are inflated with obscured sutures. The longitudinal costae occur on all chambers (although the upper portion of the final three chambers is smooth) and join together to form a spinose

protrusion from the earliest chambers. The aperture is loop-shaped with internal tooth plate and surrounded by apertural lip. The greatest width of the test is towards the apertural end.

Dimensions: The species length ranges from 125-625 µm in the current study.

Stratigraphic range: The species is recorded from the late Oligocene to Pliocene at 752 and 1168. Whereas it is confined to the Miocene (Aquitanian to Serravallian) at 1139.

Remarks: Boersma (1986) noted that *Bulimina truncana* has a highly variable morphology and thus, multiple synonyms based on differences in the number and extent of costae, their height, and orientation. Of these, small forms with fewer costae that almost completely cover the final chamber have been often been attributed to *Bulimina rostrata,* whereas those with more costae that also tend to be wavy are assigned to *Bulimina alazanensis*. Furthermore, *B. rostrata* also achieves its maximum width towards the middle of the text, is overall sub-circular in cross-section compared to *B. alazanensis* where the maximum test width occurs closer to the apertural end and the test has a more sub-triangular cross-section. *B. truncana* is very similar to *B. alazanaensis* but was separated out based on having fewer, straighter, costae that begin on the first or second chambers rather than the third (Boersma, 1986). Ultimately overlapping species occurrences at the same sites, difficulties in consistently differentiating taxa, and missing holotype specimens (*B. alazanensis*) have led to them being synonymised (Hayward et al., 2019a) in World Register of Marine Species (WoRMS). Here tests are usually sub-triangular in cross-section, having parallel, regularly formed costae with the largest width of the test towards that apertural end rather than the middle and hence are closest to the forms included in *B. truncana*. This species is considered to be cosmopolitan and has been

recorded in Southwest Pacific Ocean (Hayward et al., 2002), Tasman sea, Coral Sea (Boersma, 1986) and Indian Ocean (Nomura, 1995).

Bulimina cf. *B. elongata* d'Orbigny, 1846

Figure 3.3, 11a-b

cf. 1846 *Bulimina elongata* d'Orbigny: p. 187, pl.11, figs. 19, 20.

cf. 1826 *Bulimina elongata* d'Orbigny: (Nomen nudum), p. 269.

cf. 2004 *Bulimina elongata* d'Orbigny: De Man et al., p.187, pl. 2, fig. 9.

cf. 2008 *Bulimina elongata* d'Orbigny: Kender et al., p. 513, pl. 17, figs. 4, 5.

Description: Elongate, narrow (three times as long as wide), triserial test becoming nearly biserial in the final whorl. Little tapering of test. Chambers are flattened and broad. Sutures are depressed. The aperture is basal and rounded. The surface is mainly smooth with very few perforations.

Dimensions: The species length ranges from 150-400 μm in this study.

Stratigraphic range: This species ranges from the late Oligocene (Chattian) to mid- Burdigalian at 1168, extending into the early Tortonian at 1168. This supports the range (mid-Eocene to Pleistocene) identified by Thomas (1990). This species is not present at 752.

Remarks: This species differs from *Bulimina elongata* sensu stricto (see Holbourn et al., 2013) in that the chambers are less inflated (have a nearly polygonal outline) and a much slower rate of chamber enlargement. Holbourn et al. (2013) consider *Bulimina elongata* a cosmopolitan species.

Bulimina gibba Fornasini, 1902

Figure 3.3, 12

1902 *Bulimina gibba* Fornasini: p. 378, pl. O, figs. 32–34.

2005 *Bulimina gibba* Fornasini; Rasmussen, p. 86, pl. 11, fig. 5

2013 *Bulimina gibba* Fornasini; Holbourn et al., p.97, figs. 1–3.

Description: Triserial, elongate, fusiform shape. Nearly circular in cross-section with narrow apical tip. Chambers are inflated with clearly depressed sutures and strongly overlapping. The aperture is loop shaped, located at the base of the last chamber, with apertural lip merging with an internal tooth plate. The test surface is relatively smooth with perforation distributed across the chambers.

Dimensions: The species length ranges from 125-300 μm in the current study.

Stratigraphic range: This species occurs from the late Oligocene (Chattian) to early Tortonian at 1139. This species is not recorded at either 752 or 1168.

Remarks: This species is commonly found and described (e.g., Holbourn et al., 2013) as having an apical protrusion from the proloculus however, in this study, no spinose protrusions are observed in any specimen. This absence cannot be explained by preservation. This species has previously only been reported from the Atlantic (Holbourn et al., 2013) but the authors noted that it may well range further which is confirmed in this study. Holbourn et al. (2013) report this species from the Miocene to Recent but this work suggests it may occur earlier in the Indian Ocean.

Bulimina striata d'Orbigny in Guérin-Méneville, 1832

Figure 3.3, 13

1832 *Bulimina striata* d'Orbigny in Guérin-Méneville: p. 18, pl. 3, fig. 16.

1852 *Bulimina costata* d'Orbigny: p. 194.

1922 *Bulimina inflata* var*. mexicana* Cushman: p. 95, pI. 21, fig. 2.

1953 *Bulimina mexicana* Cushman; Phleger and others, p.33, pl.6, fig. 27.

1954 *Bulimina striata mexicana* Cushman; Parker, p.511, pl. 6, fig. 24.

1957 *Bulimina australis* Vella: p. 32, pl. 8, figs. 168-169.

1992 *Bulimina striata* d'Orbigny in Guérin-Méneville: Mackensen, p. 668, pl. 1, fig. 5.

2003 *Bulimina striata* d'Orbigny in Guérin-Méneville: Hayward et al., p. 517.

2011 *Bulimina striata* d'Orbigny in Guérin-Méneville: Kuppusamy et al., p. 46, pl. 2, figs. 7, 8.

2013 *Bulimina striata* d'Orbigny in Guérin-Méneville: Mancin et al., p. 64, pl. 2, fig. 3.

Description: Test conical and triserial. Semi-circular in cross-section, the initial part of the test (near proloculus) is acute. Chambers are inflated overhanging previous chambers, becoming broader and less ornamented near the aperture. The sutures are depressed but largely obscured by ornamentation in the earlier portion of the test. Longitudinal costae extend from the lower half of the chambers to overhang preceding chambers ending in acute points. The aperture is loop-shaped bordered by a lip with an internal tooth plate.

Dimensions: The species length ranges from 100-500 μm in this study.

Stratigraphic range: The species is recorded throughout the whole succession (late Oligocene – Pliocene) at 752. At 1139 and 1168 this species occurs from the late Oligocene (Chattian) disappearing from 1139 in the Langhian and early Tortonian at 1168.

Remarks: This species is cosmopolitan. This species is identified around New Zealand (Debenay, 2012) and by Kuppusamy et al. (2011) in North-West Atlantic Ocean. Many older Indian Ocean publications report this species as *B. mexicana* (e.g., Nomura, 1995) which does have a global distribution (Holbourn et al., 2013). Holbourn et al. (2013) consider the range of this species to be Miocene-Recent, here it is found in the late Oligocene.

Family **Turrilinidae** Cushman, 1927

Subfamily **Turrilininae** Cushman, 1927

Genus *Eubuliminella* Revets, 1993

Eubuliminella exilis (Brady, 1884)

Figure 3.4, 1

1884 *Bulimina elegans* var. *exilis* Brady: p. 399, pl.50, figs. 5, 6.

1927 *Buliminella subfusiformis* var. *tenuata* Cushman: p. 149, pl. 2, fig. 9.

1930 *Buliminella subfusiformis* (Cushman); Cushman and Moyer, p. 56, pl. 7, fig. 20.

1947 *Bulimina exilis* Brady; Cushman and Parker, p. 123, pl. 28, figs. 27, 28.

1947 *Bulimina subfusiformis* var. *tenuata* (Cushman); Cushman and Parker, p. 124, pl. 28, fig. 29.

1993 *Eubuliminella exilis* (Brady); Revets, p. 141, pl.1, figs. 1-7.

2015 *Eubuliminella exilis* (Brady); Setoyama & Kaminski, p. 8, figs. 4.2; 8.7.

Description: Elongate, narrow test that is triserial in the latter part. The test length is about four times as long as it is wide. Ovate and little inflated chambers separated by curved and depressed sutures. The aperture is basal and loop-shaped, but from the apertural opening, the tooth plate is not clear.

Dimensions: The species length ranges from 150-550 μm in the current study.

Stratigraphic range: The stratigraphic range of the species at 1168 is early Miocene (Burdigalian) to the early Pliocene (Zanclean), Holbourn et al. (2013) suggested a range from the late Miocene, the present study, therefore, extends the known stratigraphic range.

Remarks: The specimens in the current study lack the spine in the initial whorl and have more weakly inflated chambers. According to Revets (1993) and Holbourn et al. (2013), this species can be found worldwide.

Superfamily **CASSIDULINACEA** d'Orbigny, 1839a

Family **CASSIDULINIDAE** d'Orbigny, 1839a

Subfamily **CASSIDULININAE** d'Orbigny, 1839a

Genus *Globocassidulina* Voloshinova, 1960

Globocassidulina subglobosa (Brady, 1881)

Figure 3.4, 2

1881 *Cassidulina subglobosa* Brady: p. 60, illustrated in Brady, 1884, pl. 54, fig. 17.

1884 *Cassidulina subglobosa* Brady; Brady, p. 430, pl. 54, fig. 17.

1983 *Globocassidulina subglobosa* (Brady); Tjalsma and Lohmann, p. 31, pl. 16, fig. 9.

1991 *Globocassidulina subglobosa* (Brady); Nomura, p.55, pl. 5, fig. 8.

2013 *Globocassidulina subglobosa* (Brady); Holbourn et al., p.264, figs. 1, 2.

Description: Test biserial, subglobular, with a sub-circular shape in cross-section. Chambers are inflated and separated by depressed, curved sutures. The test wall is smooth and only finely perforate. The aperture is slit-like, straight or curved.

Dimensions: The species length ranges from 100-925 μm in this study.

Stratigraphic range: This is a long-ranging species, recorded from late Oligocene to early Pliocene at both 752 and 1168, and late Oligocene to the top of the studied interval (early Tortonian) at 1139.

Remarks: This species is very well preserved in all studied sites. This is a cosmopolitan species (Jones (1994) that is very long-ranging (Paleocene-Holocene; Tjalsma and Lohmann, 1983).

Genus *Paracassidulina* Nomura, 1983b

Paracassidulina minuta (Cushman)

Figure 3.4, 3a-b

1933b *Cassidulina minuta* Cushman: p. 92, pl.10, figs. 3a-c.

1951 *Cassidulina crassa* d'Orbigny; Phleger and Parker, p. 26, pl. 14, figs. 4a-b.

1954 Cassidulina aff. *crassa* d'Orbigny; Parker, p. 535, pl. 11, fig. 1.

1983b *Paracassidulina minuta* Cushman; Nomura, p. 66, pl. 5, figs. 16a-c.

1991 *Paracassidulina minuta* Cushman; Nomura, p. 55, pl. 5, fig.s 2a-b.

Description: Biserial test with slightly depressed sutures. Surface smooth, finely perforated. Chambers are strongly curved. Aperture is long, curved, and has an apertural ridge parallel to the chamber periphery.

Dimensions: The species length ranges from 125-300 µm in the current study.

Stratigraphic range: The species ranges from Chattian to early Tortonian at 752, Chattian to mid-Serravallian at 1139. The stratigraphic distribution of the species at 1168 is early Aquitanian to Zanclean.

Remarks: The chambers of the specimens found here are only slightly inflated, this differs from *Globocassidulina minuta* (Cushman, 1933b) described from the Paumotu Islands in the Southern Pacific Ocean in that the latter has more globular chambers. This species is recorded by Nomura (1991) at Broken Ridge (Site 754) in the Eastern Indian Ocean and the Gulf of Mexico (Poag, 2015).

Subfamily **EHRENBERGININAE** Cushman, 1927

Genus *Ehrenbergina* Reuss, 1850

Ehrenbergina carinata Eade, 1967

Figure 3.4, 4a-b

1967 *Ehrenbergina carinata* Eade: p. 448, pl. 9, figs. 1-4.

1991 *Ehrenbergina carinata* Eade; Nomura, p. 55, pl. 5, fig. 13.

2013 *Ehrenbergina carinata* Eade; Hayward et al., p. 442, pl. 6, figs. 12, 13.

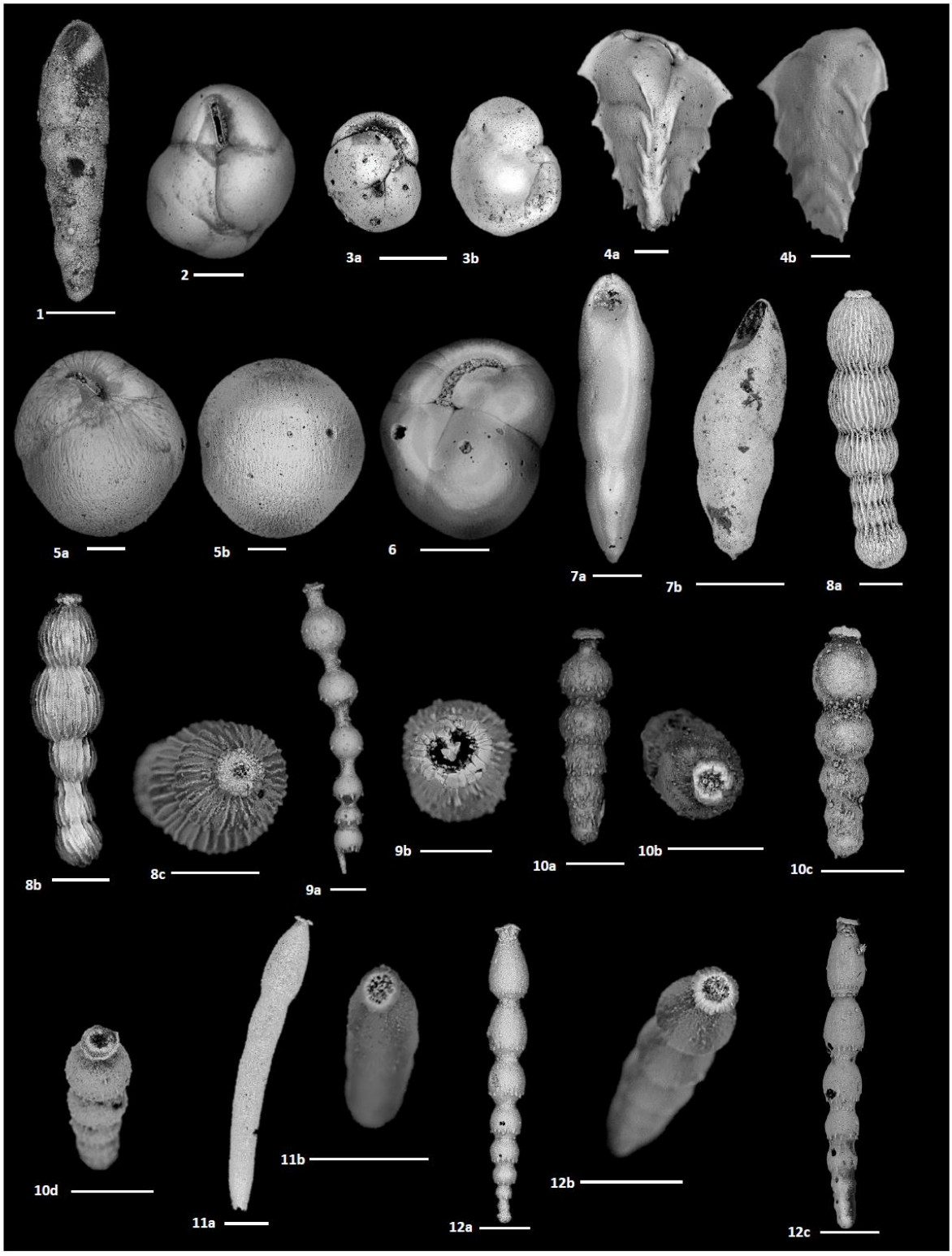


Figure 3. 4:

(Scale bar = 100 µm)

1. *Eubuliminella exilis*, 1168A, 42X-3, 70-74cm: apertural side view.

2. *Globocassidulina subglobosa*, 752A, 4H-1, 70-75cm: apertural side view.

3a-b. *Paracassidulina minuta*, 1168A, 3a. 42X-3, 70-74cm: apertural side view. 3b. 37X-6, 75-79.1cm: side view.

4a-b. *Ehrenbergina carinata*, 752A, 3H-1, 50-55cm: 4a. apertural side view; 4b. side view.

5a-b. *Burseolina pacifica*, 752A, 6H-1, 70-75cm: 5a. apertural side view; 5b. side view.

6. *Burseolina* cf. *pacifica*, 752A, 6H-1, 70-75cm: apertural side view.

7a-b. *Pleurostomella acuminata*, 7a. 752A, 7H-1, 63-68cm: apertural side view. 7b. 1168A, 22X-2, 45-49cm: lateral view.

8a-c. *Orthomorphina perversa*, 8a. 1139A, 14R-4, 65-69cm: side view. 8(b, c). 752A, 3H-1, 50-55cm: 8b. side view; 8c. apertural view.

9a-b. *Siphonodosaria lepidula*, 752A, 9a. 7H-2, 73-78cm: side view. 9b. 8H-1, 100-105cm: apertural view.

10a-d. *Siphonodosaria subspinosa*, 10a-b. 752A, 8H-6, 70-75cm: 10a, side view; 10b, apertural view. 10c. 1168A, 18X-5, 80-84cm: side view. 10d. 1168A, 15X-2, 76-80cm: apertural view.

11a-b. *Stilostomella* cf. *S. annulifera*, 1139A, 15R-4, 41-45cm: 11a, side view; 11b, apertural view.

12a-c. *Strictocostella matanzana*, 12a-b. 752A, 3H-5, 62-67cm: 12a, side view; 12b, apertural view. 12c. 1139A, 18R-1, 96-100cm: side view.

Description: Test triangular in both dorsal view and cross-section. Early chambers are not inflated, while the later chambers are slightly inflated. Well-developed peripheral keel and a spine extending from each chamber. The dorsal view is compressed. The sutures are flush, but towards the periphery become raised. The ventral view is characterised by the central keel. Aperture is slit-like and curved, with a narrow lip on the ventral side.

Dimensions: The species length ranges from 150-725 µm in the current study.

Stratigraphic range: The species range at 752 is late Miocene (Messinian) to early Zanclean. At 1168 the species is very rare and only recorded in the early and late Miocene (Tortonian). This species is not recorded at 1139.

Remarks: This species is well-preserved at 752 and reaches a very large size (up to 725 µm) in some intervals, especially in the late Miocene (Messinian). According to Eade (1967) the current species is recorded in Kermadec Islands, Fiji, Norfolk Island, Tonga and northern New Zealand. This species is also recorded by Nomura (1991) at Broken Ridge (Site 754) and New Zealand (Hayward et al., 2013).

Genus *Burseolina* Seguenza, 1880

Burseolina pacifica (Cushman, 1925)

Figure 3.4, 5a-b

1925 *Cassidulina pacifica* Cushman: p.53, figs. 14-16.

1925 *Globocassidulina pacifica* (Cushman), pl.2, fig. 16.

1983a *Burseolina pacifica* (Cushman); Nomura, pl. 6, fig. 2, pl. 21, figs. 6-10.

1983b *Burseolina pacifica* (Cushman); Nomura, pp. 57-60, pl. 5, figs. 1-4.

1991 *Burseolina* cf. *pacifica* (Cushman); Nomura, p. 53, pl. 5, figs. 14a-b.

Description: Enrolled biserial test with rounded periphery. Sutures are flush to the surface and thus, almost indistinguishable. The apertural face is flattened and the aperture is elongate, curved, with apertural flap in the lower apertural margin.

Dimensions: The species length ranges from 175-600 µm in this study.

Stratigraphic range: The distribution of the species at 752 ranges from the late Oligocene (Chattian), where it is rare, with later Miocene records from the Burdigalian to mid-Messinian. The species is rare at 1168 in the Chattian, and only appears in the late Burdigalian in the Miocene. This species is not recorded at 1139.

Remarks: According to Cushman (1925) this species is widely distributed in deep or cool waters and it has been recorded in the Pacific Ocean. It has also been reported from sub-tropical regions, along the Pacific coast of Japan (Nomura, 1983a) and in the Indian Ocean (Nomura 1991). Notably, the specimens here are more spherical in outline than *B. pacifica* reported by Nomura (1991). *Burseolina* is most abundant from the Miocene to the present.

Burseolina cf. *pacifica* (Cushman, 1925)

Figure 3.4, 6

cf. 1925 *Cassidulina pacifica* Cushman: p.53, figs. 14-16.

cf. 1925 *Globocassidulina pacifica* (Cushman), pl.2, fig. 16.

cf. 1983a *Burseolina pacifica* (Cushman); Nomura, pl. 6, fig. 2, pl. 21, figs. 6-10.

cf. 1983b *Burseolina pacifica* (Cushman); Nomura, pp. 57-60, pl. 5, figs. 1-4.

cf. 1991 *Burseolina pacifica* (Cushman); Nomura, p. 53, pl. 5, figs. 4a-b.

Description: Biserial, sub-spherical test. The surface is smooth. Flush to slightly depressed sutures. The aperture is elongated, curved, with apertural flap in the lower apertural margin.

Dimensions: The species length ranges from 100-425 μm in this study.

Stratigraphic range: The range of the species at 752 is early Miocene (Aquitanian) to early Pliocene (Zanclean). At 1139 it is very rare in the late Oligocene (Chattian) and also in the Miocene, except for Serravallian where it has its greatest abundance. The distribution at 1168 is mid-Burdigalian to Zanclean.

Remarks: This species differs from *Burseolina pacifica* by having a relatively larger and wider aperture and broader flap. The last chambers in this species are also usually separated from the preceding chambers by clearly depressed sutures. This species has a limited geographic distribution and is also observed in tropical to subtropical regions, along the Pacific coast of Japan (Nomura, 1983a) and in the Indian Ocean on the Ninetyeast Ridge (Site 756) (Nomura, 1991).

Superfamily **PLEUROSTOMELIACEA** Reuss, 1860

Family **PLEUROSTOMELLIDAE** Reuss, 1860

Subfamily **PLEUROSTOMELLINAE** Reuss, 1860

Genus *Pleurostomella* Reuss, 1860

Pleurostomella acuminata Cushman, 1922

Figure 3.4, 7a-b

1922 *Pleurostomella acuminata* Cushman: p. 50, pl. 19, fig. 6

1866 *Pleurostomella alternans* Schwager: p. 238, pl. 6, fig. 80

1934 *Pleurostomella alternans* var. *telostoma* Schubert; Cushman, pl. 16, fig. 6.

1978 *Pleurostomella acuta* Hantken; Boltovskoy, pl. 5, fig. 42.

1978 *Pleurostomella dominicana* Bermudez; Boltovskoy, pl. 6, figs. 2, 3.

2011 *Pleurostomella acuminata* (Cushman); Kuppusamy, p. 60, pl. 9, figs. 7, 8.

Description: Smooth elongate, biserial test, slightly depressed sutures. Chambers elongate, oval. Wide terminal aperture, with projecting hood on one side and two triangular or bifid teeth on the opposite side. Prolocular spine present.

Dimensions: The species length ranges from 150-725 μm in the current study.

Stratigraphic range: At 752 and 1168 it ranges from Chattian to early Zanclean, at 1139 from Chattian to early Tortonian.

Remarks: A prolocular spine is present in most specimens, but in others, it is either broken or missing. This species is cosmopolitan and recorded throughout the Indian Ocean (Hayward (2002).

Superfamily **STILOSTOMELLACEA** Finlay, 1947

Family **STILOSTOMELLIDAE** Finlay, 1947

Genus *Orthomorphina* Stainforth, 1952

Orthomorphina perversa (Schwager, 1866)

Figure 3.4, 8a-c

1866 *Nodosaria perversa* Schwager: p. 212, pl. 5, fig. 29.

1872 *Nodosaria pupoides* Silvestri: p. 65, pl. 6, figs. 148–158.

1937 *Nodogenerina challengeriana* Thalmann : p. 341, pl. 64, figs. 25-27.

1949 *Nodogenerina aminaensis* Bermudez: p. 178, pl. 11, fig. 57.

1978 *Orthomorphina challengeriana* (Thalmann); Boltovskoy, pl. 5, figs. 16-17.

1978 *Orthomorphina perversa* (Schwager); Boltovskoy, pl. 5, figs. 23-24.

1992 *Stilostomella* sp. G. Kaiho: p. 307, pl. 5, fig. 23.

2002 *Orthomorphina perversa* (Schwager); Hayward, pl. 1, figs. 50-52.

Description: Test uniserial, rectilinear. Chambers are ovoid in outline and increase in height towards the last chamber. The surface is striate with ribs perpendicularly arranged. The sutures are straight and depressed. The aperture is rounded, terminal with rim.

Dimensions: The species length ranges from 200-975 µm in the current study.

Stratigraphic range: The species ranges from Chattian to early Zanclean at 752 and 1168 but only extends into the mid-Serravallian (mid-Miocene) at 1139.

Remarks: The largest chamber is usually in the middle part of the test and the last chamber is smaller than the penultimate one. Sometimes this difference is very pronounced. This species is cosmopolitan (Hayward, 2002).

Genus *Siphonodosaria* Silvestri, 1924

Siphonodosaria lepidula Schwager, 1866

Figure 3.4, 9a-b

1866 *Nodosaria lepidula* Schwager: p. 210, pl. 5, figs. 27, 28.

1978 *Stilostomella* ex.gr. *lepidula* (Schwager). Boltovskoy, pl. 7, fig. 33–36.

1980 *Stilostomella lepidula* (Schwager); Srinivasan and Sharma, p. 46, pl. 7, figs. 1-6.

1993 *Stilostomella lepidula* (Schwager); Gupta, 1993, text-fig. 2, 1-2.

1994 *Nodogenerina lepidula* (Schwager); Loeblich and Tappan, p. 133, pl. 261, figs. 18-20.

2002 *Siphonodosaria lepidula* f. *lepidula* (Schwager); Hayward, p. 305, pl. 3, figs. 25-32.

2012 *Siphonodosaria lepidula* (Schwager); Hayward et al., p. 174, pl. 18, figs. 6-20.

Description: Elongate, uniserial test, a slightly arcuate shape, with chambers gradually increasing in size. Chambers are spherical (campanulate or pyriform) and typically become more widely spaced later with pronounced depressed sutures. A ring of small spines, annularly arranged, surrounds the base of each otherwise relatively smooth-walled chamber. Aperture is terminal with a broad neck and phialine lip; there is small tooth in the middle of the aperture giving a v- shape appearance to aperture.

Dimensions: The species length ranges from 200-1350 µm in this study.

Stratigraphic range: The distribution at 752 and 1168 is Chattian to early Zanclean, and at 1139 is Chattian to early Tortonian.

Remarks: This species is abundant, with a cosmopolitan distribution (Hayward et al., 2012; Holbourn et al., 2013). It is also highly morphologically variable showing considerable variation in ornamentation, chamber shape and the presence or absence of a prolocular spine, and hence has been frequently recorded under a number of different names (Hayward et al. (2012). After detailed population-level investigations, Hayward et al. (2012) group the different morphotypes under *S. lepidula* is known from the Late Cretaceous to Pleistocene, reports of recent occurrences are considered reworked (Hayward et al., 2012).

Siphonodosaria subspinosa (Cushman, 1943)

Figure 3.4, 10a-d

1934 *Ellipsonodosaria* sp. Cushman and Jarvis: pl. 10, figs. 4, 5.

1943 *Ellipsonodosaria subspinosa* Cushman: p. 92, pl. 16, figs. 6, 7b.

1983 *Stilostomella subspinosa* (Cushman); Tjalsma and Lohmann, p. 36, pl. 14, figs. 16, 17.

1998 *Siphonodosaria subspinosa* (Cushman); Robertson, p. 180, pl. 67, fig. 3.

2010 *Siphonodosaria subspinosa* (Cushman); Hayward et al., p. 129, pl. 14, figs. 20, 21.

Description: Test elongate, uniserial, straight to slightly arcuate shape, circular in cross-section. Chambers are spherical, separated by strongly depressed sutures. Short spines cover the surface. Chambers show a relatively rapid increase in size towards the aperture creating a tapered test outline. The aperture is terminal with broad neck and phialine lip.

Dimensions: The species length ranges from 200-1125 μm in the current study.

Stratigraphic range: The distribution at 752 and 1168 is Chattian to early Zanclean, and at 1139 Chattian to early Tortonian.

Remarks: Specimens are very well preserved and abundant at Site 752. Holbourn et al. (2013) comment that this species shows large variability in the size and ornamentation of the test, with short spines commonly found on the test sometimes converging to form fine costae in the lower portion of the test. This is consistent with the observations in this study. Distribution is worldwide (Holbourn et al., 2013).

Genus *Stilostomella* Guppy, 1894

Stilostomella cf. *S. annulifera* Cushman and Bermúdez, 1936

Figure 3.4, 11a-b

cf. 1936 *Ellipsonodosaria annulifera* Cushman and Bermudez: p. 28, pl. 5, figs. 8, 9.

1978 *Stilostomella* cf. *S. annulifera* Wright: p. 717, pl. 8, fig. 2.

cf. 1990 *Stilostomella annulifera* (Cushman and Bermudez); Thomas, 1990, p. 590, pl. 1, fig. 4.

cf. 1998 *Siphonodosaria annulifera* (Cushman and Bermudez); Robertson, p. 178, pl. 66, figs. 1, 2.

Description: Test elongate, rectilinear, arcuate in overall shape, with a smooth wall texture. Chambers are inflated to sub-spherical. Sutures are limbate and shallow. Chambers become bigger and more elongated towards the apertural end. Aperture is terminal with phialine lip.

Dimensions: The species length ranges from 225-1250 µm in this study.

Stratigraphic range: The distribution of the species at 1139 is Chattian to early Tortonian and at 1168 and 752 from Chattian to early Zanclean.

Remarks: Specimens here largely lack the prolocular spine because of preservation (see Figure 3.4, 11a). This species is similar to *Strictocostella scharbergana* Neugeboren, 1856, but the last chamber of *S. annulifera* is slightly bigger and more inflated with a shorter neck. Some publications (e.g., Hayward et al., 2012) synonymise these two species and use S. *scharbergana*. *S. consobrina* differs from this species by having sutures which are flusher to the test, as shown in Holbourn et al (2013). It has also been observed that the chambers of this species are particularly large in those specimens recorded in the Mediterranean Sea (Wright, 1978). *S.* cf. *S. annulifera* has a cosmopolitan distribution (Holbourn et al., 2013) including records in the Mediterranean Sea (Wright, 1978) and Antarctica (Thomas, 1990). *S. annulifera* ranges from the early Eocene to middle Miocene (Holbourn et al., 2013), but *S. scharbergana* is considered to range from the early Paleocene to mid-Pleistocene (Hayward et al., 2012), more consistent with this extended younger occurrence.

Genus *Strictocostella* Patterson, 1987

Strictocostella matanzana (Palmer & Bermúdez, 1936)

Figure 3.4, 12a-c

1936 *Ellipsonodosaria*? *matanzana* Palmer & Bermúdez: p. 298, pl.18, fig.12.

1940 *Ellipsonodosaria matanzana* Palmer and Bermúdez; Palmer, pl.15, fig.1.

1957 *Siphononodosaria* cf. *matanzana* (Palmer and Bermúdez); Todd, pl.67, fig.7.

1975 *Stilostomella lepidula* Saidova: p. 315, plate 87, figure 6.

1998 *Siphonodosaria matanzana* (Palmer and Bermúdez); Robertson, pl.67, fig.2.

2007 *Myllostomella matanzana* (Palmer and Bermúdez); O'Neill et al., p. 1085, pl. 1, figs. 22-23.

2010 *Strictocostella matanzana* (Palmer and Bermúdez); Hayward et al., p. 128, figs.14:27-28.

2012 *Strictocostella matanzana* (Palmer and Bermúdez); Hayward et al., p. 190, pl. 22, figs. 10-20.

Description: Test elongate, uniserial, rectilinear. The base is composed of few small, spherical chambers which become larger and more elongate towards the aperture. Sutures are straight and depressed. There are small spines forming a ring towards the base of each chamber. The aperture is terminal with a phialine lip and short, broad neck ornamented by pustular spines.

Dimensions: The species length ranges from 200-750 µm in the current study.

Stratigraphic range: The species rarely occurs in the Chattian at Site 752, and it is not recorded in Aquitanian-Langhian but appears again from early Serravallian to Zanclean. At 1139 the distribution of the species is from Chattian to early Tortonian, it is not recorded at 1168.

Remarks: The wall of the neck is folded, giving an undulation to the phialine lip. *S. matanzana* has a cosmopolitan distribution; sister species tend to be more prevalent in the Indian Ocean (Hayward et al., 2012).

Strictocostella scharbergana (Neugeboren, 1856)

Figure 3.5, 1a-b

1856 *Dentalina scharbergana* Neugeboren: p.87, pl. 4, fig. 1-4.

1856 *Strictocostella scharbergana* Neugeboren, p.87, pl. 4, fig. 1-4.

1866 *Dentalina costai* Schwager: p. 229, pl. 6, fig. 62.

1884 *Nodosaria consobrina* (d'Orbigny); Brady, pl. 62, figs. 23, 24.

1936 *Ellipsonodosaria annulifera* Cushman and Bermúdez: p. 28, pl. 5, figs. 8, 9.

1960 *Stilostomella consobrina* (d'Orbigny); Barker, pl. 62, figs. 23, 24.

1977 *Siphonodosaria consobrina* (d'Orbigny); Nishimura et al. , pl. 4, fig. 16, 17.

1994 *Stilostomella consobrina* (d'Orbigny); Jones, 1994, pl. 62, figs. 23, 24.

2000 *Stilostomella scharbergana* (Neugeboren); Sztràkos, pl. 5, fig. 19.

2005 *Myllostomella costai* (Schwager); Hayward and Kawagata, pl. 1, figs. 17, 18.

2007 *Strictocostella costai* (Schwager); Hayward et al., fig. 2.

2010 *Strictocostella scharbergana* (Neugeboren); Hayward et al., p. 128, figs. 14: 28- 29.

2012 *Strictocostella scharbergana* (Neugeboren); Hayward et al., p. 192, pl. 23, figs. 8-19.

Description: Test arcuate, uniserial, slender. Proloculus spherical but chambers become more ovate towards the aperture. Surface smooth. Sutures flush or slightly incised. Aperture is terminal with a short neck and phialine lip; internal apertural rim consists of a long, simple tooth and multiple long, fine denticles.

Dimensions: The species length ranges from 200-1400 µm in the current study.

Stratigraphic range: The species range at 752A is Chattian to early Zanclean. This species is not recorded at 1168 and 1139.

Remarks: Wall smooth throughout, occasionally with one pustular spine near the base of the proloculus. Hayward et al. (2012) consider S. *scharbergana* conspecific with *Stilostomella consobrina*, and in many works is identified as S. *scharbergana* (e.g., Jones, 1994). Cosmopolitan distribution (Hayward et al., 2012).

Family **UVIGERINIDAE** Haeckel, 1894

Subfamily **ANGULOGERININAE** Galloway, 1933

Genus *Trifarina* Cushman, 1923

Trifarina angulosa (Williamson, 1858)

Figure 3.5, 2a-c

1858 *Uvigerina angulosa* Williamson: p. 67, pl. 5, fig. 140.

1960 *Angulogerina angulosa* (Williamson); Barker, pl. 74, figs. 15, 16.

1994 *Trifarina angulosa* (Williamson); Jones, p. 86, pl. 74, figs. 15, 16.

2013 *Trifarina angulosa* (Williamson); Holbourn et al., p. 559, figs. 1-4.

Description: The test is triserial in the early portion becoming uniserial later. Test cross-section is triangular with acute periphery. The chambers are moderately inflated and increase in size towards the apertural end. The sutures are curved and depressed. Wall ornamented by discontinuous longitudinal costae. The aperture is terminal, with a rounded opening atop a short neck, with lip and internal tooth plate.

Dimensions: The species length ranges from 150-775 µm in the current study.

Stratigraphic range: This species shows a staggered appearance; first appearing sporadically at Site 752 in the Chattian then in the Aquitanian at 1168, followed by the mid-Langhian at 1139. The last appearance is in the Tortonian at 1139 and in the Zanclean at 1168 and 752.

Remarks: Specimens from 1168 usually have the typical triangular cross-section with acute periphery but those from 1139 and particularly 752 often appear nearly rounded in cross-section and lack the acute margin. This species is typically recorded from the mid-Miocene to Recent (Jones, 1994). Thus, this study extends the species range back into the latest Oligocene. The species is found worldwide (Holbourn et al. (2013).

Trifarina bradyi Cushman, 1923

Figure 3.5, 3a-c

1923 *Trifarina bradyi* Cushman: p. 99, pl. 22, figs. 3, 9.

1884 *Rhabdogonium tricarinatum* d'Orbigny; Brady, p. 525, pl. 67, figs. 1, 3.

1960 *Trifarina bradyi* Cushman; Barker, pl. 67, figs. 1, 3.

1987 *Trifarina bradyi* Cushman; Loeblich and Tappan, p. 526, pl. 574, figs. 10- 13.

2013 *Trifarina bradyi* Cushman; Holbourn et al., p. 560, figs. 1, 2.

Description: Test initially triserial becoming rectilinear and uniserial later. Test tapered at both ends and relatively smooth later chambers. Distinctive triangular cross-section with an acute peripheral keel. Chambers are moderately inflated and increase in size towards the aperture,

separated by thick, strongly curved, depressed sutures. The aperture is terminal with short neck, lip and tooth plate.

Dimensions: The species length ranges from 125-575 µm in this study.

Stratigraphic range: At 1139 and 1168 the species is rare in the Chattian but is more consistently present from the Aquitanian disappearing in the mid Serravallian at 1139 and early Zanclean at 1169. The species at 752 is restricted to the Burdigalian through Serravallian (mid-Miocene).

Remarks: Inter-site differences are observed within this species in the Indian Ocean. Specimens from 752 and 1139 are quite similar, with the lower half of the test having longitudinal striations, while at 1168 there are denticles or small nodes (see Figure 3.5, 3a and b). Distribution is worldwide according to Holbourn et al. (2013) and it has previously been recorded from the eastern Indian Ocean by Nomura (1991). As with *T. angulosa* a much earlier, late Oligocene, occurrence for this species are found in the eastern Indian Ocean than previously reported (Jones, 1994).

Subfamily **UVIGERININAE** Haeckel, 1894

Genus *Siphouvigerina* Parr, 1950

Siphouvigerina hispida (Schwager, 1866)

Figure 3.5, 4a-c

1866 *Uvigerina hispida* Schwager: p. 249, pl. 7, fig. 95.

1938 *Uvigerina rustica* Cushman and Edwards: p. 83, pl. 14, fig. 6.

1980 *Euuvigerina hispida* (Schwager); Srinivasan and Sharma, pl. 7, figs. 14, 15.

2002 *Neouvigerina hispida* (Schwager); Hayward, p. 301, pl. 1, fig. 14.

2013 *Siphouvigerina hispida* (Schwager); Patarroyo and Martínez, p. 41.

2013 *Uvigerina hispida* Schwager; Holbourn et al. p. 592, fig. 1.

Description: Triserial, elongate, nearly fusiform-shaped test with a basal spine. Nearly circular in cross-section. Chambers are inflated to sub-globular, gradually increasing in size towards the aperture and separated by depressed sutures. The surface is densely ornamented by acicular to coarse papillae/spines. The aperture is terminal, rounded, with a short neck, a phialine lip and internal tooth plate.

Dimensions: The species length ranges from 175-875 μm in the current study.

Stratigraphic range: The species distribution at 752 is from early Serravallian to late Tortonian. At 1139 the species distribution is from Chattian to early Tortonian. At 1168, this species is very rare in the Chattian, but it is consistently present from the Aquitanian to early Zanclean.

Remarks: This species is generally larger at Site 1139 than at the other study sites. This species is cosmopolitan (Hayward (2002) and Holbourn et al. (2013)) and known from the early Miocene (Aquitanian) to recent. However, it occurs earlier (latest Oligocene) here in the eastern sector of the Indian Ocean.

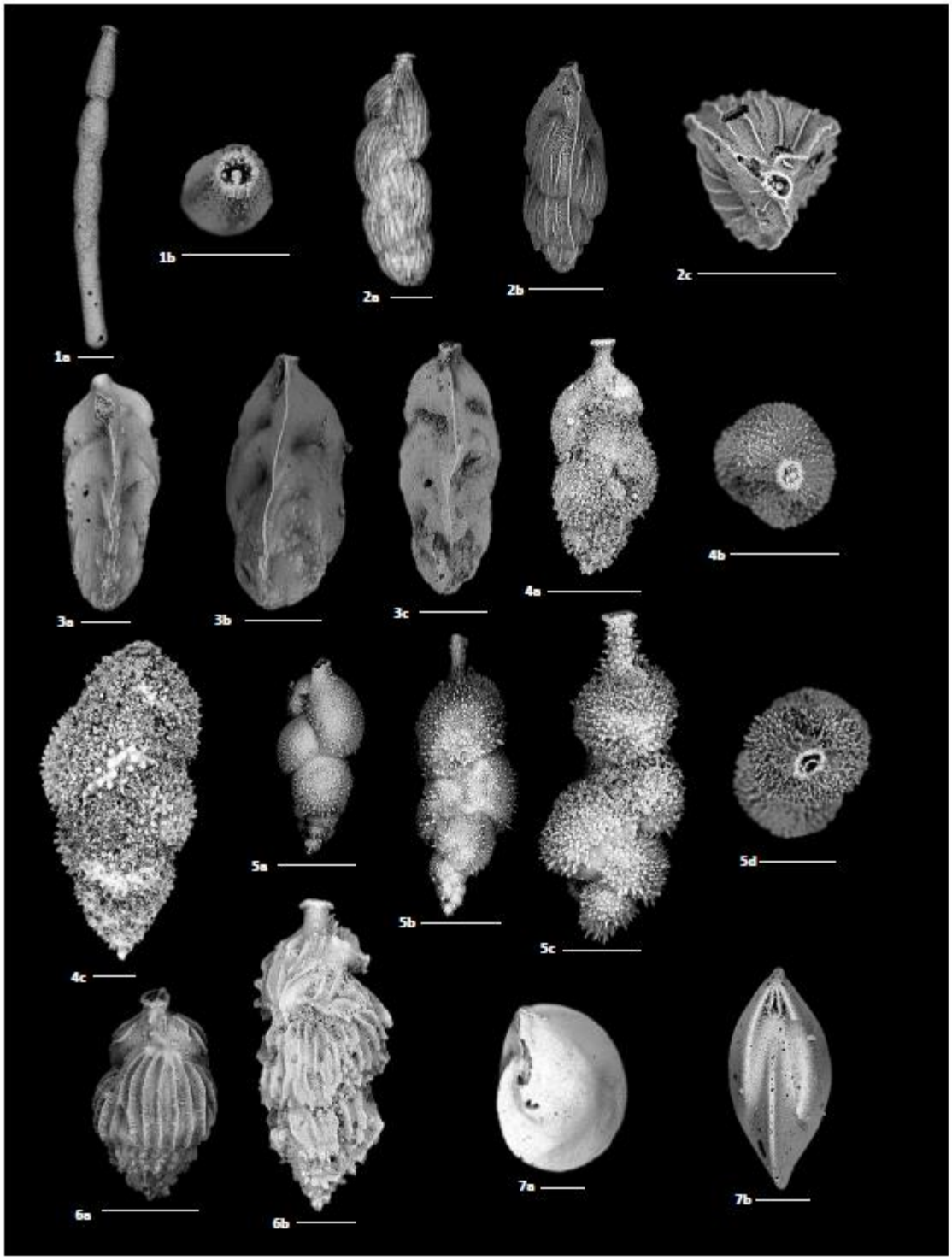


Figure 3. 5:

(Scale bar = 100 µm)

1a-b. *Strictocostella scharbergana*, 752A, 4H-1, 70-75cm: 1a. side view; 1b. aperural view.

2a-c. *Trifarina angulosa*, 2a. 752A, 6H-1, 70-75cm: side view. 2(b, c). 1168A, 23X-3, 74-78cm: 2b. side view; 2c. apertural view.

3a-c. *Trifarina bradyi*, 3a. 752A, 8H-6, 70-75cm: side view. 3b. 1168A, 15X-2, 76-80cm: side view. 3c. 1139A, 5R-1, 121-125cm: side view.

4a-c. *Siphouvigerina hispida*, 4a-b. 1168A, 20X-3, 100-104cm: 4a. side view; 4b. apertural view. 4c. 1139A, 7R-1, 111-115cm: side view.

5a-d. *Uvigerina auberiana*, 752A, 5a. 10H-2, 60-65cm: side view. 5b. 3H-5, 62-67cm: side view. 5(c, d). 4H-2, 81-85cm: 5c. side view; 5d. apertural view.

6a-b. *Uvigerina peregrina*, 6a. 752A, 9H-5, 65-70cm: side view. 6b. 1168A, 22X-2, 45-49cm: side view.

7a-b. *Lenticulina cultrata*, 752A, 10H-5, 77-81cm; 7a. side view; 7b. edge view.

Genus *Uvigerina* d'Orbigny, 1826

Uvigerina auberiana d'Orbigny, 1839a

Figure 3.5, 5a-d

1839 *Uvigerina auberiana d'Orbigny: p. 106, pl. 2, figs. 23, 24.*

1884 *Uvigerina asperula* Czjzek; Brady, p. 578, pl. 75, figs. 6, 8.

1884 *Uvigerina asperula* var. *auberiana* Brady, p. 579, pl. 75, fig. 9.

1978 *Uvigerina auberiana (d'Orbigny): Wright, p. 717,* pl. 8, fig. 10.

1984 *Uvigerina auberiana (d'Orbigny):* Lamb and Miller, p. 26, pl. 4, figs. 1-6.

2011 *Uvigerina auberiana (d'Orbigny): Kuppusamy, p. 69,* pl. 13, fig. 9.

2013 *Uvigerina auberiana (d'Orbigny):* Holbourn et al. p. 584, figs. 1-3.

Description: Test elongate, triserial, fusiform shape. Circular in cross-section. Depressed sutures, inflated chambers that gradually increase in size. Small spines usually cover the whole test. Aperture is terminal, rounded, with tubular neck, phialine lip and internal tooth plate.

Dimensions: The species length ranges from 200-525 µm in the current study.

Stratigraphic range: The species is only recorded at 752, from Aquitanian to early Zanclean.

Remarks: Some specimens are very densely covered in short spines, ranging all over the test and extending to cover the neck as well. The specimens in this study are relatively elongate (~2.5-3 times as long as broad) similar to the type material rather than the 2:1 ratio described by Holbourn et al. (2013). Cosmopolitan distribution according to Holbourn et al. (2013).

Uvigerina peregrina Cushman, 1923

Figure 3.5, 6a-b

1923 *Uvigerina peregrina* Cushman: p. 166, pl. 42, figs 7-10.

1926 *Uvigerina gardnerae* Cushman and Applin: p. 175, pl. 8, figs. 16, 17.

1984 *Uvigerina peregrina* Cushman; Lamb and Miller, p. 36-37, pl. 8, figs. 1-3; pl. 9, figs. 1-5.

1991 *Uvigerina peregrina* Cushman; Nomura, p. 55, pl. 1, fig. 10.

2013 *Uvigerina peregrina* Cushman; Hayward et al., p.442, pl.6, fig. 20.

Description: Test elongate, triserial. Chambers inflated, separated by depressed sutures. The test is ornamented by parallel, longitudinal costae. Aperture terminal, with phialine lip and short narrow neck.

Dimensions: The species length ranges from 175-700 µm in the current study.

Stratigraphic range: The range at 752 and 1139 is Chattian to Tortonian while at 1168 it ranges from Chattian to early Zanclean.

Remarks: The surface costae are usually non-continuous and parallel. The lower portion of the test is covered in isolated spines, which are randomly oriented, this is also in specimens shown in Lamb and Miller (1984) (ps. 34-37, pls. 8, 9). This species is cosmopolitan (Lamb and Miller 1984) with records including the Indian Ocean (Nomura, 1991) and New Zealand (Hayward et al., 2013).

Order LAGENIDA Lankester, 1885

Superfamily **NODOSARIACEA** Ehrenberg, 1838

Family **VAGINULINIDAE** Reuss, 1862

Subfamily **LENTICULININAE** Chapman, Parr, and Collins, 1934

Genus *Lenticulina* Lamarck, 1804

Lenticulina cultrata (Montfort, 1808)

Figure 3.5, 7a-b

1808 *Robulus cultratus* Montfort: p. 214.

1839 *Robulina canariensis* d'Orbigny: p. 127, pl. 3, figs. 3, 4.

1846 *Robulina similis* d'Orbigny: pl. 4, figs. 14, 15.

2013 *Lenticulina cultrata* Montfort; Hewaidy et al., p. 132, pl. 1, figs. 3a, b.

2016 *Lenticulina cultrata* Montfort; Amakrane et al., p. 103, pl.6, fig. 27.

Description: Test planispiral, involute, with peripheral keel. Lenticular shaped smooth test, circular in outline, biconvex in cross-section. Chambers are slightly inflated. Sutures are curved and flush to the test. The primary aperture is radiate and terminal.

Dimensions: The species length ranges from 150-1000 µm in the current study.

Stratigraphic range: The species distribution at 752 is Chattian to late Messinian. The species is only present in the early to mid-Burdigalian at 1139 and it is not recorded at all at 1168.

Remarks: This species is well-preserved and abundant at 752. It is known from the Indian Ocean (current study) and was noted from the West Pacific (Hanagata & Nobuhara, 2015) so could be considered to have a limited distribution.

Subfamily **MARGINULININAE** Wedekind, 1937

Genus *Amphicoryna* Schlumberger, in Milne-Edwards, 1881

Amphicoryna scalaris (Batsch, 1791)

Figure 3.6, 1a-b

1791 *Nautilus (Orthoceras) scalaris* Batsch: pp. 1, 4, pl. 2, fig 4a, b.

1826 *Nodosaria longicauda* d' Orbigny: p. 254.

1860 *Marginulina falx* Jones and Parker: p. 302.

1884 *Nodosaria scalaris* (Batsch); Brady, p. 510, pl. 63, figs. 28 –31.

1960 *Amphicoryna scalaris* (Batsch); Barker, p. 134, pl. 63, figs. 28 – 31.

2013 *Amphicoryna scalaris* (Batsch); Holbourn, p. 42, fig. 1.

Description: Test elongate, rectilinear, with a pronounced basal spine. Chambers are inflated, gradually increasing in size and separated by straight, depressed sutures. The wall is ornamented by long striations or fine ribs many of which are parallel and continuous in appearance. Aperture is terminal, radiate with ring-like ridges around the neck.

Dimensions: The species length ranges from 200-750 µm in this study.

Stratigraphic range: At 752 the species ranges from Chattian to Messinian. At 1139 and 1168 this species is very rare, occurring in the mid-Burdigalian at 1139, extending to the early Zanclean at 1168.

Remarks: This species is very well-preserved and recorded in highest abundance at 752. This species occurs worldwide according to Holbourn et al. (2013) and is commonly found in the Indian Ocean.

Order **ROTALIIDA** Lankester, 1885

Superfamily **ASTERIGERINACEA** d'Orbigny, 1839a

Family **EPISTOMARIIDAE** Hofker, 1954

Subfamily **NUTTALLIDINAE** Saidova, 1981

Genus *Nuttallides* Finlay, 1939

Nuttallides umbonifera (Cushman, 1933a)

Figure 3.6, 2a-d

1933a *Pulvinulinella umbonifera* Cushman: p. 90, pl. 9, fig. 9.

1884 *Truncatulina pygmaea* Hantken; Brady, p. 666, pl. 95, figs.9, 10.

1933a *Pulvinulinella umbonifera* Cushman: p. 90, pl. 9, fig. 9.

1960 *Eponides bradyi* Earland; Barker, pl. 95, figs. 9, 10.

1987 *Nuttallides umbonifera* (Cushman); Miller and Katz, p. 136, pl. 5, fig. 5.

1994 *Osangulariella umbonifera* (Cushman); Jones, p. 99, pl. 95, figs. 9, 10.

1995 *Nuttallides umboniferus* (Cushman); Nomura, p. 276, pl. 3, fig. 2.

Description: Lenticular, trochospiral form. Unequally biconvex test with a sub-acute peripheral keel. About twelve crescentic chambers in the final whorl, separated by slightly depressed, arcuate to sinuous sutures on the umbilical side and oblique sutures on the spiral side. Aperture is an intero-marginal slit extending from the umbilical boss towards the periphery.

Dimensions: The species length ranges from 100-750 µm in the current study.

Stratigraphic range: The range of the species is Chattian to Tortonian at 1139 and 752. At 1168 it ranges from Chattian to early Zanclean.

Remarks: This species is characterised by an imperforate umbilical boss. *Nuttallides umbonifera* (Cushman) is often employed as an indicator of Antarctic Bottom Water (AABW) in the Pacific and Indian Oceans (Corliss, 1979b). This species is long-ranging and distributed worldwide Mackensen et al. (1990) believed that the species is associated with carbonate

corrosive bottom water masses in the Weddell Sea. Distribution worldwide according to Holbourn et al. (2013) and found throughout the Indian and Southern Oceans (Mackensen, 1992).

Superfamily **CHILOSTOMELLACEA** Brady, 1881

Family **GAVELINELLIDAE** Hofker, 1956a

Subfamily **GAVELINELLINAE** Hofker, 1956a

Genus *Gyroidinoides* Brotzen, 1942

Gyroidinoides soldanii (d'Orbigny, 1826)

Figure 3.6, 3a-b

1826 *Gyroidina soldanii* d' Orbigny: p. 278.

1846 *Gyroidina soldanii* d' Orbigny; d' Orbigny, pl. 8, figs. 10-12.

1978 *Gyroidina soldanii* d' Orbigny; Wright, p. 715, pl. 5, figs. 7-9.

1992 *Gyroidinoides soldanii* d' Orbigny; Mackensen, p. 668, pl. 5, figs. 9, 10.

1994 *Gyroidinoides soldanii* d' Orbigny; Jones, p. 106, pl. 107, figs. 6, 7.

Description: Test trochospiral, planoconvex. The umbilical side is involute and convex, and the spiral side is flat and evolute. It has a rounded periphery. Chambers are inflated, separated by slightly depressed sutures that are straight on umbilical side but curved on spiral side. The surface is smooth. The aperture is a narrow intero-marginal slit, extending from umbilicus to the periphery. The umbilicus is open.

Dimensions: The species length ranges from 100-750 μm in this study.

Stratigraphic range: This species occurs in the Chattian at all three sites, ranging to the early Zanclean at 752 and 1168, and the early Tortonian at 1139.

Remarks: Most of the specimens observed in this study have a planar or slightly convex spiral side, and relatively small chambers in the last whorl on the spiral side. Distribution worldwide according to Holbourn et al. (2013). This species is now considered a junior synonym of *Hansenisca soldanii* (Hayward, et al., 2019b) in the World Register of Marine Species (WoRMS).

Gyroidinoides sp.1

Figure 3.6, 4a-b

Description: Test is trochospiral, plano-convex. The spiral side is flat and evolute, while the umbilical side is convex and involute. Chambers are generally inflated separated by slightly depressed sutures on both umbilical and spiral sides. The aperture is an interio-marginal slit extending from umbilicus to periphery. The surface is smooth.

Dimensions: The species length ranges from 100-550 µm in this study.

Stratigraphic range: The species is rare at 752 only occurring in the mid Serravallian and early Zanclean. At 1139 the species ranges from Chattian to early Tortonian. At 1168 it is very rare in the Chattian, with a more common range from early Burdigalian to early Zanclean.

Remarks: The chambers are more elongate and larger on the spiral side than in *Gyrodinoides soldanii* and it lacks the open, narrow umbilicus of *G. soldanii* and *G*. sp 2. The distribution of the species may be restricted to the current study (southern Indian Ocean). The stratigraphic range overlaps with that of *G. soldanii*.

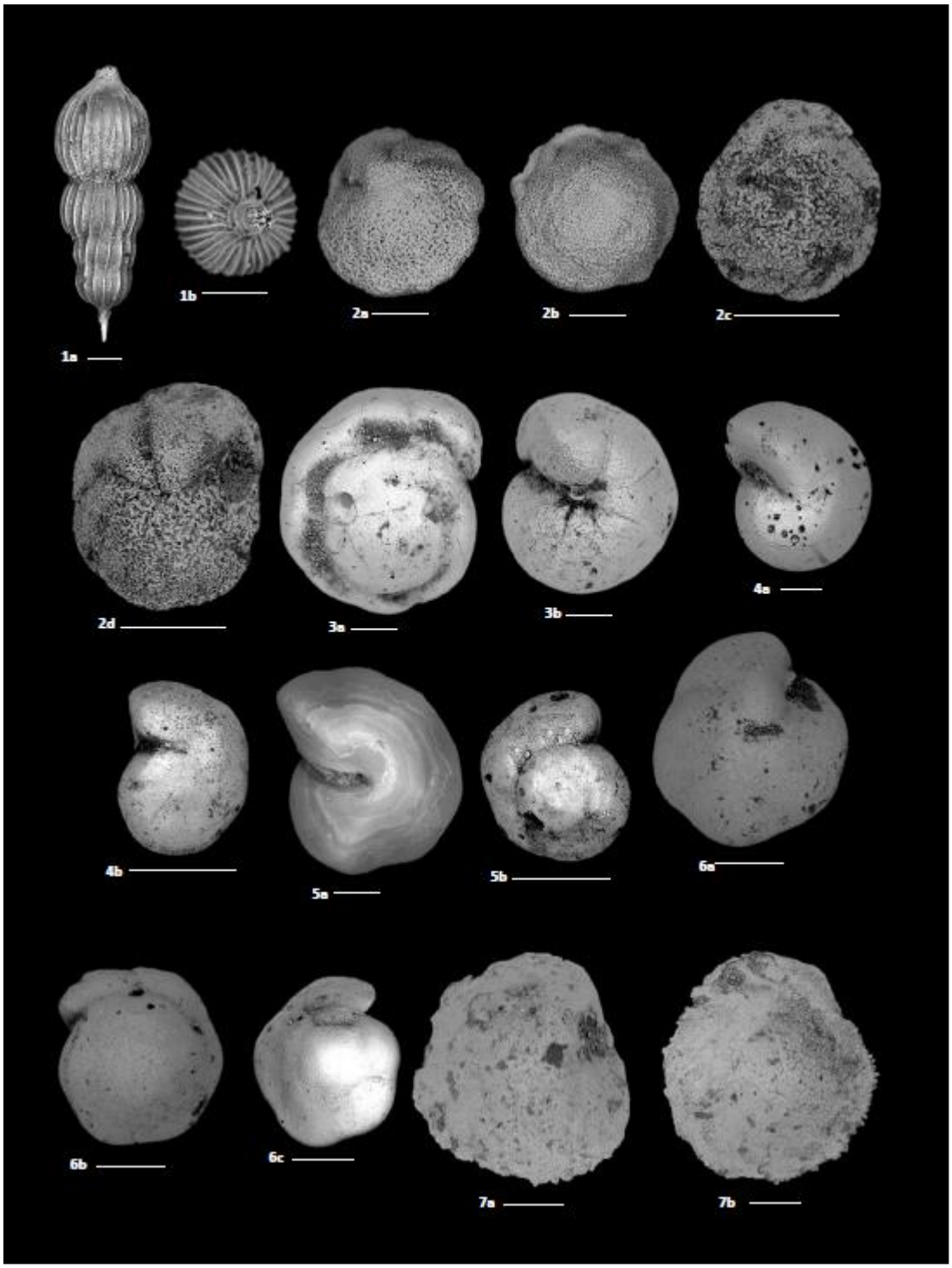


Figure 3. 6:

(Scale bar = 100 µm)

1a-b. *Amphicoryna scalaris*, 752A, 1a. 10H-5, 77-81cm: side view. 1b. 8H-1, 100-105cm: apertural view.

2a-d. *Nuttalides umbonifera*, 2a. 752A, 4H-5, 64-69cm: umbilical view. 2b. 752A, 9H-5, 65-70cm: spiral view. 2c. 1168A, 13X-1, 40-44cm: spiral view. 2d. 1168A, 14X-4, 45-49cm: umbilical view.

3a-b. *Gyroidinoides soldanii*, 1139A, 3R-4, 32-36cm: 3a. spiral view; 3b. umbilical view.

4a-b. *Gyroidinoides* sp.1, 1139A, 4a. 19R-2, 60.5-64.5cm: umbilical view. 4b. 17R-3, 91-95cm: spiral view.

5a-b. *Gyroidinoides* sp.2, 5a. 1168A, 32X-4, 80-84: umbilical view. 5b. 1139A, 15R-4, 41-45cm: spiral view.

6a-c. *Oridorsalis umbonatus*, 6a-b. 1168A, 8H-1, 100-104cm: 6a. umbilical view; 6b. spiral view. 6c. 752A, 5H-1, 65-70cm: spiral view.

7a-b. *Osangularia culter*, 1168A, 28X-3, 75-79cm: 7a. umbilical view; 7b. spiral view.

Gyroidinoides sp.2

Figure 3.6, 5a-b

Description: The test is trochospiral, planoconvex. Sutures flush to slightly depressed on the spiral side, while slightly depressed on the umbilical side. Aperture is slit-like extending from umbilicus to periphery. The aperture has a long crescentic flap covering the umbilicus.

Dimensions: The species length ranges from 100-400 µm in the current study.

Stratigraphic range: Species ranges from Chattian to mid- Serravallian at 1139 and Chattian to early Zanclean at 1168. This species is not recorded at 752.

Remarks: This species differs from *Gyroidinoides soldanii*, by having larger chambers on the spiral side, which is also more convex. *Gyroidinoides* sp.1 has slightly more inflated chambers on the spiral side and a shorter, more curved apertural slit than this species. This species may be restricted to the current study area (southern Indian Ocean).

Family **ORIDORSALIDAE** Loeblich and Tappan, 1984

Genus *Oridorsalis* Andersen, 1961

Oridorsalis umbonatus (Reuss, 1851)

Figure 3.6, 6a-c

1851 *Rotalina umbonata* Reuss: p. 75, pl. 5, fig. 35.

1884 *Pulvinulina umbonata* (Reuss); Brady, p. 695, pl. 105, fig. 2.

1884 *Truncatulina tenera* Brady: p. 665, pl. 95, fig. 11.

1932 *Eponides umbonata* (Reuss); Nuttall, p. 26, pl. 6, figs. 4, 5.

1983 *Oridorsalis umbonatus* (Reuss); Tjalsma and Lohmann, p. 18, pl. 6, fig. 8.

1988 *Oridorsalis umbonata* (Reuss); Whittaker, p. 137, pl. 19, figs. 1-3.

2011 *Oridorsalis umbonatus* (Reuss); Kuppusamy, p. 59, pl. 8, figs. 23, 24.

Description: Test trochospiral, lenticular, unequally biconvex, and nearly circular in outline. The convexity of the spiral side is greater than the umbilical side. Involute in umbilical and evolute in spiral side. Six nearly inflated chambers in the last whorl. Sutures usually slightly depressed, curved on umbilical side and radial on spiral side. The test is smooth. The aperture is an interiomarginal slit, extending from periphery to umbilicus.

Dimensions: The species length ranges from 100-750 µm in this study.

Stratigraphic range: The stratigraphic distribution of the species is Chattian to early Zanclean at 752 and 1168, Chattian to early Tortonian at 1139.

Remarks: This species generally has six chambers, some specimens possess seven chambers, in the last whorl. This species is easily identifiable, long-ranging from the Paleocene to Recent, and is common worldwide Holbourn et al. (2013).

Genus *Osangularia* Brotzen, 1940

Osangularia culter (Parker & Jones, 1865)

Figure 3.6, 7a-b

1865 *Planorbulina farcta* var. *ungeriana* subvar. *culter* Parker and Jones: pp. 382, 421, pl. 19, fig. 1.

1866 *Anomalina bengalensis* Schwager, p. 259, pl. 7, fig. 111.

1884 *Truncatulina culter* (Parker and Jones); Brady, p. 668, pl. 96, fig. 3.

1953 *Osangularia culter* (Parker and Jones); Phleger et al., p. 42, pl. 9, figs. 11– 16.

1960 *Osangularia bengalensis* (Schwager); Barker, pl. 96, fig. 3.

1994 *Osangularia bengalensis* (Schwager); Jones, p. 100, pl. 96, fig. 3.

Description: Test is trochospiral, lenticular, unequally biconvex, the umbilical side is more convex than spiral side. The umbilical side is involute, while the spiral side is evolute. Acute periphery with a serrated keel. The slightly inflated nearly ten chambers, separated by slightly

elevated, curved sutures on the spiral side, and straight with slightly depressed sutures on umbilical side. The test is smooth with some perforation in the chambers on spiral side. Aperture is slit-like interiomarginal, extending from umbilicus to periphery.

Dimensions: The species length ranges from 125-1000 µm in the current study.

Stratigraphic range: The range of the species is Chattian to early Zanclean at 752, Chattian to early Tortonian at 1139. At 1168 it ranges from Aquitanian to Langhian, and then mid Tortonian to early Zanclean.

Remarks: *Osangularia culter* is one of several species dominating intermediate water assemblages in the Miocene (Woodruff, 1985). Distribution cosmopolitan (Holbourn et al. (2013).

Superfamily DISCORBACEA Ehrenberg, 1838

Family ROSALINIDAE Reiss, 1963

Genus *Gavelinopsis* Hofker, 1951a

Gavelinopsis lobatulus (Parr, 1950)

Figure 3.7, 1

1913 *Discorbina praegeri* (Heron-Allen and Earland): p. 122, pl. 10, figs. 8-10.

1950 *Discorbis lobatulus* Parr: p. 354, pl.13, figs. 23-25.

1960 *Gavelinopsis lobatulus* (Parr); Barker, p. 182, pl. 88, figs. 1a-c.

2011 *Gavelinopsis lobatulus* (Parr); Kuppusamy et al., p. 52, pl. 5, figs 2, 3.

Description: Test trochoid. The periphery is thickened, keeled. Five slightly inflated chambers in the last whorl. Nearly flush sutures on the spiral side, with slightly depressed sutures on umbilical side. The aperture is an interiomarginal slit extending from umbilicus to periphery, having a narrow lip.

Dimensions: The species length ranges from 125-375 μm in the current study.

Stratigraphic range: The stratigraphic distribution is early Langhian to early Zanclean at 752 and mid-Burdigalian to Mid-Serravallian at 1139. This species is not recorded at 1168.

Remarks: Most of the specimens of this species are characterised by an umbilical plug and sharp periphery. Recorded from the Indian and Southern oceans including the Kerguelen Plateau (Mackensen, 1992) and eastern Indian Ocean (Nomura, 1991). This species is considered a subjective junior synonymy of *Gavelinopsis praegeri* (Hayward et al., (2019c) in WoRMS).

Family **SPHAEROIDINIDAE** Cushman, 1927

Genus *Sphaeroidina* d'Orbigny, 1826

Sphaeroidina bulloides d'Orbigny, 1828 in Deshayes, 1828

Figure 3.7, 2a-c

1828 *Sphaeroidina bulloides* d' Orbigny in Deshayes: p. 267.

1846 *Sphaeroidina austriaca* d' Orbigny: p. 284, pl. 20, figs. 19 – 21.

1848 *Sexloculina haueri* Czjzek: p. 149, pl. 13, figs. 35 – 38.

1884 *Sphaeroidina bulloides* d' Orbigny; Brady, p. 620, pI. 84, figs. 1, 2.

1949 *Sphaeroidina ciperana* Cushman and Todd: p. 67, pl. 12, fig. 14.

1949 *Sphaeroidina compacta* Cushman and Todd: p. 19, pl. 4, fig. 14.

1949 *Sphaeroidina compressa* Cushman and Todd: p. 20, pl. 4, figs. 15, 16.

1949 *Sphaeroidina nitida* Cushman and Todd: p. 20, pl. 4, fig. 13.

1953 *Sphaeroidina japonica* Asano: p. 19, pl. 2, figs. 43 – 44.

1985 *Sphaeroidina bulloides* d' Orbigny; Papp and Schmid, p. 96, pl. 90, figs. 7 – 12.

2013 *Sphaeroidina bulloides* d' Orbigny; Holbourn et al., p. 520, figs. 1- 3.

Description: Test is subglobular, usually three chambers in the final whorl. The test is variably coiled. Chambers are globular to hemispherical, separated by slightly depressed sutures. The wall is calcareous, imperforate and smooth. The aperture is a crescentic opening, bordered by a lip, occurring where the three last chambers meet.

Dimensions: The species length ranges from 125-725 µm in the current study.

Stratigraphic range: The stratigraphic distribution is Chattian to Zanclean at 752 and 1168, and Chattian to Serravallian at 1139.

Remarks: The larger specimens in the current study have a thick and opaque wall, smaller specimens are thinner-walled and appear translucent. Worldwide distribution according to Holbourn et al. (2013), including previous reports from the eastern Indian Ocean (Nomura, 1991).

Superfamily **DISCORBINELLACEA** Sigal in Piveteau, 1952

Family **DISCORBINELLIDAE** Sigal in Piveteau, 1952

Subfamily **DISCORBINELLINAE** Sigal in Piveteau, 1952

Genus *Laticarinina* Galloway and Wissler, 1927

Laticarinina pauperata (Parker & Jones, 1865)

Figure 3.7, 3a-b

1865 *Pulvinulina repanda* Fichtell and Moll var. *menardii* d' Orbigny, subvar. *pauperata* Parker and Jones: p. 395, pl. 16, figs. 50 – 51.

1884 *Pulvinulina pauperata* (Parker and Jones); Brady, p. 696, pl. 104, figs. 3-11.

1942 *Laticarinina bulbrooki* Cushman and Todd: p. 19, pl. 4, figs. 8, 9.

1942 *Laticarinina crassicarinata* Cushman and Todd: p. 18, pl. 4, figs. 11, 12.

1949 *Laticarinina pauperata* (Parker and Jones); Bermúdez, p. 309, pl. 23, figs. 43-45.

1953 *Laticarinina pauperata* (Parker and Jones); Phleger et al., p. 49, pl. 11, figs. 5, 6.

1991 *Laticarinina pauperata* (Parker and Jones); Nomura, p.55, pl. 1, fig. 6.

1992 *Laticarinina pauperata* (Parker and Jones); Mackensen, p. 668, pl. 2, figs. 1, 2.

2011 *Laticarinina pauperata* (Parker and Jones); Kuppusamy et al., p. 57, pl. 7, fig. 8.

Description: Test planoconvex, slightly trochoid. The spiral side is flat, the umbilical side is slightly convex. Chambers are inflated but becoming progressively more loosely coiled with a modest rate of enlargement. Chambers are cuneiform on the umbilical side and reniform on the spiral side and are separated by radial and slightly depressed sutures. Chambers on the

ventral side are radial, while in the dorsal side is much separated. Large, transparent peripheral keel around whole test, projecting in front of final chamber. Aperture is on the inner margin of last formed chamber.

Dimensions: The species length ranges from 175-1300 µm in the current study.

Stratigraphic range: The range of the species at 752 is Chattian to early Burdigalian and then again late Langhian to early Zanclean. At 1139 the species appears in the Chattian and later from the mid-Aquitanian to mid-Serravallian. At 1168, it is recorded from the mid- Aquitanian to mid-Messinian.

Remarks: Most specimens are easily distinguished by the presence of a very broad, transparent keel on the periphery.

Biogeography: This species has previously been reported from the eastern Indian Ocean (Nomura, 1991) and Kerguelen Plateau (Mackensen, 1992) but can be found worldwide (Holbourn et al. (2013).

Family **PSEUDOPARRELLIDAE** Voloshinova, 1952

Subfamily **PSEUDOPARRELLINAE** Voloshinova, 1952

Genus *Epistominella* Husezima and Maruhasi, 1944

Epistominella exigua (Brady, 1884)

Figure 3.7, 4a-b

1884 *Pulvinulina exigua* Brady: p. 696, pl. 103, figs. 13 – 14.

1951 *Pseudoparrella exigua* (Brady); Phleger and Parker, p. 28, pl. 15, fig. 6.

1994 *Pseudoparrella exigua* (Brady); Loeblich and Tappan, p. 146, pl. 307, figs. 1-7.

1951a *Pulvinulinella exigua* (Brady); Hofker, p. 322, text figs. 219-221.

1960 *Epistominella exigua* (Brady); Barker, pl. 103, figs. 13, 14.

1992 *Epistominella exigua* (Brady); Mackensen, p. 668, pl. 4, figs. 5, 6.

1994 *Alabaminoides exiguus* (Brady); Jones, p. 103, pl. 103, figs. 13, 14.

2011 *Epistominella exigua* (Brady); Kuppusamy et al., p. 50, pl. 4, figs 11, 12.

2013 *Epistominella exigua* (Brady); Holbourn et al., p. 240, figs. 1- 6.

Description: Test trochoid, unequally biconvex. Slightly convex spiral side, convex umbilical side. The periphery is acute. Five to six moderately inflated chambers in the last whorl, separated by curved, flush sutures on the spiral side and curved, depressed sutures on umbilical side. Aperture is an interiomarginal slit on the umbilical side extending to the face of the final and largest chamber.

Dimensions: The species length ranges from 100-275 µm in the current study.

Stratigraphic range: The species is rare at 752 ranging from early Langhian to early Zanclean. The range is Chattian to early Tortonian at 1139 and to early Zanclean at 1168.

Remarks The abundance of this species is employed as a proxy for constraining the flux of pulsed organic matter (Holbourn et al., 2013). This species is found worldwide including local to this study in the Timor Sea (Loeblich and Tappan, 1994), Kerguelen Plateau (Mackensen, 1992) and the Weddell Sea, Antarctic (Thomas, 1990).

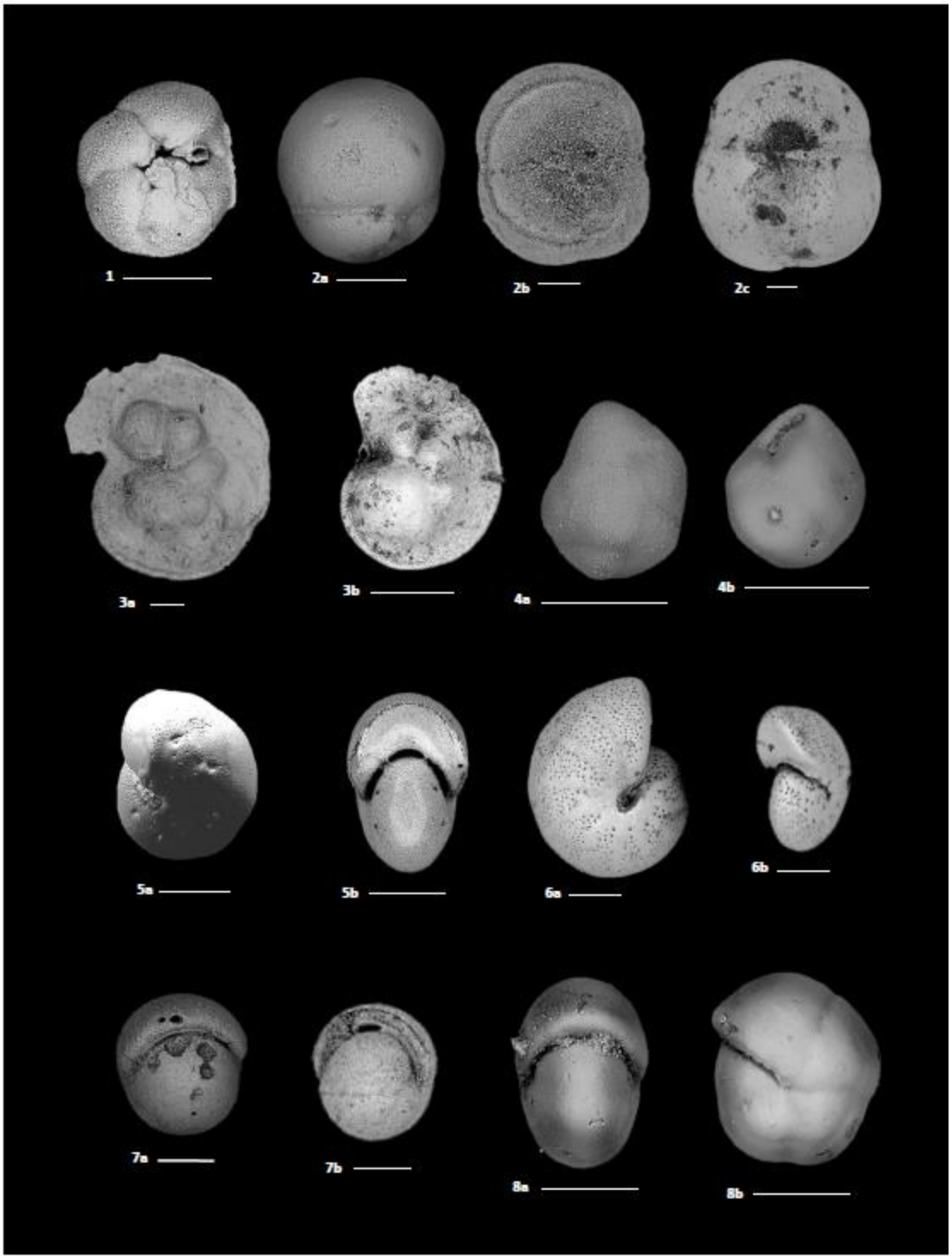


Figure 3. 7:

(Scale bar = 100 µm)

1. *Gavelinopsis lobatulus*, 752A, 3H-5, 62-67cm: umbilical view.

2a-c. *Sphaeroidina bulloides*, 2a. 752A, 8H-1, 100-105cm: side view. 2b. 1139A, 8R-1, 45-49cm: apertural side view. 2c. 1168A, 26X-2, 73-77cm: apertural side view.

3a-b. *Laticarinina pauperata*, 3a. 752A, 7H-2, 73-78cm: umbilical view. 3b. 1139A, 18R-1, 96-100cm: umbilical view.

4a-b. *Epistominella exigua*, 1168A, 36X-6, 62.5-66.5cm: 4a. spiral view; 4b. umbilical view.

5a-b. *Astrononion umbilicatulum*, 1139A, 5a. 19R-2, 60.5-64.5cm: side view. 5b. 17R-3, 91-95cm: edge view.

6a-b. *Melonis barleeanus*, 1139A, 6a. 4R-2, 105-109cm: side view. 6b. 19R-2, 60.5-64.5cm: edge view.

7a-b. *Pullenia bulloides*, 7a. 752A, 9H-5, 65-70cm: edge view. 7b. 1139A, 16R-2, 55-59cm: edge view.

8a-b. *Pullenia quinqueloba*, 1168A, 35X-1, 65-69cm: 8a. edge view; 8b. side view.

Superfamily **NONIONACEA** Schultze, 1854

Family **NONIONIDAE** Schultze, 1854

Subfamily **ASTRONONIONINAE** Saidova, 1981

Genus *Astrononion* Cushman & Edwards, 1937

Astrononion umbilicatulum Uchio, 1952

Figure 3.7, 5a-b

1952 *Astrononion umbilicatulum* Uchio: p. 36, pl. 32, fig. 1.

1978 *Astrononion umbilicatulum* Uchio; Wright, p.710, pl. 1, fig. 12.

2011 *Astrononion umbilicatulum* Uchio; Kuppusamy et al., p. 44, pl. 1, figs 7–9.

Description: Planispiral involute test. Periphery rounded, elliptical in lateral view. Chambers large and increasing gradually in size. Approximately seven to eight chambers in the last whorl, separated by curved, thickened radial sutures. Aperture is a narrow interiomarginal, crescentic slit, extending across the periphery to the umbilicus.

Dimensions: The species length ranges from 100-350 μm in the current study.

Stratigraphic range: The distribution of the species at 752 is early Aquitanian to early Zanclean and Chattian to early Zanclean at 1168. The range is Chattian to early Tortonian at 1139.

Remarks: The flaps that partially cover the sutures in the last whorl leave a small cavity beneath, which look like secondary chamberlets. This species was originally described from the lower Pleistocene of Japan (Uchio, 1952) but has not been widely reported from elsewhere. It is known from the Indian Ocean (current study), ODP Site 757 (Singh and Gupta, 2004), North West Atlantic Ocean (Kuppusamy et al., 2011) and the Mediterranean (Wright, 1978).

Subfamily **PULLENIINAE** Schwager, 1877

Genus *Melonis* de Montfort, 1808

Melonis barleeanus (Williamson, 1858)

Figure 3.7, 6a-b

1858 *Noniona barleeana* Williamson: p. 32, pl. 3, figs. 68, 69.

1930 *Nonion barleeanum* (Williamson); Cushman, p. 11, pl. 4, fig. 5.

1953 *Nonion barleeanum* (Williamson); Phleger et al., p. 30, Plate 6, Fig. 4.

1979 *Melonis barleeanum* (Williamson); Corliss, p. 10, pl. 5, fig. 78.

1987 *Melonis barleeanum* (Williamson); Loeblich and Tappan, pl. 696, figs. 5, 6.

1992 *Melonis barleeanus* (Williamson); Mackensen, p.668, pl. 5, fig. 2.

1997 *Melonis barleeanus* Williamson, 1858; Bergamin et al., p. 38, pl. 2, figs. 1-9.

Description: Test planispiral, bi-umbilicate, involute, compressed test. The umbilicus is open. The test is elliptical, elongated in lateral view, rounded periphery. Ten to eleven flattened chambers, separated by broad, flush sutures. The test is smooth and perforated. The aperture is an interiomarginal slit extending to the umbilicus, possessing an apertural lip.

Dimensions: The species length ranges from 150-600 μm in this study.

Stratigraphic range: The stratigraphic distribution of the species at 752 is split into two phases, early Langhian to mid-Serravalian and then again late Messenian to Zanclean. At 1139 it ranges from Chattian to mid-Tortonian while at 1168 it ranges from Chattian to Zanclean.

Remarks: Forms identified here have a prominent apertural lip distinguishing them from morphologically similar *Melonis affinis* separated out by some authors (see details in Holbourn et al., 2013). However, we consider the morphologically similar *Melonis affinis* synonymous with *M. barleeanus* following molecular analyses by Schweizer (2006).

Biogeography: The species is found worldwide, but Holbourn et al. (2013) suggest that it is not present at very high latitudes. The highest southern-recorded occurrence is on the Kerguelen Plateau by Mackensen (1992), which is supported by the current study observations.

Geuns *Pullenia* Parker & Jones, 1862 in Carpenter et al., 1862

Pullenia bulloides (d'Orbigny, 1846)

Figure 3.7, 7a-b

1826 *Nonionina bulloides* d'Orbigny: p. 293.

1884 *Pullenia sphaeroides* (d'Orbigny); Brady, p. 615, pl. 84, figs. 12, 13.

1945 *Pullenia bulloides* (d'Orbigny); Cushman and Todd, p. 64, Pl. 11, Fig. 5.

1949 *Pullenia bulloides* (d'Orbigny); Bermüdez, p. 276, Plate 21, Figs. 28-29.

1978 *Pullenia bulloides* (d'Orbigny); Wright, p. 716, pl. 7, fig. 7.

2011 *Pullenia bulloides* (d'Orbigny); Kuppusamy et al., p. 62, pl. 9, figs 18, 19.

Description: Test planispiral, involute, globular, sub-circular in outline. Four to five inflated chambers in the last whorl, separated by flush to slightly depressed sutures. Very compact test. Aperture is a narrow interiomarginal, crescentic slit, extending from the periphery to umbilicus.

Dimensions: The species length ranges from 125-425 µm in this study.

Stratigraphic range: The stratigraphic distribution of the species at 752 and 1168 is Chattian to Zanclean. At 1139 the species ranges from Chattian to mid-Tortonian.

Remarks: This species usually has a broad periphery and a smooth surface. Up to five chambers are present in the final whorl compared to four or five in the holotype and topotype specimens. Distribution is worldwide (Holbourn et al., 2013) including previous reports from the Indian Ocean by Nomura (1991) and (Singh and Gupta, 2004).

Pullenia quinqueloba (Reuss, 1851)

Figure 3.7, 8a-b

1851 *Nonionina quinqueloba* Reuss: p. 71, pl. 5, fi g. 31a, b.

1960 *Pullenia subcarinata* (d'Orbigny); Barker, pl. 84, figs. 14, 15.

1949 *Pullenia quinqueloba* (Reuss); Bermüdez, p. 276, Pl. 21, figs. 32, 33.

1983 *Pullenia quinqueloba* (Reuss); Tjalsma and Lohmann, p. 36, Pl. 16, fig. 2.

1987 *Pullenia quinqueloba* (Reuss); Miller and Katz, p. 138, Pl. 4, figs. 2a-b.

Description: Test planispiral, involute. Sub-globular, slightly compressed test, rounded periphery. Chambers are triangular, inflated. Five chambers present in the final whorl, separated by depressed and radial sutures. Aperture is a narrow crescentic, interiomarginal slit, extending from periphery to umbilicus.

Dimensions: The species length ranges from 125-500 µm in the current study.

Stratigraphic range: The range of the species at 752 is Chattian to Zanclean at 1139 Chattian to mid- Serravallian and at 1168 early Aquitanian to Zanclean.

Remarks: This species is distinguished from five chambered forms of *P. bulloides* by the more open coiling and less circular outline. This species is recorded worldwide (Holbourn et al., 2013) but is common in the continental shelf sediments of the Yellow Sea and the East China Sea (Lei and Li, 2016) and the Indian Ocean (Nomura, 1991; (Singh and Gupta, 2004).

Superfamily **PLANORBULINACEA** Schwager, 1877

Family **CIBICIDIDAE** Cushman, 1927

Subfamily **CIBICIDINAE** Cushman, 1927

Genus *Cibicidoides* Saidova, 1975

Cibicidoides bradyi (Trauth, 1918)

Figure 3.8, 1a-b

1918 *Truncatulina bradyi* Trauth, p. 235.

1884 *Truncatulina dutemplei* (d'Orbigny); Brady, p. 665, pl. 95, fig. 5.

1976 *Cibicidoides bradyi* (Trauth); Pflum and Frerichs, pl. 3, figs. 6, 7.

1994 *Gyroidina bradyi* (Trauth); Jones, p. 99, pl. 95, fig. 5.

2013 *Cibicidoides bradyi* (Trauth); Holbourn et al., p. 162, figs. 1- 6.

Description: Test trochospiral, unequally biconvex. The umbilical side is involute, and the spiral side is evolute, more convex. Nine inflated chambers in the last whorl, separated by radial curved sutures in the umbilical side, and oblique sutures in the spiral side. The aperture is a slit-like opening with lip extending from periphery to spiral side.

Dimensions: The species length ranges from 100-450 μm in this study.

Stratigraphic range: The species first appears in the Chattian and ranges to the Zanclean at 752 and 1168, at 1139 it ranges from Chattian to early Tortonian.

Remarks: Distinguished from *Cibicidoides robertsonianus* (Brady, 1881), with which it can be confused (Holbourn et al. (2013), by having fewer chambers (typically <10) in the last whorl,

smaller test and a more rounded periphery. Recorded worldwide (Holbourn et al., 2013), including from the central Indian Ocean by Boersma (1990). While this species is perhaps most commonly referred to as *C. bradyi* in the literature (e.g., Holbourn et al., 2013), accepted alternate names include *Parrelloides bradyi* and *Heterolepa bradyi* (Hayward et al., (2019d) in WoRMS database).

Cibicidoides mundulus (Brady, Parker & Jones, 1888)

Figure 3.8, 2a-c

1888 *Truncatulina mundula* Brady, Parker and Jones: p. 228, pl. 45, fig. 25a-c.

1953 *Cibicides kullenbergi* Parker in Phleger et al.: p. 49, pl. 11, figs. 7, 8.

1955 *Cibicidoides mundulus* (Brady, Parker and Jones); Loeblich and Tappan, p. 25, fig. 4a-c.

1960 *Cibicidoides mundulus* (Brady, Parker and Jones); Barker, pl. 95, fig. 6.

1992 *Cibicidoides mundulus* (Brady, Parker and Jones); Mackensen, p. 668, pl. 3, figs. 5-7.

Description: Unequally biconvex test, trochospiral. The umbilical side is more convex than the spiral side. Chambers are low, inflated, ten to twelve chambers in the last whorl, separated by curved sutures. The primary aperture is a long, narrow interiomarginal slit, extending from periphery to spiral side. The test is smooth on the umbilical side and highly perforated on the spiral side.

Dimensions: The species length ranges from 125-800 µm in this study.

Stratigraphic range: The stratigraphic distribution of the species at 752 and 1168 is Chattian to Zanclean. At 1139A it ranges from the Chattian to early Tortonian.

Remarks: The specimens here all show a pronounced umbilical boss, as also illustrated by Holbourn et al. (2013, p. 196, pl. 1-8), and Setoyama and Kaminski (2015, p. 14, fig. 5, pls. 4(a-c)). Common species found worldwide (Holbourn et al., 2013), including in the eastern Indian Ocean (Nomura, 1991) and Kerguelen Plateau (Mackensen, 1992).

Cibicidoides wuellerstorfi (Schwager, 1866)

Figure 3.8, 3a-c

1866 *Anomalina wuellerstorfi* Schwager: p. 258, pl. 7, figs. 105, 107.

1884 *Truncatulina wuellerstorfi* (Schwager); Brady, pp. 627, 662, pl. 93, figs. 8, 9.

1960 *Planulina wuellerstorfi* (Schwager); Barker, pl. 93, fig. 9.

1976 *Cibicides wuellerstorfi* (Schwager); Pflum and Frerichs, p. 116, pl. 4, figs. 2-4.

1994 *Cibicidoides wuellerstorfi* (Schwager); Jones, p. 98, pl. 93, figs. 8, 9.

2015 *Cibicidoides wuellerstorfi* (Schwager); Setoyama and Kaminski, p.14, fig.5, pls. 10a-c.

Description: Planispiral, to low trochospiral and plano-convex test. Up to twelve elongated and curved chambers in the last whorl; increasing rapidly in size. Peripheral keel so acute periphery. The sutures are depressed and strongly curved. The wall is coarsely perforate on the spiral side. The aperture is a narrow slit, having a narrow lip extending from the periphery to the spiral side.

Dimensions: The species length ranges from 125-1000 μm in the current study.

Stratigraphic range: The stratigraphic distribution of the coarse type at 752 is early Aquitanian to Tortonian and mid-Aquitanian to Zanclean at 1168. At 1139 it ranges from mid-Burdigalian to mid- Serravallian. The smooth type ranges from early Tortonian to Zanclean at 752. At 1139 it ranges from Burdigalian to Serravallian, while at 1168 it ranges from Aquitanian to Zanclean.

Remarks: This species has two different styles of test ornamentation as noted by Nomura (1991) in the eastern Indian Ocean (ODP Hole 754A) – a 'smooth' and a 'coarse' type. The smooth type (Figure 3.8, 4(a-c)) has a smooth umbilical side and is relatively inflated in the side view compared with the 'coarse' type which is highly adorned with nodes on the umbilical side and is more compressed in the side view. The smooth type is recorded at all three localities in the current study. The coarse type *Cibicidoides wuellerstorfi* has previously been assigned to three different genera: *Fontobia* (Schwager), *Planulina* Revets (1996) and *Cibicidoides*. Following the molecular phylogenetic studies of Schweizer (2006) and Schweizer et al. (2009, 2011) the latter genus has now been accepted and applied in the literature (Setoyama and Kaminski (2015). Worldwide distribution (Holbourn et al., 2013), widely reported in the Indian Ocean (e.g. Boersma, 1990; Nomura, 1991).

Family **PLANULINIDAE** Bermúdez, 1952

Genus *Planulina* d'Orbigny, 1826

Planulina costata (Hantken, 1875)

Figure 3.8, 5a-c

1875 *Truncatulina costata* Hantken: p. 73, pl. 9, figs. 2a-c.

1932 *Planulina wuellerstorfi* Schwager; Nuttall, p. 31, pl. 4, figs. 14, 15.

1979 *Planulina wuellerstorfi* Schwager; Sztràkos, p. 86, pl. 26, fig. 4.

1934 *Planulina marialana* Hadley: p. 27, pl. 4, figs. 4-7.

1941 *Planulina palmerae* van Bellen: in van Bellen et al., 1941, p. 1144, figs. 7-9.

1986 *Planulina costata* (Hantken); van Morkhoven et al., p. 212, pl. 72.

1991 *Planulina costata* (Hantken); Nomura, p. 55, pl. 4, figs. 5a-c.

Description: Low trochoid test. The spiral side is evolute and flattened. While the umbilical side is involute, slightly convex. Chambers number ten to twelve, with a low inflated shape, separated by slightly too highly curved sutures. The test is smooth on the umbilical side and highly perforated with small pores on the spiral side. Aperture is slit-like, peripheral, with a small lip extending towards the umbilicus.

Dimensions: The species length ranges from 150-1150 µm in the current study.

Stratigraphic range: This species only occurs at 752 where it ranges from early Aquitanian to early Serravallian.

Remarks: Van Morkhoven et al. (1986) considered that this species may have evolved from *Planulina cocoaensis* and that *P. costata* and *Planulina renzi* may have evolved separately through the Oligocene and early Miocene. The current species is similar to the 'smooth' form of *C. wuellerstorfi* in overall test shape and by having a smooth umbilical surface, but differs by having a smaller apertural opening, more compressed test and more irregular periphery. It is similar to *Planulina karsteni* (Petters and Sarmiento, 1956), but the spiral side of *P. karsteni* is slightly convex, while in *Planulina costata* it is plano-convex. Species is widely distributed (van Morkhoven et al., 1986) and has previously been recorded from the eastern Indian Ocean (Nomura, 1991).

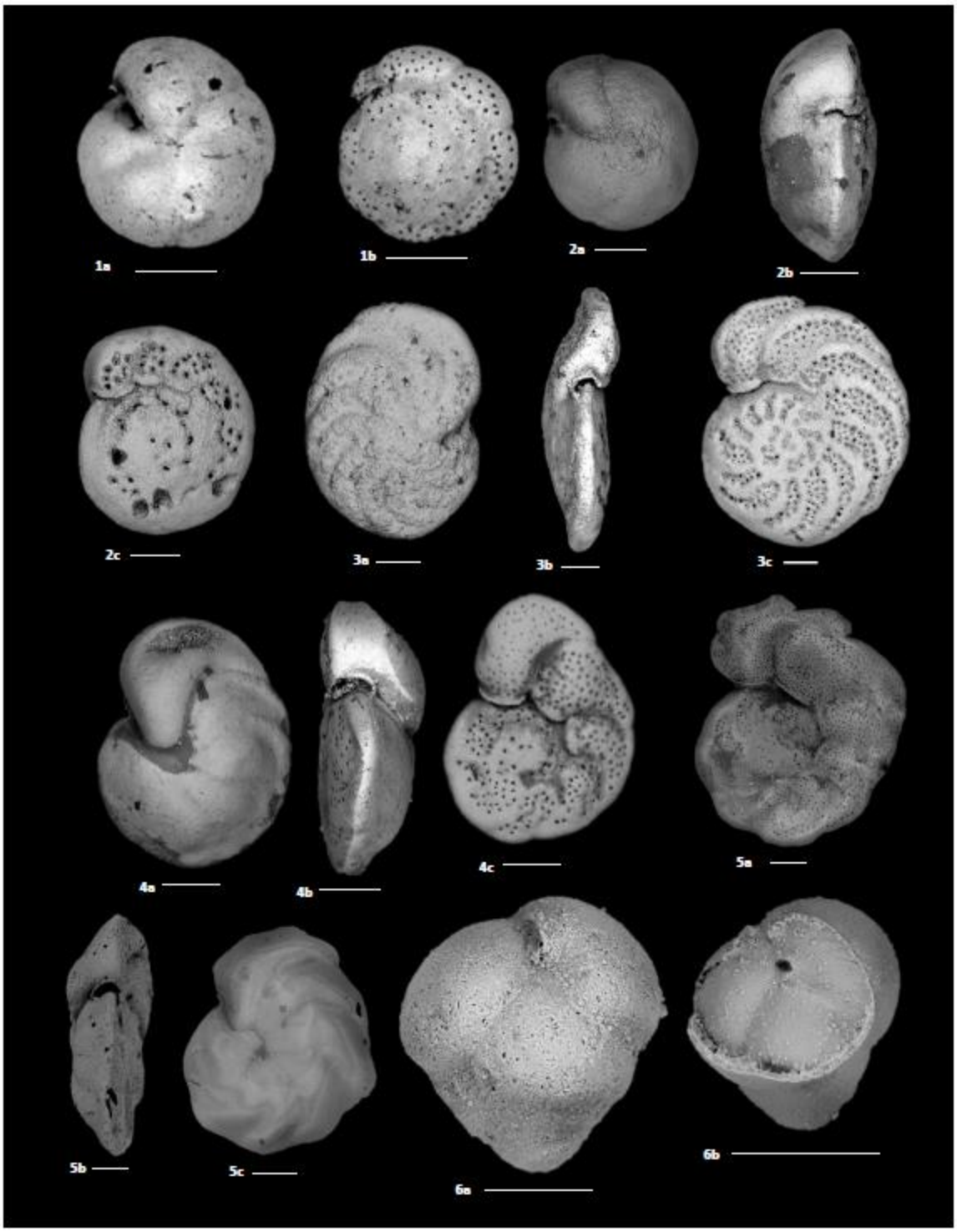


Figure 3. 8:

(Scale bar = 100 µm)

1a-b. *Cibicidoides bradyi*, 1139A, 1a. 9R-4, 105-110cm: umbilical view. 1b. 8R-1, 45-49cm: spiral view.

2a-c. *Cibicidoides mundulus*, 752A, 3H-1, 50-55cm: 2a. umbilical view; 2b. edge view; 2c. spiral view.

3a-c. *Cibicidoides wuellerstorfi*, (coarse) 752A, 7H-2, 73-78cm: 3a. umbilical view; 3b. edge view; 3c. spiral view.

4a-c. *Cibicidoides wuellerstorfi*, (smooth) 752A, 5H-1, 65-70cm: 4a. umbilical view; 4b. edge view; 4c. spiral view.

5a-c. *Planulina costata*, 7H-2, 73-78cm: 5a. spiral view; 5b. edge view; 5c. umbilical view.

6a-b. *Eggerella bradyi*, 1168A, 6a. 42X-3, 70-74cm: side view. 6b. 10H-2, 80-84cm: apertural view.

Order TEXTULARIIDA Lankester, 1885

Superfamily **TEXTULARIACEA** Ehrenberg, 1838

Family **EGGERELLIDAE** Cushman, 1937b

Subfamily **EGGERELLINAE** Cushman, 1937b

Genus *Eggerella* Cushman, 1933a

Eggerella bradyi (Cushman, 1911)

Figure 3.8, 6a-b

1911 *Verneuilina bradyi* Cushman: p. 54, fig. 87.

1937b *Eggerella bradyi* (Cushman); Cushman, p. 52, pI. 5, fig. 19.

1951 *Eggerella bradyi* (Cushman); Phleger and Parker, p. 6, pl. 3, figs. 1, 2.

1960 *Eggerella bradyi* (Cushman); Barker, pl. 47, figs. 4-7.

1987 *Eggerella bradyi* (Cushman); Loeblich and Tappan, p. 170, pl. 189, figs. 1, 2.

1991 *Eggerella bradyi* (Cushman); Nomura, p. 55, pl. 1, figs. 12(a,b).

Description: The test is trochoid in the initial portion, subsequently changing to a triserial arrangement. The test is nearly conical. Chambers are highly inflated, separated by depressed sutures. The wall is agglutinated, with calcareous cement. The aperture is a semi-circular slit, with narrow lip, located at the base of the last biggest chamber.

Dimensions: The species length ranges from 125-550 µm in the current study.

Stratigraphic range: The species ranges from the Chattian to Zanclean at 752 and 1168. At 1139 it ranges from Chattian to early Tortonian.

Remarks: This species is considered cosmopolitan (Kender et al. (2008) and has previously been recorded in the Miocene of the East Indian Ocean by Nomura (1991) and on the Kerguelen Plateau (Mackensen, 1992).

3.5 Summary

Benthic foraminiferal assemblages from ODP Sites 752, 1139 and 1168 were identified from the >63 um fraction for the late Oligocene through Pliocene. Assemblages are highly diverse comprising more than 200 species at each individual site. Hole 752A yielded 268 species, of which 143 do not occur at the other two sites, at 1139A 224 species were recorded, 92 of which only at that site and at 1168A, 331 species with 189 taxa not present at the two other

sites. The 52 most-abundant species, chosen as they represent at least 1% of the total fauna encountered in this study, are described, and illustrated here providing a useful reference work for the southern Indian Ocean.

Author contributions

DR has undertaken all sample processing, data collection and analyses under the supervision of IB and KE. All authors have contributed to the writing of the paper.

Competing Interests

The authors declare that they have no conflict of interest.

Acknowledgements

This research used samples and data provided by the International Ocean Discovery Program (IODP). The completion of this study could not have been possible without the support of HCED (The Higher Committee for Education Development in Iraq) supporting DR during the course of this work. The authors wish to thank Dr Chris Smart (University of Plymouth) for his useful discussions during this project.

Chapter Four

Foraminifera: Results and Discussion

4.1 Introduction:

Different parameters are used (Cluster analysis, Diversity, Benthic Foraminifera Accumulation Rate (BFAR) and Rarefaction curves) to examine deep-sea benthic foraminifera at the different ODP Sites of Indian Ocean (752A, 1168A and 1139A). Results of these parameters combined with abundance of dominant benthic foraminifera and high productivity taxa (*Bolivina*, *Bulimina*, *Uvigerina* and *Melonis* species). The above-mentioned parameters used to reveal significant palaeoceanographic changes in Indian Ocean during the late Oligocene, Miocene, and the early Pliocene.

Characteristic species of each clusters at the three studied sites are indicative of different nutrient and oxygen levels. For instance, the characteristic species of cluster A at 752A is *Ehrenbergina carinata*; this species is more indicative of high nutrient, low oxygenated environments, and high temperatures (Gupta and Satapathy, 2000). Both *Cibicidoides wuellerstorfi* (coarse type) and *Nuttalides umbonifera* in clusters C and D (752A) are associating with AABW (Antarctic Bottom Water) (Corliss, 1979a, Corliss, 1983).

The highest peak of *Trifarina angulosa* is recorded during the late Miocene at 1168A. *Trifarina angulosa* is species that indicate colder periods, and it has bloomed during the intensification

of bottom currents (Mackensen, 1992). *Oridorsalis umbonatus* (cluster A) (1139A) is indicative of well-oxygenated water, and it peaks during low organic conditions (Mackensen et al., 1985).

4.2 Results:

4.2.1 ODP Site 752 Hole A:

4.2.1.1 Cluster analysis:

The first sample 2H-4 (4.14 Ma) has the least similarity index of less than 0.2 (Figure 4.1), while cluster A has the highest similarity. Cluster (A) (See Appendix D) represents samples 3H-1 and 3H-2, both have an average diversity of 59. Cluster (B) is representing samples 3H-5- 5H-2 (six samples). Sample 3H-4 (6.62 Ma) is not making a direct cluster with clusters A & B while it is a part of a larger cluster that includes clusters A, B & C. Samples of cluster B have average diversity of 53.

Sample 5H-3 (10.23 Ma) does not make a direct cluster with adjacent clusters (B &C), while it is a part of the larger cluster including clusters A, B & C. Cluster C is represented by samples 5H-4- 6H-5 having average diversity of 66 benthic foraminifera species. Sample 6H-6 (12.83 Ma) forms one larger cluster at nearly 0.3 with clusters A, B & C and clusters D, E and F are grouped at around 0.3 as well. These two larger clusters are separated at around 12.83 Ma before they group to form one larger cluster at about 0.2. Sample 7H-6 (15.21 Ma) has not directly clustered with clusters D & E. Cluster D is composed of three samples (7H-1, 7H-2 & 7H-4), the diversity of these samples is 69, 94 and 67 species, respectively.

Cluster E is composed of four samples (8H-1- 9H-2) having an average diversity of 70 species per sample. Cluster F is composed of five samples (9H-4-10H-5). The average species diversity for this cluster (F) is 73 benthic species.

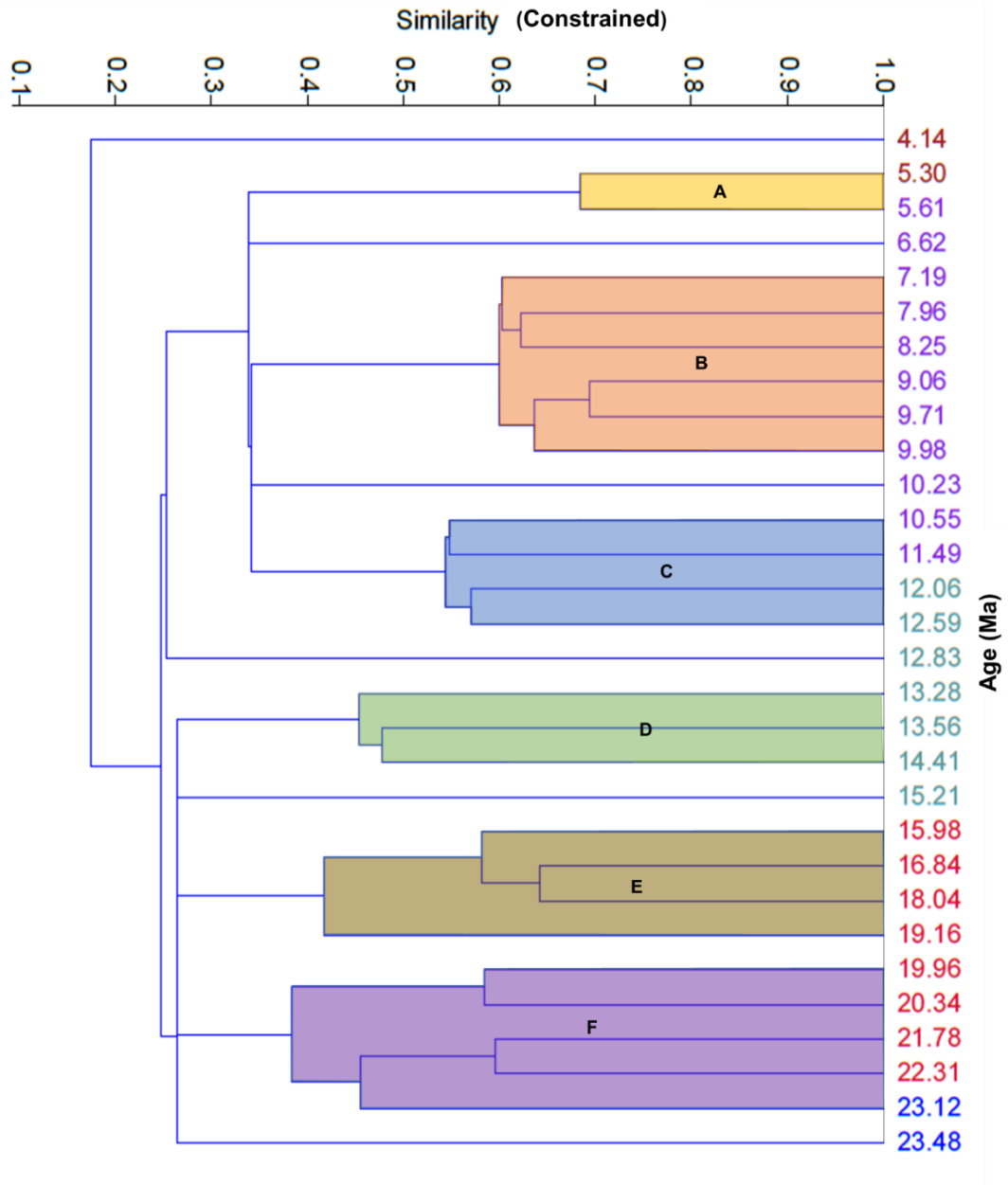


Figure 4. 1: Constrained cluster diagram of samples in the late Oligocene and Neogene (Miocene & early Pliocene) at the Site 752 Hole A, exhibiting the presence of six major cluster groups.

The above dendrogram (Figure 4.1) was mainly grouped into two major clusters, the first cluster group (A-C) which has higher similarity index than the second cluster group (D-F). These two groups were separated at 12.83 Ma (Serravalian). By comparing the diversity of two groups, the first group (Cluster A, B & C) have slightly declined in diversity which showing in species richness (Taxa_S) and the Shannon diversity curve. The drop is apparent especially in Cluster A and B until it starts to increase in Cluster A. However, the second Group (Cluster D, E & F) showing nearly the same inclination of diversity and higher trend than the first group (Cluster A, B & C) (Figure 4.2).

There are some species that each cluster is characterised with such as, *Bolivinellina* cf. *B. translucens* and *Ehrenbergina carinata* in cluster A, *Strictocostella scharbergana and Trifarina angulosa* in cluster B, *Bolivina viennensis*, *Cibicidoides wuellerstorfi* (coarse type) and *Burseolina pacifica* in cluster C, *Nuttalides umbonifera*, *Bolivina reticulata* and *Trifarina bradyi* in cluster D, *Lenticulina cultrata* and *Planulina costata* in cluster E and *Bolivina huneri* and *Nuttalides umbonifera* in cluster F.

The separation of cluster group (A-C) which has higher similarity index than the second cluster group (D-F) is shown by the differences between two assemblages (Figure 4.2) for example, the shifting from high Shannon-index assemblages (characterised by *Siphonodosaria, Nuttalides* and *Trifarina bradyi)* to lower Shannon-index assemblages (characterised by *C. wuellerstorfi and Trifarina angulosa*) at about 13 Ma (Figure 4.5).

4.2.1.2 Diversity:

Diversity indices curves were plotted versus age (See Appendix E). Shannon diversity index is used in the current study and compared with other parameters. Shannon diversity accounts both number of individuals and number of taxa. The species richness (Taxa_S) only represents the number of taxa counted in the studied samples. Dominance is ranged between 0 to 1 which 1 represent only 1 taxon dominated the community completely. The details of diversity indices can be found in Harper (1999).

Shannon index was high during the early Miocene and the early-mid Miocene until dropped suddenly at around 15.21 Ma. The highest peak of diversity has recorded in 13.56 Ma, and it started to decline gradually with fluctuations in the late Miocene until about 6.62 Ma. The diversity values slightly recovered and increased at 5.61 Ma (Figure 4.2).

The species dominance recorded the highest peak at around 10-8 Ma (Figure 4.2) coincided with the time when all diversity and evenness values decreased and, in some intervals, it reaches the lowest values.

4.2.1.3 Benthic Foraminifera Accumulation Rate (BFAR):

In the current study, the first peak of BFAR (See Appendix F) was in the late Oligocene (23.48 Ma) and it declined until it peaks again during the early Miocene at 19.16 Ma (Figure 4.3). The curve dropped again towards late early Miocene (15.98 Ma). From mid- Miocene towards late Miocene, the peak shows many fluctuations. Despite these fluctuations, the peak has an

increasing trend, starts from 13.56 Ma until 8.25 Ma. Three highest peaks had recorded from the mid- Miocene until the latest Miocene. The first peak was at 12.83 Ma, the second peak was at 10.23 Ma, and the last peak was at 6.62 Ma.

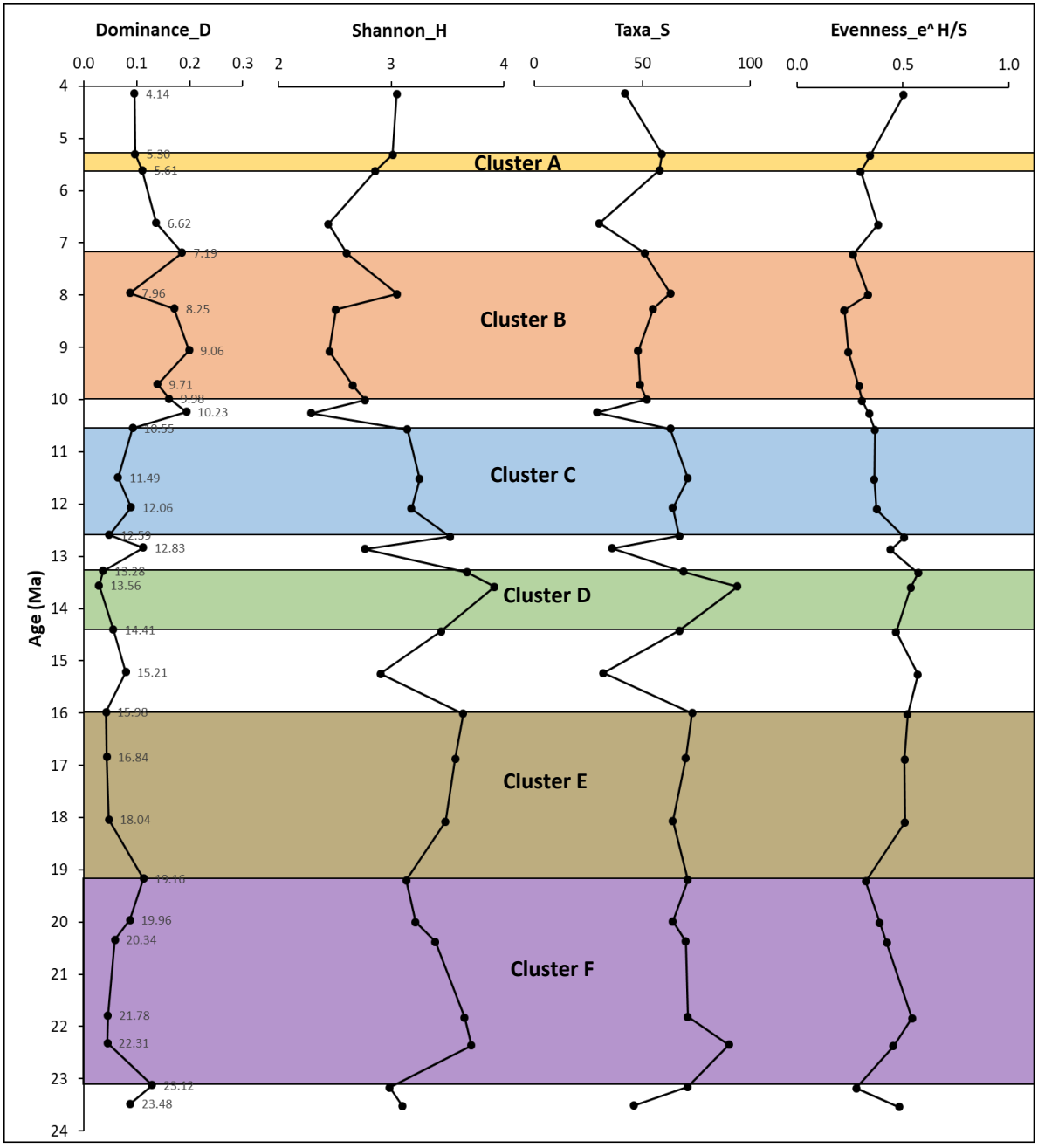


Figure 4. 2: Diversity indices, dominance, species richness and evenness at the Site 752 Hole A, the shaded area are six clusters formed from samples with similar composition, separated from each other in the places where diversity changed.

High productivity taxa calculated by adding the percentages of high productivity benthic taxa such as *Bolivina*, *Bulimina*, *Uvigerina* and *Melonis* species (See Appendix A). The first peak recorded at the latest Oligocene, while the highest peak during the early Miocene was around 19 Ma then the peak is dropped suddenly. The values started to increase during the early mid-Miocene with high fluctuations. The highest peak has recorded during the late Miocene starting from ~ 10 Ma and continued until around 5.6 Ma (Figure 4.3).

4.2.1.4 Rarefaction curves:

The reason for having the rarefaction curve is to examine samples completeness by comparing the relative composition of two or more samples. Rarefaction is used for comparing the diversity of two or more different sized samples (Hammer et al., 2001). One or more columns of counted individuals of different species are required, and samples must be taxonomically similar and from similar habitats (Hammer et al., 2001). Prothero (2013) supposed that rarefaction analysis used for comparing two different sized samples and make sure that the differences are real and not caused by the sampling process.

As shown in the plot below the diversity increased rapidly at the beginning until it becomes more flattened when fewer new taxa added. From the curves below (Figure 4.4) it is shown that the diversity of most of the samples shows the range between ~45-70 taxa except for a few samples, at 13.56 and 22.31 Ma. Most of the curves become more flattened around 400-600 specimens; it shows that this range of counting may apply for most of the samples at the current study.

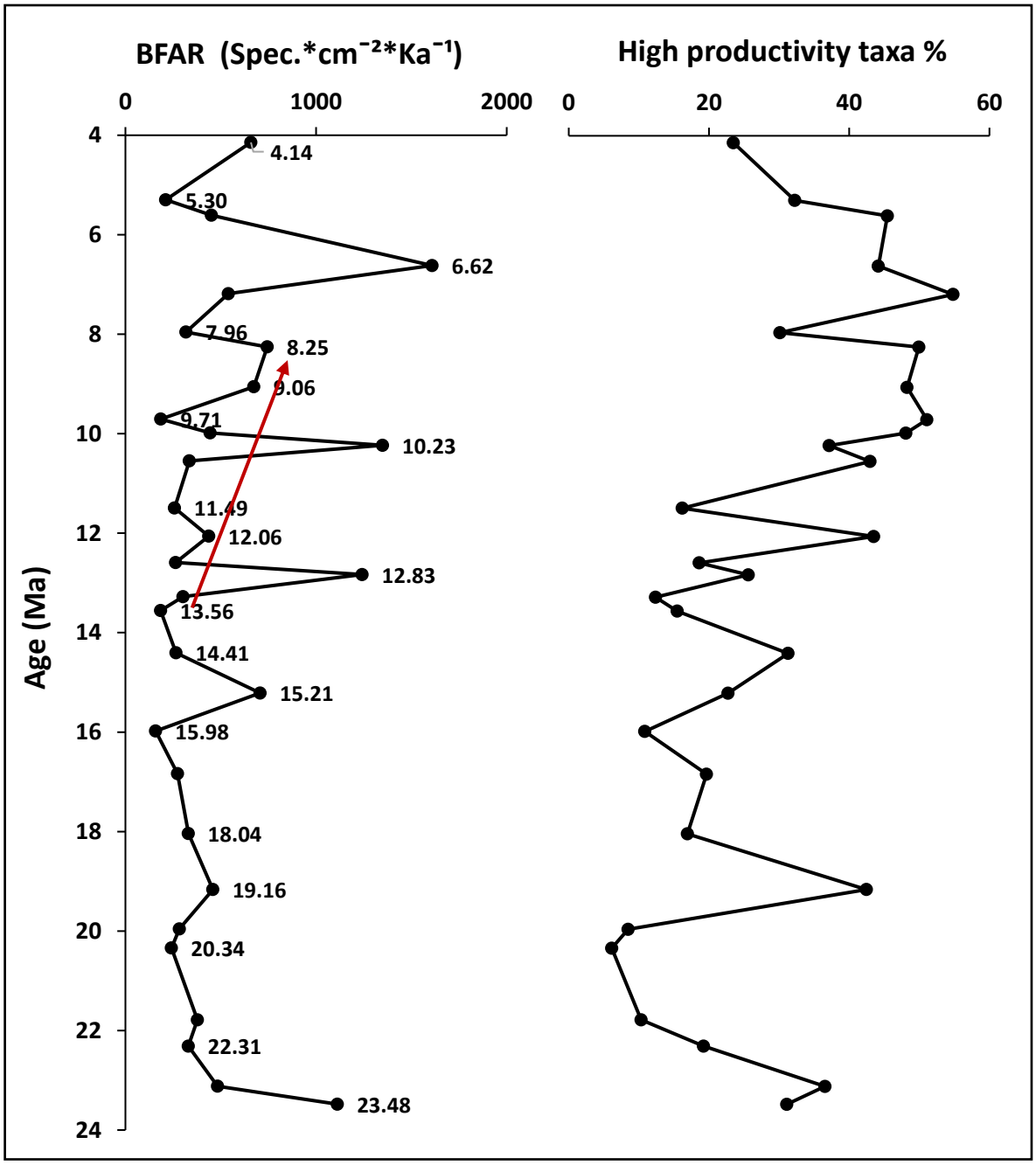


Figure 4. 3: Benthic Foraminifera Accumulation Rate (BFAR) and High productivity taxa relative abundance versus age at Hole 752A. The red arrow points to an increasing trend of BFAR values.

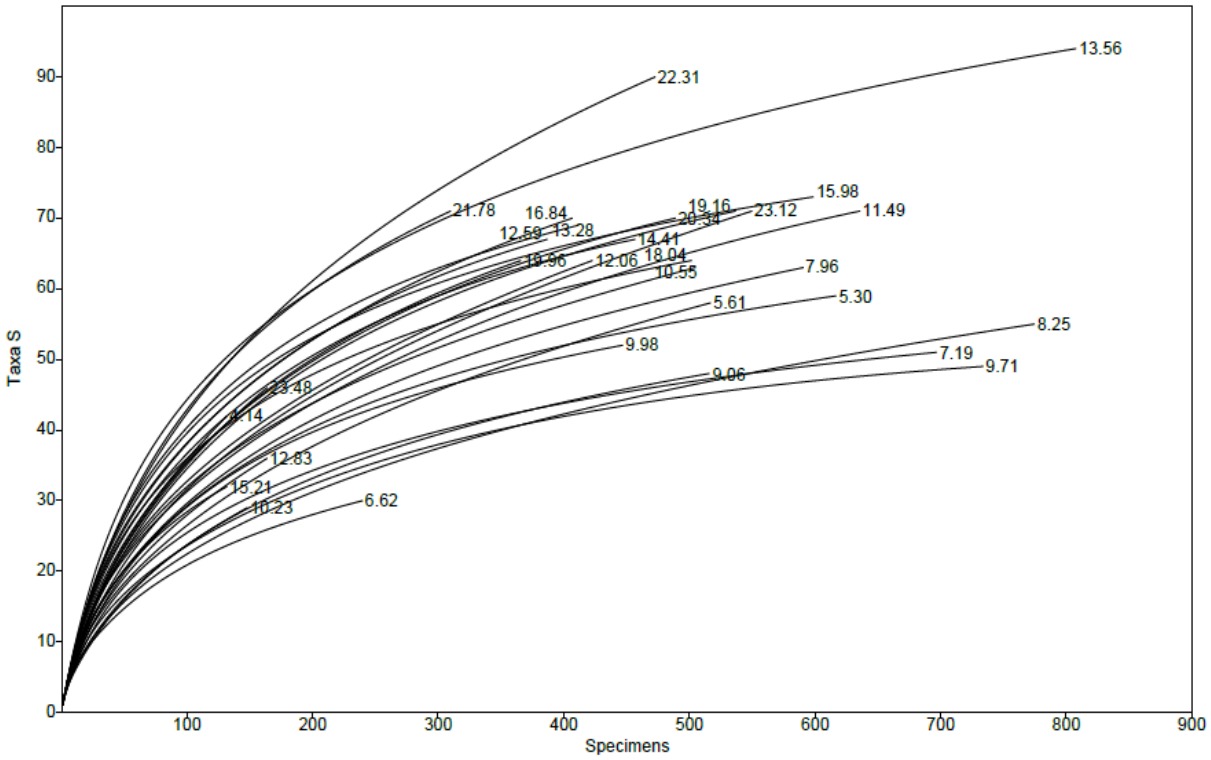


Figure 4. 4: Rarefaction curve of the thirty samples at the Site 752 Hole A. The numbers on each curve represent the Age (Ma). The vertical axis is species diversity, and the horizontal axis is the number of collected specimens.

4.2.1.5 Faunal composition:

The relative abundance of thirteen most abundant species are plotted and compared with both BFAR and diversity (Shannon_H) (Figure 4.5). These relative species abundances have increased and decreased during Latest Oligocene, Miocene, and early Pliocene. Some species have peaked during late Oligocene-early Miocene, such as *Globocassidulina subglobosa* and *Strictocostella scharbergana*. In the early Miocene species like *Nuttalides umbonifera*, *Astrononion umbilicatulum* and *Globocassidulina subglobosa* are peaked then rapidly declined at 19.16 Ma at the same time BFAR slightly recorded higher value, and the diversity dropped suddenly.

After 19.16 Ma species like *Siphonodosria subspinosa*, *Trifarina bradyi* and *Globocassidulina subglobosa* started to peak. At the time when the maximum value of diversity recorded (13.56 Ma) the first peak of *Cibicidoides wuellerstorfi* (coarse type) and *Trifarina angulosa* are recorded, and the highest peak of *Astrononion umbilicatulum* is also recorded. Most of the species abundance decreased and dropped suddenly at around 12.83 Ma except some species such as *Bulimina truncana* and *Astrononion umbilicatulum*.

The diversity started to decline again after it shows the highest value at 13.56 Ma. At the same time, BFAR started to increase also species such as *Bolivina* cf*. B. reticulata*, *Bulimina truncana*, *B*. *striata*, *Cibicidoides wuellerstorfi*, *Trifarina angulosa* become most popular species during late- middle Miocene to late Miocene. While *Burseolina pacifica*, *Globocassidulina subglobosa*, *Strictocostella scharbergana*, *Siphonodosaria subspinosa* started to peak again. *Cibicidoides wuellerstorfi* (coarse type) has substituted by smooth type (red peak) *C. wuellerstorfi* at around 10 Ma. In the late Miocene and early Pliocene species such as *Gavelinopsis lobatulus* increase rapidly and shows the highest peak.

Both correlation coefficient and significant values are calculated between the relative abundance of each species in Figure 4.5 and diversity values (Shannon_H) (See Appendix K). Correlation coefficient (R-value) has either negative or positive values. The best correlation represented by highest positive values (0.43) which recorded between *Trifarina bradyi* and diversity. The significant value (P-value) is represented by statistically significant value when the value is small and < 0.05 while the value will be non-statistically significant when P>0.05. the more stratigraphically significant value is 0.02 between *Trifarina bradyi* and diversity.

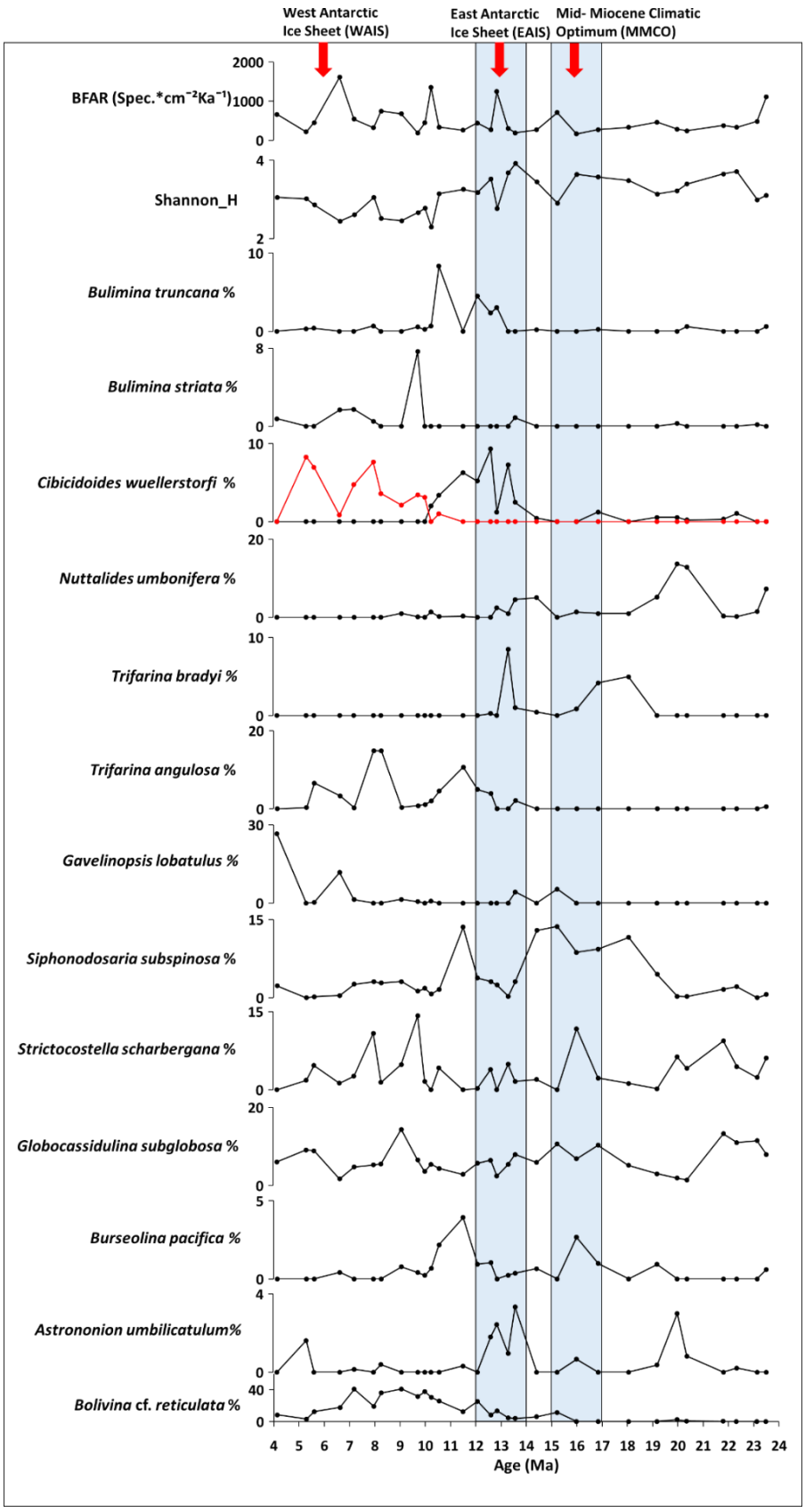


Figure 4. 5: Species relative abundance, diversity (Shannon_H) and Benthic Foraminifera accumulation Rate (BFAR) versus age at Site 752 Hole A.

4.2.2 ODP Site, 1168 Hole A:

4.2.2.1 Cluster analysis:

The dendrogram divided into six main clusters. Most clusters have a similarity index of nearly 0.5, except cluster F, which has less similarity around 0.36. Cluster A (See Appendix D) represented by samples 8H-1- 15X-2 (eight samples) with an average diversity of 64 benthic foraminifera species (Figure 4.6).

Cluster B is represented by samples 16X-2- 25X-2 (ten samples) with the average diversity of 62 benthic foraminifera species. Cluster C is represented by samples 25X-5- 30X- 3 (seven samples) having an average diversity of 54 benthic foraminifera species. Cluster D is represented by samples 31X-5- 37X- 6 (seven samples) having an average diversity of 59 benthic foraminifera species. Cluster E is represented by samples 38X-3- 42X-3 (five samples) with an average diversity of 54 benthic foraminifera species. Cluster F is represented by samples 45X-6- 52X-4 (five samples) having an average diversity of 45 benthic foraminifera species.

There are some characteristic species in each cluster such as *Melonis barleeanus* and *Siphouvigerina hispida* in cluster A, *Nuttalides umbonifera* and *Bolivina* sp.3 in cluster B, *Nuttalides umbonifera* and *Sphaeriodina bulloides* in cluster C, *Cibicidoides mundulus*, *Bolivina* sp.3 and *Bulimina truncana* in cluster D, *Bulimina* cf. *B*. *elongata*, *Bolivina dilatata* and *Cibicidoides mundulus* in cluster E and *Bolivina dilatata* and *Melonis barleeanus* in cluster F.

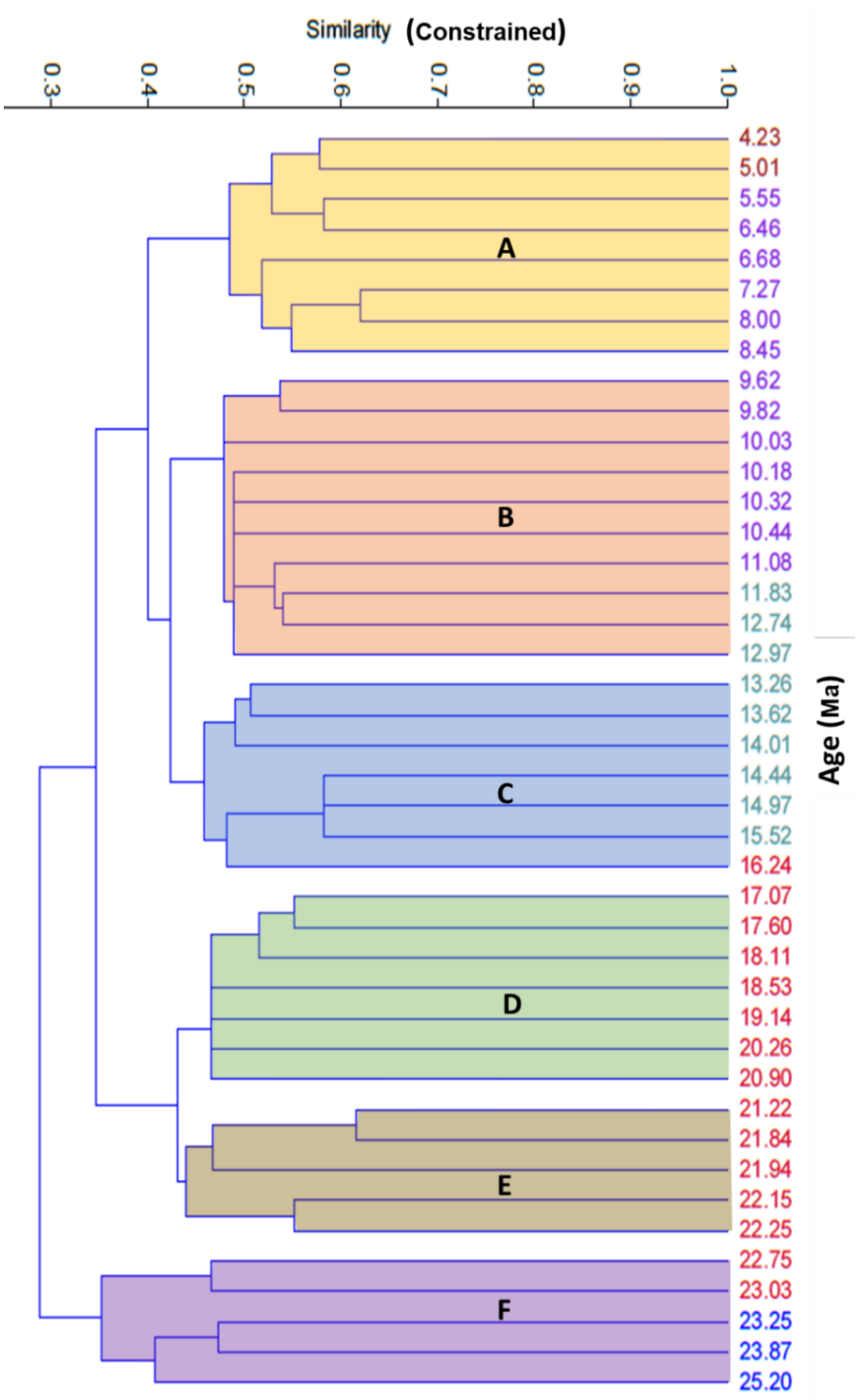


Figure 4. 6: Constrained Cluster diagram of samples in the late Oligocene and Neogene (Miocene and early Pliocene) at the Site 1168 Hole A, exhibiting the presence of six major cluster groups.

4.2.2.2 Diversity:

Commonly the diversity values (Figure 4.7) have not changed a lot, while in some intervals records high values (See Appendix G). In the late Oligocene and earliest Miocene, the values increased then dropped suddenly at 21.84 Ma, and after that, the values have not changed a lot until it decreased rapidly to record the lowest value at 18.53 Ma.

In 18.11 Ma the diversity records the highest value and remains high until it drops suddenly in 14.01 Ma. The range between 14.01 and 11.83 Ma shows low diversity values except for the intervals between 12.97 and 13.62 Ma, which have a slightly higher peak. The peak of the diversity rapidly dropped down at 9.62 Ma and another lower value also recorded at 6.46 Ma. Commonly the range between 10.44 to 7.27 Ma has low diversity values.

Evenness values have the same pattern of increasing and decreasing with diversity indices while dominance peak almost opposite to the diversity and evenness peaks.

4.2.2.3 Benthic Foraminifera Accumulation Rate:

The lowest value of the BFAR (See Appendix H) was in late Oligocene (23.87 Ma), and it has gradually increased until it reaches the highest value in the earliest Miocene (22.75 Ma) (Figure 4.8). The value dropped again in 20.9 Ma. The values remain relatively similar and low until it peaks again in 14.01 Ma. High values also recorded at around 10 and 8 Ma. In The current Site (1168A) the BFAR values increase maybe during the periods of cooling.

The high productivity taxa calculated from the sum of *Bolivina*, *Bulimina*, *Uvigerina* and *Melonis* species (See Appendix B). The highest peak recorded during the latest Oligocene and early Miocene and continued until about 21 Ma. The values are gradually decreased until recording the lowest value at 13.62 Ma. The values gradually increase during the mid-Miocene and continued until about 10 Ma (Figure 4.8).

4.2.2.4 Rarefaction curves:

At the beginning of the rarefaction curve, diversity increased rapidly until it becomes more flattened when fewer new taxa added (Figure 4.9). The diversity of the most samples has a range between ~40 to 70 species except few samples, especially at 7.27, 18.11 and 10.44 Ma which record slightly higher values. Most of the curves become more flattened around 200-350 specimens. The range of 200- 350 specimens may represent the best range of specimens counting at the current study.

4.2.2.5 Faunal composition:

Thirteen most abundance species have been plotted and compared with both diversity (Shannon_H) and Benthic Foraminifera Accumulation Rate (BFAR) (Figure 4.10). Some species peaked during the latest Oligocene to the early Miocene such as *Astrononion umbilicatulum*, *Siphonodosaria subspinosa* and *Epistominella exigua*. Species such as *Globocassidulina subglobosa*, *Trifarina bradyi*, *Cibicidoides wuellerstorfi* (both types), *Bulimina truncana* and *Sphaeroidina bulloides* peaked during the early Miocene.

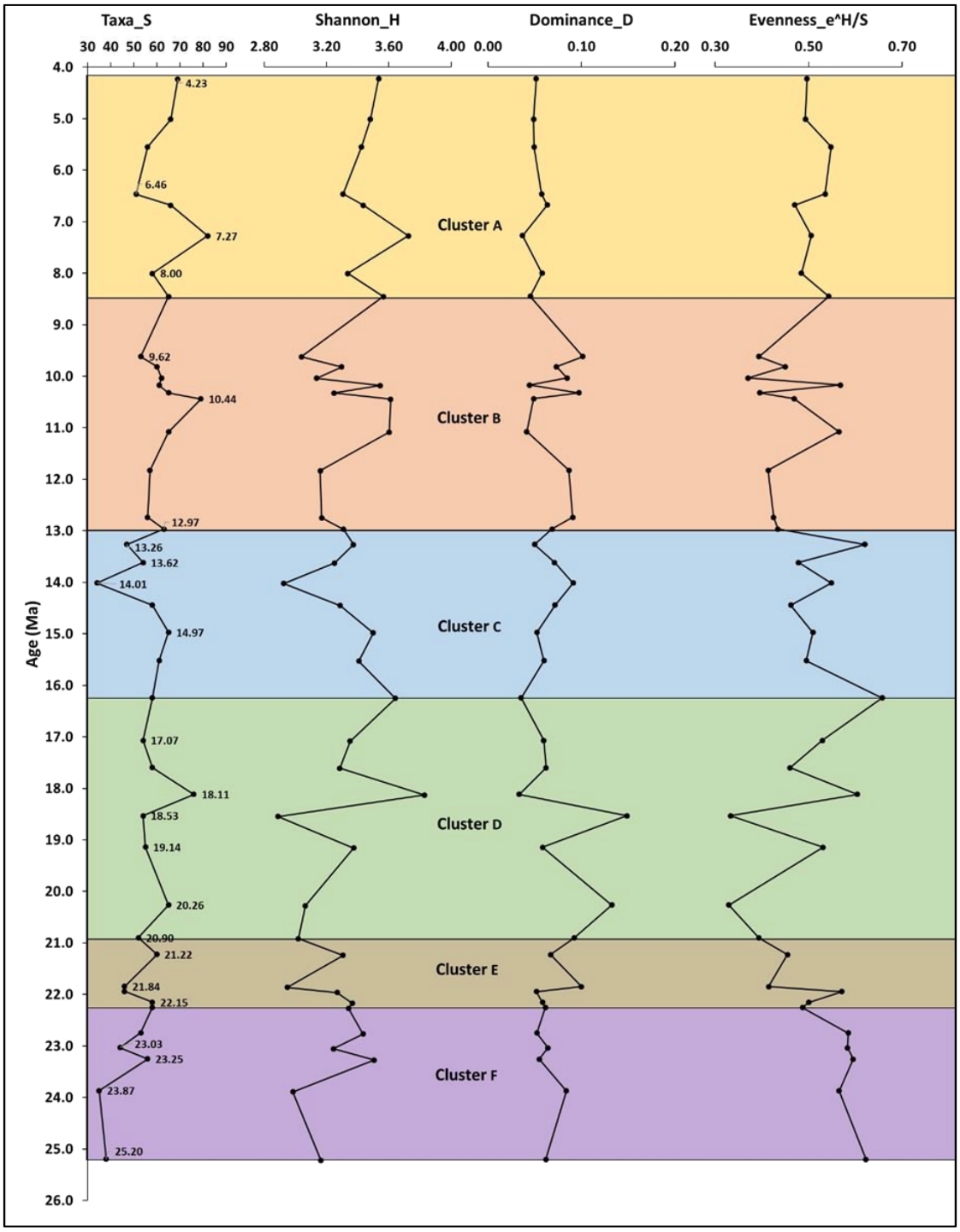


Figure 4. 7: Diversity indices, dominance, species richness and evenness at the Site 1168 Hole A, the shaded area are six clusters formed from samples with similar composition.

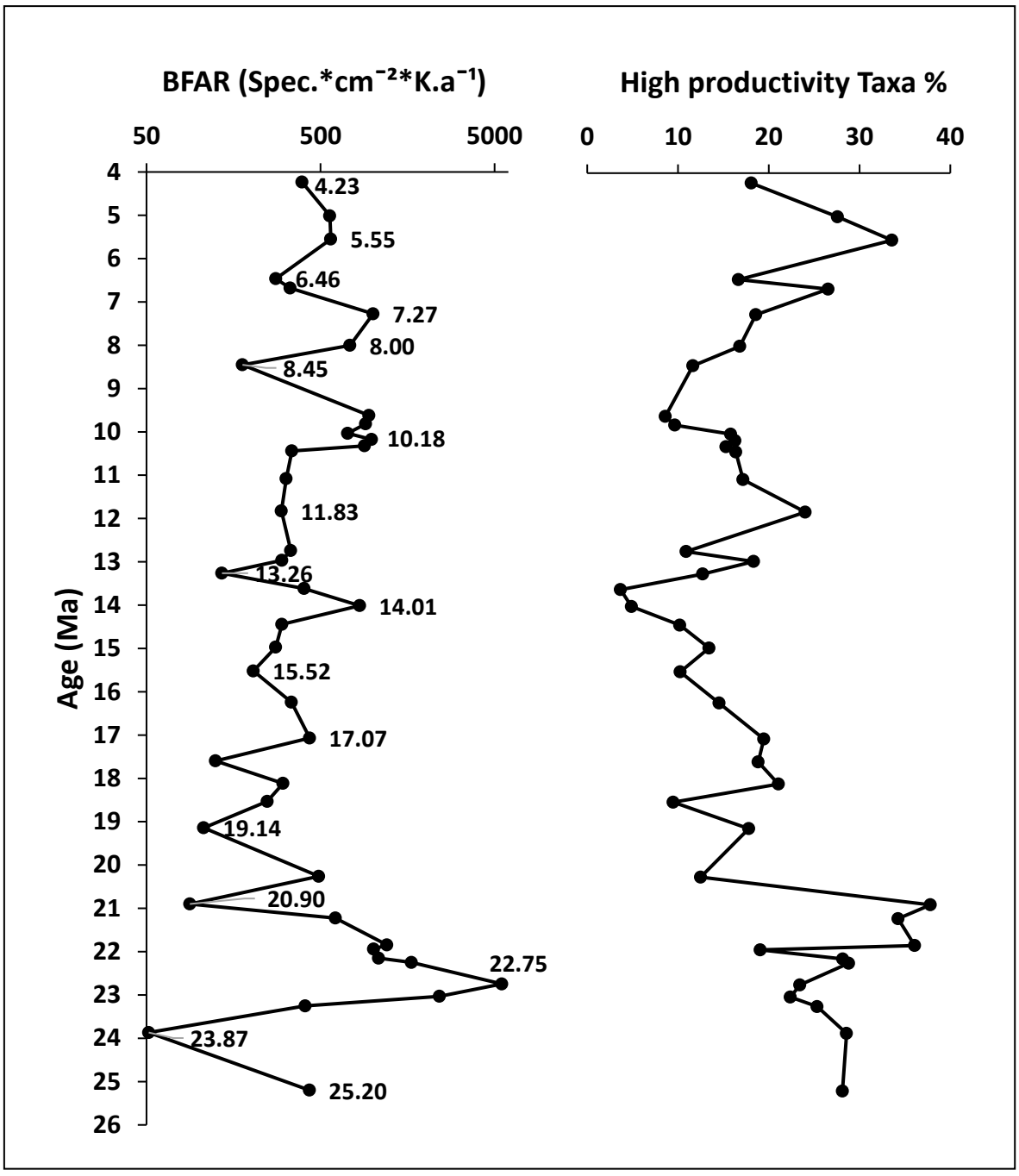


Figure 4. 8: Benthic Foraminifera Accumulation Rate (BFAR) and High productivity taxa versus age at the Hole 1168A. The x-axis of BFAR is a logarithmic scale.

The highest peak of *Bolivina dilatata* occurred at around 21.84 Ma. *Sphaeroidina bulloides* dominated during the early Miocene to the late mid- Miocene. *Abdetodentrix peudothalmanni* is less dominated and has low abundance during the latest Oligocene and the early Miocene, while it starts to peak again during the late mid-Miocene and continued until the early Pliocene.

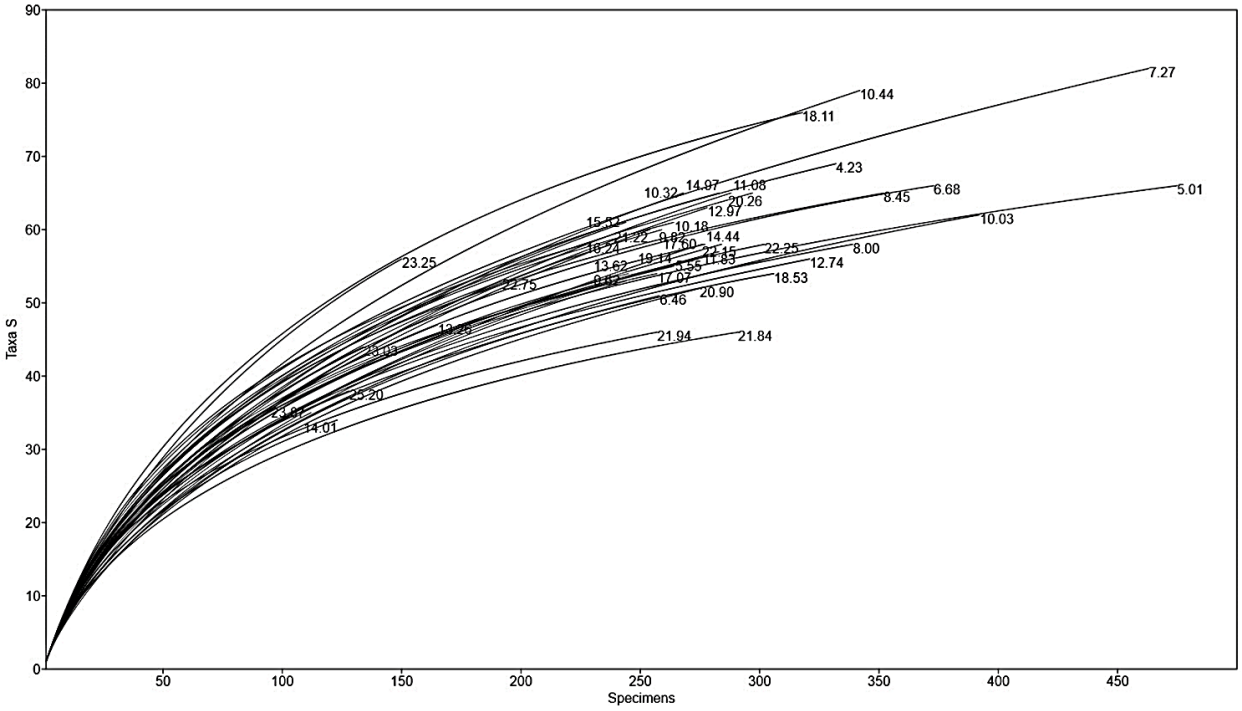


Figure 4. 9: Rarefaction curve of the forty-two samples at the Site 1168 Hole A. The numbers on each curve represent the Age (Ma). The vertical axis is species diversity, and the horizontal axis is the number of collected specimens.

Astrononion umbilicatulum increase in abundance during mid and the late Miocene and dropped in the early Pliocene. The highest peak of *Stilostomella* cf. *S*. *annulifera* was at 8.45 Ma and dropped suddenly in the latest Miocene. Both *Siphonodosaria subspinosa* and *Trifarina angulosa* has a highest peaked during the late Miocene, while the *Siphonodosaria subspinosa* peak drop earlier at around 8 Ma. Species such as *Globocassidulina subglobosa*, *Nuttalides umbonifera Cibicidoides wuellerstorfi* (coarse type), *Bulimina truncana* and

Sphaeroidina bulloides peaked again during the mid- Miocene. The highest peak of both *Nuttalides umbonifera* and *Sphaeroidina bulloides* recorded in the mid-Miocene which coincided with the East Antarctic Ice Sheet expansion.

The peaks of relative abundance, diversity and BFAR highly fluctuate during ~ 10.5 to 10 Ma. During the early late Miocene, *Trifarina bradyi* peaked again and declined in the latest Miocene when the peak of *Trifarina angulosa* remains high.

Both correlation coefficient (R-value) and significant values (P-value) are calculated by using the relative abundance of the species shown in the Figure 4.10 and diversity values (Shannon_H) (See Appendix K). The highest correlation coefficient is 0.3 between the relative abundance of *Stilostomella* cf. *S*. *annulifera* and diversity which also record statistically significant value (0.04).

4.2.3 ODP Site, 1139 Hole A:

4.2.3.1 Cluster analysis:

The dendrogram has divided into five main clusters. The similarity, of all clusters around 0.4 to 0.5. Cluster A (See Appendix D) is composed of two samples (3R-1 & 3R-2) with an average diversity of 43 benthic foraminifera species. Cluster B is represented by samples 4R-1, 4R-2, and 4R-4 it has an average diversity of 44 benthic foraminifera species. Sample 3R-4 (12.77 Ma) is not clustered directly with cluster A and B. Cluster C represents samples 6R-1 and 7R-1 and has a species diversity of 39 and 68, respectively. Sample 5R-1 (17.98 Ma) is not clustered directly with cluster C (Figure 4.11).

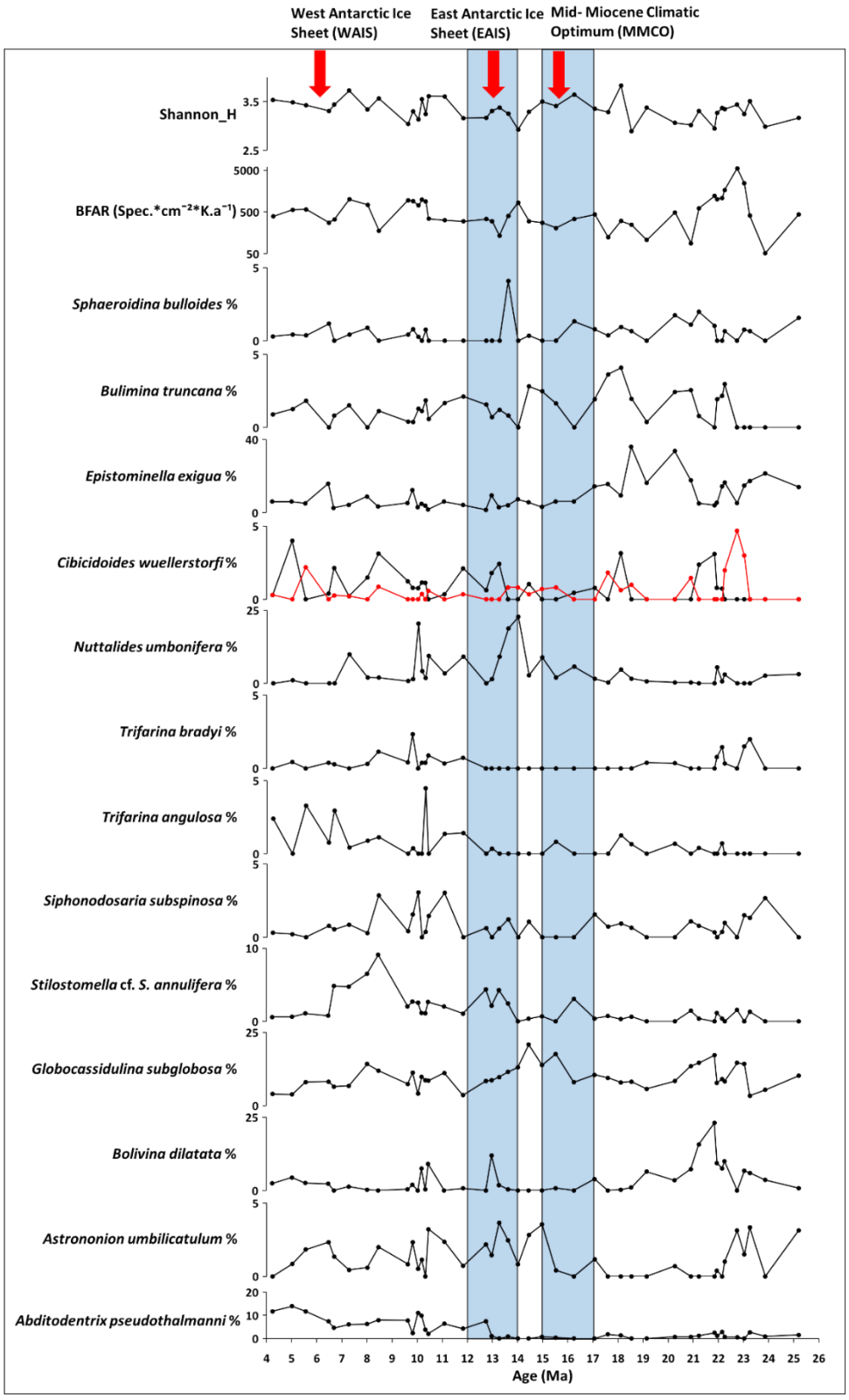


Figure 4. 10: Species relative abundance, diversity (Shannon_H) and Benthic Foraminifera accumulation Rate (BFAR) versus age at Site 1168 Hole A. The red curve is *Cibicidoides wuellerstorfi* (smooth type).

Cluster D represented by samples 8R-1- 14R-4 (19.42-2.10 Ma) and it has an average diversity of 51 species. Sample 15R-2 (22.39 Ma) is not clustered directly with cluster D or E. Cluster E is represented by samples 15R-4 – 19R-2. The average diversity of this cluster (E) is 55 species.

There are some characteristic species at 1139A such as, *Oridorsalis umbonatus* and *Trifarina angulosa* in cluster A, *Strictocostella matanzana*, *Bulimina truncana* and *Cibicidoides wuellerstorfi* (smooth and coarse types) in cluster B, *Bulimina* cf. *B*. *elongata*, *Bulimina striata* and *Laticarinina pauperata* in cluster C, *Sphaeroidina bulloides*, *Uvigerina peregrina* and *Bulimina gibba* in cluster D and *Stilostomella* cf. *S*. *annulifera*, *Pullenia quinqueloba* and *Eggerella bradyi* in cluster E.

4.2.3.2 Diversity:

Commonly the Shannon index values are not changing much except for some intervals (See Appendix I). The diversity values are high during the late Oligocene and decline rapidly in the latest Oligocene (23.18 Ma) (Figure 4.12). The diversity curve declined then records the highest peak in the early Miocene (22.1 Ma). The values do not record high changes while dropped suddenly at 21.14 Ma and the second-highest decrease was at 18.61 Ma. During the late early Miocene, the diversity records the highest value at around 18 Ma and the second-highest value was around 12.77 Ma then it declined rapidly in the late mid-Miocene. The evenness peak has a similar inclination with the diversity curve, especially in the early to mid-Miocene. While dominance is relatively low during the latest Oligocene and has the highest peak at around 18.61 Ma. The dominance peaked again at 14.49 Ma then dropped rapidly.

4.2.3.3 Benthic Foraminifera Accumulation Rate (BFAR):

The highest BFAR value recorded in the late Oligocene during 23.6 – 23.18 Ma (Figure 4.13). The values of BFAR decreased in the early Miocene except at 22.39 Ma until it increased again at 21.34 Ma. The value remains relatively high until peaks again at around 19.14 Ma and the second peak is at 14.49 Ma. The value decreased sharply at about 12.77 Ma when the high value of diversity recorded. While increased at 11.99 Ma (See Appendix J).

The High productivity taxa calculated from the sum of *Bolivina*, *Bulimina*, *Uvigerina* and *Melonis* species (See Appendix C). The high productivity values are high during the latest Oligocene and early Miocene and decrease suddenly after about 22.7 Ma. The values remain low then increase again at about 21 Ma. Another dropping happens after that then another peak records at around 19 Ma. After that, the values continuously decrease until around 14.4 Ma. During the late mid-Miocene, the values are slightly increase and drop again at around 11.2 Ma (Figure 4.13).

4.2.3.4 Rarefaction curves:

From the rarefaction curves, the diversity values increase rapidly at the beginning until it becomes more flattened when fewer new taxa added (Figure 4.14).

The range of the diversity of the current study samples is around ~40-60 taxa for most of the samples except few of them, especially samples at 16.3 and 17.98 Ma. Most of the curves

become more flattened around 300-500 specimens; it shows that this range of counting may apply for most of the samples at the current study.

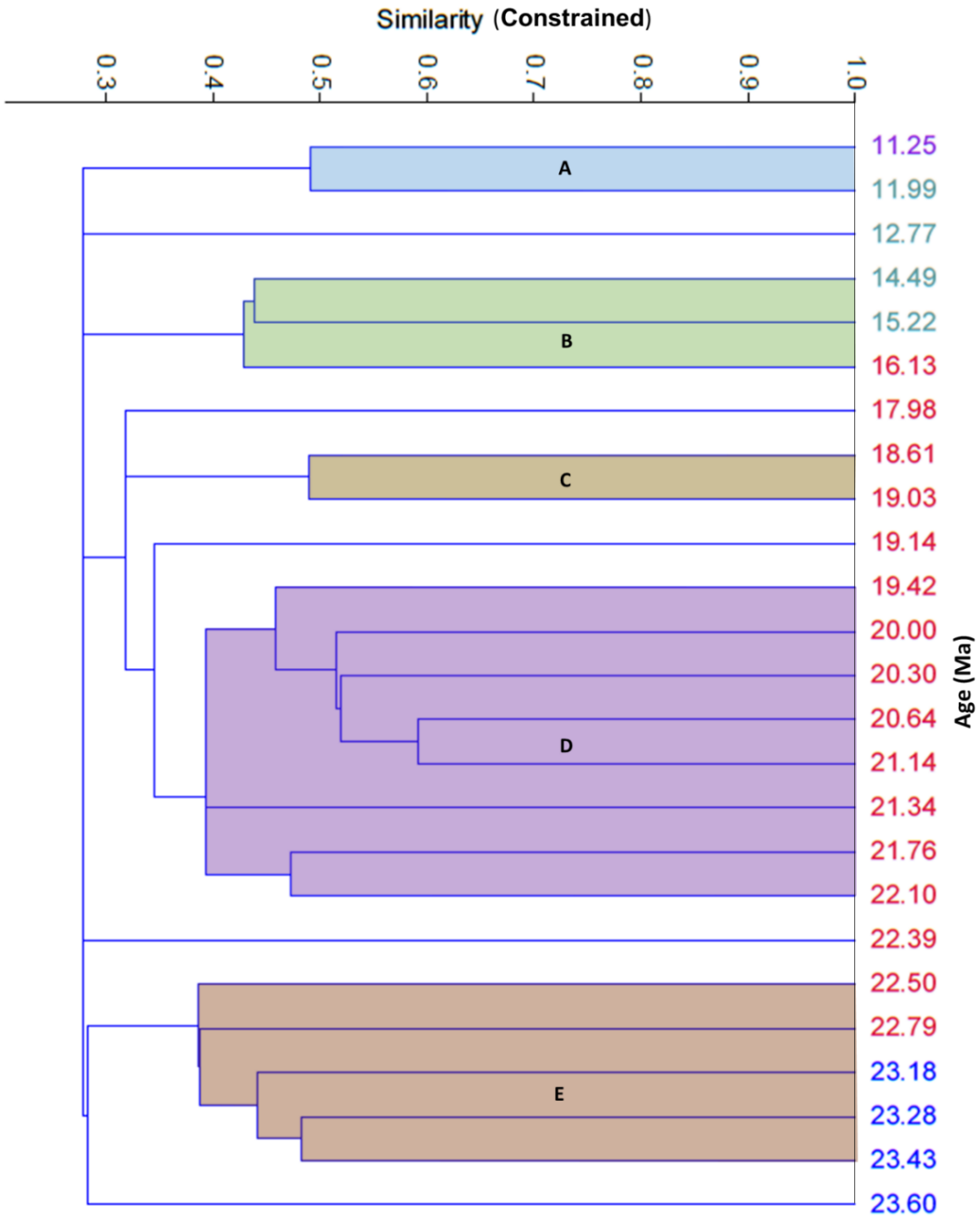


Figure 4. 11: Cluster diagram of samples in the late Oligocene and Miocene (early & early late Miocene) at the Site 1139 Hole A, exhibiting the presence of five major cluster groups.

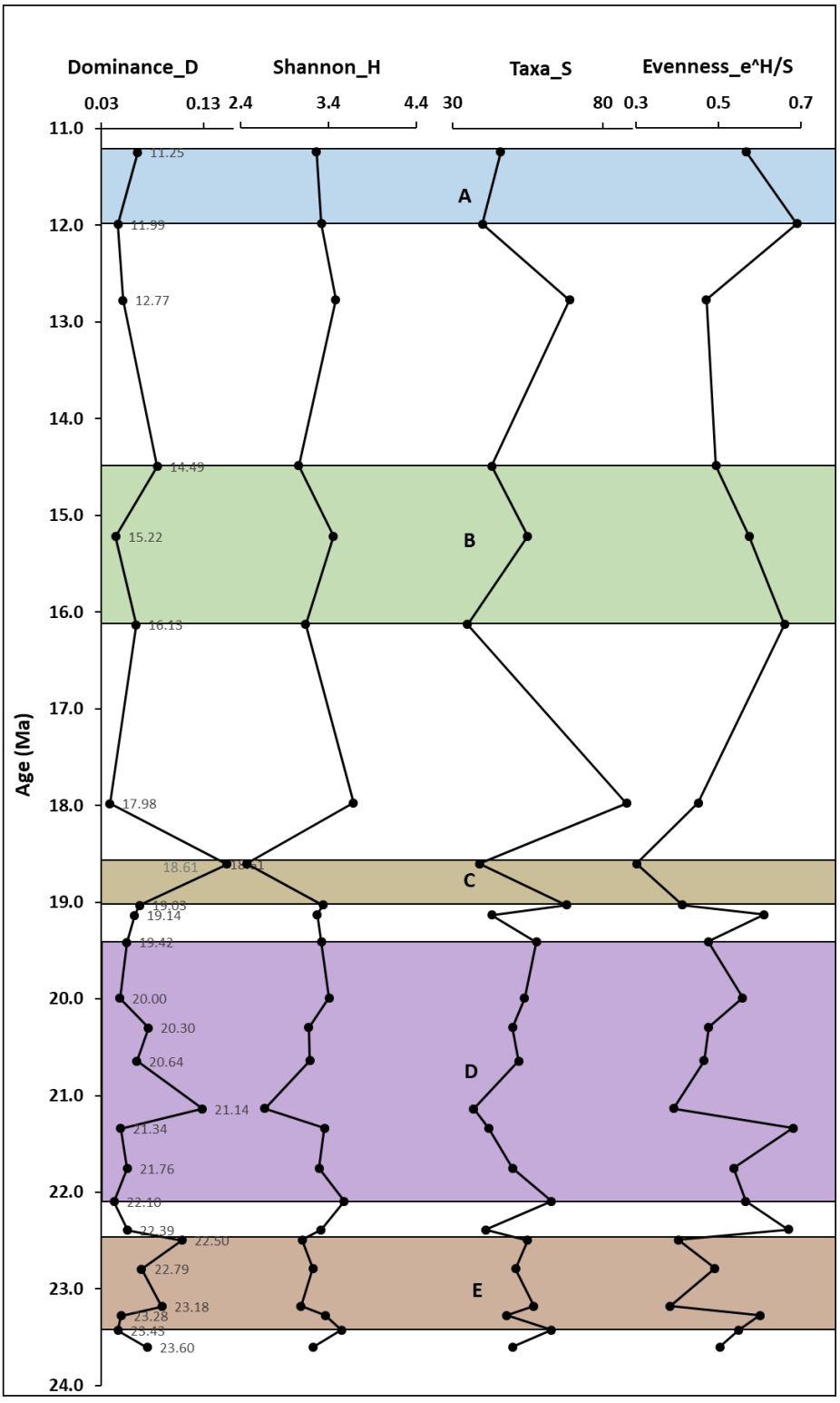


Figure 4. 12: Diversity indices, dominance, species richness and evenness at the Site 1139 Hole A, the shaded area are five clusters formed from samples with similar composition.

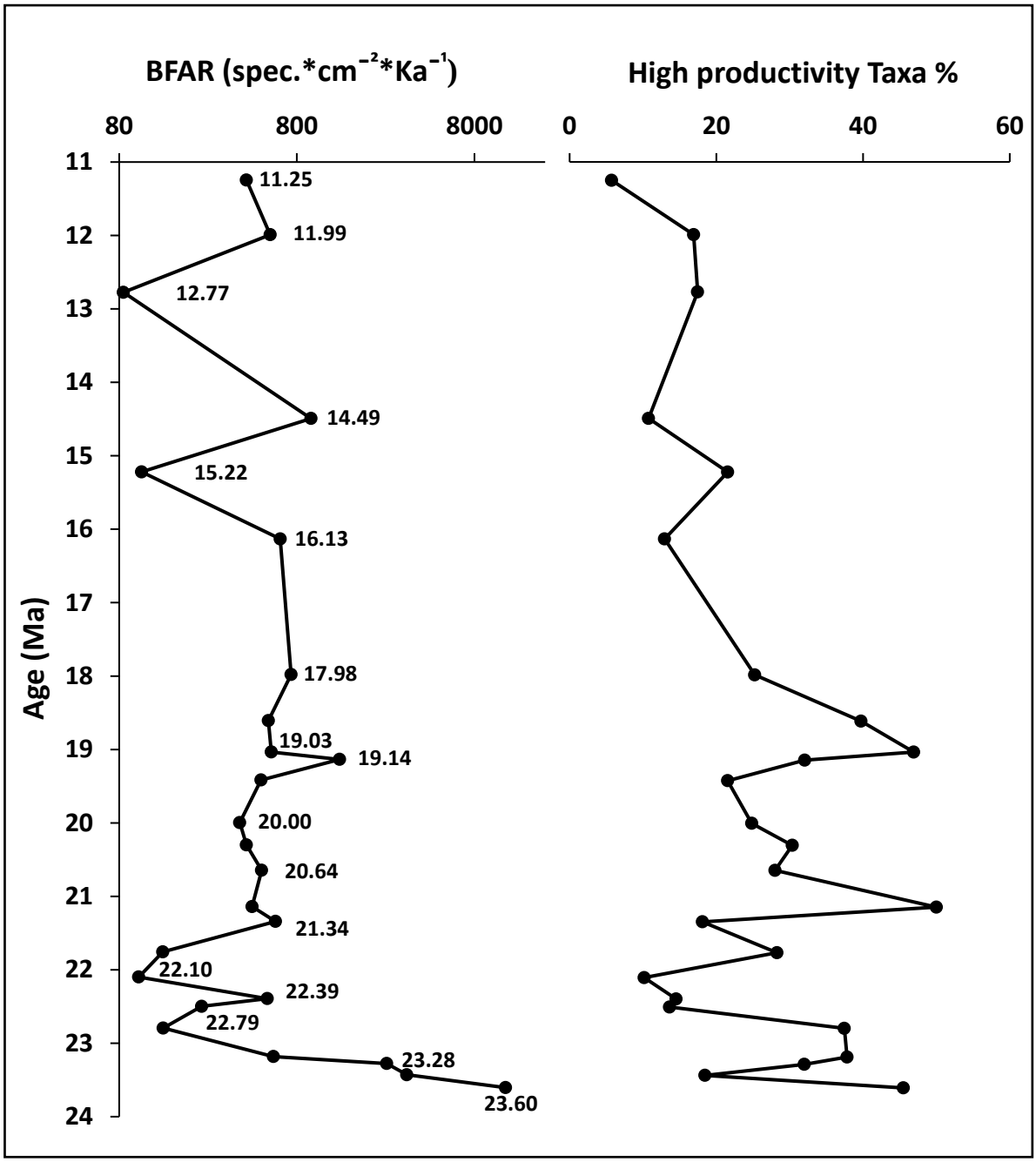


Figure 4. 13: Benthic Foraminifera Accumulation Rate (BFAR) and High productivity taxa versus age at the Hole 1139A. The x-axis of BFAR is a logarithmic scale.

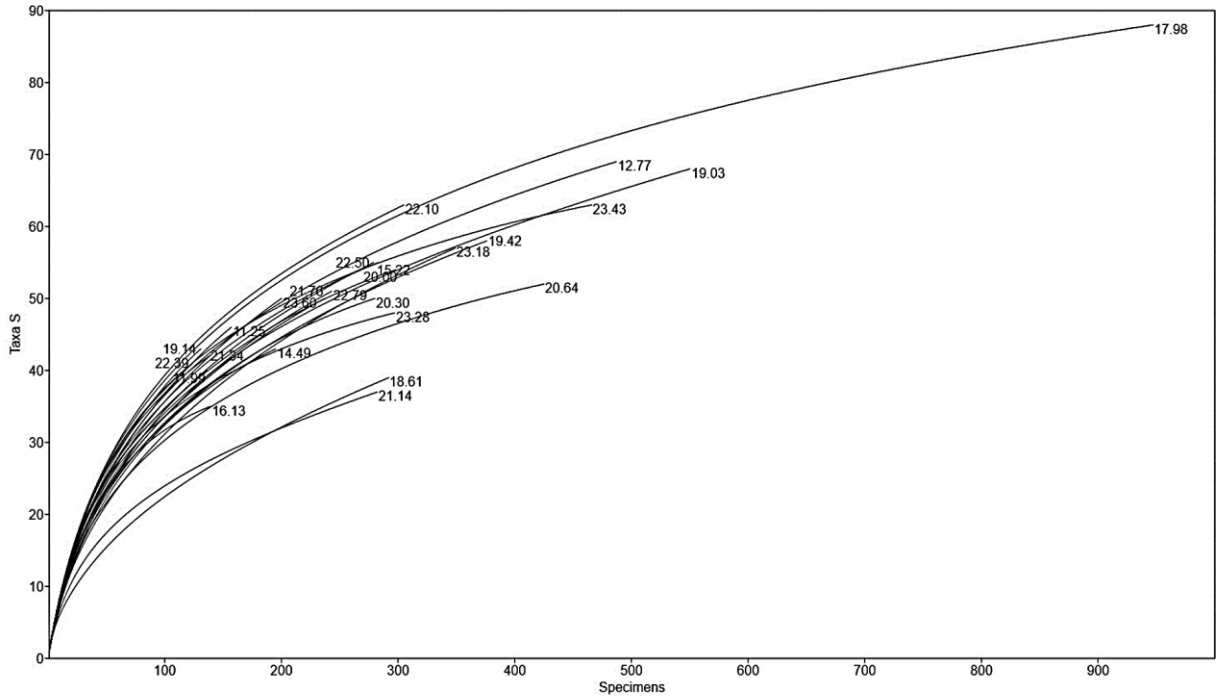


Figure 4. 14: Rarefaction curve of the twenty-five samples at the Site 1139 Hole A. The numbers on each curve represent the Age (Ma). The vertical axis is species diversity (richness), and the horizontal axis is the number of collected specimens.

4.2.3.5 Faunal composition:

The relative abundance of thirteen most abundance species are plotted and compared with both diversity (Shannon_H) and Benthic Foraminifera Accumulation Rate (BFAR) (Figure 4.15). Peaks of all selected species have fluctuated differently during the late Oligocene to the Neogene (Miocene and early Pliocene). Species like *Globocassidulina subglobosa*, *Astrononion umbilicatulum*, *Stilostomella* cf. *S. annulifera*, *Siphonodosaria subspinosa* and *Bulimina striata* have peaked during the late Oligocene and the earliest Miocene. The *Astrononion umbilicatulum* highest peak was at 23.43 Ma at the time where the BFAR has high value during the late Oligocene. The highest peak of *Stilostomella* cf. *S. annulifera* at 22.5 Ma coincided

with the first peak of both *Siphonodosaria subspinosa* and *Bulimina truncana*. The first peak of *Globocassidulina subglobosa* at 22.10 Ma coincided with the first highest peak of diversity and the lowest value of BFAR.

The first highest peak of *Bulimina striata* was at 21.76 Ma at the time when the value of BFAR is still low, and the diversity value remains high. The peak of *Bulimina truncana* more or less dropped and increased, contrary to BFAR values. In the current study *Epistominella exigua* responding to any changes to BFAR values (Figure 4.15).

Sphaeroidina bulloides recorded high values during the late Oligocene and the early Miocene and dropped rapidly at 17.98 Ma at the same time *Abdetodentrix peudothalmanni* bloomed. *Abdetodentrix peudothalmanni* dropped suddenly at 19.14 Ma. Some species recorded high values during the late early Miocene and the mid- Miocene such as *Trifarina bradyi* and *Cibicidoides wuellerstorfi*.

The highest peak of species such as *Globocassidulina subglobosa*, *Cibicidoides wuellerstorfi* (the coarse type), *Trifarina bradyi* and *Epistominella exigua* were at 16.13 Ma during mid-Miocene Climatic Optimum (MMCO). During the mid- Miocene, the peak of *Trifarina bradyi* declined suddenly at the time *Trifarina angulosa* recorded the highest peak at 15.22 Ma. The highest peak of both *Nuttalides umbonifera* and *Cibicidoides wuellerstorfi* (the smooth type) were recorded at 12.77 Ma which coincided with East Antarctic Ice Sheet expansion.

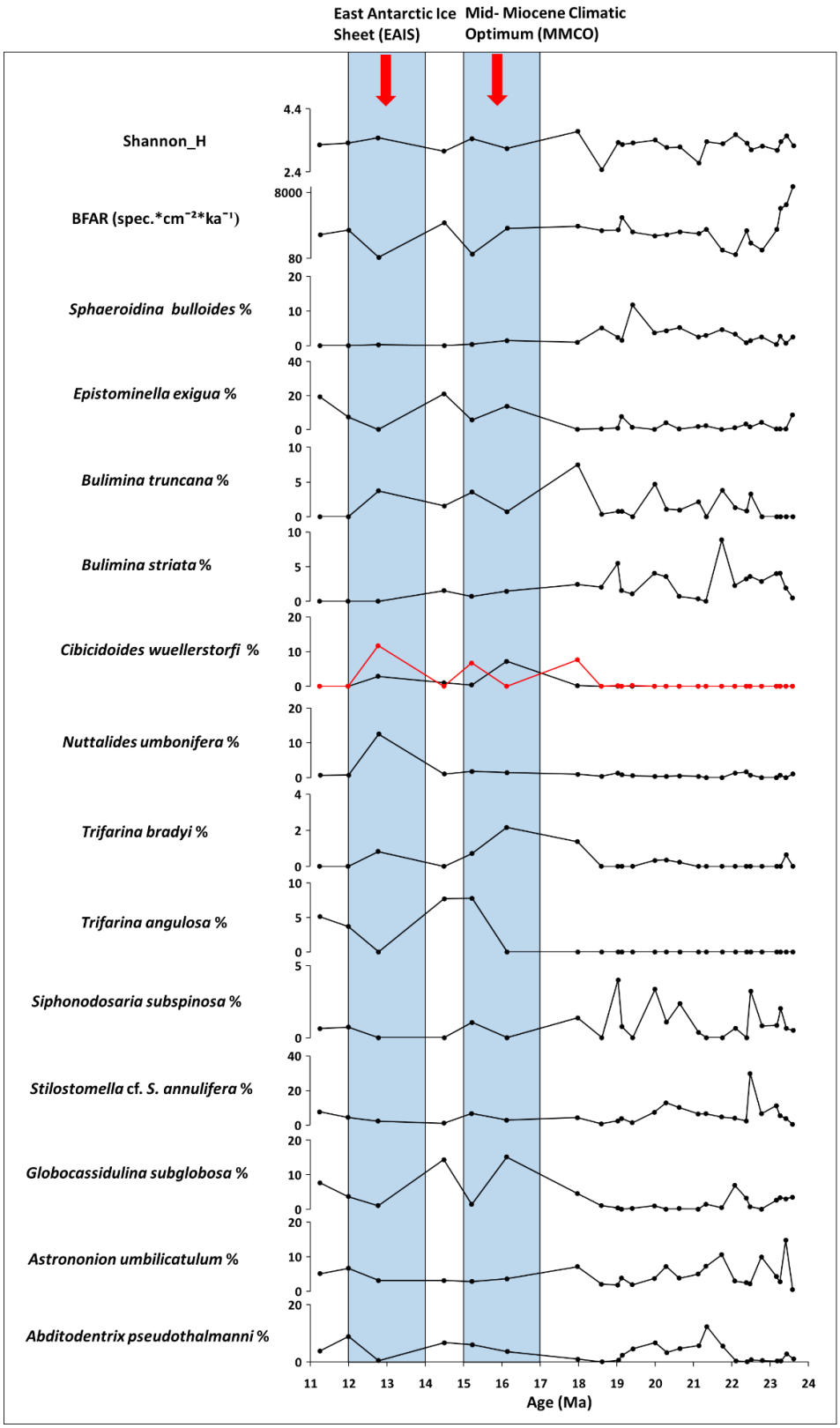


Figure 4. 15: Species relative abundance, diversity (Shannon_H) and Benthic Foraminifera accumulation Rate (BFAR) versus age at Site 1139 Hole A. The red curve is *Cibicidoides wuellerstorfi* (smooth type).

Both correlation coefficient (R-value) and significant values (P-value) are calculated by using the relative abundance of the species shown in the Figure 4.15 and diversity values (Shannon_H) (See Appendix K). The highest correlation coefficient is 0.4 between the relative abundance of *Cibicidoides wuellerstorfi* (smooth) and diversity which also record statistically significant value (0.05).

4.3 Discussion:

4.3.1 ODP Site 752 Hole A:

4.3.1.1 Cluster analysis:

The characteristic species of cluster A is *Ehrenbergina carinata*; this species is more indicative of high nutrient, low oxygenated environments and high temperatures (Gupta and Satapathy, 2000). In the central Indian Ocean, *E. carinata* is a good indicator of intermediate to high input of organic matter and low oxygen condition (Gupta et al., 2006). *Trifarina angulosa* in cluster B is indicative species of colder periods, and it peaks during bottom currents intensification (Mackensen, 1992). Both *Cibicidoides wuellerstorfi* (coarse type) and *Nuttalides umbonifera* in clusters C and D are associating with AABW (Antarctic Bottom Water) (Corliss, 1979a, Corliss, 1983). Singh and Gupta (2004) suggested that the blooming of *Nuttalides umbonifera* in the south-eastern Indian Ocean coincided with time were growing of other species could not be maximal. According to Corliss (1979a) in the modern southeastern Indian Ocean, the species such as *Globocassidulina subglobosa* and *Nuttalides umbonifera* have coexisted with AABW (Antarctic Bottom Water), *Globocassidulina subglobosa* is dominated in warmer AABW (0.6-0.8 C°), while *Nuttalides umbonifera* had dominated in coolest AABW (-0.2-0.4 C°).

Lenticulina cultrata (cluster E) is one of the most common species during the early Miocene until the late mid- Miocene at 752A (see appendix A). At the Site 754, *Lenticulina* spp. were abundant in the early Miocene but, it dropped from the mid- Miocene and upward (Nomura, 1991). *Nuttalides umbonifera* is the most common species in cluster F and shows the highest peak during the early Miocene. At the current Site (752A) the first peak of BFAR was in the late Oligocene (23.48 Ma) it may be due to deep glacial maximum within Oligocene/ Miocene boundary (Zachos et al., 2001) and it has declined until it peaks again during the early Miocene at 19.16 Ma (Figure 4.3).

The separation of two larger clusters at ~ 13 Ma may have controlled by a climactic event such as faunal change due to Antarctic ice sheet expansion (Woodruff and Savin, 1989). According to Nomura (1991), the development of the benthic foraminifera assemblages has recorded from Eastern Indian Ocean at sites 754 and 756 at around 13.8 Ma which supposed to be related to decreasing in water temperature of the intermediate oceanic waters due to Antarctic ice sheet expansion (Badger et al., 2013, Holbourn et al., 2005).

4.3.1.2 Diversity:

Singh et al. (2012) studied the diversity of deep-sea benthic foraminifera at the Hole 752A. They have noted that all diversity parameters values declined from 25 to 23 Ma and then increased with a peak value recorded at ~13.5 Ma. According to Singh et al. (2012), the interval between Late Oligocene to Earliest Miocene at Hole 752A showed highly unstable conditions.

This interval was an interval of low organic carbon, high energy (carbonate corrosive), and well-oxygenated conditions. The peak of diversity parameters coincided with the early Middle Miocene climatic optimum (Singh et al., 2012). The trend of all diversity parameters declined from 13.5 to 4.5 Ma, which believed to cooccurred with major Antarctic ice sheets build up (Singh et al., 2012). In the current study the interval between 13.56 to 6.62 Ma shows gradual declining of diversity.

According to Holbourn et al. (2005), the Antarctic Ice Sheet expansion (14.7 to 12.7 Ma) and global cooling over Antarctica coexisted with decreasing atmospheric carbon dioxide levels from the northwest and southeast subtropical Pacific Ocean. While according to Holbourn et al. (2013), a continuous deep-water cooling and glaciation episodes happened from ~ 13 Ma until ~ 9 Ma.

4.3.1.3 Benthic Foraminifera Accumulation Rate (BFAR):

Three highest peaks for BFAR recorded from the mid- Miocene until the latest Miocene. The first peak was at 12.83 Ma which may have been triggered by global productivity increase in oceans at ~13 Ma. High values recorded around 10- 8 Ma this may be due to Antarctic glaciation (Gupta et al., 2004, Singh et al., 2012, Woodruff, 1985). In the current study, productivity also records very high values during around 10- 8 Ma (Figure 4.3). The second peak was at 10.23 Ma; this is possibly due to high productivity as well (Smart et al., 2007). Increasing organic carbon, low oxygen zone intensification and deep ocean dissolution

triggered and changed benthic foraminifera abundance and depth distribution during late Miocene, between 8 to 10 Ma (Nomura, 1991).

Increase abundance of *Bolivina* species during the late-mid Miocene to the late Miocene at the current Site (752A) are indicative for low oxygen level (Oxygen Minimum Zone (OMZ)), higher organic matter input (Boersma and Mikkelsen, 1990, Poag and Low, 1984). Smart et al. (2007) believed that the relation between BFAR and high productivity taxa is not considerable at any of the studied sites in the western equatorial Indian Ocean. They believe that the overall productivity increase is coincided with very high values of BFAR especially during the high-productivity time (8-10 Ma) at the two shallower sites (237 and 707). The last peak of BFAR was at 6.62 Ma which may be due to the expansion of the West Antarctic Ice Sheet (Zachos et al., 2001). In the current study productivity increase coincided mostly with high values of BEAR, this has been reported clearly in the late mid- Miocene to the late Miocene, also in the latest Oligocene (Figure 4.3).

Wollenburg and Kuhnt (2000) believed that there is a negative correlation between BFAR and carbon flux in the Arctic Ocean. They believed that the highest value of BFAR would be at the area of the permanent ice sheet, while at the area of seasonality ice-free the BFAR value will be lowest.

4.3.1.4 Faunal composition:

In the early Miocene *Nuttalides umbonifera*, *Astrononion umbilicatulum* and *Globocassidulina subglobosa* are peaked then rapidly declined at 19.16 Ma. Singh and Gupta (2004) suggested that blooming of *Nuttalides umbonifera* in the south-eastern Indian Ocean was during the time when other taxa could not grow optimally. According to Corliss (1979a) in the modern southeastern Indian Ocean, the species such as *Globocassidulina subglobosa* and *Nuttalides umbonifera* coexisted with AABW (Antarctic Bottom Water) *Globocassidulina subglobosa* is dominated in warmer AABW (0.6-0.8 C°), while *Nuttalides umbonifera* had dominated in coolest AABW (-0.2-0.4 C°).

In the current Site (752A) *Bolivina* cf*. B. reticulata* was most popular species during the late-middle Miocene to the late Miocene. Increase abundance of *Bolivina* species are indicative for low oxygen level (Oxygen Minimum Zone (OMZ)), higher organic matter input (Boersma and Mikkelsen, 1990, Poag and Low, 1984).

4.3.2 ODP Site 1168 Hole A:

4.3.2.1 Cluster analysis:

Trifarina angulosa has a highest peaked during the late Miocene. According to Mackensen (1992), *Trifarina angulosa* is species that indicate colder periods, and it has bloomed during the intensification of bottom currents. In the Tasman Plateau the early Neogene dominated by *Melonis barleeanus* (Shipboard Scientific Party, 2001c). In the current study (1168A) this

species is dominated during the early Miocene and the late Miocene. *Nuttalides umbonifera* is a characteristic species of cluster B and C. Singh and Gupta (2004) believed that *N. umbonifera* bloomed in very high oligotrophic condition and insufficient organic supply. *Cibicidoides mundulus* (see Figure 4.17) is a characteristic species of cluster D and E; this species is a common species of the early Miocene (Nomura, 1991), however, its peak recorded during the late mid- Miocene to the late Miocene at 754 (Nomura, 1991). *Bolivina dilatata* is a characteristic smooth-walled species of cluster E and F. According to Ramsay et al. (1998), smooth-walled species are a typical species of intermediate and deep-water Sites (237 and 709).

Depending on isotopic composition, apertural morphology and sedimentation rate small biserial foraminifera in the eastern Atlantic and western Indian Oceans which previously assigned to genus *Bolivina* were planktic (genus *Streptochilus*) (Smart and Thomas, 2006). Smart and Thomas (2007) identified three different species of *Streptochilus* in the eastern Atlantic and western Indian Oceans which previously assigned to genus *Bolivina*.

4.3.2.2 Diversity:

In the late Oligocene and earliest Miocene, the diversity values increased until dropped suddenly at 21.84 Ma. In 18.11 Ma the diversity records the highest value and remains high then dropped suddenly at 14.01 Ma. Smart et al. (2007) supposed that the world exhibited another global warming and reached a maximum in the late early Miocene (17-15 Ma), which

represent the warmest interval in the Miocene. Banerjee et al. (2017) also reported a global warming during the late early Miocene at about 17-14 Ma. Commonly the range between 10.44 to 7.27 Ma has low diversity values. Gupta et al. (2004) supposed that the event of high oceanic productivity (10-8 Ma) might have triggered by increase Antarctic ice sheet volume and global cooling.

4.3.2.3 Benthic Foraminifera Accumulation Rate (BFAR):

The highest value of the BFAR was in the earliest Miocene (22.75 Ma) (Figure 4.8). The current configuration of the oceanic basin had started in the earliest Miocene (~22 Ma), which coexisted with the formation of the separate Antarctic continent (Ramstein et al., 1997). In the current study, the highest record of the productivity is during the late Oligocene and early Miocene which coincided with the greatest value of the BFAR.

According to Smart et al. (2007), the surface productivity increase started at around 13 Ma and intensified at about 11 Ma, the similar situation has also observed in the current study through observing the peak of the high productivity taxa during around 11.8 Ma. During the high productivity event (10- 8 Ma) the high productivity values at the current study show the continuous increase and continued until around 5 Ma, while BFAR does not record the highest values but remains relatively high (Figure 4.8).

According to Smart et al. (2007), BFAR is a useful proxy for food flux estimation, and they believe that the amount of organic flux to the ocean floor depends on the water depth. At a

depth of greater than 1000 m, only a few amounts of organic matter will deposit in the oceanic floor which only represents a few percentages of organic production in the euphotic zone (0.01- 1 %) (Murray et al., 1996).

4.3.2.4 Faunal composition:

Some species peaked during the latest Oligocene to the early Miocene such as *Astrononion umbilicatulum*, *Siphonodosaria subspinosa* and *Epistominella exigua*. *Astrononion* is a good indicator of high organic flux, blooms particularly during cool periods where the supply of organic flux to the sediment increases (Gooday, 1994). *Nuttalides umbonifera* and *Sphaeroidina bulloides* recorded highest peak in the mid-Miocene which coincided with the East Antarctic Ice Sheet expansion. According to Badger et al. (2013), the development of the East Antarctica Ice Sheet happened at about 14 Ma. In the late Miocene *Trifarina angulosa* recorded high peaks. According to Mackensen (1992), *Trifarina angulosa* is species that indicate colder periods, and bloomed during the intensification of bottom currents.

4.3.3 ODP Site 1139 Hole A:

4.3.3.1 Cluster analysis:

Oridorsalis umbonatus (cluster A) is indicative of well-oxygenated water, and it peaks during low organic conditions (Mackensen et al., 1985). *Cibicidoides wuellerstorfi* (cluster B) is a species which bloom in a high energy environment (Lutze and Thiel, 1989). This species dominated around 5-15 Ma at ODP Site 757 (Singh and Gupta, 2004). The most sensitive

species and responding to any change to BFAR values in the current study is *Epistominella exigua* (characteristic species of cluster B) (Figure 4.15). Deepwater assemblage's abundance increase which dominated by *Epistominella exigua* When $\delta^{18}O$ increased from 14.5 to 14.1 Ma (early Mid-Miocene) during significant growth of EAIS and deep-water cooling, (Kurihara and Kennett, 1992).

Bulimina cf. *B*. *elongata*, *Bulimina striata* are characteristic species of cluster C. Most of the elongated species, especially biserial and triserial forms have high abundances in low oxygenated conditions (Corliss, 1991, Corliss and Fois, 1990). According to Johnson et al. (2011) the environmental changes that associated with the mid-Miocene global cooling did not affect the elongated group.

Cluster D mainly characterised by infaunal species such as *Uvigerina peregrina* and *Bulimina gibba*. According to Thomas (1990), infaunal species has dominated at Maud Rise; this may refer to high productivity and low oxygenated bottom water. *Uvigerina* species are dominant in the Southern Indian Ocean at Sites 747, 748 and 751 (Kerguelen Plateau) during the early Miocene, the high abundance of *Uvigerina* indicate productivity area (Woodruff, 1985) highly.

According to Nomura (1991), *Sphaeroidina bulloides* (cluster D) is a common species during early Miocene at 754 (Broken Ridge), and its peak also found during late mid- Miocene to late Miocene. *Uvigerina* and *Eggerella bradyi* (characteristic species of cluster E) highly linked to IDW (Indian Deep Water) (Nomura, 1991, Peterson, 1984). The dominance of *Uvigerina* in the southern Indian Ocean is indicative of Circumpolar Deep Water (Corliss, 1983, Nomura, 1991).

4.3.3.2 Diversity:

During the late early Miocene, the diversity records the highest value at around 18 Ma and the second-highest value was around 12.77 Ma after that it declined rapidly in the late mid-Miocene. In the north-eastern Indian Ocean, the diversity recorded lower values at the shallow Site 214, medium values at the intermediate Site 216, while it recorded higher values at the deeper Site 758 (Gupta et al., 2001a).

Recording different diversity values may be related to environmental turbulence in intermediate water and highly stratification of Indian Ocean during the Miocene, which may be coincided with a cooling of deeper water at the time when the tropical surface water temperature did not change a lot (Gupta et al., 2001a). Gupta et al. (2001a) supposed that low fluctuation of diversity means high stable conditions.

4.3.3.3 Benthic Foraminifera Accumulation Rate (BFAR):

The highest BFAR value recorded in the late Oligocene during 23.6 – 23.18 Ma, also the diversity value decreased at about 23.18 Ma. Zachos et al. (2001) stated that one of the most famous aberrations which limit the boundary of Oligocene-Miocene is around ~23 Ma, which represents the deep glacial maximum. The high productivity values increase during the late Oligocene are coincided with the highest values of the BFAR and remains high during the early Miocene. The high productivity curve shows nearly similar inclination with the BFAR at the current study especially during the late Oligocene and the early Miocene (Figure 4.13).

The sharp drop of both BFAR and high productivity values have recorded during around 17-15 Ma during the late early Miocene global warming (Banerjee et al., 2017) at all studied sites, at the time when the sedimentation rates also record low values (See Appendices F, H & J).

4.3.3.4 Faunal composition:

Astrononion umbilicatulum recorded highest peak at 23.43 Ma. According to Gooday, 1994 *Astrononion* is a good indicator of high organic flux, blooms particularly during cool periods where the supply of organic flux to the sediment increases. Deepwater assemblage's abundance increase which dominated by *Epistominella exigua* when $\delta^{18}O$ increased from 14.5 to 14.1 Ma (early Mid-Miocene) during significant growth of EAIS and deep-water cooling, (Kurihara and Kennett, 1992). *Trifarina angulosa* recorded the highest peak at 15.22 Ma and remains high then dropped suddenly at 12.77 Ma. Mackensen (1992) supposed that *Trifarina angulosa* is an indicator species for colder periods, and it dominated during the intensification of bottom currents.

4.3.4 Species diversity and abundance comparison:

4.3.4.1 Species diversity comparison at three studied Sites (752A, 1168A and 1139A):

The diversity values have similar peaks during the latest Oligocene in all three sites (Figure 4.16) with an abrupt decrease at about ~23 Ma at the sites 752A and 1139A, which coincided with the early Miocene glaciation (Mi 1). This aberration is short but deep followed by small

sporadic glaciations (Zachos et al., 2001). The low diversity value recorded during the latest Oligocene at 23.87 Ma at 1168A.

After around 22 Ma in all sites, the diversity values dropped down continuously then recorded the lowest value during early Miocene at about 19.16 Ma at 752A. In comparison, at 1168A and 1139A, it recorded the lowest value slightly later at around 18.5 Ma.

Singh and Gupta (2004) recorded short time peaks of intermediate organic flux and low oxygen around ~19 and ~18 Ma at the Site 757, which indicates a short time disturbance in the deep sea. This event is nearly similar to the late early Miocene Climatic Optimum (Singh and Gupta, 2004). The diversity values increase in all sites at around 18 Ma and record the highest value in deeper sites (1168A and 1139A). Singh et al. (2012), during their study at 752A, observed that the sharp increase in $\delta^{18}O$ value of *Cibicidoides* sp. at 19.5 is indicative of deep-sea cooling and causing in sea level lowering. This event coincided with the NH1 hiatus of Keller and Barron (1983) (20-18 Ma), and it is indicated by decreasing diversity parameters and number of species while dominated by *C. wuellerstorfi*.

Singh et al. (2012) noted that the diversity E (Equitability), H (Information Function), S (Species Diversity) and Sander's values were reduced from 25 to 23 Ma and stayed low until 20.5 Ma, however, increased afterwards up to ~13.5 Ma. The gradual decrease of the previously mentioned parameters recorded from ~13.5 to 4.5 Ma, which co-occurred with major ice sheet intensification in the Antarctic region (Kennett, 1990, Singh et al., 2012). Short period increasing of the E, H, S and Sander's values have been recorded from ~4.5 to 3 Ma followed

by a sudden decrease in later times, co-occurred with North Hemisphere major Glaciation (NHG) (Singh et al., 2012).

The diversity values and peaks are quite similar to the diversity values recorded by Singh et al. (2012) at 752A, and the highest diversity value at the current study is recorded at 13.56 Ma, which has also been recorded at ~ 13.5 Ma by Singh et al. (2012). The diversity values show high correspondence with isotope values (Singh et al., 2012).

According to Woodruff and Savin (1991), the high $\delta^{13}C$ values at an interval between 17 to 13.5 Ma was contemporaneous with periodic fluctuations of $\delta^{13}C$. Both carbon and oxygen values increased during that time, which coincided with a cooling period. The $\delta^{18}O$ values decreased and reached a minimum between 16.7 to 14.9 Ma and this followed by 2 million years increasing of $\delta^{18}O$ values by 1.5 per mil. During around 13.8 Ma the bottom water temperature decreased by ~ 2 °C in the eastern equatorial Pacific Sites (Sites U1338 and 1146), this decrease coincided with the increasing of $\delta^{18}O_{sw}$ by 0.9–1.0 ‰ (Kochhann et al., 2017).

Seven events for both carbon and oxygen isotopes have been recorded in a different part of the world by Woodruff and Savin (1991) and the periods of high $\delta^{13}C$ have referred to as a carbon excursion (Holbourn et al., 2007). Banerjee et al. (2017) reported the global warmth period at ~17–14 Ma which coincided to increase of organic carbon deposition (Monterey excursion). The diversity values show a gradual increase during the Mid-Miocene Climatic Optimum (MMCO) and dropped down suddenly at around 15- 14 Ma in all studied sites (752A,

1168A and 1139A). The diversity values peaked again with fluctuations between ~14- 12 Ma, which may coincide with East Antarctic ice sheet expansion (EAIS) (Flower and Kennett, 1993).

Because of the erosion in early late Miocene at 1139A, the data was not enough to see the diversity fluctuations during the late Miocene and early Pliocene. The diversity values for both Sites (752A and 1168A) are increased during the late mid- Miocene, while decreased rapidly at ~ 10.3 Ma. The interval between ~10.5- 8 Ma shows low diversity values in both Sites (752A and 1168A). According to Zachos et al. (2001), the renovation of the major Antarctic ice sheet started again at around 10 Ma, and through the late Miocene, the mean value of $\delta^{18}O$ increased slowly until early Pliocene ~6 Ma which coincided with a small expansion of West Antarctic Ice Sheet (WAIS). In the current study in both Sites (752A and 1168A) the diversity shows low value at ~6.5 Ma. This may have coincided with small ice sheet expansion (WAIS) (Zachos et al., 2001). The diversity values at both Sites (752A and 1168A) start to increase in the latest Miocene and the early Pliocene which may be coincided with a short warm interval of Pliocene which continued until ~3.2 Ma (Zachos et al., 2001). As mentioned before that the E, H, S and Sander's values also increased from ~4.5 to 3 Ma at 752A (Singh et al., 2012) which may have coincided with Pliocene short warm interval.

4.3.4.2 Most abundant taxa comparison between the studied Sites (752A, 1168A and 1139A) and other Miocene localities around the world:

Eight most abundant and environmentally important species have used in the studied Sites (752A, 1168A and 1139A) and these are compared to their global occurrence. In the current study, *Abdetodentrix peudothalmanni* peak is started from the early-mid Miocene at 752A and

the late mid- Miocene at 1168A, while it bloomed in the early Miocene during ~ 22-19 Ma at 1139A and peaked again at around 16 Ma (Figure 4.17). *Abdetodentrix* is closely related to *Bolivina* existing in a productive area, having the same infaunal niche and blooms in lower dissolved oxygen conditions (Thomas and Gooday, 1996, Hayward et al., 2002).

The peak of this species is similar at 1168A with *Bolivina dilata* (smooth-walled Bolivinids) (see Figure 4.10), while the latter records the highest peak at around 21.84 Ma (early Miocene). Smart and Ramsay (1995) believed that the smooth-walled bolivinids high abundances between 19.5 and 16.5Ma in the Indian Ocean coincided with their high abundances in the Atlantic Ocean. This been related to the oxygen reduction within Northern Component Water (NCW). Small biserial foraminifera in the eastern Atlantic and western Indian Oceans which previously assigned to genus *Bolivina* were planktic (genus *Streptochilus*) (Smart and Thomas, 2006, 2007).

According to Hayward et al. (2002), *Abdetodentrix peudothalmanni* was considered as bathyal species; its distribution is parallel to the Antarctic Intermediate Water (AAIW) distribution. This water mass is located directly under the surface water and occupies the depth between 600-1450 m, and it is considered as a significant northward spreading water mass (Hayward et al., 2002).

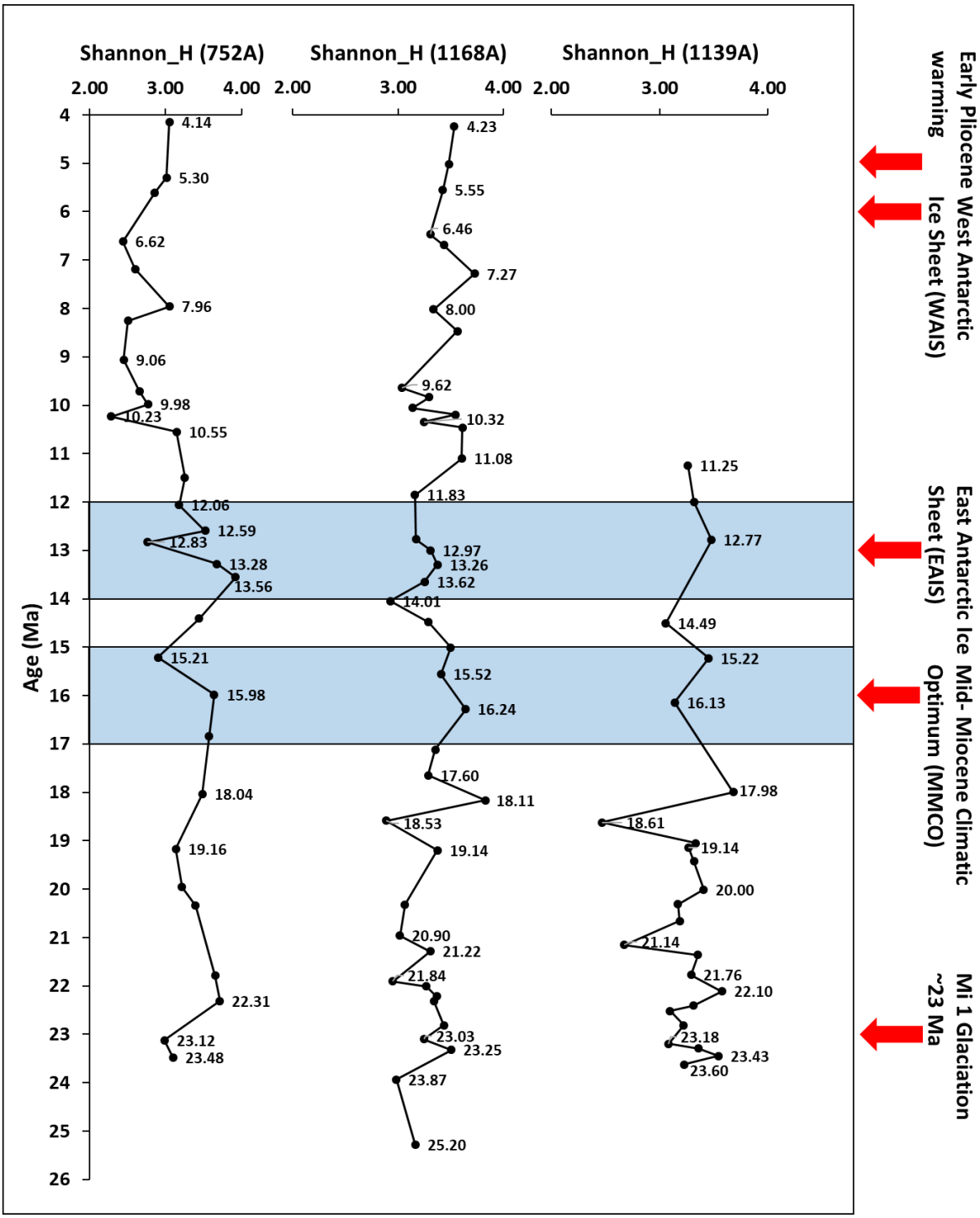


Figure 4. 16: Diversity versus age of studied Sites 752A, 1168A and 1139A. The red arrows pointed to the periods of glaciation and inter-glaciation. The shaded areas are Miocene cooling and warming events.

The first peak of *Astrononion umbilicatulum* was around 23-22 Ma at 1168A and 1139A, and its first peak was about 20 Ma at 752A (Figure 4.17). This species peaks again in the mid-Miocene at 752A and the middle to late Miocene at 1168A, while it started to peak back at around 12 Ma at 1139A.

Astrononion umbilicatulum peaks generally coincided with cooling events during the earliest Miocene (23-22 Ma) and the mid and Late Miocene during the expansion of the Antarctic Ice sheets (EAIS & WAIS) (Figure 4.17). Gooday (1994) believed that *Uvigerina, Melonis* (*M. barleeanum*) and *Astrononion* are high organic flux indicators. They are bloomed during increasing organic flux and cooling periods.

The peak of *Globocassidulina subglobosa* at all studied Sites (752A, 1168A and 1139A) was high during the latest Oligocene and early Miocene until around ~20 Ma (Figure 4.17). The peak dropped after ~ 20 Ma gradually at all sites. The peak started again at around ~ 18 Ma and second highest peak recorded in the mid- Miocene at all sites. The peak drops suddenly at ~ 12 Ma at the study sites. The relative abundance was high during the late Miocene at 1168A while the peak at 752A was relatively lower during the late Miocene except ~ 9 Ma which recorded the highest peak. *Globocassidulina subglobosa* is considered to be cosmopolitan species living in a different bathymetry and linked to different water masses (Gooday, 1994).

Corliss (1979a) noted the association of this species in the south-eastern Indian Ocean with AABW (Antarctic Bottom Water). The blooming of this species in the southeast Indian Ocean

is indicative of highly oxygenated (oligotrophic) and strongly pulsed food supply (Singh and Gupta, 2004). According to Singh et al. (2012), this species was dominant during the early and mid- Miocene and decreased continuously until ~ 2 Ma at 752A.

The peak of *Cibicidoides mundulus* was in the early and late Miocene while the peak highly depleted in the mid- Miocene at 752A (Figure 4.17). The peak of this species at the Site 1168A was during the early Miocene and dropped from ~ 21- 18 Ma and then peaked again with gradually decreasing until the late Miocene. The relative abundance of *C. mundulus* was high during the early Miocene, and the peak highly fluctuated during mid- Miocene at 1139A. According to Nomura (1991), *C. mundulus* was a common species of the early Miocene at 754 (Broken Ridge), and its relative abundance increased again in the late mid- Miocene and the late Miocene. *C. mundulus* was a dominant species of late Oligocene and earliest Miocene at the Site 756 (Ninetyeast ridge) (Nomura, 1991). *C. mundulus* was a characteristic species of the late Miocene at the shallow Site 748 (1288 mbsf) (Southern Kerguelen Plateau) (Mackensen, 1992).

Epistominella exigua was a common species in the early Miocene at 1168A while at 752A only appear in few intervals during the mid and the late Miocene (Figure 4.18). *Epistominella exigua* peak was recorded during the mid- Miocene at 1139A. Kurihara and Kennett (1992) observed that species such as *G. subglobosa* and *E. exigua* were dominant during the early Miocene in the South Western Pacific Ocean at the deep Site 206, these species existed when relatively low $\delta^{18}O$ values recorded. The relative abundance of *E. exigua* increase during the early-mid Miocene at the shallower Sites (588, 590 and 591) in the South-Western Pacific

Ocean at ~ 15 Ma, this had been interpreted by shallowing of water masses which characterised by *E*. *exigua* during ~ 15 Ma (Kurihara and Kennett, 1992). This species is a high productivity species associated with increased upwelling near the Antarctic convergence (Schroder-Adams, 1991). A large population of phytodetritus species such as *E*. *exigua* build up during the seasonal arrival of phytodetritus. This was observed in oligotrophic condition when pulsed inputs of food in form of phytodetritus arrived and make this opportunistic species (*E*. *exigua*) increase in abundance notably (Smart et al., 2007).

Nuttalides umbonifera is a dominant early Miocene species at 752A; its relative abundance was lower at ~ 14 Ma until it abruptly decreases and disappears in the late Miocene (Figure 4.18). This species dominated during mid- Miocene at both deeper Sites 1168A and 1139A, while the relative abundance peak continued at 1168A during the late Miocene. According to Badger et al. (2013), the development of the East Antarctica Ice Sheet happened at about 14 Ma which is the time when *Nuttalides umbonifera* started to dominate at the Sites 1139A and 1168A.

The high relative abundance of *Nuttalides umbonifera* has been linked to the corrosive bottom water or AABW (Antarctic Bottom Water) (Bremer and Lohmann, 1982). Loubere and Fariduddin (1999) believed that this species might be a good indicator of low productivity. Mackensen et al. (1990) recorded this species as a characteristic species of the mid- Miocene in the southern Kerguelen Plateau and Maud Rise.

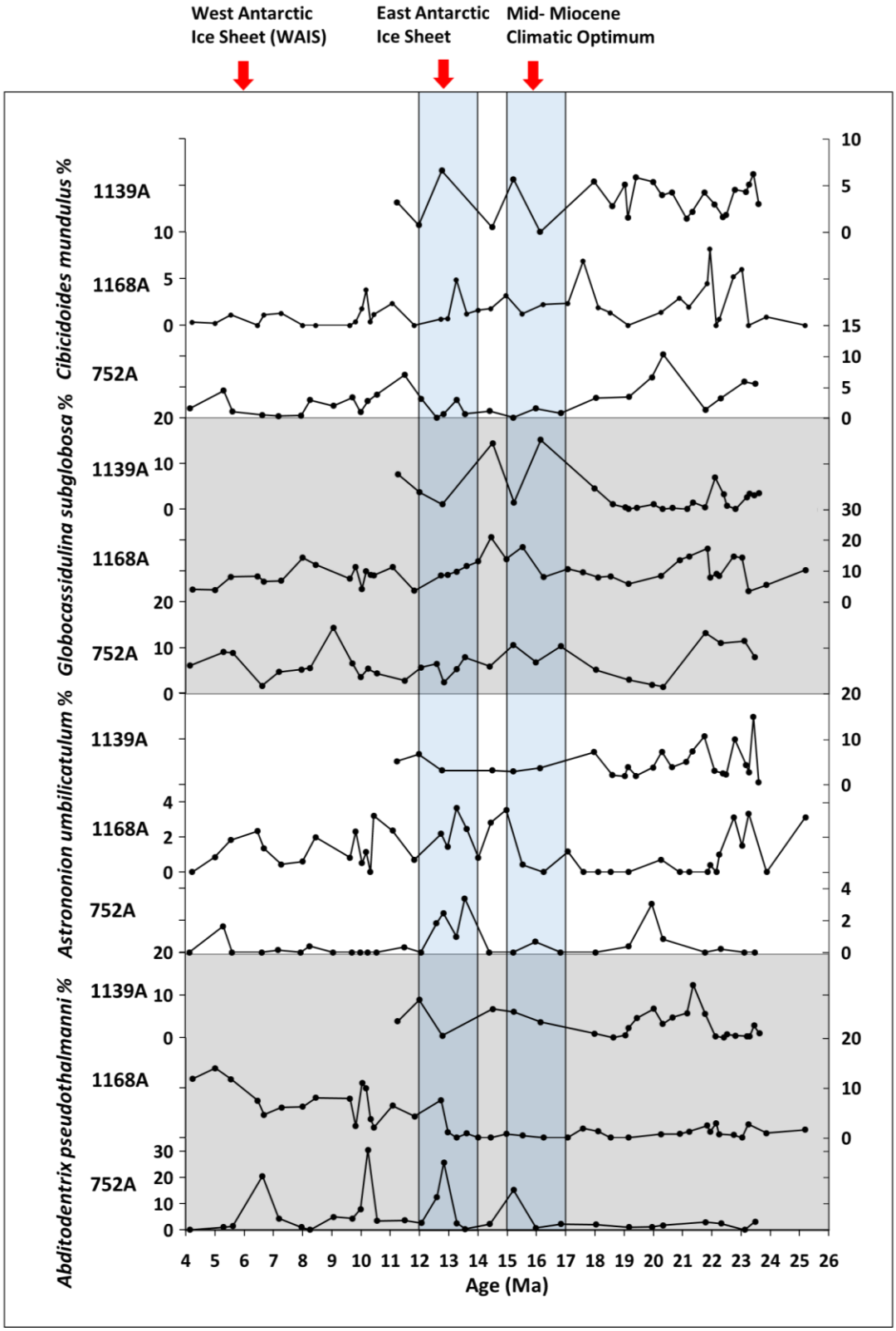


Figure 4. 17: Comparing between four most abundant species at the study sites 752A, 1168A and 1139A plotted versus age. The shaded areas with the red arrows point to global climatic events.

Nuttalides umbonifera recorded as dominant during 22- 19.5 Ma and again during 15- 14 Ma at 752A (south-eastern Indian Ocean) (Singh et al., 2012). According to Ramsay et al. (1998) *Nuttalides umbonifera* dominated simultaneously at ~ 13 Ma at both Indian Ocean Sites 237 and 710. This may be affected by EAIS (East Antarctic Ice Sheet) expansion.

Siphonodosaria lepidula is a common species during the early Miocene at the present Sites (752A, 1168A and 1139A) (Figure 4.18). The abundance of this species has relatively increased during the mid- Miocene with lower peaks at 752A and 1168A. The peak of this species was observed again during the late Miocene at 1168A.

Stilostomella lepidula lives in highly organic carbon sediments with relatively low oxygen (Boersma, 1990). Singh and Gupta (2010) believed that *Stilostomella lepidula* is a cosmopolitan species it has observed in a complex ecological system, and it does not have a clear distribution. This species widely distributed in the Central Indian Ocean, it is an index fauna of the late Oligocene - early Miocene at Sites 714 and 238 and index early Miocene species at Sites 214, 219 and 715 (Boersma, 1990). This species was a common mid- Miocene species at Sites 714 and 709, and it is considered as an index species at 219 (1764 mbsf) during the late Miocene (Central Indian Ocean) (Boersma, 1990).

Boersma (1990), used a group of benthic foraminifera species (index species) for paleoenvironmental interpretations, these species are occurred under specific environmental conditions, different water depths and water masses.

Stilostomella lepidula was a common species during the early and the mid- Miocene at Hole 757B (South-eastern Indian Ocean), while it decreased in abundance in the early late Miocene during ~12-10 Ma, coinciding with major decrease of *Oridorsalis umbonatus* abundance (Singh and Gupta, 2010). The lowering of relative abundance of *Stilosomella lepidula* at around 12-11 Ma at 757B also coincided with a gradual increase in the relative abundance of *Nuttalides umbonifera* (Singh and Gupta, 2010).

Trifarina angulosa was a common late Miocene species at the current Sites 752A and 1168A and dominant mid- Miocene species (~ 15Ma) at 1139A. This species was only seen in very low abundance during the early Miocene at 1168A.

According to Mackensen (1992), *Trifarina angulosa* was a common species when Antarctic Circumpolar Current (ACC) strengthen during the Pliocene and Pleistocene in the southern Indian Ocean (Kerguelen Plateau) at the Sites 747, 748 and 751. This species bloomed during the period of global cooling during the late Pliocene and Pleistocene in the southern Indian Ocean (Kerguelen Plateau) (Mackensen, 1992).

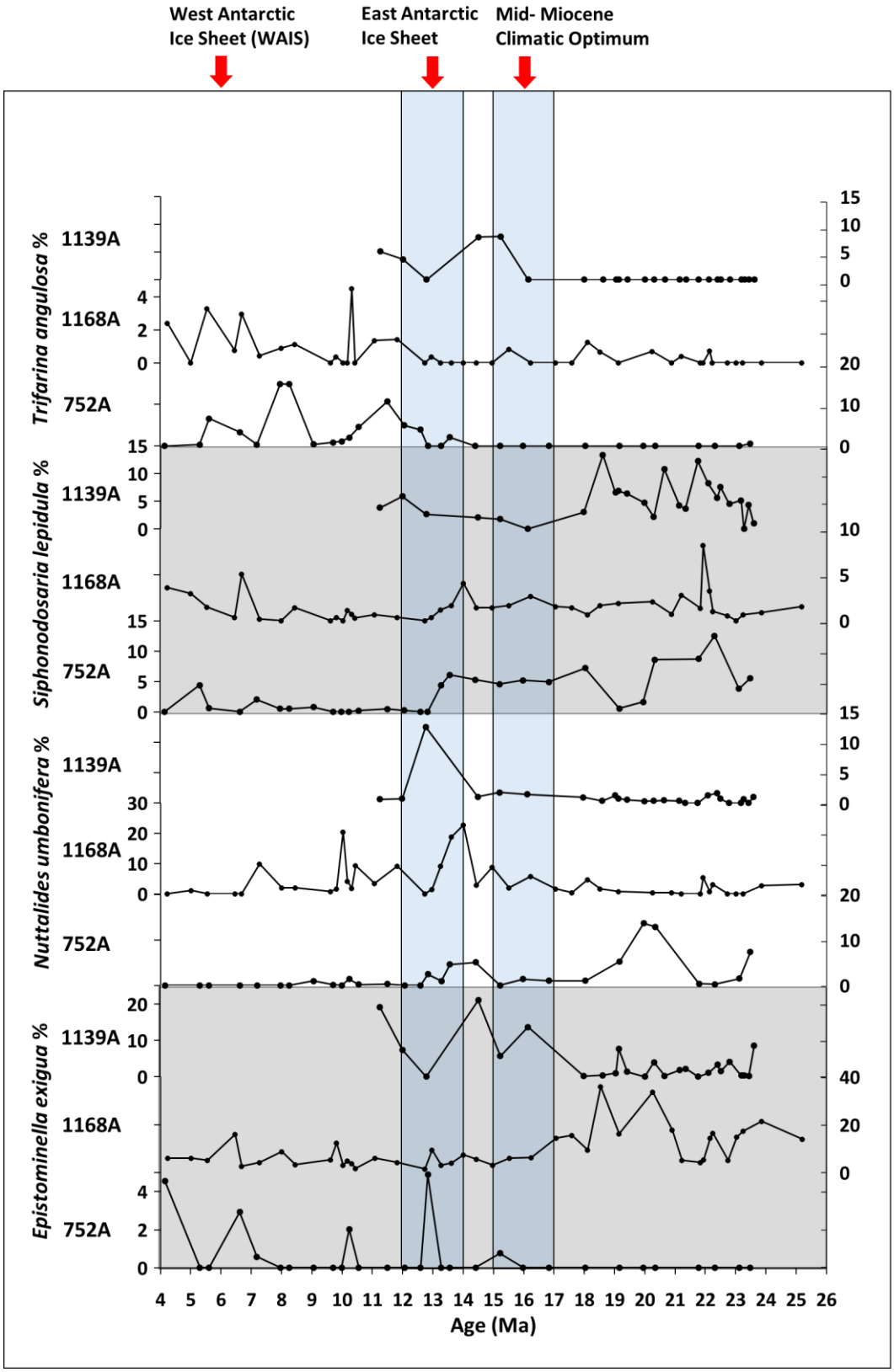


Figure 4. 18: Comparing between four most abundant species at the study Sites 752A, 1168A and 1139A plotted versus age. The shaded area with the red arrows pointing to the global events.

Chapter Five

Test sizes, Carbonate crash and Biogenic blooms

5.1 Test sizes:

5.1.1 Introduction:

The size of five different benthic foraminifera species (*Abdetodentrix pseudothalmani*, *Globocassidulina subglobosa*, *Cibicidoides mundulus*, *Nuttalides umbonifera* and S*phaeroidina bulloides*) are testified and compared with their relative abundance form all studied Sites (752A, 1168A and 1139A). Most of the species size values (mean size, smallest and largest size) show rapid change at around 12- 13 Ma in all sites. This drop followed by a rapid shift in sizes at the time where most of the species show increasing in size.

The maximum size of the biserial form such as *Abdetodentrix pseudothalmani* increased significantly after MMCO, the same increase has recorded for all other species maximum and mean sizes, this has coincided with primary productivity increase at the studied sites especially at the Sites 752A and 1168A (Figures 4.3 and 4.8). Kaiho (1999) believed that variations in oceanic primary productivity, organic carbon flux and dissolved-oxygen levels in the water column has significant effect in controlling of benthic foraminiferal test size.

During the testing of a maximum size of ten genera over a past 120 Ma, Kaiho (1999) noted that the test size increased in general. This long-term increase of the test size coincided with increasing $\delta^{18}O$ of deep-water benthic foraminifera. According to Kaiho (1999), the test size

minima coexists with low oxygen dissolution and warming periods. The warming period caused slow circulation and coincided with high CO_2 levels (Kaiho, 1999). In contrast, the test size maxima during the late Oligocene- early Miocene and the late Miocene- early Pliocene co-occurred with high oxygen dissolution conditions and cooling events (Kaiho, 1999).

5.1.2 Results:

In each figure, the size (mean, largest test, smallest test, and standard deviation) and relative abundance for each site are plotted side by side to show the variations of each of them during different times. The peaks of maximum sizes of all species highly show fluctuation; however, size values become higher from the mid- Miocene towards the late Miocene except the interval between ~20 to 18 Ma. In this interval most of the species maximum and mean size shows higher peaks if compared with the earlier Miocene except some species where these (maximum size and mean) values started to increase earlier. For instance, the high peaks of species such as *Cibicidoides mundulus* at both 1139A and 1168A recorded around 21- 22 Ma also *Abdetodentrix pseudothalmani* maximum size was relatively high during this time.

The maximum size of the *Globocassidulina subglobosa* recorded higher values at around 22 Ma at 1168A (Figure 5.2). The general trend of a mean and maximum size of all species at all studied sites show a drop at about 17 Ma; this may have coincided with MMCO.

The average size curve of *Abdetodentrix pseudothalmani* (Figure 5.1) shows peak before the Mid Miocene Climatic Optimum and also during East Antarctic Ice Sheet expansion (EAIS) at

the Sites 752A and 1139A, while at the Site 1168A the peak starting from the late mid-Miocene (during EAIS expansion) and upward.

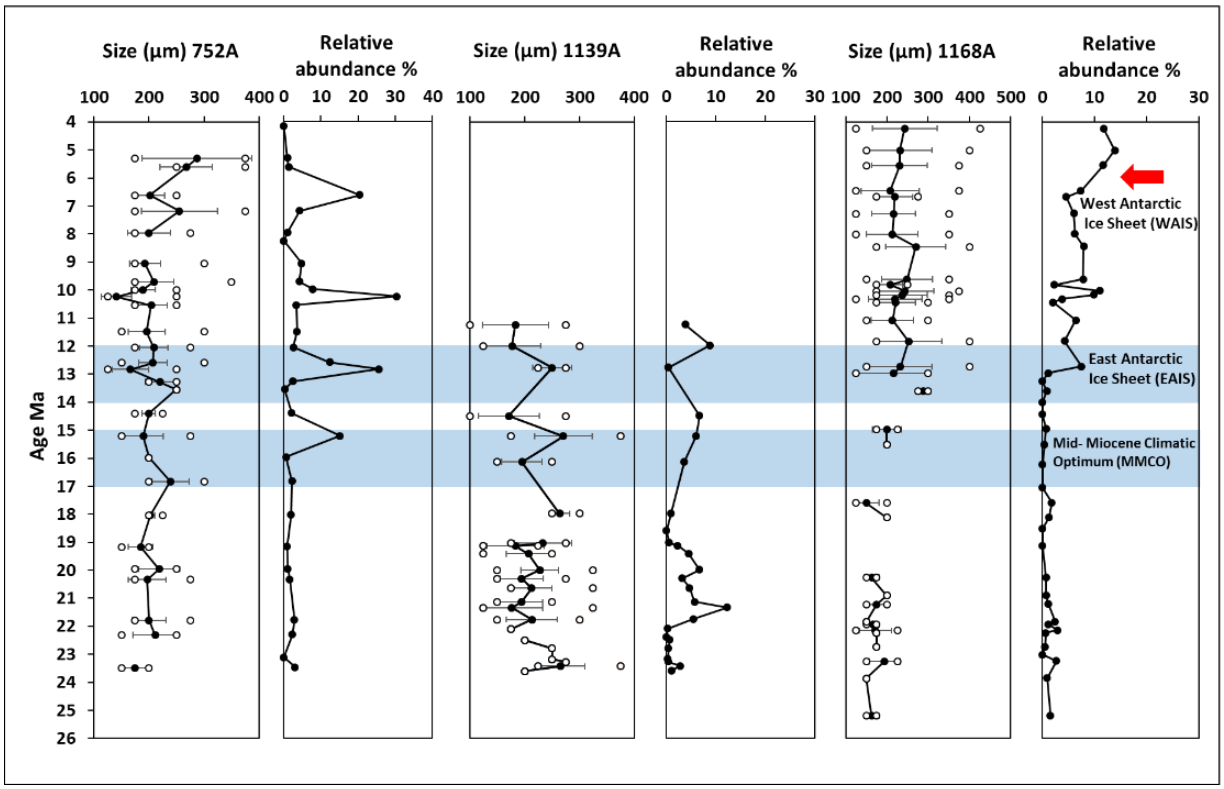


Figure 5. 1: Size and relative abundance of *Abdetodentrix pseudothalmani* at the studied Sites versus age. The solid line in the size graph is the mean size, and the empty circles are representing the smallest and largest test. The horizontal lines in size graphs are standard deviation (STDV).

The relative abundance and maximum size of *Abdetodentrix pseudothalmani* increase gradually from the early mid-Miocene to late Miocene at 752A and from the late mid-Miocene to the early Pliocene at the Site 1168A. While the relative abundance and maximum size of this species were high at 1139A during early Miocene until around ~19 Ma, this has also happened at 752A. The relative abundance and maximum size of this species at 1139A

increase again until it dropped suddenly in the Mid Miocene during MMCO and increased again at the end of EAIS expansion.

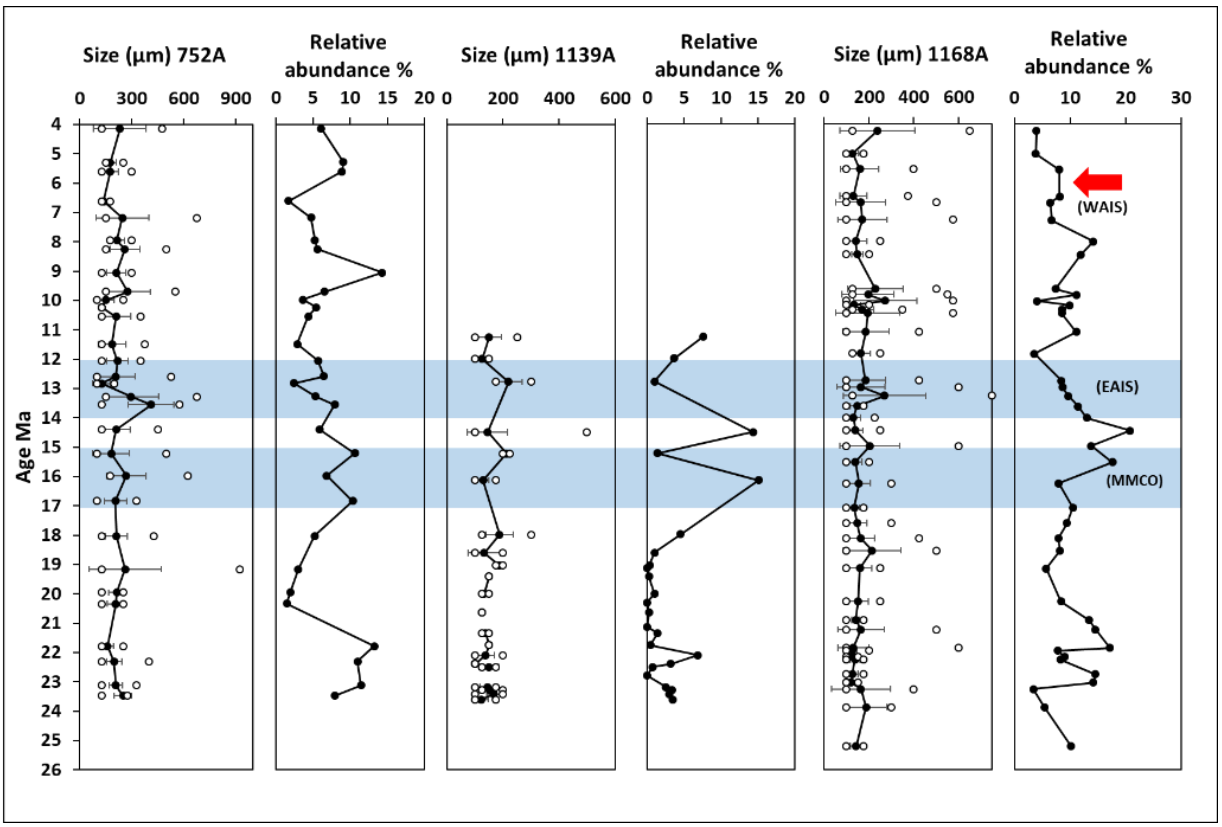


Figure 5. 2: Size and relative abundance of *Globocassidulina subglobosa* at the studied Sites versus age. The solid line in the size graph is the mean size, and the empty circles are representing the smallest and largest test. The horizontal lines in size graphs are standard deviation (STDV).

Due to the unconformity at 1139A, there is not enough data to see what happened during the late Miocene and the early Pliocene.

The mean and maximum size of *Cibicidoides mundulus*, *Nuttalides umbonifera* and S*phaeroidina bulloides* (Figures 5.3- 5.5) at all studied Sites (752A, 1139A and 1168A) increase

gradually followed by sharp drop at around 6-5 Ma of both *Cibicidoides mundulus* and S*phaeroidina bulloides*. This dropping has also been observed in *Globocassidulina subglobosa* curves.

The correlation coefficient calculated between the maximum size and the relative abundance of each species. Correlation coefficient for *Abdetodentrix pseudothalmani* is highest at 1168 (0.83). The value for *Globocassidulina subglobosa* is 0.49 at 1139A (highest value). *Cibicidoides mundulus* records highest value (0.62) at 1139A (highest value). The value for *Nuttalides umbonifera* is highest (0.8) at 1168A. S*phaeroidina bulloides* records highest correlation coefficient (0.43) at 1139A (See Appendix K).

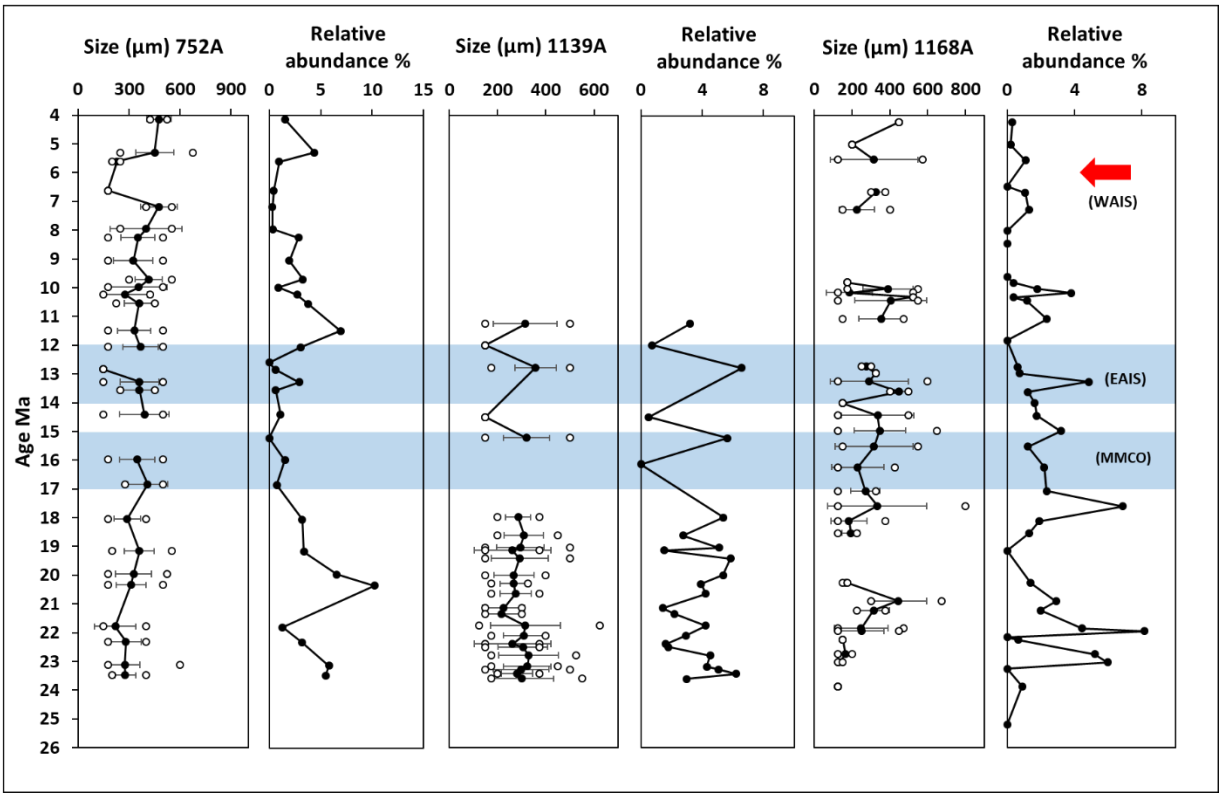


Figure 5. 3: Size and relative abundance of *Cibicidoides mundulus* at the studied Sites versus age. The solid line in the size graph is the mean size, and the empty circles are representing the smallest and largest test. The horizontal lines in size graphs are standard deviation (STDV).

5.1.3 Discussion:

Increasing of *Abdetodentrix pseudothalmani* (Figure 5.1) size coincided with cooling events, for an instant the increasing of the maximum size at around 19 Ma as well. This time is indicative of deep-sea cooling which associated with sea level lowering. This cooling event coincided with the NH1 hiatus of Keller and Barron (1983) (20-18 Ma). The general trend of a mean and maximum size of all species at all studied sites dropped at about 17 Ma; this may have coincided with MMCO.

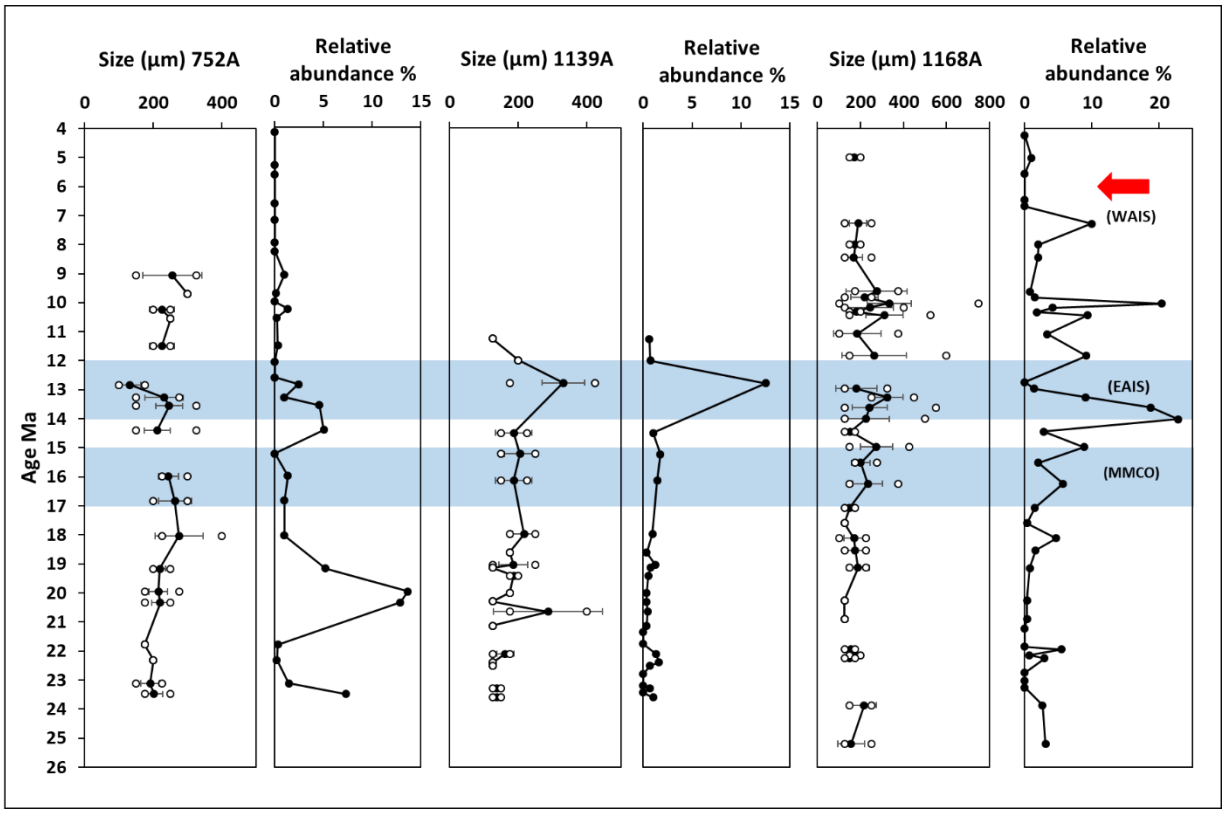


Figure 5. 4: Size and relative abundance of *Nuttalides umbonifera* at the studied Sites versus age. The solid line in the size graph is the mean size, and the empty circles are representing the smallest and largest test. The horizontal lines in size graphs are standard deviation (STDV).

The composition and different water masses during geologic times may have triggered the abundance and size variability of the deep-sea benthic foraminifera. It has been observed that the development of water mass similar to modern North Atlantic Deep Water (NADW) had started between 14.5 and 8 Ma (Woodruff and Savin, 1989), this water mass supposedly co-existed with highly oxygenated, cooler deep water (Smart and Ramsay, 1995). Kaiho (1994) presumed that slow horizontal and vertical circulation due to increasing temperature (warming periods) led to oxygen lowering and low oxygen index values.

Slow vertical and horizontal deep-water circulations during global warming cause the high oxygen consumptions, high CO_2 levels and precipitation of dissolved nutrients (Kaiho, 1999), this, in turn, decrease the test calcifications and test size of trochospiral benthic foraminifera (Peypouquet et al., 1988). According to Greenop et al. (2014) two intervals of Antarctic ice sheet regression reported during the Mid Miocene Climatic Optimum. This retreating coincided with recording high CO2 and orbital obliquity variability.

Most of the species size values show a rapid drop at around 12- 13 Ma in all sites. This drop followed by a rapid shift in sizes and most of the species show increasing in size.

In the current study sharp drop of both *Cibicidoides mundulus* and S*phaeroidina bulloides* at around 6-5 Ma (Figures 5.3, 5.5) may have been affected by an early Pliocene warming event (Zachos et al., 2001), this also been observed in *Globocassidulina subglobosa* curves (Figure 5.2).

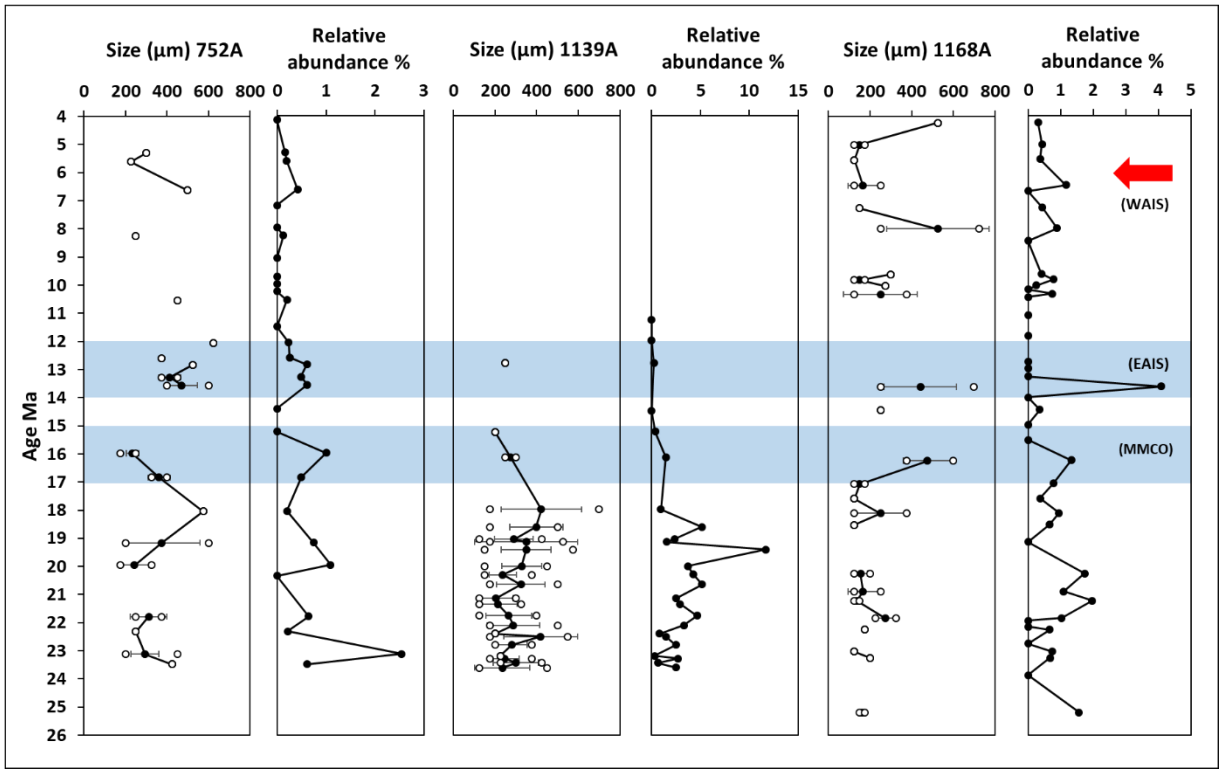


Figure 5. 5: Size and relative abundance of *Sphaeroidina bulloides* at the studied Sites versus age. The solid line in the size graph is the mean size, and the empty circles are representing the smallest and largest test. The horizontal lines in size graphs are standard deviation (STDV).

The characteristic benthic species of oxic environments has a thick wall and large tests (>350 µm) which live in high oxygen bottom water and are absent in low oxygen conditions, such as biconvex trochospiral and rounded forms (*Cibicidoides, Nuttallides, Stensioina, Gavelinella,* and *Globocassidulina*) (Kaiho, 1994).

The nutrient and oxygen levels change along the deep-water circulation direction had affected the MDLS (Maximum Diameter of Largest specimens) values and make it variable not just stratigraphically, but also geographically (Kaiho, 1999). That is what have been noted when each species records slightly different maximum size values at all studied sites.

5.2 Carbonate crash and Biogenic blooms:

5.2.1 Introduction:

Previous studies recorded a change in a deposition with sediments of high calcium carbonate content to an interval of carbonate content fluctuations and increased intervals of silica-rich sediments at about 9.1- 10,1 Ma (Mayer et al., 1985, Mayer et al., 1986). The abrupt rise of carbonate compensation depth (CCD) at ~ 10 Ma which lasted 2 to 3 million years was called carbonate crash which reported in the tropical eastern Pacific Ocean (Lyle et al., 1995).

Many possibilities have been explained in Lubbers et al. (2019) regarding carbonate crash among them: 1) increasing primary production of siliceous and organic-walled phytoplankton in the equatorial Pacific which may cause the decreasing of organic carbon (C_{org}), 2) the releasing of C_{org} which may have caused by high latitude cooling and Antarctic ice sheet expansion. 3) EAIS expansion during the mid to late Miocene which followed by expansion of south-sourced intermediate and deep water massed. 4) Indonesian seaway closure which may have triggered the oceanic circulations and affected the equatorial productivity.

Biogenic bloom is related to primary production (Dickens & Owen, 1999). During the late Miocene-early Pliocene, primary productivity substantially increased at Indo-Pacific upwelling zones in the north and the western Indian Ocean, this increase has been reported between 9 to 3 Ma (Dickens & Owen, 1999). Gupta et al. (2004) recorded high productivity increase with a declination of benthic foraminiferal diversity in the eastern equatorial Indian Ocean between 10 and 8 Ma.

Increase in biogenic accumulations and sedimentation rates towards the Equator following the carbonate crash is called “biogenic bloom” was recognised at Site U1443 around 8.7 Ma (Lubber et al., 2019).

In the current study benthic foraminifera stable isotopes ($\delta^{18}O$ and $\delta^{13}C$) (discussed in detail in chapter 6), benthic foraminifera abundance and diversity, and carbonate accumulations (carbonate content (%) and carbonate mass accumulation rates ($MAR_{carbonate}$)) integrated to reconstruct changes in carbonate depositions and climate evolution over the interval 13.5 to 8.2 Ma. Lubbers et al. (2019) reported the range between 13.5 to 8.2 Ma as an interval of declination of carbonate percentages and carbonate accumulation rates at International Ocean Discovery Program Site U1443 (Ninetyeast Ridge, Indian Ocean). The current study at all Sites (752A, 1168A and 1139A) attempted to observe the carbonate accumulations and biogenic blooms during the mid and the late Miocene.

5.2.2 Results:

5.2.2.1 ODP Site 752 Hole A:

Carbonate content (%), carbonate mass accumulation rates ($MAR_{carbonate}$) (See Appendix F) are plotted (Figure 5.6) with parameters mentioned above (abundance, diversity, etc.) to show the carbonate declination interval and biogenic blooms.

The first dropping of the $MAR_{carbonate}$ has seen after about 13.28 Ma and continued to record the lowest value during the early late Miocene (~ 9 Ma). In contrast, the carbonate content remains high, and it does not show a high declination during the mid to the late Miocene

despite the interval between ~ 9 to 7 Ma, which records lower values. MAR $_{carbonate}$ dropping coincided with lowering of diversity and carbon isotope ($\delta^{13}C$) and increasing of both benthic foraminiferal abundance and oxygen isotope ($\delta^{18}O$). MAR $_{carbonate}$ improvement recorded at about 8 Ma and suddenly dropped at the latest Miocene.

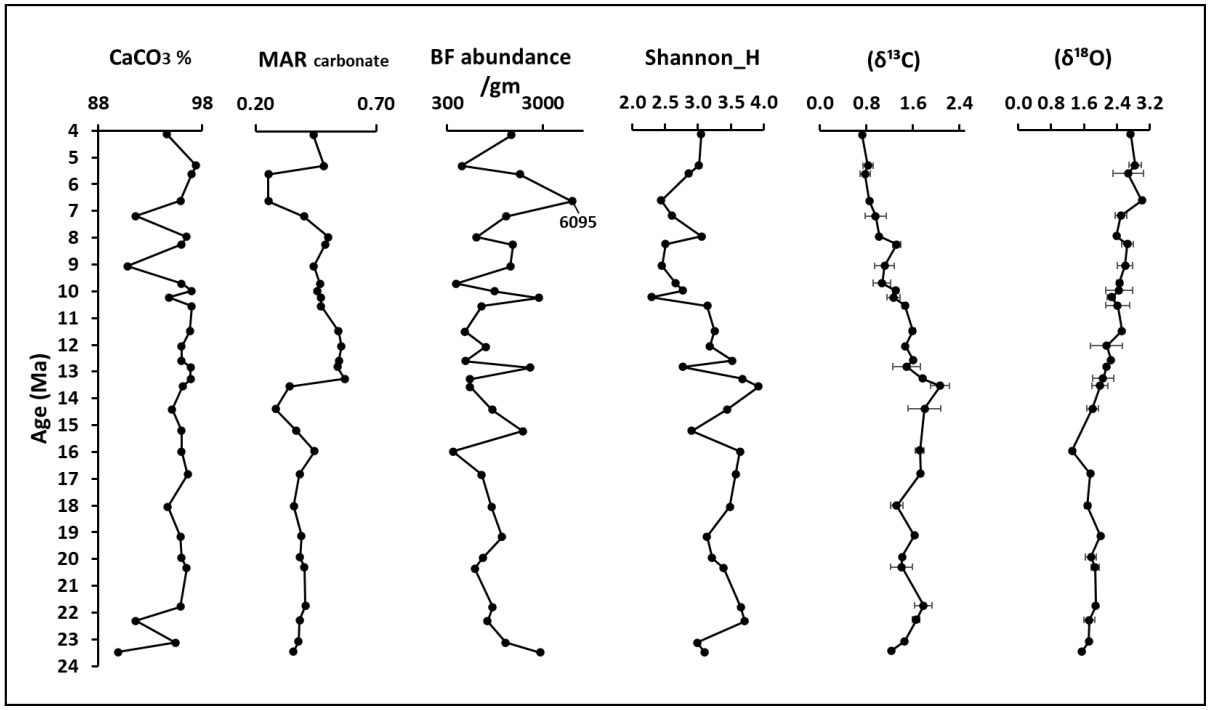


Figure 5. 6: Carbonate content (%), carbonate mass accumulation rates (MAR $_{carbonate}$), benthic foraminiferal abundance, diversity and isotope values plotted versus age at the studied Site 752 Hole A.

5.2.2.2 ODP Site 1168 Hole A:

The values of carbonate content (%) (See Appendix H) gradually increase during the Miocene with fluctuation and it records the highest value at 13.26 Ma (Figure 5.7). The carbonate content gradually decreased until it records ~ 68% at around 11 Ma. MAR $_{carbonate}$ values are

picked during the early Miocene and early late Miocene at about 10 Ma at the same time the carbonate content values increased gradually.

During the peak of MAR $_{carbonate,}$ both carbon ($\delta^{13}C$) and oxygen isotopes ($\delta^{18}O$) gradually increased, while diversity values sharply decreased with slightly depleting of benthic foraminiferal abundance. At about 8 Ma MAR $_{carbonate}$ rapidly dropped, this has coincided with a rapid dropping of both carbon ($\delta^{13}C$) and oxygen isotopes ($\delta^{18}O$) and both abundance and diversity are peaked.

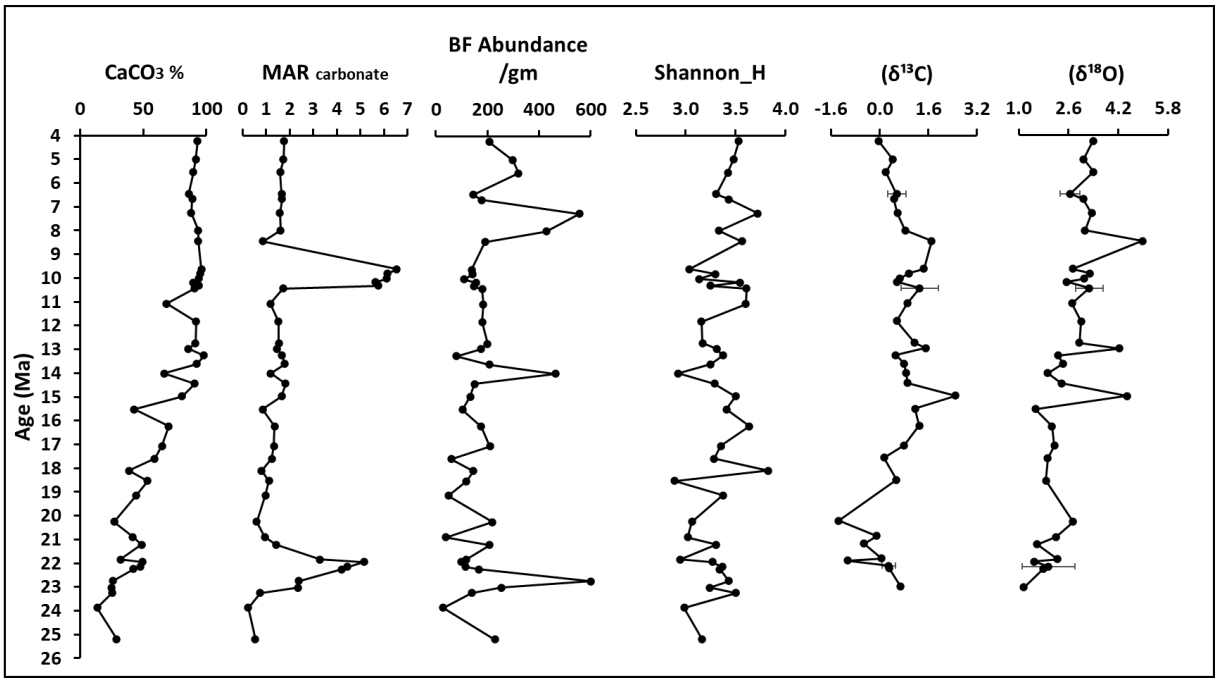


Figure 5. 7: Carbonate content (%), carbonate mass accumulation rates (MAR $_{carbonate}$), benthic foraminiferal abundance, diversity and isotope values plotted versus age at the studied Site 1168 Hole A.

5.2.2.3 ODP Site 1139 Hole A:

Carbonate content (%) and MAR $_{carbonate}$ (See Appendix J) have low values during the latest Oligocene and early Miocene this has coincided with dropping of benthic foraminiferal

abundance and carbon ($\delta^{13}C$) isotope, while oxygen isotope ($\delta^{18}O$) remain slightly high (Figure 5.8). Both isotope records with abundance values are increased gradually at around 18 Ma which coincided with the increasing of carbonate content (%). During around 19 Ma MAR $_{carbonate}$ recorded the lowest value and it remains low until the early late Miocene, while the diversity does not show a big change.

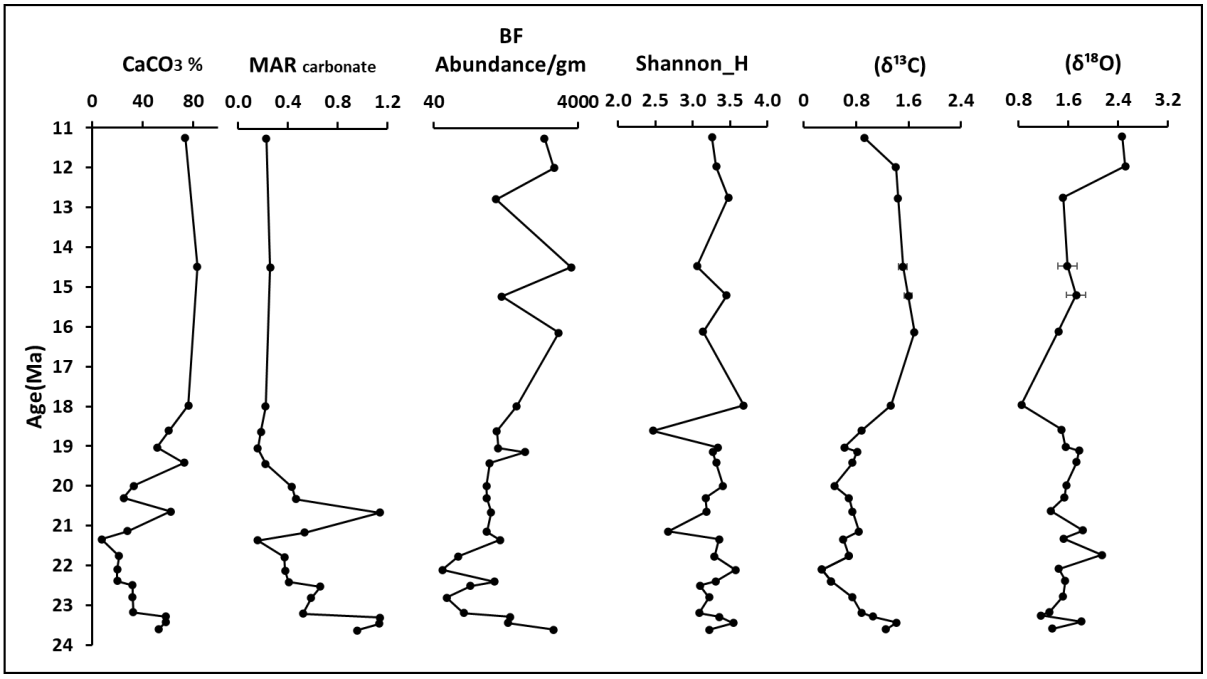


Figure 5. 8: Carbonate content (%), carbonate mass accumulation rates (MAR $_{carbonate}$), benthic foraminiferal abundance, diversity and isotope values plotted versus age at the studied Site 1139 Hole A.

5.2.3 Discussion:

5.2.3.1 ODP Site 752 Hole A:

The declination of MAR $_{carbonate}$ in the current Site continued from around 13 Ma to around 8 Ma coincides with the middle to late Miocene carbonate crash (Lubbers et al., 2019). Reduced carbonate deposition in all major tropical ocean basins coincided with intense carbonate impoverishment at Site U1443 (~11.5 to ~10 Ma) (Lubbers et al., 2019). The continuous

increase of high productivity during around 10.5 to 8 Ma (Figure 4.3) may have coincided with the global onset of the biogenic bloom this has also coincided with diversity and carbon ($\delta^{13}C$) isotope decrease in the current Site. Gupta et al. (2004) also recorded high productivity increase with a decreasing of benthic foraminiferal diversity in the eastern equatorial Indian Ocean between 10 and 8 Ma.

5.2.3.2 ODP Site 1168 Hole A:

The declination of the carbonate content at around 13 Ma is gradual until recorded a low value at around 11 Ma at the time when carbon ($\delta^{13}C$) isotope record low values as well. At the Site U1443 the intense carbonate crash phase has reported during around 12.2 Ma and continued until it records lowest $MAR_{carbonate}$ at about 11.5 to 10 Ma (Lubbers et al., 2019). While at the current study the carbonate content and $MAR_{carbonate}$ records high values coincided with the high rate of the sedimentation during the interval between 10.32 to 9.62 Ma. The surface productivity started at around 13 Ma and intensified at about 11 Ma (Smart et al., 2007), while in the current study the high productivity taxa recorded during around 11.8 Ma and another high value recorded at around 5 Ma (Figure 4.8).

5.2.3.3 ODP Site 1139 Hole A:

The erosion of the upper part of the current Site does not give the opportunity to see the late Miocene succession. The mid- Miocene is poorly interpreted because of the low data availability. The values of the carbonate content and $MAR_{carbonate}$ are missing because of the erosion of the upper succession, for that there is no evidence about the carbonate crash and biogenic blooms.

Chapter Six

Stable Isotopes

6.1 Introduction

6.1.1 Background

Oxygen and Carbon isotope records of benthic foraminifera from deep-sea ocean cores in the different part of the world provide useful information about the oceanic temperature and organic productivity (Cramer et al., 2009). Benthic foraminiferal oxygen isotope ($\delta^{18}O$) fluctuations show the different properties of deep marine water and changes in ice sheet volume during different times while, changes in carbon isotope ($\delta^{13}C$) values reflect the carbon transportation between sediments, atmosphere and ocean (Cramer et al., 2009).

Global deep-sea nutrient and density differences (temperature and salinity) have been revealed from measuring oxygen and carbon isotopes (Cramer et al., 2009). The modern ocean deep water masses formed in the North Atlantic (North Atlantic Deep Water (NADW)) and in the Southern Ocean close to Antarctica (Antarctic Bottom Water (AABW)) both have different density and nutrients (Cramer et al., 2009). The bipolar water masses, which made a framework for palaeoceanographic reconstruction of deep-water source regions were Northern Component Water (NCW) and Southern Component Water (SCW) (Cramer et al., 2009).

According to Woodruff and Savin (1989), the development of Miocene thermohaline circulation was during the early, mid and the late Miocene. Stepwise climatic change during

the Miocene was observed. This started from the late Oligocene and continued until a climatic optimum during the late early Miocene, then mid- Miocene rapid cooling (Flower and Kennett, 1994, Shackleton and Kennett, 1975). The significant climatic evolution was recorded during the mid- Miocene (Flower and Kennett, 1994). Another important period during the late Neogene was global cooling and Northern hemisphere ice sheet initiation (Flower and Kennett, 1994).

The modern ocean circulation is dissimilar qualitatively with the Miocene ocean circulation before 11 Ma (Woodruff and Savin, 1989). During the early Miocene continuous decreasing of dissolved oxygen and carbon values observed because of oxidation of organic matter and water transported further away at the ocean surfaces (Woodruff and Savin, 1989).

Woodruff and Savin (1989) considered that the early Miocene global circulation of temperature and salinity of the oceans might have strongly impacted by flowing of saline warm Tethyan Indian Saline Water (TISW). From the global isotopic and faunal records it has been suggested that the flux of TISW had terminated at around 14 Ma at the same time where the formation of North Atlantic Deep Water has not evidenced except in short intervals during the early Miocene (Woodruff and Savin, 1989).

The average values of $\delta^{13}C$ during ~ 17 – 13.5 Ma have largely increased (Monterey Carbon Excursion) globally; this positive excursion has several $\delta^{13}C$ maxima which represent huge variations in organic flux (Flower and Kennett, 1994, Woodruff and Savin, 1991). During the mid- Miocene, a high organic carbon deposition coincided with partial and continuous

depleting of atmospheric CO_2 (Flower and Kennett, 1994). Tectonic movements have another impact on oceanographic development during the mid-Miocene, such as eastern Tethys closure (Flower and Kennett, 1994) and Indonesian Seaway restriction (Kennett et al., 1985). A significant increase of $\delta^{18}O$ from 1.0 to 1.3‰ was observed during ~ 16 to 12.5 Ma which coincided with EAIS (East Antarctic Ice Sheet) expansion and bottom water cooling (Shackleton and Kennett, 1975, Woodruff and Savin, 1989).

Another establishment of the Antarctic Ice Sheet has been reported at around 10 Ma during recording a high mean value of $\delta^{18}O$; then the values continued to increase slowly until about 6 Ma which indicates the expansion of the West Antarctic Ice Sheet (Zachos et al., 2001).

6.1.2 Aim of study

The oxygen and carbon isotope values are determined for three sites at the Southern Indian Ocean (752A, 1168A and 1139A). The current study aimed to understand and observe the changes and shifting of isotope values during the early, middle and the late Miocene at the current studied sites and compare the present study curves with the global curves.

6.2 Methodology

For the stable-isotope analysis of foraminiferal carbonate in this study, approximately 80-150 µg of benthic foraminifera were placed into 4 ml glass vials then sealed by a lid and pierceable septum. The number of specimens required varied depending on the weight of individual taxa. A total of 136 specimens are used and their sizes ranged between 125µm to >355µm. The vials were placed in a heated sample rack (30°C) where the vial headspace was replaced by pure

helium via an automated needle system as part of an Isoprime Multiflow preparation system. Samples were then manually injected with approximately 50 µl of phosphoric acid and left to react for at least 4 hours before the headspace gas was sampled by automated needle and introduced into a continuous-flow Isoprime mass-spectrometer. Duplicate samples were extracted from each vial and a mean value obtained for both $\delta^{13}C$ and $\delta^{18}O$. Samples were calibrated using IAEA standards NBS-18 and NBS-19 and reported as ‰ on the VPDB scale. An external precision of better than 0.10‰ was typically achieved for $\delta^{13}C$ and better than 0.15‰ for $\delta^{18}O$ (Ian Boomer, *pers. comm.*, 2019).

Both oxygen and carbon isotope data have been calculated by using three different species at 752A, *Cibicidoides mundulus*, *C. wuellerstorfi* and *Planulina costata* (See Appendix Q). The values have been corrected to *Cibicidoides mundulus* by calculating the difference between this species and *C. wuellerstorfi* and *Planulina costata* for those samples in which they co-occur. Ideally, the stable-isotope analysis will be for just one species, but the same species wasn't always present throughout any core, and it is clear that there are fractionation differences in the oxygen and carbon isotopes of benthic foraminifera between taxa due to biological (vital) effects and also environmental factors (Grossman, 1987). The mean calculated difference is shown in the appendix Q for each species (the bold numbers at the bottom of the table) with *C. mundulus* and then corrected values are calculated from subtracting the original isotope values of each species (*C. wuellerstorfi* and *Planulina costata*) added to mean difference value. Finally, a composite mean isotope record is determined for the carbon and oxygen isotopes in each core.

The oxygen and carbon isotope at 1168A have been calculated from eight different species such as *Cibicidoides mundulus*, *Oridorsalis umbonatus*, *Globocasssidulina subglobosa*, *Gyrodinoides soldanii*, *Epistominella exigua*, *C. wuellerstorfi*, *Nuttalides umbonifera*, *Cibicidoides* sp. and *Cibicidoides* sp.11. The distribution of *Cibicidoides mundulus* throughout the whole succession is not good enough to be the only species used to determine the isotope values.

Isotope data from species other than *Cibicidoides mundulus* are corrected to that species to provide a standardised benthic foraminifera isotope record, as outlined above. Some species such as *Cibicidoides* sp. and *Cibicidoides* sp.11 are not corrected to *C. mundulus* because they do not co-exist with *C. mundulus* in samples 11H-5 and 41X-5. The mean difference between the species as mentioned above is calculated by subtracting the mean of each species with the mean of *Cibicidoides mundulus,* and then the corrected mean of each species calculated. Finally, the composite mean (standardised benthic foraminifera) of oxygen and carbon is derived from the mean of all selected species (See Appendices R & S).

The oxygen and carbon isotopes data at 1139A calculated from three different species such as *Cibicidoides mundulus*, *Epistominella exigua* and *Sphaeroidina bulloides* (See Appendix T). The mean values of *Epistominella exigua* are corrected depending on the mean values of *C. mundulus* while the oxygen and carbon isotope values of *Sphaeroidina bulloides* directly used because it is the only species that has good preservation and abundance at the samples 13R-5, 14R-4 and 15R-2.

The mean difference between *Cibicidoides mundulus* and *Epistominella exigua* has been calculated for two samples (4R-1 and 4R-2, 1139A) and mean difference is used to derive the mean corrected value of *Epistominella exigua* which is 0.54 for carbon and -0.18 for oxygen. Finally, the composite mean values are calculated for carbon and oxygen isotopes which represent the standardised benthic foraminifera isotope values (See Appendix T).

6.3 Results:

6.3.1 Site 752 Hole A

The mean value of the oxygen isotope was lower during the Oligocene, and the early Miocene (Figure 6.1). The highest peak occurs at around 19.16 Ma. The $\delta^{18}O$ value decreases rapidly at 15.74 Ma; and after 14.41 Ma, the $\delta^{18}O$ values show rapid increase. The values increase continuously with fluctuations until the early Pliocene. The highest value of oxygen isotope has recorded at 6.62 Ma

The $\delta^{13}C$ values recorded the first peak at around 21.78 Ma then decrease rapidly until it records a slightly high value at 19.16 Ma. The carbon isotope values increase rapidly from 16.84- 13.56 Ma.

The increasing productivity at ~ 13 Ma may have coexisted with EAIS expansion and shows its highest peak during 10- 8 Ma. The maximum carbon excursion followed by rapid and gradual decreasing of $\delta^{13}C$ at 752A from late mid- Miocene to early Pliocene (Figure 6.1).

6.3.2 Site 1168 Hole A

The oxygen values decreased before 23 Ma and slowly increased until peaks around 20 Ma. The values decrease rapidly at ~ 15.5 Ma. The significant shifting of oxygen isotope values at 1168A (6.2 (A)) was after 13.26 Ma which was higher by ~ 0.3 ‰ with the late mid- Miocene values. The oxygen values started to increase continuously after 13.26 Ma until it shows another shift during about 10- 8 Ma. This may be related to global cooling and Antarctic ice sheet expansion. After 6.45 Ma, the oxygen isotope values increase again.

The carbon values ($\delta^{13}C$) were high during the late Oligocene- early Miocene (Figure 6.2 (B)) then these values decreased and had very low values (~ 20- 22 Ma) in the current study. The $\delta^{13}C$ values started to increase and record the highest values at 1168A during MMCO (~ 17- 15 Ma). The $\delta^{13}C$ values at 1168A decrease gradually after ~ 15 Ma and peak again around 10- 8 Ma and then decreased rapidly towards the latest Miocene and early Pliocene.

6.3.3 Site 1139 Hole A

The oxygen isotope values fluctuated (Figure 6.3) during the early Miocene at 1139A. The highest value is recorded at 21.76 Ma and dropped down at 20.64 Ma. The oxygen isotope values become relatively high at about 20- 18 Ma until dropped suddenly at 17.98 Ma. Significant shifting of oxygen isotope values happened towards the heavier values during around 14.5- 12 Ma. The erosion at 1139A made most of the late Miocene successions disappear. At 11.25 Ma oxygen isotope recorded higher value than the preceding times.

There is a high carbon excursion (Figure 6.3) during the latest Oligocene and the earliest Miocene at 1139A. The carbon values gradually decrease and remain low during the early Miocene at 1139A; these values increase until records the highest excursion at around 16 Ma. This excursion continued until about 12 Ma; then the carbon values depleted rapidly towards the late Miocene.

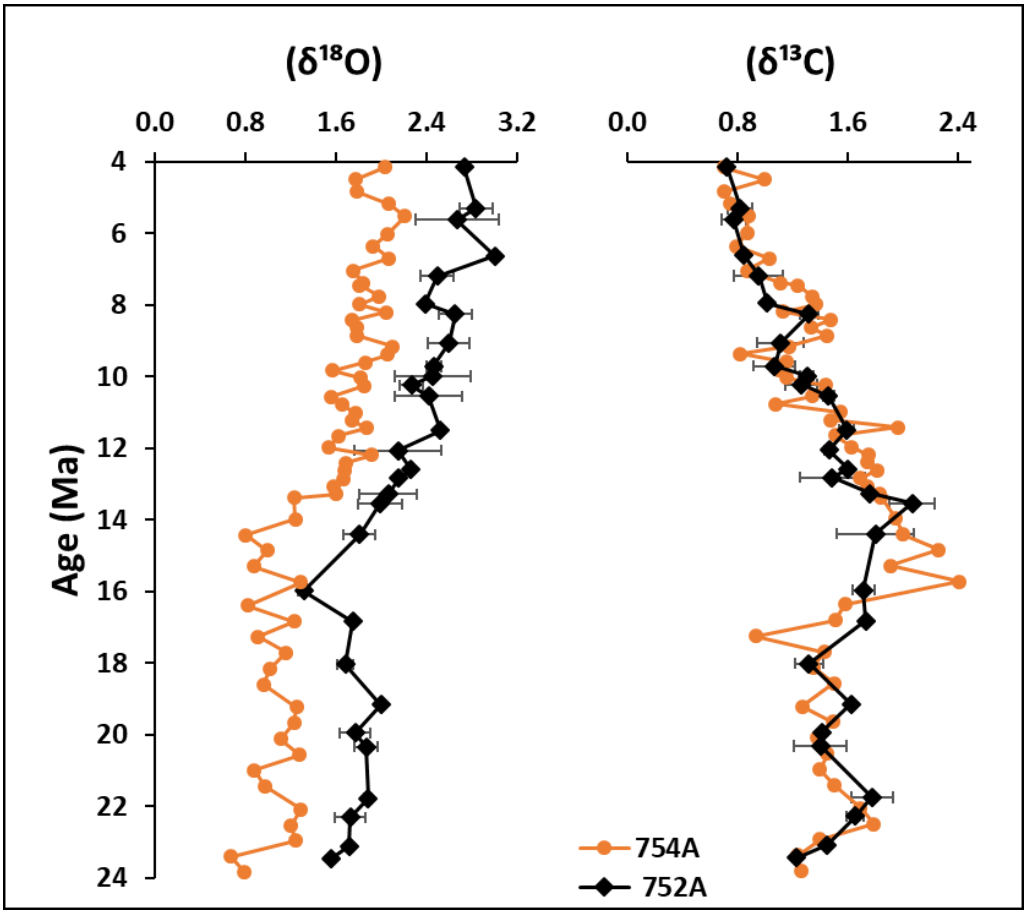


Figure 6. 1: Oxygen ($\delta^{18}O$) and carbon ($\delta^{13}C$) stable isotope records for the ODP Holes 752A and 754A. The isotope values corrected to *Cibicidoides mundulus* for 752A while, the values at 754A conducted on *Cibicidoides* sp. Oxygen and carbon data of 754A provided by Rea et al. (1991).

6.4 Discussion:

6.4.1 Site 752 Hole A

The highest peak of $\delta^{18}O$ occurs at around 19.16 Ma. Singh and Gupta (2012) supposed that the abrupt increase in the $\delta^{18}O$ values of *Cibicidoides* sp. at 19.5 Ma (752A) indicates deep-sea cooling causing sea level lowering. This event coincides with the hiatus NH1 of Keller and Barron (1983). The rapid decreasing of $\delta^{18}O$ value at 15.74 Ma may be coincided with MMCO (Mid Miocene Climatic Optimum) (Zachos et al., 2001). Banerjee et al. (2017) also recorded the interval between 17 to 14 Ma as an interval of Miocene global warming (MMCO). After 14.41 Ma, the $\delta^{18}O$ values increase rapidly this coincided with EAIS expansion (14- 12 Ma) (Badger et al., 2013, Zachos et al., 2001). The highest value of oxygen isotope has recorded at 6.62 Ma. This may have coincided with West Antarctic Ice Sheet Expansion (Zachos et al., 2001).

The rapid increase of carbon isotope values from 16.84- 13.56 Ma coincided with the early to the mid-Miocene carbon isotope excursion (Monterey Carbon Isotopic Excursion from 17.0 to 13.5 Ma) (Flower and Kennett, 1993, Holbourn et al., 2007). Large storage of organic carbon in the Monterey formation of California have been attributed by maximum carbon excursion during around 17.0 to 13.5 Ma. This large storage contributed significantly to the global cooling and lowering the atmospheric CO2 during the mid- Miocene (Flower and Kennett, 1993).The increasing productivity at ~ 13 Ma might cause the Oxygen Minimum Zone (OMZ) expansion and biogenic bloom (Gupta et al., 2004, Singh et al., 2012).

In the Indian Ocean, the coincidence of OMZ expansion, productivity increase and trade wind increase during the late Miocene in the intermediate depths may have triggered the low values of $\delta^{13}C$ (Gupta et al., 2004, Gupta and Thomas, 1999, Singh et al., 2012).

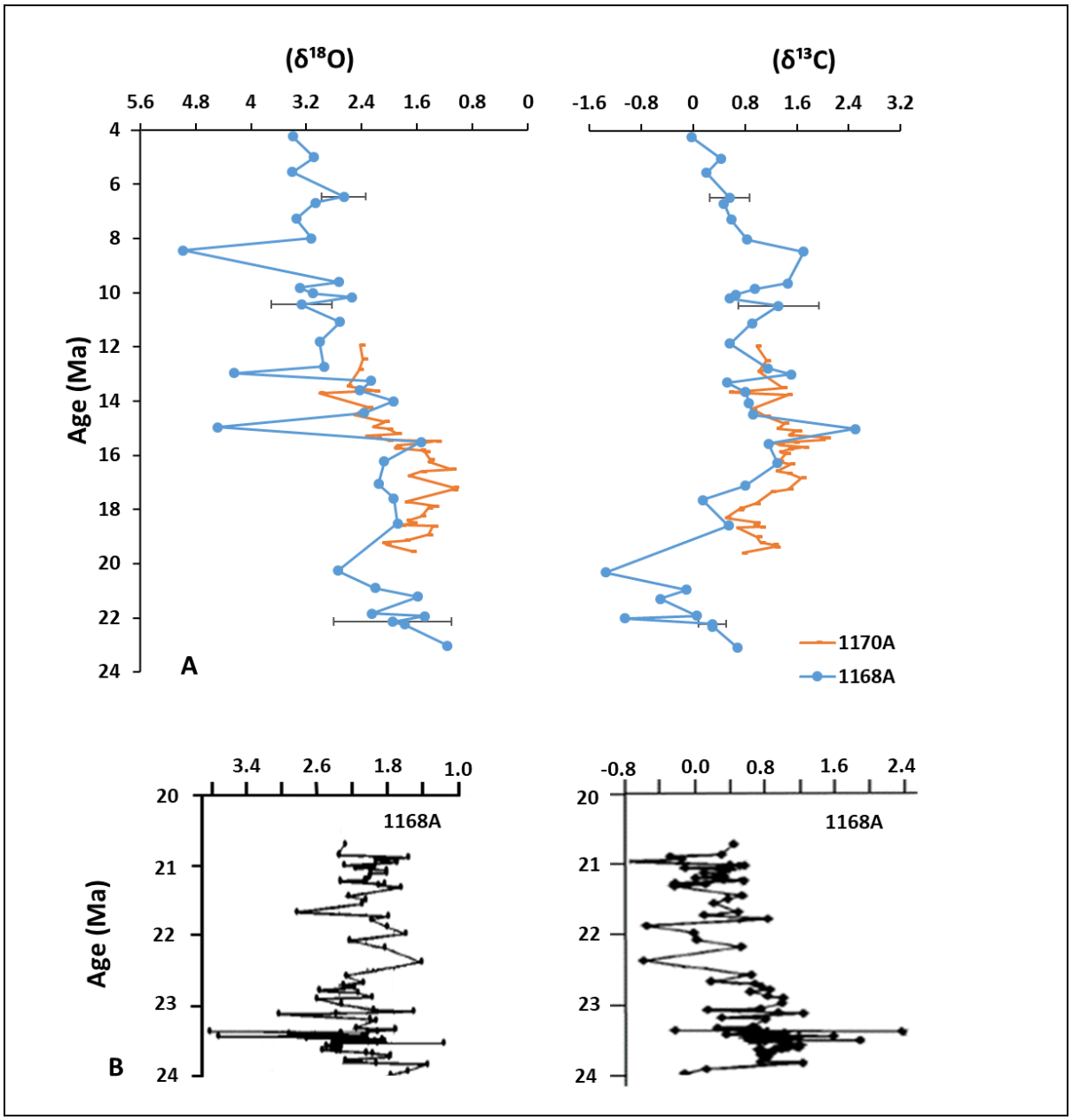


Figure 6. 2: Oxygen ($\delta^{18}O$) and carbon ($\delta^{13}C$) stable isotope records for the ODP Holes 1168A and 1170A. Most of the isotope values corrected to *Cibicidoides mundulus* for 1168A while the values at 1170A are for *Cibicidoides mundulus* (A). The oxygen and carbon curves from the interval between ~ 20.5 to ~24 Ma at 1168A (B) provided by Pfuhl et al. (2004), and the age is after Cande and Kent (1992, 1995).

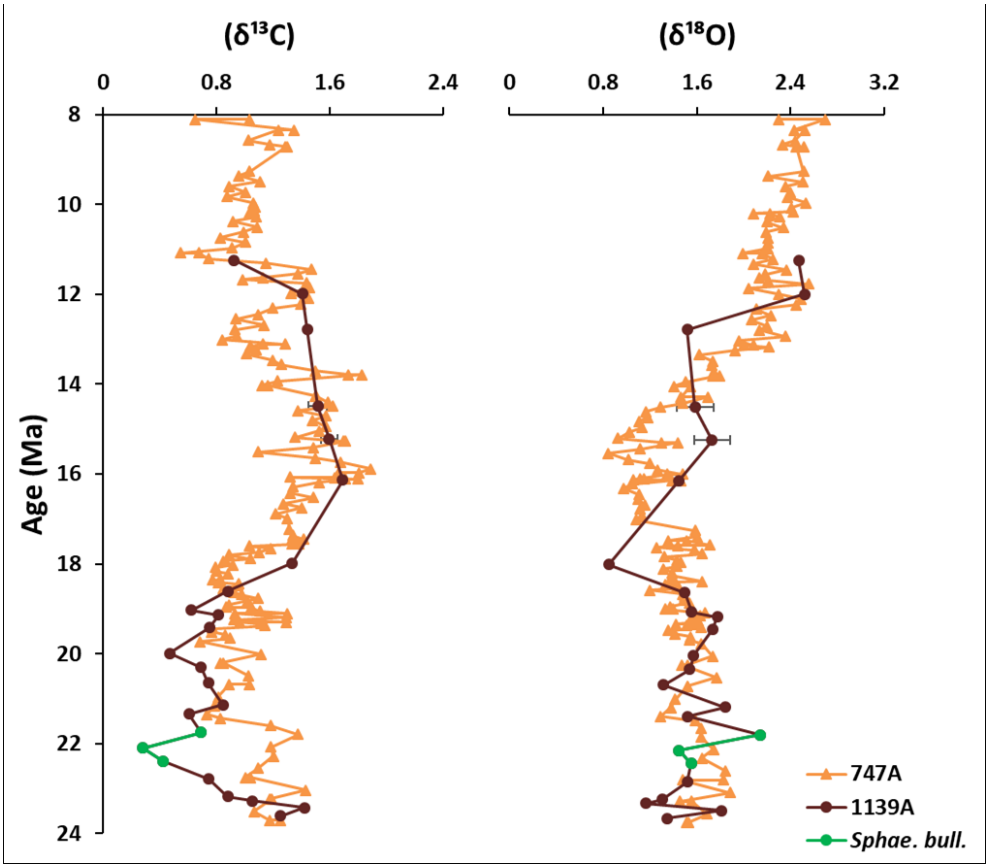


Figure 6. 3: Oxygen ($\delta^{18}O$) and carbon ($\delta^{13}C$) stable isotope records for the ODP Holes 1139A and 747A. Most of the isotope values corrected to *Cibicidoides mundulus* for 1139A while the values at 747A are for *Cibicidoides* spp. The green line represents *Sphaeroidina bulloides* at 1139A.

The isotope results of 752A compared with 754A, and the latter located near the crest of the Broken Ridge (1063.6 mbsf) with latitude 30°56.44´ and longitude 93°33.99´ (Shipboard Scientific Party, 1989b). The age of the Site 754A is determined based on the first and last occurrence of nine nannofossil species which provided by Shipboard Scientific Party (1989b) and revised by ATNTS2012 in GTS2012 (Hilgen et al., 2012) (see appendix U). Oxygen and carbon data of 754A are provided by Rea et al. (1991) and the data conducted on *Cibicidoides*

sp. (see appendix U). The oxygen isotope values of 754A were low during the late Oligocene and early Miocene these values rapidly changed after 14.41 Ma (Figure 6.1). The interval between 14.41 and 13.26 shows the increasing by 0.8 ‰. After 13.26 the oxygen values continuously increase with fluctuations up to early Pliocene (Figure 6.1).

The oxygen isotope peak is similar to the current Site 752A with an offset between the two curves. This offset may only represent the temperature differences between both sites. There is no significant offset between carbon isotope curves between 752A and 754A while the carbon excursion at 754A started at nearly the same time (16.83 Ma) and ended earlier at 14. 86 Ma. The carbon values at 754A rapidly decreased with some fluctuation from mid- Miocene to the early Pliocene.

The Southern Component Deep Water has influenced the site 752 Hole A during the whole Neogene (Peirce et al., 1989). According to Singh et al. (2012), the Site 752A have been impacted by Antarctic Intermediate Water (AAIW) in the present day as this water mass flows in the Indian Ocean at 1200 m. According to Rea et al. (1991), the oxygen isotope values of *Cibicidoides* at 752A represent the heaviest values among other Sites (754,756 and 757) in the Eastern Indian Ocean. The increasing of $\delta^{18}O$ values by 0.8 to 1.0 per mil in the Ninetyeast Ridge and Broken Ridge during 14.4 to 13 Ma may represent the cooling event (EAIS expansion) (Holbourn et al., 2005, Rea et al., 1991). Rea et al. (1991) observed the increase of $\delta^{13}C$ values by 0.8 to 0.9 ‰ during around 17- 15 Ma. This may be produced by removing light organic carbon from the ocean.

6.4.2 Site 1168 Hole A

The isotope results of 1168A are compared with the results at 1170A (see appendix V). Site 1170 Hole A located at latitude 470°9.0'S and longitude 146°02.0'E at the South Tasmanian Rise (STR) on the western slope, having a water depth of 2704 mbsf (Ennyu and Arthur, 2004b). The chronozones and nannofossil ages are provided by (Stickley et al., 2004) and revised by ATNTS2012 in GTS2012 (Hilgen et al., 2012).

The isotope values are supplied by Ennyu and Arthur (2004a). For the current study, the data of *C. mundulus* are selected to compare with current Hole (1168A) (See Appendix V).

The oxygen values during the late Oligocene to the early Miocene were high at 1168A, which considered as a heavier $\delta^{18}O$ during that time as shown in Figure 6.2 (B). The isotope values of the Figure 6.2 (B) were provided by Pfuhl et al. (2004). Pfuhl et al. (2004) recorded high oxygen isotope values during the late Oligocene and the early Miocene at 1170A. This heavy record of oxygen isotope values (positive oxygen excursion) coincided with the period of short and deep glacial maximum which represented by Mi-1 event (Zachos et al., 2001).

The oxygen values decreased before 23 Ma and it peaks again at around 20 Ma; this have been coincided with the lowering of the eustatic sea level and NH1 hiatus of Keller and Barron (1983). The values decrease rapidly at ~ 15.5 Ma in both Sites (1168A and 1170) as shown in Figure 6.2 (A). The decrease was also similar to the early-mid Miocene decrease (15.74 Ma) at 752A (Figure 6.1) which may have also been affected by MMCO (Banerjee et al., 2017). The

oxygen values increased gradually and continuously towards the late mid- Miocene at 1168A and 1170A and showed relatively higher values than the late early Miocene.

The increase in oxygen isotope values after ~ 15.6 Ma and recording high values during around 13.8 Ma in the South-West Pacific may reflect increase Southern Component Water (SCW) sources and coincided with EAIS expansion (Badger et al. 2013, Flower and Kennett, 1995). The termination of TISW and disappearing of meridional heat transportation to high southern latitudes led to increasing production of SCW during around 15.6 Ma (Flower and Kennett, 1995). The oxygen values started to increase continuously after 13.26 Ma until it shows another shift during about 10- 8 Ma. This may be related to global cooling and Antarctic ice sheet expansion which increased the wind intensity in the Indian Ocean (Gupta et al., 2004). After 6.45 Ma, the oxygen isotope values increase again. This may have been affected by West Antarctic Ice Sheet Expansion (Zachos et al., 2001).

The carbon values ($\delta^{13}C$) were high during the late Oligocene- early Miocene (Figure 6.2 (B)) then these values decreased and had very low values (~ 20- 22 Ma) in the current study and the previous study (Pfuhl et al., 2004) (Figure 6.2 (A & B)). This negative carbon excursion has been interpreted by the location of the Hole 1168A near the land and transporting a high organic matter from the land (Pfuhl et al., 2004).

The $\delta^{13}C$ values started to increase and record the highest values at 1168A and 1170A during MMCO (~ 17- 15 Ma), and this event is within a range of Monterey Carbon Isotopic Excursion event (Flower and Kennett, 1993, Holbourn et al., 2007).

Benthic foraminifera oxygen isotopes have been measured near the Tasmanian Gateway for four ODP sites 1168A, 1170, 1171 and 1172 (Pfuhl et al., 2004). The oxygen values during the late Oligocene and the early Miocene increased and remained high until ~ 22.6 Ma, especially at the Sites 1170, 1171 and 1172 (Pfuhl et al., 2004). The Hole 1168A situated to the north of the ACC (Antarctic Circumpolar Current) is under the effect of Leeuwin current (Shipboard ScientificParty, 2001a).

According to Pfuhl et al. (2004), $\delta^{18}O$ and $\delta^{13}C$ records of benthic foraminifera have a low resolution in 1168 and have similar records with the Sites 1170, 1171 and 1172. The low isotope values at restricted Site 1168 are similar to the lowest values at the Site 1090 on Agulhas Ridge (abyssal depth). These low values represent warmer temperatures and high organic oxidation (Pfuhl et al., 2004). It has been suggested that the proximity of the Site 1168 to land sources organic impute may have been affected and decreased the $\delta^{13}C$ values during the early Miocene which recorded the lowest value (-0.8 ‰) at around 21 Ma (Pfuhl et al., 2004). According to Pfuhl et al. (2004), the $\delta^{13}C$ values from similar paleolatitudes and paleodepths sites (1170 and 747 (Central Kerguelen Plateau)) have no offsets during the early Miocene. The fluvial bicarbonate increases, and higher rates of organic carbon may have been attributed to the positive carbon excursion in the benthic foraminifera records during Mi- 1 event (24-22.5 Ma) and mid-Miocene shifting events (Vincent and Berger, 1985).

According to Ennyu and Arthur (2004b) the oxygen isotope values of *Cibicidoides mundulus* at the Site 1172 recorded the highest values if compared with the Sites 1170, 289 and 747 throughout the Miocene. This may suggest the impact of cold SCW on the Site 1172. The

oxygen isotope values of the site 1170 were quite similar with those at the Sites 289 and 747 especially during the early and the early-mid- Miocene. Oxygen isotope recorded higher values at 1170 during and after expansion of the EAIS (East Antarctic Ice Sheet) this may prove the diminishing of TISW (Tethyan Indian Saline Water) after ~ 14.5 Ma (Ennyu and Arthur, 2004b). At around 14 Ma deep waters temperatures decreased by 1.5 to 3.0°C at the Site 1171 (Shevenell et al., 2008, Majewski and Bohaty, 2010).

6.4.3 Site 1139 Hole A

The isotope values of the Site 1139A are compared to the Site 747 Hole A. The Site 747 Hole A is located at the centre of Kerguelen Plateau (54°48.68'S, 76°47.64'E) at the south of 1139A with the water depth of 1695 mbsf, it is situated south of the recent polar front under the influence of ACC (Antarctic Circumpolar Current) (Wright and Miller, 1992).

The isotope values and chronozones of the Site 747 Hole A were provided by Wright and Miller (1992), and the Chronozone C6cn2 provided by Berggren (1992). The isotope values for 747A were measured on *Cibicidoides* spp. (Wright and Miller, 1992) and the age is revised by ATNTS2012 in GTS2012 (Hilgen et al., 2012) (see appendix W).

The oxygen isotope values at 747A remain relatively constant during the early Miocene but have a declining trend towards the early-mid Miocene; this shift is also observed at 1139A. The low data availability at 1139A makes the shift during the late- early Miocene less obvious than the one at 747A. Significant shifting of oxygen isotope values happened towards the heavier values during around 14.5- 12 Ma in both Sites (1139A and 747A); this may have been

affected by EAIS expansion (Zachos et al., 2001, Holbourn et al., 2005). An overall increase of benthic foraminifera oxygen isotope values recorded at 747A during ~15.0 to 12.2 Ma through the interval which spans the Middle Miocene Climate Transition (MMCT) (Majewski and Bohaty, 2010). During ~14 Ma, sea surface temperatures (SSTs) were decreased by ~6–7°C in the Southern Ocean (747A) (Verducci et al., 2007).

There is a high carbon excursion (Figure 6.3) during the latest Oligocene and the earliest Miocene at 1139A, which have also observed at 747A and 1168A. The high carbon excursion in the benthic foraminifera records during Mi- 1 event (24-22.5 Ma) may have triggered by the fluvial bicarbonate increase, and higher rates of organic carbon (Vincent and Berger, 1985). The carbon values gradually decrease and remain low during the early Miocene at 1139A and 747A; these values increase until records the highest excursion at around 16 Ma at Sites 1139A and 747A (Holbourn et al., 2007). This excursion continued until about 12 Ma; then the carbon values depleted rapidly towards the late Miocene.

6.4.4 Stable isotope comparison

Oxygen and carbon isotope values have been calculated for three localities (752A (Broken Ridge), 1168A (Western Tasmania margin) and 1139A (Kerguelen Plateau)). Most of the isotope values at all Sites have been corrected to *Cibicidoides mundulus*.

The current sites oxygen and carbon isotopes are compared with each other, then compared with global isotope records (Cramer et al., 2009). The provided age model of Cramer et al. (2009) are modified to the GTS2012 time scale (Gradstein, 2012) as presented in Edgar et al.

(2017). The oxygen values at 1168A are higher if compared with other sites. This Site is situated at higher latitudes and have a water depth of 2463 mbsf. The main pattern of the isotope curves, during the whole Miocene, are similar to the global curve (Cramer et al., 2009) at all studied sites.

The lower resolution values in the mid- Miocene for the site 1139A, was because of the few data availability during this interval. Important events for the current sites are shown in Figure 6.4. Most of these bio-events have coincided to the global climatic events (Figure 6.4).

The oxygen isotope of 1168A are compared with a sea surface temperature (SST) during the Miocene by using alkenones as SST biomarkers (Figure 6.5). The temperature values provided by Knee-Robinson (2018) (see appendix X). The sea surface temperature has nearly a similar pattern with the oxygen curve; this shows the similarity of the temperature gradient between the surface and deep-water masses during the Miocene. The alkenones show an overall cooling of about 6 C° SST from 24 to 4 Ma with a distinct cooling at about 15 Ma (and possibly, 8.5 Ma). The former of these is also indicated in the benthic foraminifera $\delta^{18}O$. The foraminifera oxygen isotopes also suggest an overall cooling trend during this period. Gradual decrease of alkenones and continuous increase in benthic foraminifera $\delta^{18}O$ values were reported after about 14 Ma. This were continued until the early Pliocene.

The sea surface temperature in the North Atlantic Ocean from about 23.03 to 14.5 Ma was ~ 15°C higher than modern temperature. During MMCT (14,5- 12,5 Ma) ~6 °C decrease of SST

reported, this lowering coincided with a *p*CO2 decrease from an average of ~430 ppm in MMCO to ~305 ppm after the MMCT (Super et al., 2018).

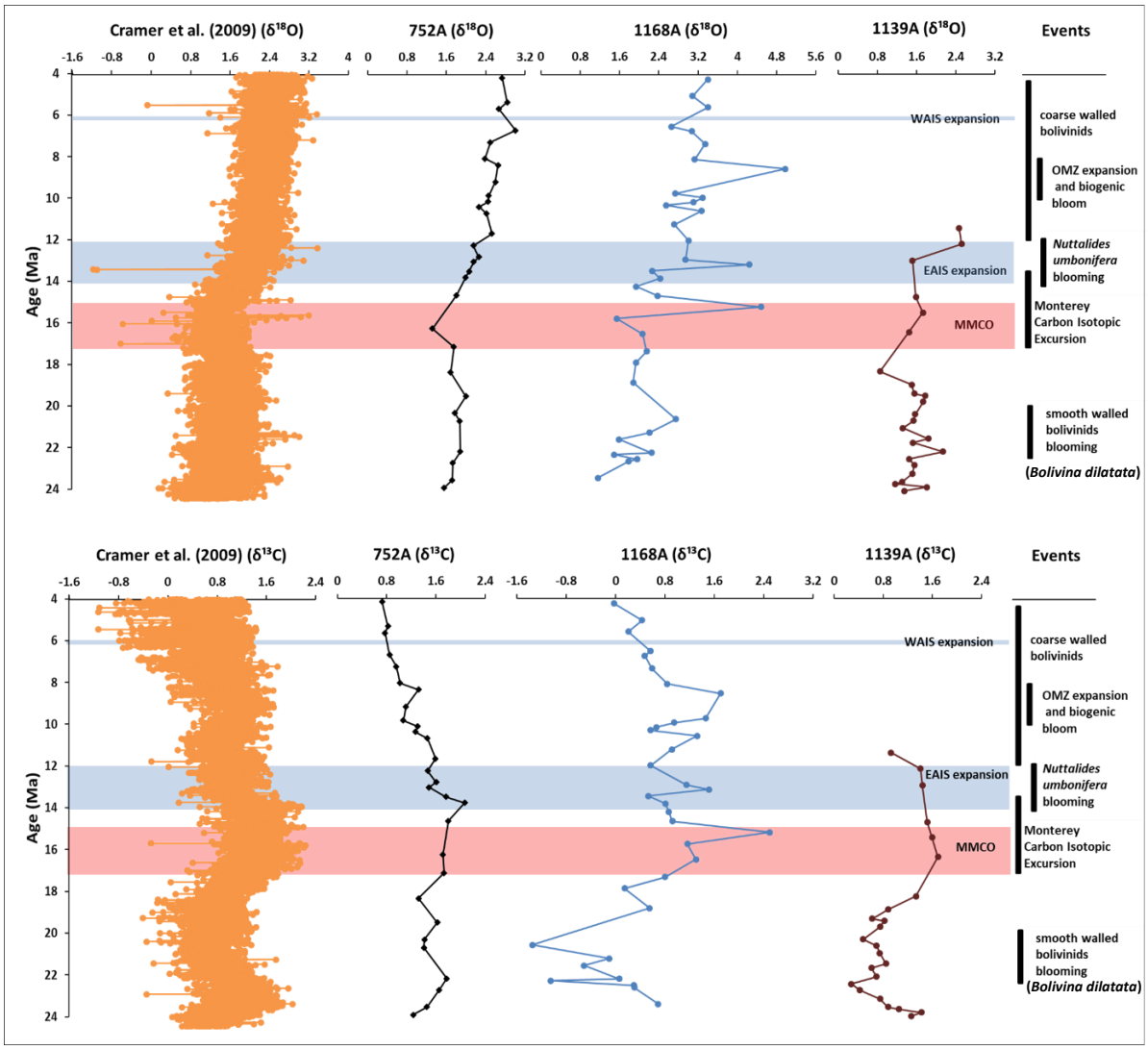


Figure 6. 4: Oxygen ($\delta^{18}O$) and carbon ($\delta^{13}C$) stable isotope records for the ODP Holes 752A, 1168A and 1139A compared with global isotopic records (Cramer et al., 2009). Both Climatic and bio- events have shown. The ranges of the important species at all sites have shown in the right.

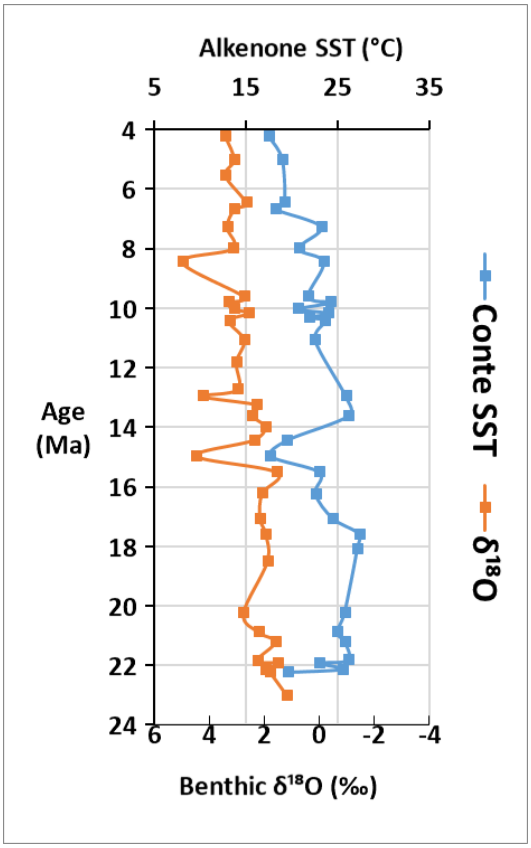


Figure 6. 5: Sea surface temperature and oxygen isotope at 1168A. The temperature (SST) data are provided by Knee-Robinson (2018).

Chapter Seven

Summary and Conclusions

Overall Faunal Summary

Ninety-seven samples from the latest Oligocene, Miocene and early Pliocene have been analysed from three ODP Sites (752A, 1168A and 1139A). More than 200 species of benthic foraminifera were recorded at each site, and fifty-two (52) of the most abundant species are illustrated (these represent ~78 % of the whole benthic foraminifera record by abundance). The high diversity includes a large number in the smaller size fraction (>63 µm). Benthic foraminiferal assemblages are well-preserved and similar at all sites with mostly complete specimens. There was little faunal turnover in the most abundant taxa during the palaeoclimatic shifts of the Miocene. The described species are assigned to 33 different genera and were subdivided into four orders, 15 superfamilies, 20 families and 16 subfamilies. Four species were recorded with open nomenclature, two each from *Bolivina* and *Gyroidinoides*. All the described taxa are calcareous hyaline forms, apart from one agglutinated species (*Eggerella bradyi*). The Buliminida (31 species) are the major constituents of those records, at all studied sites. The next most important components of the benthic foraminifer assemblages are species of the Rotaliida.

Some species are distributed in different intervals across the three cores, for instance, *Bolivina huneri* is recorded in the early Miocene of Hole 752A, and the mid- to late Miocene of Hole 1168A, while it is not reported at Hole 1139A. Smooth-walled bolivinids are typical species of intermediate and deep water sites. *Bolivina dilatata* has been recorded as a common smooth-

walled bolivinid at 1168A and appears in a short interval at 1139A but is not recorded at all at 752A.

High BFAR values recorded, in the latest Oligocene- early Miocene in all studied sites.

One of the climatic events (Mi-1) (deep glacial maximum) which marks the boundary of Oligocene-Miocene is around ~23 Ma. Small and discontinuous glaciations followed this event. It has been observed that the BFAR peaks generally coincided with Antarctic glaciations at all studied sites.

The highest peak of high productivity taxa at 752A was recorded during the late Miocene starting from ~ 10 Ma and continued until around 5.6 Ma. At 1168A the highest peak recorded during the latest Oligocene and early Miocene and continued until about 21 Ma. The values gradually increase during the mid-Miocene and continued until about 10 Ma. The high productivity values at 1139A recorded high values during the latest Oligocene and early Miocene and decreased suddenly after about 22.7 Ma. During the late mid-Miocene, the values are slightly increase and drop again at around 11.2 Ma

Age Depth Models

New age-depth models have been established for each site based on revised timescales, and up to date studies of planktonic and geomagnetic polarity datums. This allowed the timing of events to be considered with best possible accuracy. The average sedimentation rate at 752A in the Neogene and late Oligocene is 0.44 cm ka^{-1}. Changes in the rate of sedimentation at 752A are recorded at around 5.61 Ma and 13.56 Ma, with a lower rate of sedimentation during

early Miocene and a higher rate of sedimentation during the mid- Miocene to the late Miocene. This may have been related to expansion of Antarctic ice sheets.

The average rate of sedimentation for Hole 1168A is 1.82 cm ka^{-1}. The highest rate of sedimentation is recorded in two different intervals, first at around 9.6-10.3 Ma (5.67 cm ka^{-1}). This increase may indicate higher oceanic productivity associated with expansion of the Antarctic Ice volume, and the second-highest rate is at around 21.84-23.03 (6.68 cm ka^{-1}). This may coincide with a large and short glacial maximum recorded at 22.95 and 21.1 Ma.

The lowest rate of sedimentation is recorded (0.30 cm ka^{-1}) at 1139A from 16.13 to 11.25 Ma, and from 22.79 to 18.61 Ma the rate of sedimentation increases very rapidly (2.32 cm ka^{-1}), while the highest rate of sedimentation (7.06 cm ka^{-1}) is recorded from 23.6 to 23.18 Ma. The high pelagic input and the derivation of terrigenous clastic deposits from the exposed volcanic edifice at Skiff Bank affected the high sedimentation rates at 1139A.

Cluster Analysis

Quantitative techniques (cluster analysis) were used at all studied sites, to investigate the foraminifera assemblages at each site further.

752A

At 752A, there are two main clusters separated at ~13 Ma coincided with the shifting from high Shannon-index assemblages (characterised by *Siphonodosaria, Nuttalides* and *Trifarina bradyi)* to lower Shannon-index assemblages (characterised by *C. wuellerstorfi and Trifarina*

angulosa) at about 13 Ma. This distinction may have been controlled by climatic events associated with Antarctic ice sheet expansion.

1168A

Six clusters were identified at 1168A. There are characteristic species for each cluster. *Bolivina dilatata* is an essential component during the late Oligocene- earliest Miocene. It is believed that such smooth-walled species are typical of intermediate and deep-water sites. The high abundance of this species was recorded when the BFAR was also high. *Nuttalides umbonifera* and *Sphaeriodina bulloides* are species indicative of the late early Miocene and mid- Miocene. *N*. *umbonifera* is thought to increase in abundance in very high oligotrophic conditions and insufficient organic supply. *Cibicidoides mundulus* is a characteristic species of cluster D and E which represent common species of early Miocene at this site. This species was also common during the early Miocene at the sites 752A and 1139A. The Shannon diversity index recorded a drop at about 14 Ma which may be due to EAIS expansion during the mid- Miocene.

Abdetodentrix pseudothalmani and *Trifarina angulosa* dominate the mid-late Miocene at Sites 752A, and 1168A. *Abdetodentrix* is similar to *Bolivina,* indicative of a productive area, blooms in lower dissolved oxygen conditions with the same infaunal niche. In the southern Indian Ocean (Kerguelen Plateau), *Trifarina angulosa* has a high abundance during global cooling in the late Pliocene and Pleistocene.

1139A

There are characteristic species recorded at 1139A during the Miocene. *Oridorsalis umbonatus* (11.99-11.25 Ma) low organic condition species indicative of well-oxygenated water. *Cibicidoides wuellerstorfi* (mid-Miocene) is a species which has a high abundance in a higher energy environment.

The Shannon diversity index at 1139A recorded a significant drop in the values during about 14.5 Ma which may be due to EAIS expansion during the mid- Miocene. This event has the most marked effect on deep-sea benthic foraminifera in this region, and it appears to be synchronous for all studied sites.

The characteristic species of the late- early Miocene are *Bulimina* cf. *B*. *elongata* and *Bulimina striata*. Most of the biserial and triserial species occur in high abundances in low oxygenated conditions. The Early Miocene of 1139A is characterised by a high abundance of *Sphaeroidina bulloides* and *Uvigerina* spp, which indicate a high productivity area. *Uvigerina* and *Eggerella bradyi* (latest Oligocene- early Miocene) are highly linked to IDW (Indian Deep Water). It is believed that the dominance of *Uvigerina* in the southern Indian Ocean is indicative of Circumpolar Deep Water.

Changing test size through time

Five species (*Abdetodentrix pseudothalmani, Cibicidoides mundulus, Globocassidulina subglobosa*, *Nuttalides umbonifera* and *Sphaeroidina bulloides*) were examined to study changing test size during the late Oligocene and the Neogene at all three sites. Most of the

species size values (mean size, smallest and largest size) show a rapid reduction in size at around 12- 13 Ma in all sites. A rapid increase follows this reduction in size. According to Kaiho (1999), test size minima coincides with warming periods and low dissolved oxygen.

Most of the species mentioned above increase in size notably during the glaciation periods in the late Oligocene-early Miocene and the late Miocene-early Pliocene, and a significant shift (becoming larger) is observed after the MMCO event and during about 13 Ma and later which may have been triggered by Antarctic ice sheet expansion. This size-shift is particularly well marked in *Abdetodentrix pseudothalmani, Cibicidoides mundulus* and *Nuttalides umbonifera*. This increase in size has coincided with primary productivity increase and biogenic blooms at the studied sites especially at the Sites 752A and 1168A. It is suggested that variations in oceanic primary productivity, organic carbon flux and dissolved-oxygen levels in the water column has significant effect in controlling of benthic foraminiferal test size.

Carbonate crash and Biogenic blooms

752A

The first decreasing of the $MAR_{carbonate}$ recorded after about 13.28 Ma and continued to record the lowest value during the early late Miocene (~ 9 Ma). In contrast, the carbonate content remains high, and it does not show a high declination during the mid to the late Miocene despite the interval between ~ 9 to 7 Ma. The high productivity continuously increases during around 10.5 to 8 Ma. This may have coincided with the global onset of the biogenic bloom.

1168A

Gradual declination of carbonate content was at around 13 Ma and it recorded a low value at around 11 Ma at the time when carbon ($\delta^{13}C$) isotope record low values as well. At the current study, the carbonate content and $MAR_{carbonate}$ records high values during the interval between 10.32 to 9.62 Ma. This coincided with the high rate of the sedimentation. The high productivity taxa recorded high values during around 11.8 Ma and another high value recorded at around 5 Ma.

1139A

The upper part of the current Site is eroded, and it does not give opportunity to see the late Miocene successions. Because of the low data availability, the mid- Miocene is poorly interpreted. The values of the carbonate content and $MAR_{carbonate}$ are missing because of the erosion of the upper succession, for that the carbonate crash and biogenic blooms are not recorded.

Stable isotopes

Oxygen and carbon isotope values have been calculated from the benthic foraminifera for all Sites (752A, 1168A and 1139A). Most of the isotope values have been corrected to *Cibicidoides mundulus* so that data from different species can be incorporated into a single composite record. The shifts, and the main pattern of the isotope curves at all sites during the Miocene, are similar to those seen in the global curve of Cramer et al. (2009). Oxygen isotope values decrease rapidly at around 15 Ma in all studied Sites; this coincides with MMCO (Mid Miocene Climatic Optimum). At about 14 Ma, the oxygen isotope values increase rapidly at all Sites;

this coincides with EAIS expansion (14- 12 Ma). High oxygen isotope values at 752A and 1168A at about ~ 6 Ma, coincided with West Antarctic Ice Sheet Expansion (Zachos et al., 2001).

The high carbon isotope values in the benthic foraminifera at 1168A and 1139A records during the Mi-1 event (24-22.5 Ma) may have been triggered by the fluvial bicarbonate increase and higher rates of organic carbon; similar high values were recorded at 752A around ~22 Ma. Lower trends in the carbon isotope values have been recorded at 1168A in the current study at ~ 22-20 Ma. This is interpreted as representing enhanced transportation of high organic matter from the land. The carbon isotope values increase rapidly from the late- early Miocene to mid- Miocene in all studied sites. This increase coincided with the early to the mid-Miocene carbon isotope excursion (Monterey Carbon Isotopic Excursion from 17.0 to 13.5 Ma).

Sea surface temperatures at 1168A, established through organic biomarkers, has nearly the same pattern as the oxygen isotope curve. This shows the similarity of the temperature gradient between the surface and deep-water masses during the Miocene at 1168A.

Recommendation and Future work

More samples are needed to test the oxygen and carbon isotope at the 1139A, especially in the upper succession (late-mid Miocene and early late Miocene). Only a few samples tested for the isotope from the upper successions at 1139A and need more samples to show more details. For nearly ~7 Ma from the late early Miocene (18.61 Ma) until early late Miocene

(11.25 Ma), only seven samples were tested which represent only ~ 30 m sediments (thickness).

The low resolution of geomagnetic polarity datums at 1139A need to be fixed by providing and updating geomagnetic polarity datums. The geomagnetic polarity updating will improve the age model and this, in turn, provides a more adequate age model.

More study is needed to understand the palaeoceanographic changes at the Southern Ocean, especially deep-sea benthic foraminifera by testing the smaller sizes > 63 µm. By testing smaller sizes, the diversity of the benthic foraminifera will increase which provides and adds significant tools for palaeoceanographic changes because some small-sized species are a good indicator for climatic changes.

References

ALVE, E. & MURRAY, J. W. 2001. Temporal variability in vertical distributions of live (stained) intertidal foraminifera, southern England. *The Journal of Foraminiferal Research,* 31**,** 12-24.

AMAKRANE, J., AZDIMOUSA, A., REZQI, H., EL HAMMOUTI, K., EL OUAHABI, M. & FAGEL, N. 2016. Paleoenvironment and sequence stratigraphy of the late Miocene from the Guercif basin (Northeastern of Morocco). *Bulletin de l'Institut Scientifique***,** 95-110.

ANDERSEN, H. V. 1961. Foraminifera of the mudlumps, lower Mississippi River Delta. In: Genesis and Paleontology of the Mississippi River Mudlumps. *Louisiana Geol. Survey, Geol. Bull,* 35**,** 1-208.

ASANO, K. J. 1953. Miocene foraminifera from the Noto Peninsula, Ishikawa Prefecture. *Tohoku University, Institute of Geological Paleontology Short Papers,* 5**,** 1-21.

BADGER, M. P. S. et al. 2013. CO2 drawdown following the middle Miocene expansion of the Antarctic Ice Sheet. Paleoceanography, 28, 42-53, doi:10.1002/palo.20015

BALDI, K. & HOHENEGGER, J. 2008. Paleoecology of benthic foraminifera of the Baden-Sooss section (Badenian, Middle Miocene, Vienna Basin, Austria). *Geol. Carpathica,* 59**,** 411-424.

BANERJEE, B. et al. 2017. Paleoceanographic changes in the Northeast Indian Ocean during middle Miocene inferred from carbon and oxygen isotopes of foraminiferal fossil shells. Palaeogeography, Palaeoclimatology, Palaeoecology, 466, 166-173.

BARKER, W. R. 1960. Taxonomic Notes on the species figured by H.B. Brady in his report on the foraminifera dredged by HMS Challenger during the years 1873-1876. *Society of Economic Paleontologists Mineralogists, Special Publication,* 9**,** 1-238.

BATSCH, A. I. G. C. 1791. Sechs Kupfertafeln mit Conchylien des Seesandes, gezeichnet und gestochen von AJGK Batsch. University Press, Jena, 6 pls.

BELLEN, R. C. V., RUTGERS, J. G., SOEST, J. V., WITT PUYT, J. F. C. D. & RUTGERS, A. C. 1941. Smaller Foraminifera from the Lower Oligocene of Cuba. *Koninklijke Nederlandse Akademie van Wetenschappen Proceedings,* 9**,** 1140-1146.

BERGAMIN, L., CARBONI, G. & BELLA, L. 1997. *Melonis pompilioides (Fichtel & Moll) and Melonis barleeanus (Williamson) from Pliocene, Pleistocene and Holocene sediments of Central Italy*.

BERGGREN, W. A. 1992. Neogene planktonic foraminifer magnetobiostratigraphy of the southern Kerguelen Plateau (Sites 747, 748, and 751). *In:* WISE JR, S. & SCHLICH, R., ET AL (eds.) *Proceedings of the Ocean Drilling Program: Scientific results.* College Station, TX (Ocean Drilling Program).

BERMÚDEZ, P. J. 1949. Tertiary smaller foraminifera of the Dominican Republic. *Cushman Laboratory for Foraminiferal Research,* 25**,** 1-322.

BERMUDEZ, P. J. J. B. D. G., VENEZUELA 1952. Estudio sistematico de los Foraminiferos Rotaliformes. *Boletin de Geologia, Venezuela,* 2**,** 230.

BIALIK, Or. M. et al. 2019. Two-step closure of the Miocene Indian Ocean Gateway to the Mediterranean. Scientific Reports, 9:8842, https://doi.org/10.1038/s41598-019-45308-7.

BOERSMA, A. 1986. Benthic foraminifera in Tertiary sediments of DSDP Leg 90 holes. *Supplement to: Boersma, A (1986): Biostratigraphy and biogeography of Tertiary bathyal benthic foraminifers: Tasman Sea, Coral Sea, and on the Chatham Rise (Deep Sea Drilling Project, Leg 90). In: Kennett, JP; von der Borch, CC; et al. (eds.), Initial Reports of the Deep Sea Drilling Project, Washington (U.S. Govt. Printing Office), 90, 961-1035, https://doi.org/10.2973/dsdp.proc.90.120.1986.* PANGAEA.

BOERSMA, A. 1990. Late Oligocene to late Pliocene benthic foraminifers from depth traverses in the central Indian Ocean. In Duncan, R.A., Backman, J., Peterson, L.C., et al. *Proc. ODP, Sci. Results.* College Station, TX (Ocean Drilling Program).

BOERSMA, A. & MIKKELSEN, N. 1990. Miocene-age primary productivity episodes and oxygen minima in the central equatorial Indian Ocean. *Proceedings of Ocean Drilling Program Scientific Results* College Station, TX (Ocean Drilling Program).

BOLTOVSKOY, E. 1978. Late Cenozoic benthonic foraminifera of the Ninetyeast Ridge (Indian Ocean). *Elsevier Oceanography Series,* 21**,** 139-175.

BOLTOVSKOY, E. & DE KAHN, G. G. 1981. Cinco nuevos taxones en Orden Foraminiferida. *Comunicaciones des Museo Argentino de Ciencias Naturales "Bernardino Rivadavia" e Instituto Nacional de investigación de las Ciencias Naturales, Hydrobiologia,* 2**,** 43-51.

BOOMGAART, L. 1949. Smaller Foraminifera from Bodjonegoro (Java): Smit and Dontje. 1-175.

BRADY, H. B. 1881. Notes on some of the reticularian Rhizopoda of the Challenger Expedition, Part III. *Quarterly Journal of Microscopical Science (New Series),* 21**,** 31-71.

BRADY, H. B. 1884. Report on the scientific results of the voyage of the HMS Challenger during the years 1873-1876, Report on the foraminifera dredged by HMS Challenger during the years 1873-1876. *Zoology,* 9**,** 1-814.

BRADY, H. B., PARKER, W. K. & JONES, T. R. 1888. XI. On some Foraminifera from the Abrohlos Bank. *The Transactions of the Zoological Society of London,* 12**,** 211-239.

BREMER, M. & LOHMANN, G. 1982. Evidence for primary control of the distribution of certain Atlantic Ocean benthonic foraminifera by degree of carbonate saturation. *Deep Sea Research Part A. Oceanographic Research Papers,* 29**,** 987-998.

BROTZEN, F. 1940. Flintrännans och trindelrännans geologi (Öresund): Zusammenfassung. *Die Geologie der Flint-und Trindelrinne (Öresund), Norstedt,* 34**,** 1-33.

CANDE, S. C. & KENT, D. V. 1992. A new geomagnetic polarity time scale for the Late Cretaceous and Cenozoic. *Journal of Geophysical Research: Solid Earth,* 97**,** 13917-13951.

CANDE, S. C. & KENT, D. V. 1995. Revised calibration of the geomagnetic polarity timescale for the Late Cretaceous and Cenozoic. *Journal of Geophysical Research: Solid Earth,* 100**,** 6093-6095.

CANE, M. A. & MOLNAR, P. 2001. Closing of the Indonesian seaway as a precursor to east African aridification around 3–4 million years ago. *Nature,* 411**,** 157.

CARPENTER, W. B., PARKER, W. K. & JONES, T. R. 1862. *Introduction to the study of the Foraminifera*, Ray society.

CHAPMAN, F., W. J. PARR, AND A. C. COLLINS, 1934. Tertiary foraminifera of Victoria, Australia-The Balcombian deposits of Port Phillip, Part lll. *Journal of the Linnean Society of London, Zoology,* 38**,** 553-577.

COMPTON, J. S., SNYDER, S. W. & HODELL, D. A. 1990. Phosphogenesis and weathering of shelf sediments from the southeastern United States: Implications for Miocene δ13C excursions and global cooling. *Geology,* 18**,** 1227-1230.

CORLISS, B. H. 1979a. Quaternary Antarctic bottom-water history: deep-sea benthonic foraminiferal evidence from the southeast Indian Ocean. *Quaternary Research,* 12**,** 271-289.

CORLISS, B. H. 1979b. Taxonomy of Recent deep- sea benthonic foraminifera from the Southeast Indian Ocean. *Micropaleontology,* 25**,** 1-19.

CORLISS, B. H. 1983. Distribution of Holocene deep-sea benthonic foraminifera in the southwest Indian Ocean. *Deep Sea Research Part A. Oceanographic Research Papers,* 30**,** 95-117.

CORLISS, B. H. 1985. Microhabitats of benthic foraminifera within deep-sea sediments. *Nature,* 314**,** 435-438.

CORLISS, B. H. 1991. Morphology and microhabitat preferences of benthic foraminifera from the northwest Atlantic Ocean. *Marine Micropaleontology,* 17**,** 195-236.

CORLISS, B. H. & FOIS, E. 1990. Morphotype analysis of deep-sea benthic foraminifera from the northwest Gulf of Mexico. *Palaios,* 5**,** 589-605.

CRAMER, B., TOGGWEILER, J., WRIGHT, J., KATZ, M. & MILLER, K. 2009. Ocean overturning since the Late Cretaceous: Inferences from a new benthic foraminiferal isotope compilation. *Paleoceanography,* 24.

CUSHMAN, J. A. 1911. A monograph of the foraminifera of the North Pacific Ocean. Part 2. Textulariidae. *Bulletin of the United States National Museum,* 71(2)**,** 1-108.
CUSHMAN, J. A. 1922. The foraminifera of the Atlantic Ocean. Part 3. Textulariidae. *Bulletin of the United States National Museum,* 104**,** 1 – 149.
CUSHMAN, J. A. 1923. The foraminifera of the Atlantic Ocean. Part 4. Lagenidae. *Bulletin of the United States National Museum,* 104**,** 1-228.
CUSHMAN, J. A. 1925. Some new foraminifera from the Velasco Shale of Mexico. *Contributions from the Cushman Laboratory for Foraminiferal Research,* 1**,** 18-23.
CUSHMAN, J. A. 1927. An outline of a reclassification of foraminifera. *Contributions from the Cushman laboratory for foraminiferal research,* 3**,** 105.
CUSHMAN, J. A. 1930. The foraminifera of the Atlantic Ocean, Part 7. Nonionidae, Camerinidae, Peneroplidae and Alveolinellidae. *Bulletin of the United States National Museum,* 104**,** 1-79.
CUSHMAN, J. A. 1933a. Some new foraminiferal genera. *Contributions from the Cushman Laboratory for Foraminiferal Research,* 9**,** 33.
CUSHMAN, J. A. 1933b. Some new Recent foraminifera from the tropical Pacific. *Contributions from the Cushman Laboratory for Foraminiferal Research,* 9**,** 77-95.
CUSHMAN, J. A. 1934. Smaller foraminifera from Vitilevu, Fiji. *Bulletin of Bernice P. Bishop Museum,* 119**,** 102–142.
CUSHMAN, J. A. 1937b. A monograph of the foraminiferal family Valvulinidae. Special Publications. *Cushman Laboratory for Foraminiferal Research,* 8**,** 1-210.
CUSHMAN, J. A. 1943. Some new foraminifera from the Tertiary of the Island of St. Croix. *Contributions from the Cushman Laboratory for Foraminiferal Research,* 19**,** 90-93.
CUSHMAN, J. A. & APPLIN, E. R. 1926. Texas Jackson foraminifera. *AAPG Bulletin,* 10**,** 154-189.
CUSHMAN, J. A. & BERMUDEZ, P. J. 1936. New genera and species of foraminifera from the Eocene of Cuba. *Contributions from the Cushman Laboratory for Foraminiferal Research,* 12**,** 27-38.
CUSHMAN, J. A. & EDWARDS, P. G. 1937. *Astrononion* a new genus of the foraminifera, and its species. *Contributions from the Cushman laboratory for foraminiferal research,* 13**,** 29-36.
CUSHMAN, J. A. & EDWARDS, P. G. 1938. Notes on the Oligocene species of *Uvigerina* and *Angulogerina*. *Contributions from the Cushman Laboratory for Foraminiferal Research,* 14**,** 74-89.
CUSHMAN, J. A. & JARVIS, P. W. 1934. Some interesting new uniserial foraminifera from Trinidad. *Contributions from the Cushman Laboratory for Foraminiferal Research,* 10**,** 71-75.
CUSHMAN, J. A. & MOYER, D. A. 1930. Some recent foraminifera from off San Pedro, California. *Contributions from the Cushman Laboratory for Foraminiferal Research,* 6**,** 49-62.
CUSHMAN, J. A. & PARKER, F. L. 1947. *Bulimina* and related foraminiferal genera. *Professional Paper of the United States Geological Survey,* 210- D**,** 55-176.
CUSHMAN, J. A. & TODD, R. 1942. The Recent and fossil species of *Laticarinina*. *Contributions from the Cushman Laboratory for Foraminiferal Research,* 18**,** 14-20.
CUSHMAN, J. A. & TODD, R. 1945. Miocene foraminifera from Buff Bay, Jamaica. *Cushman Laboratory for Foraminiferal Research, Special Publication* ,15**,** 73.
CUSHMAN, J. A. & TODD, R. 1949. The genus *Sphaeroidina* and its species. *Contributions from the Cushman Laboratory for Foraminiferal Research,* 25**,** 11-21.
CZJZEK, J. 1848. Beitrag zur Kenntniss der fossilen Foraminiferen des Wiener Beckens. *Naturwissenschaftliche Abhadlungen, Wien,* 2**,** 137-150.
D'ORBIGNY, A. D. 1826. Tableau méthodique de la classe des Céphalopodes. *Annales des Sciences Naturelles*
D'ORBIGNY, A. D. 1839a. Foraminifères. *In:* SAGRA, R. D. L. (ed.) *Histoire physique, politique et naturelle de l'île de Cuba.* Paris: A. Bertrand.
D'ORBIGNY, A. D. 1839b. Foraminifères. *In:* BARKER-WEBB, P. & BERTHELOT, S. (eds.) *Histoire Naturelle des iles Canaries.* Paris: Bethune.

D'ORBIGNY, A. D. 1839c. *Voyage dans l'Amérique méridionale: foraminifères,* Paris and Strasbourg, P. Bertrand.

D'ORBIGNY, A. D. 1846. *Foraminiferes fossiles du Bassin Tertiaire de Vienne (Autriche)* Paris: Gide et Camp.

D'ORBIGNY, A. D. 1849-1852. *Prodrome de paléontologie stratigraphique universelle des animaux mollusques & rayonnés, faisant suite au Cours élémentaire de paléontologie et de géologie stratigraphiques,* Paris, V. Masson.

DE MAN, E., VAN SIMAEYS, S., DE MEUTER, F., KING, C. & STEURBAUT, E. 2004. Oligocene benthic foraminiferal zonation for the southern North Sea Basin. *Bulletin van het Koninklijk Belgisch Instituut voor Natuurwetenschappen. Aardwetenschappen= Bulletin de l'Institut Royal des Sciences Naturelles de Belgique. Sciences de la Terre,* 74 177-195.

DESHAYES, G. P. 1828. Les mollusques [in] Cuvier, Le Règne Animal distribué d'après son organisation, pour servir de base à l'histoire naturelle des animaux et d'introduction à l'anatomie comparée. ed. 2., 310 pp. available online at https://archive.org/stream/lesmollusquesave00desh#page/34/

DICKENS, G.R. & OWEN, R.M., 1999. The latest Miocene–early Pliocene biogenic bloom: a revised Indian Ocean perspective. *Marine Geology*, 161, 75-91.

DIESTER-HAASS, L., BILLUPS, K. & EMEIS, K. C. 2006. Late Miocene carbon isotope records and marine biological productivity: Was there a (dusty) link? *Paleoceanography and Paleoclimatology,* 21.

DUNCAN, R. A. & STOREY, M. 1992. The life cycle of Indian Ocean hotspots. *Washington DC American Geophysical Union Geophysical Monograph Series,* 70**,** 91-103.

EADE, J. V. 1967. New Zealand Recent foraminifera of the families Islandiellidae and Cassidulinidae. *New Zealand journal of marine freshwater research,* 1**,** 421-454.

EARLAND, A. 1934. Foraminifera. Part III. The Falklands sector of the Antarctic (excluding South Georgia). *Discovery Reports, University Press, Cambridge***,** 1-208.

EDGAR, K. M., HULL, P. M. & EZARD, T. H. 2017. Evolutionary history biases inferences of ecology and environment from δ 13 C but not δ 18 O values. *Nature communications,* 8**,** 1106.

EHRENBERG, C. G. 1838. Über dem blossen Auge unsichtbare Kalkthierchen und Kieselthierchen als Hauptbestandtheile der Kreidegebirge. *Bericht über die zu Bekanntmachung geeigneten Verhandlungen der Königlichen Preussischen Akademie der Wissenschaften zu Berlin* 192-200.

ENNYU, A. & ARTHUR, M. A. 2004a. 13. Data Report: Oxygen and Carbon Stable Isotope Records of the Miocene Calcareous Microfossils from ODP Leg 189 Sites 1170 (South Tasman Rise) and 1172 (East Tasman Plateau).

ENNYU, A. & ARTHUR, M. A. 2004b. Early to Middle Miocene paleoceanography in the southern high latitudes off Tasmania. *The Cenozoic Southern Ocean: Tectonics, Sedimentation, and Climate Change Between Australia and Antarctica, Geophys. Monogr. Ser,* 151**,** 215-233.

EXON, N. F., KENNETT, J. P. & MALONE, M. J., ET AL. 2001. Leg 189 Summary. *Proc. ODP, Init. Repts.* College Station, TX (Ocean Drilling Program).

FICHTEL, L. & MOLL, J. P. C. 1798. *Testacea Microscopica aliaque Minuta ex Generibus Argonauta et Nautilus ad Naturam Delineat et Descripta,* Vienna.

FIEUX, M., ANDRIÉ, C., CHARRIAUD, E., ILAHUDE, A., METZL, N., MOLCARD, R. & SWALLOW, J. 1996. Hydrological and chlorofluoromethane measurements of the Indonesian throughflow entering the Indian Ocean. *Journal of Geophysical Research: Oceans,* 101**,** 12433-12454.

FINLAY, H. J. 1939. New Zealand foraminifera: key species in stratigraphy – no. 1. *Transactions of the Royal Society of New Zealand,* 68**,** 504-543.

FINLAY, H. J. 1940. New Zealand foraminifera: key species in stratigraphy–no. 4. *Transactions of the Royal Society of New Zealand,* 69**,** 448-472.

FINLAY, H. J. 1947. New Zealand Foraminifera: Key Species in Stratigraphy - no. 5. *New Zealand journal of science and technology,* 28**,** 259-292.

FLOWER, B. & KENNETT, J. 1993. Middle Miocene ocean-climate transition: High-resolution oxygen and carbon isotopic records from Deep Sea Drilling Project Site 588A, southwest Pacific. *Paleoceanography and Paleoclimatology,* 8**,** 811-843.

FLOWER, B. P. & KENNETT, J. P. 1994. The middle Miocene climatic transition: East Antarctic ice sheet development, deep ocean circulation and global carbon cycling. *Palaeogeography, Palaeoclimatology, Palaeoecology,* 108**,** 537-555.

FLOWER, B. P. & KENNETT, J. P. 1995. Middle Miocene deepwater paleoceanography in the southwest Pacific: relations with East Antarctic Ice Sheet development. *Paleoceanography,* 10**,** 1095-1112.

FORNASINI, C. 1902. Contributo a la conoscenza de le Bulimine adriatiche. *Memorie della Reale Accademia delle Scienze dell'Istituto di Bologna,* 9**,** 371-382.

FURSENKO, A. 1958. Osnovnye etapy razvitiya faun foraminifer v geologicheskom proshlom. *Trudy Instituta Geologicheskikh Nauk, Akademiia Nauk Belorusskoi SSR,* 1**,** 10-29.

GALLOWAY, J. J. 1933. *A manual of Foraminifera,* Bloomington, Principia press.

GALLOWAY, J. J. & WISSLER, S. G. 1927. Correction of names of foraminifera. *Journal of Paleontology,* 1**,** 193-193.

GLAESSNER, M. F. 1937. Die Entfaltung der Foraminiferenfamilie Buliminidae. *Problemy Paleontologii, Paleontologicheskaya Laboratoriya Moskovskogo Gosudarstvennogo Universiteta,* 2**,** 411-3.

GOODAY, A. J. 1988. A response by benthic Foraminifera to the deposition of phytodetritus in the deep sea. *Nature,* 332**,** 70-73.

GOODAY, A. J. 1994. The biology of deep-sea foraminifera: a review of some advances and their applications in paleoceanography. *Palaios***,** 14-31.

GOODAY, A. J. 2003. Benthic foraminifera (Protista) as tools in deep-water palaeoceanography: environmental influences on faunal characteristics. *Advances in Marine Biology.*

GORDON, A. L. & FINE, R. A. 1996. Pathways of water between the Pacific and Indian oceans in the Indonesian seas. *Nature,* 379**,** 146.

GORDON, A. L., GIULIVI, C. F. & ILAHUDE, A. G. 2003. Deep topographic barriers within the Indonesian seas. *Deep Sea Research Part II: Topical Studies in Oceanography,* 50**,** 2205-2228.

GRADSTEIN, F. M., OGG, J.G., SCHMITZ, M.D., OGG, G.M., ET AL. 2012. *The Geologic Time Scale 2012,* Boston, USA, Elsevier.

GREENOP, R. et al. 2014. Middle Miocene climate instability associated with high-amplitude CO2 variability. Paleoceanography, 29,845-853, doi:10.1002/2014PA002653.

GRIFFITH, J. W. & HENFREY, A. 1875. *The micrographic dictionary: a guide to the examination and investigation of the structure and nature of microscopic objects,* London, J. Van Voorst.

GROSSMAN, E. L. 1987. Stable isotopes in modern benthic foraminifera; a study of vital effect. *The Journal of Foraminiferal Research,* 17**,** 48-61.

GUÉRIN-MÉNEVILLE, F. E. 1829-1844. *Iconographie du règne animal de G. Cuvier : ou, Représentation d'après nature de l'une des espèces les plus et souvent non encore figurées de chaque genre d'animaux,* Paris ; London.

GÜMBEL, C. W. 1868. Beiträge zur Foraminiferenfauna der nordalpinen, älteren Eocängebilde oder der Kressenberger Nummulitenschichten. *Abhandlungen der Mathematisch-Physikalischen Klasse der Königlich Bayerischen Akademie der Wissenschaften,* 10**,** 581-730.

GUPPY, R. J. L. 1894. On some Foraminifera from the Microzoic deposits of Trinidad, West Indies. *Proceedings of the Zoological Society of London,* 4**,** 647-653.

GUPTA, A., JOSEPH, S. & THOMAS, E. 2001a. Species diversity of Miocene deep-sea benthic foraminifera and water mass stratification in the Northeastern Indian Ocean. 47**,** 111-124.

GUPTA, A. K. 1993. Biostratigraphic vs. paleoceanographic importance of *Stilostomella lepidula* (Schwager) in the Indian Ocean. *Micropaleontology*, 47-51.

GUPTA, A. K. 1994. Taxonomy and bathymetric distribution of Holocene deep-sea benthic foraminifera in the Indian Ocean and the Red Sea. *Micropaleontology*, 351-367.

GUPTA, A. K. 1997. Paleoceanographic and paleoclimatic history of the Somali Basin during the Pliocene-Pleistocene; multivariate analyses of benthic foraminifera from DSDP Site 241 (Leg 25). *The Journal of Foraminiferal Research,* 27, 196-208.

GUPTA, A. K., DHINGRA, H., MÉLICE, J. L. & ANDERSON, D. M. 2001b. Earth's eccentricity cycles and Indian Summer Monsoon variability over the past 2 million years: Evidence from deep-sea benthic foraminifer. *Geophysical Research Letters,* 28, 4131-4134.

GUPTA, A. K., SARKAR, S. & MUKHERJEE, B. 2006. Paleoceanographic changes during the past 1.9 Myr at DSDP Site 238, Central Indian Ocean Basin: benthic foraminiferal proxies. *Marine Micropaleontology,* 60, 157-166.

GUPTA, A. K. & SATAPATHY, S. 2000. Latest Miocene–Pleistocene abyssal benthic foraminifera from west-central Indian Ocean DSDP Site 236: Paleoceanographic and paleoclimatic inferences. *Journal of Paleontological Society of India,* 45, 33-48.

GUPTA, A. K., SINGH, R. K., JOSEPH, S., THOMAS, E. & 2004. Indian Ocean high-productivity event (10-8 Ma): Linked to global cooling or to the initiation of the Indian monsoons? *Geology,* 32, 753-756.

GUPTA, A. K. & THOMAS, E. 1999. Latest Miocene-Pleistocene Productivity and Deep-Sea Ventilation in the Northwestern Indian Ocean (Deep Sea Drilling Project Site 219). *Paleoceanography and Paleoclimatology,* 14, 62-73.

HADLEY , W. H. 1934. Some Tertiary foraminifera from the north coast of Cuba. *Bulletin of American Paleontology,* 20, 1-40.

HAECKEL, E. 1894. *Systematische Phylogenie. Entwurf eines Natürlichen Systems der Organismen auf Grund ihrer Stammesgeschichte. Theil l, Systematische Phylogenie der Protisten und Pflanzen,* Berlin, Georg Reimer.

HALL, R. 1998. The plate tectonics of Cenozoic SE Asia and the distribution of land and sea. *Biogeography and geological evolution of SE Asia*, 99-131.

HALL, R., COTTAM, M. A. & WILSON, M. E. 2011. The SE Asian gateway: history and tectonics of the Australia–Asia collision. *Geological Society, London, Special Publications,* 355, 1-6.

HAMMER, Ø., HARPER, D. A. & RYAN, P. D. 2001. PAST: paleontological statistics software package for education and data analysis. *Palaeontologia electronica,* 4, 9.

HANAGATA, S. & NOBUHARU, T. 2015. Illustrated guide to Pliocene foraminifera from Miyakojima, Ryukyu Island Arc, with comments on biostratigraphy. *Palaeontologia Electronica*. 18(1).

HANTKEN, M. V. 1875. Die fauna der Clavulina Szabói-Schichten. Theil I - Foraminiferen. *Kaiserlich Ungarische Anstalt, Mitteilungen, Jahrbuch,* 4, 1-93.

HARPER, D.A., 1999. *Numerical palaeobiology: computer-based modelling and analysis of fossils and their distributions*. John Wiley & Sons Inc.

HAYWARD, B. W. 2002. Late Pliocene to middle Pleistocene extinctions of deep-sea benthic foraminifera ("*Stilostomella* extinction") in the southwest Pacific. *Journal of Foraminiferal Research,* 32, 274-307.

HAYWARD, B. W., GRENFELL, H. R., SABAA, A. & HAYWARD, J. J. 2003. Recent benthic foraminifera from offshore Taranaki, New Zealand. *New Zealand Journal of Geology and Geophysics,* 46, 489-518.

HAYWARD, B. W. & KAWAGATA, S. 2005. Extinct foraminifera figured in Brady's Challenger Report. *Journal of Micropalaeontology,* 26, 171–175.

HAYWARD, B. W., KAWAGATA, S., SABAA, A., GRENFELL, H., KERCKHOVEN, L. V., LEWANDOWSKI, K. & E, T. 2012. *The last global extinction (Mid-Pleistocene) of deep sea benthic foraminifera*

(Chrysalogoniidae, Ellipsoidinidae, Glandulonodosariidae, Plectofrondicularіidae, Pleurostomellidae, Stilostomellidae), their Late Cretaceous-Cenozoic history and taxonomy.

HAYWARD, B. W., NEIL, H., CARTER, R., GRENFELL, H. R. & HAYWARD, J. J. 2002. Factors influencing the distribution patterns of Recent deep-sea benthic foraminifera, east of New Zealand, Southwest Pacific Ocean. *Marine Micropaleontology,* 46**,** 139-176.

HAYWARD, B. W., S. KAWAGATA, GRENFELL, H. R., SABAA, A. T. & O'NEILL, T. 2007. Last global extinction in the deep sea during the mid-Pleistocene climate transition. *Paleoceanography* 22**,** PA3103.

HAYWARD, B. W., SABAA, A., GRENFELL, H., NEIL, H. & BOSTOCK, H. 2013. Ecological distribution of Recent deep-water foraminifera around New Zealand. 43**,** 414-441.

HAYWARD, B. W., SABAA, A. T., THOMAS, E., KAWAGATA, S., NOMURA, R., SCHRÖDER-ADAMS, C., GUPTA, A. K. & JOHNSON, K. 2010 Cenozoic record of elongate, cylindrical, deep-sea benthic foraminifera in the Indian Ocean (ODP Sites 722, 738, 744, 758, and 763). *The Journal of Foraminiferal Research,* 40**,** 113-133.

HAYWARD, B. W., LE COZE, F., VACHARD, D., GROSS, O. 2019. World Foraminifera Database. *Bulimina alazanensis* Cushman, 1927. Accessed at: http://www.marinespecies.org/foraminifera/aphia.php?p=taxdetails&id=113032 on 2019-07-07.

HAYWARD, B. W., LE COZE, F., VACHARD, D., GROSS, O. 2019. World Foraminifera Database. *Hansenisca soldanii* (d'Orbigny, 1826). Accessed through: World Register of Marine Species at: http://www.marinespecies.org/aphia.php?p=taxdetails&id=113418 on 2019-07-07.

HAYWARD, B. W., LE COZE, F., VACHARD, D., GROSS, O. 2019. World Foraminifera Database. *Gavelinopsis praegeri* (Heron-Allen & Earland, 1913). Accessed through: World Register of Marine Species at: http://www.marinespecies.org/aphia.php?p=taxdetails&id=113159 on 2019-07-07.

HAYWARD, B. W., LE COZE, F., VACHARD, D., GROSS, O. 2019. World Foraminifera Database. *Heterolepa bradyi* (Trauth, 1918). Accessed through: World Register of Marine Species at: http://www.marinespecies.org/aphia.php?p=taxdetails&id=736954 on 2019-07-07.

HAYWARD, B. W., LE COZE, F., VACHARD, D., GROSS, O. 2020. World Foraminifera Database. *Bolivina dilatata* Reuss, 1850. Accessed through: World Register of Marine Species at: http://www.marinespecies.org/aphia.php?p=taxdetails&id=112973 on 2020-05-25.

HERGUERA, J. C. & BERGER, W. 1991. Paleoproductivity from benthic foraminifera abundance: Glacial to postglacial change in the west-equatorial Pacific. *Geology,* 19**,** 1173-1176.

HERMELIN, J. 1991. The benthic foraminiferal faunas of sites 725, 726, and 728 (Oman Margin, northwestern Arabian Sea). *Proceedings of the Ocean Drilling Program. Scientific Results,* 117**,** 55-87.

HERMOYIAN, C. S. & OWEN, R. M. 2001. Sedimentation rates and geochemistry of the Atlantic and Indic Ocean of Late Miocene - Early Pliocene. *Supplement to: Hermoyian, CS; Owen, RM (2001): Late Miocene-early Pliocene biogenic bloom: Evidence from low-productivity regions of the Indian and Atlantic Oceans. Paleoceanography, 16(1), 95-100, https://doi.org/10.1029/2000PA000501.* PANGAEA.

HERON-ALLEN, E. & EARLAND, A. 1913. Clare Island survey *Foraminifera: Proceedings of the Royal Irish Academy,* 31**,** 1-188.

HEWAIDY, A. G. A., SALLAM, M. M. & KHALIFA, M. F. 2013. Miocene calcareous foraminifera of the Nile delta area, Egypt. *Egypt. J. Paleontol.,* 13**,** 121-171.

HILGEN, F. J., LOURENS, L. J., VAN DAM, J. A., BEU, A. G., BOYES, A. F., COOPER, R. A., KRIJGSMAN, W., OGG, J. G., PILLER, W. E. & WILSON, D. S. 2012. Chapter 29 - The Neogene Period. *In:*

GRADSTEIN, F. M., OGG, J. G., SCHMITZ, M. D. & OGG, G. M. (eds.) *The Geologic Time Scale.* Boston: Elsevier.

HOFKER, J. 1951a. The foraminifera of the Siboga expedition. Part III *Siboga-Expeditie, Monographie IVa* 1-513.

HOFKER, J. 1954. Über die Familie Epistomariidae (Foram.). *Palaeontographica Abteilung A,* A105**,** 166-206.

HOFKER, J. 1956a. Tertiary foraminifera of coastal Ecuador: Part II, Additional notes on the Eocene species. *Journal of Paleontology***,** 891-958.

HOLBOURN, A., HENDERSON, A. & MACLEOD, N. 2013. *Atlas of Benthic Foraminifera*, John Wiley & Sons.

HOLBOURN, A., W. Kuhnt, M. Schulz, and H. Erlenkeuser (2005), Impacts of orbital forcing and atmospheric carbon dioxide on Miocene ice-sheet expansion, *Nature*, 438, 483-487.

HOLBOURN, A., Kuhnt, W., Schulz, M., Flores, J.A. and Andersen, N., 2007. Orbitally-paced climate evolution during the middle Miocene "Monterey" carbon-isotope excursion. *Earth and Planetary Science Letters*, 261, 534-550.

HOLBOURN, A., Kuhnt, W., Clemens, S., Prell, W. and Andersen, N., 2013. Middle to late Miocene stepwise climate cooling: Evidence from a high-resolution deep water isotope curve spanning 8 million years. *Paleoceanography*, 28, 688-699.

HOUTZ, R. E., HAYES, D. E. & MARKL, R. G. 1977. Kerguelen Plateau bathymetry, sediment distribution and crustal structure. *Marine Geology,* 25**,** 95-130.

HOWE, H. V. 1939. Louisiana Cook Mountain Eocene Foraminifera. *Bulletin of the Geological Survey of Louisiana,* 14**,** 1-122.

HSU, K. J. & BERNOULLI, D. 1978. Genesis of the Tethys and the Mediterranean. In: lnit. Rep. DSDP.

HUANG, X., STÄRZ, M., GOHL, K., KNORR, G. & LOHMANN, G. 2017. Impact of Weddell Sea shelf progradation on Antarctic bottom water formation during the Miocene. *Paleoceanography,* 32**,** 304-317.

HUSEZIMA, R. & MARUHASI, M. 1944. A new genus and thirteen new species of foraminifera from the core-sample of Kashiwazaki oil field, Niigata-ken. *Journal of the Sigenkagaku Kenkyusho,* 1**,** 391-400.

INGLE, S., WEIS, D., DOUCET, S. & MATTIELLI, N. 2003. Hf isotope constraints on mantle sources and shallow-level contaminants during Kerguelen hot spot activity since∼ 120 Ma. *Geochemistry, Geophysics, Geosystems,* 4**,** 1-28.

JONES, R. W. 1994. *The Challenger Foraminifera,* Oxford, Oxford University Press

JONES, T. R. 1875. The micrographic dictionary; a guide to the examination and investigation of the structure and nature of microscopic objects. *In:* GRIFFITH, J. W. & HENFREY, A. (eds.). London.

JONES, T. R. & PARKER, W. K. 1860. On the rhizopodal fauna of the Mediterranean, compared with that of the Italian and some other Tertiary deposits. *Quarterly Journal of the Geological Society,* 16**,** 292-307.

JOHNSON, K. et al. 2011. Impact of the Middle Miocene climate transition on elongate, cylindrical foraminifera in the subtropical Pacific. Marine Micropaleontology, 78, 50-64.

KAIHO, K. 1992. Eocene to Quaternary benthic foraminifers and paleobathymetry of the Izu-Bonin Arc, Legs 125 and 126. *Proceedings of the Ocean Drilling Program, Scientific Results,* 126**,** 285-310.

KAIHO, K. 1994. Benthic foraminiferal dissolved-oxygen index and dissolved-oxygen levels in the modern ocean. *Geology,* 22**,** 719-722.

KAIHO, K. 1999. Evolution in the test size of deep-sea benthic foraminifera during the past 120 m.y. *Marine Micropaleontology,* 37**,** 53-65.

KAMINSKI, M. A. 2004. The year 2000 classification of the agglutinated Foraminifera. In: Bubík, M., Kaminski, M.A. (Eds.). *Proceedings of the Sixth International Workshop on Agglutinated Foraminifera, 237-255.* Grzybowski Foundation, Special Publication.

KELLER, G. & BARRON, J. A. 1983. Paleoceanographic implications of Miocene deep-sea hiatuses. *Geological Society of America Bulletin,* 94**,** 590-613.

KENDER, S., KAMINSKI, M. A. & JONES, R. W. 2008. Early to middle Miocene foraminifera from the deep-sea Congo Fan, offshore Angola. *Micropaleontology***,** 477-568.

KENNETT, J. P. Latest Cretaceous to Cenozoic climate and oceanographic developments in the Weddell Sea, Antarctica: an ocean-drilling perspective. Proceedings of the Ocean Drilling Program, Scientific Results, 1990. College Station, 937-962.

KENNETT, J. P., HOUTZ, R. E., ANDREWS, P. B., EDWARDS, A. R., GOSTIN, V. A., HAJÓS, M., HAMPTON, M., JENKINS, D. G., MARGOLIS, S. V. & OVENSHINE, A. T. 1975. Cenozoic paleoceanography in the southwest Pacific Ocean, Antarctic glaciation, and the development of the Circum-Antarctic Current. *Initial reports of the deep sea drilling project,* 29**,** 1155-1169.

KENNETT, J. P., SRINIVASAN, M. S. & AND KELLER, G. 1985. Miocene planktonic foraminiferal biogeography and pale-oceanographic development of the Indo-Pacific region. *The Miocene Ocean: Paleoceanography and biogeography: Boulder, Colorado Geologic Society of America Memoir***,** 197-236.

KNEE-ROBINSON, S. 2018. *Miocene climate reconstruction in the Southern Indian Ocean* Master University of Birmingham.

KOCHHANN, K. G. D. et al. 2017. Eastern equatorial Pacific benthic foraminiferal distribution and deep water temperature changes during the early to middle Miocene. Marine Micropaleontology, 133, 28-39.

KUPPUSAMY, M., GUPTA, A. & BHAUMIK, A. 2011. Distribution of deep-sea benthic foraminifera in the Neogene of Blake Ridge, NW Atlantic Ocean. *Journal of Micropalaeontology,* 30**,** 33-74.

KURIHARA, K. & KENNETT, J. P. 1992. Paleoceanographic significance of Neogene benthic foraminiferal changes in a southwest Pacific bathyal depth transect. *Marine Micropaleontology,* 19**,** 181-199.

LAMARCK, J. B. 1804a. Suite des mémoires sur les fossiles des environs de Paris *Annales Muséum National d'Histoire Naturelle,* 5**,** 179-188.

LAMB, J. L. & MILLER, T. H. 1984. *Stratigraphic Significance of Uvigerinid Foraminifers in Western Hemisphere*.

LANKESTER, E. R. 1885. Protozoa. *Encyclopaedia Britannica.* 9th ed.

LEAR, C. H., COXALL, H. K., FOSTER, G. L., LUNT, D. J., MAWBEY, E. M., ROSENTHAL, Y., SOSDIAN, S. M., THOMAS, E. & WILSON, P. A. 2015. Neogene ice volume and ocean temperatures: Insights from infaunal foraminiferal Mg/Ca paleothermometry. *Paleoceanography,* 30**,** 1437-1454.

LEE, J. J. 1990. Phylum Granuloreticulosa (Foraminifera). *In:* L. MARGULIS, J. O. C., M. MELKONIAN, AND D. J. CHAPMAN (ed.) *Handbook of Protoctista.* Boston: Jones and Bartlett, Publishers, 524-528.

LEI, Y. & LI, T. 2016. *Atlas of Benthic Foraminifera from China Seas: The Bohai Sea and the Yellow Sea*, Springer.

LINKE, P. & LUTZE, G. 1993. Microhabitat preferences of benthic foraminifera—a static concept or a dynamic adaptation to optimize food acquisition? *Marine micropaleontology,* 20**,** 215-234.

LOEBLICH, A. & TAPPAN, H. 1955. Re-vision of some Recent Foraminiferal genera. *Smithsonian Miscellaneous Collections,* 128**,** 1-37.

LOEBLICH, A. R. & TAPPAN, H. 1984. Suprageneric classificationof the Foraminiferida (Protozoa). *Micropaleontology,* 30**,** 1-70.

LOEBLICH, A. R. & TAPPAN, H. 1987. *Foraminiferal genera and their classification,* New York, Van Nostrand Reinhold.

LOEBLICH, A. R. & TAPPAN, H. 1992. Present status of Foraminiferal Classification. In: Takayanagi, Y. & Saito, T (eds), Studies in Benthic Foraminifera. Tokai University Press, 93-102.

LOEBLICH, A. R. & TAPPAN, H. 1994. Feraminifera of the Sahul Shelf and Timor Sea. *Special Publications of the Cushman Laboratory for Foraminiferal Research,* 31**,** 1-661.

LOUBERE, P. & FARIDUDDIN, M. 1999. Benthic foraminifera and the flux of organic carbon to the seabed. *Modern foraminifera.* Springer.

LUBBERS, J., KUHNT, W., HOLBOURN, A. E., BOLTON, C. T., GRAY, E., USUI, Y., ET AL. 2019. The middle to late Miocene "carbonate crash" in the equatorial Indian Ocean. Paleoceanography and Paleoclimatology, 34, 813–832. https:// doi.org/10.1029/2018PA003482

LUTZE, G. & THIEL, H. 1989. Epibenthic foraminifera from elevated microhabitats; Cibicidoides wuellerstorfi and Planulina ariminensis. *The Journal of Foraminiferal Research,* 19**,** 153-158.

Lyle, M., DADEY, K.A. & FARREL, J.W., 1995. The Late Miocene (11–8 Ma) Eastern Pacific Carbonate Crash: evidence for reorganization of deep-water Circulation by the closure of the Panama Gateway. *Proceedings of the Ocean Drilling Program, Scientific Results*, 138, 821- 838.

MACKENSEN, A. 1992. Neogene benthic foraminifers from the southern Indian Ocean (Kerguelen Plateau): biostratigraphy and paleoecology. In Wise, S.W., Jr., Schlich, R., et al. *Proc. ODP, Sci. Results.* College Station, TX (Ocean Drilling Program).

MACKENSEN, A. & BERGGREN, W. A. Paleogene benthic foraminifers from the southern Indian Ocean (Kerguelen Plateau): biostratigraphy and paleoecology. Proceedings of the Ocean Drilling Program, Scientific Results, 1992. Ocean Drilling Program College Station TX, 603-630.

MACKENSEN, A., GROBE, H., KUHN, G. & FU¨TTERER, D. K. 1990. Benthic foraminiferal assemblages from the eastern Weddell Sea between 68 and 73°S: Distribution, ecology and fossilization potential. *Marine Micropaleontology,* 16**,** 241-283.

MACKENSEN, A., SEJRUP, H. & JANSEN, E. 1985. The distribution of living benthic foraminifera on the continental slope and rise off southwest Norway. *Marine Micropaleontology,* 9**,** 275-306.

MAJEWSKI, W. & BOHATY, S.M., 2010. Surface-water cooling and salinity decrease during the Middle Miocene climate transition at Southern Ocean ODP Site 747 (Kerguelen Plateau). *Marine Micropaleontology*, 74, 1-14.

MANCIN, N., HAYWARD, B., I, T., COBIANCHI, M. & LUPI, C. 2013. *Can the morphology of deep-sea benthic foraminifera reveal what caused their extinction during the mid-Pleistocene Climate Transition?*

MARKS, P. 1951. A revision of the smaller foraminifera from the Miocene of the Vienna Basin. *Contributions from the Cushman Foundation for Foraminiferal Research,* 2**,** 33-73.

MARTIN, E. E. & SCHER, H. 2006. A Nd isotopic study of southern sourced waters and Indonesian throughflow at intermediate depths in the Cenozoic Indian Ocean. *Geochemistry, Geophysics, Geosystems,* 7.

MAYER, L.A., SHIPLEY, T.H. & WINTERER, E.L., 1986. Equatorial Pacific seismic reflectors as indicators of global oceanographic events. *Science*, 233, 761-764.

MAYER, L. A., THEYER, F., BARRON, J. A., DUNN, D. A., HANDYSIDE, T., HILLS, S., ET AL. 1985. Initial reports of the Deep Sea Drilling Project, 85, 1-1021. Washington: U.S. Government Printing.

MAZUMDER, A., HENRIQUES, P. & NIGAM, R. 2003. Distribution of benthic foraminifera within oxygen minima zone, off central west coast, India. *Gondwana Geological Magazine,* 6**,** 5-10.

MCGONIGAL, K. L. 2007. *Miocene climate transitions in the southwest Pacific, Tasmania: Interpretations based on calcareous nannofossils.* The Florida State University.

MILLER, K. G. & KATZ, M. E. 1987. Oligocene to Miocene benthic foraminiferal and abyssal circulation changes in the North Atlantic. *Micropaleontology,* 33**,** 97-149.

MILLER, K. G., KOMINZ, M. A., BROWNING, J. V., WRIGHT, J. D., MOUNTAIN, G. S., KATZ, M. E., SUGARMAN, P. J., CRAMER, B. S., CHRISTIE-BLICK, N. & PEKAR, S. F. 2005. The Phanerozoic record of global sea-level change. *science,* 310**,** 1293-1298.

MILNE-EDWARDS, A. 1881. Compte rendu sommaire d'une exploration zoologique faite dans l'Atlantique à bord du navire de l'etat" le Travailleur". *Compte Rendu Hebdomadaire des Séances de l' Académie des Sciences,* 93**,** 876-882.

MONTFORT, P. D. D. 1808. *Conchyliologie systématique et classification méthodique des coquilles,* Paris.

MURRAY, J. W., YOUNG, J., NEWTON, J., DUNNE, J., CHAPIN, T., PAUL, B. & MCCARTHY, J. J. 1996. Export flux of particulate organic carbon from the central equatorial Pacific determined using a combined drifting trap-234Th approach. *Deep Sea Research Part II: Topical Studies in Oceanography,* 43**,** 1095-1132.

MUTTER, J. C. & CANDE, S. C. 1983. The early opening between Broken Ridge and Kerguelen Plateau. *Earth and Planetary Science Letters,* 65**,** 369-376.

NEUGEBOREN, J. L. 1856. Die foraminiferen aus der Ordnung der Stichostegier von Ober-Lapugy in Siebenbürgen. *Denkschriften der Kaiserlichen Akademie der Wissenschaften, Mathematisch-Naturwissenschaftliche Classe,* 12**,** 65-108.

NISHIMURA, A., KONDA, I., MATSUOKA, K., NISHIDA, S. & OHNO, T. 1977. Microfossils of the core sample GDP-11-15 from the Amami Plateau, the northern margin of the Philippines Sea. *Memoirs of the Faculty of Science, Kyoto University. Series of geology and mineralogy* 43**,** 111-129.

NISHIMURA, S. & SUPARKA, S. 1997. Tectonic approach to the Neogene evolution of Pacific-Indian Ocean seaways. *Tectonophysics,* 281**,** 1-16.

NOMURA, R. 1983a. Cassidulinidae (foraminiferida) from the uppermost Cenozoic of Japan (part I). *The science reports of the Tohoku University. Second series, Geology,* 53**,** 1-101.

NOMURA, R. 1983b. Cassidulinidae (Foraminiferida) from the uppermost Cenozoic of Japan (Part 2). *Science Reports of the Tohoku University. Sendai, Series. 2 (Geology)* 54**,** 1- 93.

NOMURA, R. 1991. Oligocene to Pleistocene benthic foraminifer assemblages at sites 754 and 756 eastern Indian Ocean. *Proceedings Oceanic Drilling Program (ODP), Scientific Results,* 121**,** 31-75.

NOMURA, R. 1995. Paleogene to Neogene deep-sea paleoceanography in the eastern Indian Ocean: benthic foraminifera from ODP Sites 747, 757 and 758. *Micropaleontology***,** 251-290.

NUTTALL, W. L. F. 1932. Lower Oligocene foraminifera from Mexico. *Journal of Paleontology,* 6**,** 3-35.

O'NEILL, T. A., HAYWARD, B. W., KAWAGATA, S., SABAA, A. T. & GRENFELL, H. R. 2007. Pleistocene extinctions of deep-sea benthic foraminifera: the South Atlantic record. *Palaeontology,* 50**,** 1073-1102.

OHKUSHI, K. I., THOMAS, E. & KAWAHATA, H. 1999. Abyssal benthic foraminifera from the northwestern Pacific (Shatsky Rise) during the last 298 kyr. *Marine Micropaleontology,* 38**,** 119-147.

OKADA, H. & BUKRY, D. 1980. Supplementary modification and introduction of code numbers to the low-latitude coccolith biostratigraphy (Bukry, 1973; 1975). *Mar. Micropaleontol.,* 5**,** 321-325.

PALMER, D. K. 1940. Foraminifera of the Upper Oligocene Cojimar Formation of Cuba. *Sociedad Cubana de Historia Natural,* 14**,** 19-35, 113–132, 277–304.

PALMER, D. K. & BERMÚDEZ, P. J. 1936. Late Tertiary foraminifera from the Matanzas Bay region, Cuba. *Memorias de la Sociedad Cubana de Historia Natural "Felipe Poey,* 9**,** 237–257.

PAPP, A. & SCHMID, M. E. 1985. Die fossilen Foraminiferen des tertiaeren Beckens von Wien: Revision der Monographie Alcide d' Orbigny (1846). *Abhandlungen der Geologischen Bundesanstalt,* 37**,** 1-311.

PARKER, F. L. 1954. Distribution of the foraminifera in the North- eastern Gulf of Mexico. *Bulletin of the Museum of Comparative Zoology* 111**,** 453-588.

PARKER, W. K. & JONES, T. R. 1865. On some foraminifera from the North Atlantic and Arctic Oceans, including Davis Straits and Baffin's Bay. *Philosophical Transactions of the Royal Society* 155**,** 325-441.

PARR, W. 1932. Victorian and South Australian shallow-water foraminifera. *Part II: Proceedings of the Royal Society of Victoria,* 44**,** 226.

PARR, W. J. 1950. Foraminifera, BANZ Antarctic Research Expedition 1929–31, Report, ser. *B,* 5**,** 232-392.

PATTERSON, R. T. 1985. *Abditodendrix*, a new foraminiferal genus in the family Bolivinitidae. *Journal of Foraminiferal Research,* 15**,** 138-140.

PATTERSON, R. T. 1987. Four new foraminiferal (Protozoa) genera from the Rio Grande Rise, southwest Atlantic Ocean. *Transactions of the American Microscopical Society,* 106**,** 139-148.

PAUL, H. A., ZACHOS, J. C., FLOWER, B. P. & TRIPATI, A. 2000. Orbitally induced climate and geochemical variability across the Oligocene/Miocene boundary. *Paleoceanography,* 15**,** 471-485.

PEIRCE, J., WEISSEL, J. & TAYLOR, E., ET AL. 1989. *Proc. ODP, Sci. Results.* College Station, TX (Ocean Drilling Program).

PERSICO, D., WISE JR, S. W. & JIANG, S. Oligocene–Holocene calcareous nannofossil biostratigraphy and diagenetic etch patterns on Quaternary placoliths at ODP Site 1139 on Skiff Bank, Northern Kerguelen Plateau. Proc. ODP, Sci. Results, 2003. 1-19.

PERYT, D. 2013. Foraminiferal record of the Middle Miocene climate transition prior to the Badenian salinity crisis in the Polish Carpathian Foredeep Basin (Central Paratethys). *Geological Quarterly,* 57**,** 141-164, doi: 10.7306/gq. 1080.

PETERSON, L. C. 1984. Recent abyssal benthic foraminiferal biofacies of the eastern equatorial Indian Ocean. *Marine Micropaleontology,* 8**,** 479-519.

PETTERS, V. & SARMIENTO, S. R. 1956. Oligocene and Lower Miocene Biostratigraphy of the Carmen-Zambraon Area, Colombia. *Micropaleontology,* 2**,** 7-35.

PEYPOUQUET, J., CARBONEL, P., DUCASSE, O., TÖULDERER-FARMER, M. & LÉTÉ, C. 1988. Environmentally Cued Polymorphism of Ostracods A Theoretical and Practical Approach. A Contribution to Geology and to the Understanding of Ostracod Evolution. *Developments in Palaeontology and Stratigraphy.* Elsevier.

PFLUM, C. E. & FRERICHS, W. E. 1976. *Gulf of Mexico deep-water foraminifers*, Cushman Foundation for Foraminiferal Research.

PFUHL, H. A., MCCAVE, I. N., SCHELLENBERG, S. A. & FERRETTI, P. 2004. Changes in Southern Ocean circulation in late Oligocene to early Miocene time. *The Cenozoic Southern Ocean: Tectonics, Sedimentation, and Climate Change Between Australia and Antarctica,* 151**,** 173-189.

PHLEGER, F. B. & PARKER, F. L. 1951. Ecology of foraminifera, northwest Gulf of Mexico. Pt. II. Foraminifera species. *Memoirs of the Geological Society of America,* 46**,** 1-64.

PHLEGER, F. B., PARKER, F. L. & PEIRSON, J. F. 1953. North Atlantic foraminifera: Swedish Deep-Sea Exped. *Repts., Göteborg,* 7**,** 1-122.

PIVETEAU, J. 1952. *Traité de Paléontologie*, Masson et Cie, Paris.

POAG, C. W. 2015. *Benthic Foraminifera of the Gulf of Mexico: Distribution, ecology, paleoecology,* Texas A&M University Press.

POAG, C. W. & LOW, D. 1984. Environmental trends among Neogene benthic foraminifers at DSDP Site 548, Irish continental margin. In: Graciansky, P.C., de, Poag, C.W., et al. (Eds.). *Initial Report of Deep Sea Drilling Program.* Washington (U.S.Govt. Printing Office).

POPESCU, G. & CRIHAN, I.-M. 2005. Middle Miocene foraminifera from Romania: order Buliminida, part II. *Acta Palaeontol. Rom.,* 5**,** 397-412.

PROTHERO, D. R. 2013. *Bringing fossils to life: An introduction to paleobiology*, Columbia University Press.

RAMSAY, A. T., SMART, C. W. & ZACHOS, J. C. 1998. A model of early to middle Miocene deep ocean circulation for the Atlantic and Indian Oceans. *Geological Society, London, Special Publications,* 131**,** 55-70.

RAMSTEIN, G., FLUTEAU, F., BESSE, J. & JOUSSAUME, S. 1997. Effect of orogeny, plate motion and land–sea distribution on Eurasian climate change over the past 30 million years. *Nature,* 386**,** 788.

RASMUSSEN, T. L. 2005. Systematic paleontology and ecology of benthic foraminifera from the Plio-Pleistocene Kallithea Bay section, Rhodes, Greece. *Cushman Foundation Special Publication,* 39**,** 53-157.

REA, D. K., DEHN, J., DRISCOLL, N. W., FARRELL, J. W., JANECEK, T. R., OWEN, R. M., POSPICHAL, J. J. & RESIWATI, P. 1990. Paleoceanography of the eastern Indian Ocean from ODP Leg 121 drilling on Broken Ridge. *Geological Society of America Bulletin,* 102**,** 679-690.

REA, D. K., LOHMANN, K. C., MACLEOD, N. D., HOUSE, M. A., HOVAN, S. A. & AND MARTIN, G. D. 1991. Oxygen and carbon isotopic records from the oozes of Sites 752, 754, 756, and 757. *In:* WEISSEL, J., PEIRCE, J., TAYLOR, E., ALT, J., ET AL. (ed.) *Proc. ODP, Sci. Results.* College Station, TX (Ocean Drilling Program).

REISS, Z. 1963. Reclassification of perforate foraminifera. *Bulletin of the Geological Survey of Israel* 35**,** 1-111.

RENZ, H. H. 1948. *Stratigraphy and fauna of the Agua Salada group, State of Falcon, Venezuela*, Geological Society of America.

REUSCH, D. N. Oligocene–Miocene terrigenous and pelagic sediments, Skiff Bank, Kerguelen Plateau (ODP Leg 183, Site 1139). Proceedings of the Ocean Drilling Program, Scientific Results, 2002. 1-31.

REUSS, A. E. 1850. Neue Foraminiferen aus den Schichten des österreichischen Tertiärbeckens. *Denkschriften der Kaiserlichen Akademie der Wissenschaften,* 1**,** 365-390.

REUSS, A. E. 1851. Ueber die fossilen Foraminiferen und Entomostraceen der Septarienthone der Umgegend von Berlin. *Zeitschrift der Deutschen Geologischen Gesellschaft,* 3**,** 49-92.

REUSS, A. E. 1860. Die Foraminiferen der westphälischen Kreideformation. *Sitzungsberichte der mathematisch-naturwissenschaflichen Classe der kaiserlichen Akademie der Wissenschaften,* 40**,** 147-238.

REUSS, A. V. 1862. Entwurf einer systematischen Zusammenstellung der Foraminiferen. *Sitzungsberichte der Kaiserlichen Akademie der Wissenschaften zu Wien, mathematish-naturwissenschaftlichen Classe,* 44**,** 355-396.

REVETS, S. A. 1993. The revision of the genus *Buliminellita* Cushman and Stainforth, 1947, and Eubuliminella gen. nov. *The Journal of Foraminiferal Research,* 23**,** 141-151.

REVETS, S. A. 1996. The generic revision of five families of rotaliine foraminifera. Part I The Bolivinitidae Cushman, 1927. *Cushman Foundation for Foraminiferal Research, Special Publication,* 34**,** 1–55.

ROBERTSON, B. E. 1998. Systematics and paleoecology of the benthic Foraminiferida from the Buff Bay section, Miocene of Jamaica. *Micropaleontology,* 44**,** 1 – 266.

ROLLET, N. 1997. Plate-tectonic setting of the Tasmanian region. *Australian Journal of Earth Sciences* 44**,** 543-560.

SAIDOVA, K. M. 1975. *Bentosnye Foraminifery Tikhogo Okeana [Benthonic foraminifera of the Pacific Ocean],* Moscow, Institut Okeanologii P. P. Shirshova, Akademiya Nauk SSSR.

SAIDOVA, K. M. 1981. [On an up-to-date system of supraspecific taxonomy of Cenozoic benthonic foraminifera]-"In Russian". *Akademiya Nauk SSSR***,** 1-73.

SCHLICH, R., SCHAMING, M., WEIS, D., MONTIGNY, R. & DAMASCENO, D. 1998. New structural and tectonic data in the Northern Kerguelen Plateau. *Eos Trans. AGU,* 79**,** F871.

SCHLICH, R. & WISE JR, S. Leg 120. Proceedings of the Ocean Drilling Program, Initial Reports, 1989.

SCHRODER-ADAMS, C. 1991. Middle Eocene to Holocene Benthic Foraminifer Assemblages from the Kerguelen Plateau (Southern Indian Ocean). In: Barron, J., Larsen, B., et al., 1991. *Proceedings of the Ocean Drilling Program, Scientific Results.* College Station, Texas.

SCHUBERT, R. J. 1899. Die Miocäne Foraminiferen fauna von Karwin (Oestern Schlesien). *Lotos,* 19**,** 211-247.

SCHULTZE, M. S. 1854. *Über den Organismus der Polythalamien (Foraminiferen), nebst Bermerkungen über die Rhizopoden im Allgemeinen,* Leipzig.

SCHWAGER, C. 1866. Fossile Foraminiferen von Kar Nikobar. *Reise der Österreichischen Fregatte Novara um die Erde in den Jahren 1857, 1858, 1859 unter den Befehlen des Commodore B. von Wüllerstorf-Urbair,* 2**,** 187-268.

SCHWAGER, C. 1877. Quadro del proposto sistema di classificazione dei foraminiferi con guscio. *Bolletino R. Comitato Geologico d'Italia,* 8**,** 18-27.

SCHWEIZER, M. 2006. Evolution and molecular phylogeny of Cibicides and Uvigerina (Rotaliida, Foraminifera). *Geologica Ultraiectina,* 261**,** 1-167.

SCHWEIZER, M., FONTAINE, D. & PAWLOWSKI, J. 2011. Phylogenetic position of two Patagonian Cibicididae (Rotaliida, foraminifera): *Cibicidoides dispars* (d'Orbigny, 1839) and *Cibicidoides variabilis* (d'Orbigny, 1826). *Revue de Micropaléontologie,* 54**,** 175-182.

SCHWEIZER, M., PAWLOWSKI, J., KOUWENHOVEN, T. & VAN DER ZWAAN, B. 2009. Molecular phylogeny of common Cibicidids and related Rotaliida (Foraminifera) based on small subunit rDNA sequences. *Journal of Foraminiferal Research* 39**,** 300-315.

SEGUENZA, G. 1880. Le formazioni terziarie nella provincia di Reggio (Calabria). *Memorie della Classe di Scienze Fisiche Matematiche e Naturali della Regia Accademia del Lincei,* 3**,** 1-445.

SETOYAMA, E. & KAMINSKI, M. 2015. Neogene Benthic Foraminifera from the southern Bering Sea (IODP Expedition 323). *Palaeontologia Electronica,* 18**,** 1-30.

SHACKLETON, N. J. & KENNETT, J. P. 1975. Paleotemperature history of the Cenozoic and the initiation of Antarctic glaciation: oxygen and carbon isotope analyses in DSDP sites 277, 279 and 281. *Init. Repts. DSDP.* College Station, TX (Texas A&M University).

SHEVENELL, A.E., KENNETT, J.P. & LEA, D.W., 2008. Middle Miocene ice sheet dynamics, deep-sea temperatures, and carbon cycling: A Southern Ocean perspective. *Geochemistry, Geophysics, Geosystems*, 9, doi:10.1029/2007GC001736.

SHIPBOARD SCIENTIFIC PARTY. 1989a. Site 752. *In:* PEIRCE, J., WEISSEL, J., TAYLOR, E., ALT, J. & AL., E. (eds.) *Proc. ODP, Init. Repts.* College Station, TX (Ocean Drilling Program).

SHIPBOARD SCIENTIFIC PARTY. 1989b. Site 754. *In:* PEIRCE, J. & WEISSEL, J., ET AL. (eds.) *Proc. ODP, Init. Repts.* College Station, TX (Ocean Drilling Program).

SHIPBOARD SCIENTIFIC PARTY. 2000. Site 1139. *In:* COFFIN, M. F., FREY, F. A. & WALLACE, P. J., ET AL. (eds.) *Proc. ODP, Init. Repts.* College Station, TX (Ocean Drilling Program).

SHIPBOARD SCIENTIFIC PARTY. 2001a. Site 1168. *In:* EXON, N. F., KENNETT, J. P. & MALONE, M. J., ET AL. (eds.) *Proc. ODP, Init. Repts.* College Station, TX (Ocean Drilling Program).

SHIPBOARD SCIENTIFIC PARTY. 2001b. Site 1171. *In:* EXON, N. F., KENNETT, J. P. & MALONE, M. J., ET AL. (eds.) *Proc. ODP, Init. Repts.* College Station, TX (Ocean Drilling Program).

SHIPBOARD SCIENTIFIC PARTY. 2001c. Site 1172. *In:* EXON, N., KENNETT, J. P. & MALONE, M., ET AL. (eds.) *Proc. ODP, Init. Repts.* College Station, TX (Ocean Drilling Program).

SILVESTRI, A. 1924. Revisione di fossili della Venezia e della Venezia Giulia. *Atti dell'Accademia Scientifica Veneto− Trentino− Istriana, Padova (ser. 3),* 14**,** 7-12.

SILVESTRI, O. 1872. Saggio di studi sulla fauna microscopia fossile appartenente al terreno subappenino italiano. Mem. I - monografia delle Nodosarie. *Academia Gioenia Scienze Naturali Catania,* 3**,** 1-108.

SINGH, R. K. & GUPTA, A. K. 2004. Late Oligocene–Miocene paleoceanographic evolution of the southeastern Indian Ocean: evidence from deep-sea benthic foraminifera (ODP Site 757). *Marine Micropaleontology,* 51**,** 153-170.

SINGH, R. K. & GUPTA, A. K. 2010. Deep-sea benthic foraminiferal changes in the eastern Indian Ocean (ODP Hole 757B): their links to deep Indonesian (Pacific) flow and high latitude glaciation during the Neogene. *Episodes,* 33**,** 74-82.

SINGH, R. K., GUPTA, A. K. & DAS, M. 2012. Paleoceanographic significance of deep-sea benthic foraminiferal species diversity at southeastern Indian Ocean Hole 752A during the Neogene. *Palaeogeography, Palaeoclimatology, Palaeoecology,* 361**,** 94-103.

SMART, C. W. & RAMSAY, A. T. S. 1995. Benthic foraminiferal evidence for the existence of an early Miocene oxygen-depleted oceanic water mass? *Journal of the Geological Society,* 152**,** 735-738.

SMART, C. W. and Thomas, E. 2006. The enigma of early Miocene biserial planktic foraminifera. Geology, 34, 1041-1044.

SMART, C. W. and Thomas, E. 2007. Emendation of the genus *Streptochilus* Brönnimann and Resig 1971 (Foraminifera) and new species from the lower Miocene of the Atlantic and Indian Oceans. Micropaleontology, 53, 73-103.

SMART, C. W., THOMAS, E. & RAMSAY, A. T. 2007. Middle–late Miocene benthic foraminifera in a western equatorial Indian Ocean depth transect: paleoceanographic implications. *Palaeogeography, Palaeoclimatology, Palaeoecology,* 247**,** 402-420.

SRINIVASAN, M. & SHARMA, V. 1980. *Schwager's Car Nicobar Foraminifera in the Reports of the Novara Expedition: a revision*, Today and Tomorrow Publisher.

STAINFORTH, R. 1952. Classification of uniserial calcareous Foraminifera. *Contributions from the Cushman Foundation for Foraminiferal Research,* 3**,** 6-14.

STICKLEY, C., BRINKHUIS, H., MCGONIGAL, K., CHAPRONIERE, G., FULLER, M., KELLY, D., NÜRNBERG, D., PFUHL, H., SCHELLENBERG, S. & SCHÖNFELD, J. Late Cretaceous–Quaternary biomagnetostratigraphy of ODP Sites 1168, 1170, 1171, and 1172, Tasmanian Gateway. Proceedings of the Ocean Drilling Program, Scientific Results, 2004. Ocean Drilling Program, College Station TX, 1-57.

SUPER, J. R. et al. 2018. North Atlantic temperature and *p*CO2 coupling in the early-middle Miocene. Geology, 46, 519-522.

SZTRĂKOS, K. 1979. *La stratigraphie, paléoécologie, paléogéographie et les foraminifères de l'Oligocène du nord-est de la Hongrie*, Éditions du Centre national de la recherche scientifique.

SZTRÀKOS, K. J. R. D. M. 2000. Les foraminifères de l'Eocène du Bassin de l'Adour (Aquitaine, France): biostratigraphie et taxinomie. *Revue de micropaléontologie,* 43**,** 71-172.

THALMANN, H. E. 1937. Mitteilungen über Foraminiferen III. *Eclogae Geologicae Helvetiae,* 30**,** 337–356.

THOMAS, E. 1990. Late Cretaceous through Neogene deep-sea benthic foraminifera (Maud Rise, Weddell Sea, Antarctica). *Proceedings Oceanic Drilling Program (ODP), Scientific Results,* 113**,** 571-594.

THOMAS, E., BOOTH, L., MASLIN, M. & SHACKLETON, N. 1995. Northeastern Atlantic benthic foraminifera during the last 45,000 years: changes in productivity seen from the bottom up. *Paleoceanography and Paleoclimatology,* 10**,** 545-562.

THOMAS, E. & GOODAY, A. J. 1996. Cenozoic deep-sea benthic foraminifers: Tracers for changes in oceanic productivity? *Geology,* 24**,** 355-358.

TJALSMA, R. 1983. EOCENE TO MIOCENE BENTHIC FORAMINIFERS FROM DEEP-SEA DRILLING PROJECT SITE-516, RIO-GRANDE RISE, SOUTH-ATLANTIC. *Initial Reports of the Deep Sea Drilling Project,* 72**,** 731-755.

TJALSMA, R. C. & LOHMANN, G. P. 1983. Paleocene-Eocene bathyal and abyssal benthic foraminifera from the Atlantic Ocean *Micropaleontology, Special Publication* 4**,** 1-90.

TODD, R. 1957. Smaller Foraminifera. *Geology of Saipan, Mariana Islands. Part 3. Palaeontology.* Professional Papers U.S. Geological Survey.

TRAUTH, F. 1918. Das Eozanvorkommen bei Radstadt im Pongau und seine Beziehungen zu den gleichalterigen Ablagerungen bei Kirchberg am Wechsel und Wimpassing am Leithagebirge. *Kaiserlichen Akademie der Wissenschaften in Wein, Mathematisch-Naturwissenschaftliche Classe,* 95**,** 171-278.

UCHIO, T. 1952. Foraminiferal assemblages from Hachijo Island, Tokyo Prefecture, with descriptions of some new genera and species. *Japanese Journal of Geology and Geography,* 22**,** 145-159.

VAN AKEN, H., PUNJANAN, J. & SAIMIMA, S. 1988. Physical aspects of the flushing of the east Indonesian basins. *Netherlands Journal of Sea Research,* 22**,** 315-339.

VAN MARLE, L. J. 1988. Bathymetric distribution of benthic foraminifera on the Australian-Irian Jaya continental margin, eastern Indonesia. *Marine Micropaleontology,* 13**,** 97-152.

VAN MORKHOVEN, F. P., BERGGREN, W. A., EDWARDS, A. S. & OERTLI, H. 1986. *Cenozoic cosmopolitan deep-water benthic foraminifera*, Elf Aquitaine.

VELLA, P. 1957. Studies in New Zealand Foraminifera; Part I- Foraminifera from Cook Strait. Part II- Upper Miocene to Recent Species of the Genus *Notorotalia*. *New Zealand Geological Survey Paleontological Bulletin,* 28**,** 1-64.

VERDUCCI, M., FORESI, L. M., SCOTT, G. H., SPROVIERI, M., LIRER, F. & PELOSI, N. 2009. The Middle Miocene climatic transition in the Southern Ocean: Evidence of paleoclimatic and hydrographic changes at Kerguelen plateau from planktonic foraminifers and stable isotopes. *Palaeogeography, Palaeoclimatology, Palaeoecology,* 280**,** 371-386.

VERDUCCI, M., FORESI, L. M., SCOTT, G. H., TIEPOLO, M., SPROVIERI, M., & LIRER, F. 2007. East Antarctic Ice Sheet fluctuations during the Middle Miocene Climatic Transition inferred from faunal and biogeochemical data on planktonic foraminifera (Kerguelen Plateau). *US Geological Survey and The National Academics; USGS OF− 2007− 1047, Short Re− search Paper*, 37.

VINCENT, E. & BERGER, W. H. 1985. Carbon dioxide and polar cooling in the Miocene: The Monterey hypothesis. *The carbon cycle and atmospheric CO2: Natural variations Archean to present,* 32**,** 455-468.

VINCENT, E., KILLINGLEY, J. S. & BERGER, W. H. 1985. Miocene oxygen and carbon isotope stratigraphy of the tropical Indian Ocean. *The Miocene Ocean: Paleoceanography and Biogeography.* Geological Society of America Memoir 163.

VOLOSHINOVA, N. A. 1952. Pseudoparellinae, P. 80. *In:* VOLOSHINOVA, N. A. & DAIN, L. G., 1952 (eds.) *Iskopaemye Foraminifery SSSR. Nonionidy, Kassidulinidy I Khilostomellidy.* Trudy Vsesoyuznogo Neftyanogo Nauchnoissledovatel'skogo Geologo-razvedochnogo Instituta (VNIGRI), (New Series). [In Russian].

VOLOSHINOVA, N. A. 1960. Uspekhi mikropaleontologii v dele izucheniya vnutrennego stroeniya foraminifer. *Trudy Pervogo Seminara po Mikrofaune***,** 48-87.

WEATHERALL, P., MARKS, K. M., JAKOBSSON, M., SCHMITT, T., TANI, S., ARNDT, J. E., ROVERE, M., CHAYES, D., FERRINI, V. & WIGLEY, R. 2015. A new digital bathymetric model of the world's oceans. *Earth and Space Science,* 2**,** 331-345.

WEDEKIND, R. 1937. *Einführung in die Grundlagen der historischen Geologie: Mikrobiostratigraphie. Die Korallen-u. Foraminiferenzeit*, Enke.

WESTERHOLD, T., BICKERT, T. & RÖHL, U. 2005. Middle to late Miocene oxygen isotope stratigraphy of ODP site 1085 (SE Atlantic): new constrains on Miocene climate variability and sea-level fluctuations. *Palaeogeography, Palaeoclimatology, Palaeoecology,* 217**,** 205-222.

WHITTAKER, J. E. 1988. *Benthic Cenozoic Foraminifera from Ecuador: Taxonomy and Distribution of Smaller Benthic Foraminifera from Coastal Ecuador (Late Oligocene-Late Pliocene)*, British Museum of Natural.

WIJFFELS, S., BRAY, N., HAUTALA, S., MEYERS, G. & MORAWITZ, W. 1996. The WOCE Indonesian throughflow repeat hydrography sections: I10 and IR6. *International WOCE Newsletter,* 24**,** 25-28.

WILLIAMSON, W. C. 1858. *On the recent foraminifera of Great Britain*, Ray Society.

WOLLENBURG, J. E. & KUHNT, W. 2000. The response of benthic foraminifers to carbon flux and primary production in the Arctic Ocean. *Marine Micropaleontology,* 40**,** 189-231.

WOODRUFF, F. 1985. Changes in Miocene deep-sea benthic foraminiferal distribution in the Pacific Ocean: relationship to paleoceanography. *Geological Society of America Memoir,* 163**,** 131-175.

WOODRUFF, F. & SAVIN, S. 1991. Mid-Miocene isotope stratigraphy in the deep sea: High-resolution correlations, paleoclimatic cycles, and sediment preservation. *Paleoceanography,* 6**,** 755-806.

WOODRUFF, F. & SAVIN, S. M. 1989. Miocene deepwater oceanography. *Paleoceanography and Paleoclimatology,* 4**,** 87-140.

WRIGHT, J. D. & MILLER, K. G. 1992. Miocene stable isotope stratigraphy, Site 747, Kerguelen Plateau. *In:* WISE, S. W., JR., SCHLICH, R., ET AL. (ed.) *Proc. ODP, Sci. Results.* College Station, TX (Ocean Drilling Program).

WRIGHT, J. D. & MILLER, K. G, & FAIRBANKS, R. G. 1992. Early and Middle Miocene stable isotopes: Implications for Deepwater circulation and climate, *Paleoceanography*, 7(3), 357– 389, doi:10.1029/92PA00760.

WRIGHT, R. 1978. Neogene benthic foraminifera from DSDP leg 42A, Mediterranean Sea. Init. Rept. *DSDP* 42**,** 709-726.

ZACHOS, J., PAGANI, M., SLOAN, L., THOMAS, E. & BILLUPS, K. 2001. Trends, rhythms, and aberrations in global climate 65 Ma to present. *science,* 292**,** 686-693.

ZACHOS, J. C., DICKENS, G. R. & ZEEBE, R. E. 2008. An early Cenozoic perspective on greenhouse warming and carbon-cycle dynamics. *Nature,* 451**,** 279.

Appendices

Appendix A: Benthic foraminifera species checklist at ODP Site 752 Hole A.

752A (core, section, interval (cm))	Age (Ma)	Depth (mbsf)	*Abditodentrix pseudothalmanni*	*Amphicoryna scalaris*	*Amphicoryna* sp.1	*Amphicoryna* sp.2	*Anomalinoides alazanensis*	*Anomalinoides* sp.1	*Anomalinoides* sp.4	*Anomalinoides* sp.4?	*Anomalinoides* sp.13	*Astacolus crepidulus*	*Astacolus* sp.1	*Astrononion umbilicatulum*	*Bolivina albatrossi*	*Bolivina digitata*	*Bolivina Huneri*	*Bolivina reticulata*	*Bolivina* cf. *reticulata*
2H-4, 65-70	**Early Pliocene**	13.32													1				11
3H-1, 50-55		18.30	6								4			10					19
3H-2 ,60-65	**Late Miocene**	19.85	7	1						2									65
3H-4 ,40-45		22.78	49																42
3H-5 ,70-75		24.42	30											1					283
4H-1 ,70-75		28.00	6							5									114
4H-2 ,85-90		29.61												3					278
4H-5 ,70-75		33.94	25																210
5H-1 ,70-75		37.45	31																231
5H-2 ,70-75		38.95	35							1									167
5H-3 ,90-95		40.30	45																45
5H-4 ,70-75		41.99	17	1															130
6H-1 ,70-75		47.10	23	8						4		1		2					79
6H-3 ,75-80	**Mid-Miocene**	50.16	11	3			6				1								107
6H-5 ,70-75		53.03	48	3								1		7					31
6H-6 ,20-25		54.33	42					1						4					22
7H-1 ,65-70		56.73	10	3								3		4					19
7H-2 ,80-85		58.33	2	17				1	3			5		27				8	33
7H-4 ,70-75		61.30	10	13				1				2						63	28
7H-6 ,100-105		64.13	20	6															15
8H-1 ,100-105	**Early Miocene**	66.80	4	18			1				1	3		4		29		12	
8H-3 ,100-105		69.80	9	12			2					1	1			3		28	
8H-6 ,70-75		74.00	10	9			3					3	1					46	
9H-2 ,100-105		77.94	5	8								6		2				47	
9H-4 ,80-85		80.71	4	2		1						5		11		3	2		9
9H-5 ,65-70		82.05	8					1				13	2	4				2	3
10H-2 ,60-65		87.10	9	3		1	1					2					3		1
10H-3 ,100-105		88.95	11	3	1							3		1			23		1
10H-5 ,80-85	**Late Oligocene**	91.77		9								2					177		
10H-6 ,110-115		93.03	5	1			1					2					40	2	

Appendix A (continued)

Depth (mbsf)	*Bolivina striatula*	*Bolivinellina* cf. *B. translucens*	*Bolivina viennensis*	*Bolivina* sp.2	*Bolivina* sp.3	*Bolivina* sp.11	*Bolivina* sp.6	*Bolivina* sp.7	*Bolivina* sp.8	*Bolivina* sp.9	*Bolivina* sp.10	*Bolivina* sp.12	*Bolivina* sp.16	*Bulimina aculeata*	*Bulimina truncana*	*Bulimina striata*	*Bulimina* sp.3	*Bulimina* sp.5	*Bulimina* sp.6	*Bulimina* sp.9	*Bulimina tuxpamensis*	*Burseolina pacifica*	*Burseolina* cf. *pacifica*	*Cassidulina* sp.3	*Cibicides* sp.1	*Cibicides* sp.2	*Cibicides* sp.3	*Cibicides* sp.4	*Cibicides* sp.5
13.32		4	4					1		2						1							4						
18.30		150	23												2														
19.85	1	136	23						1						2					1			4						
22.78		51	8													4						1							
24.42		9	62													12							4						
28.00	1	1	34							7					4	3				4			3						
29.61		6	81						1	1													6						
33.94		1	33																			4							
37.45		6	33												4	56						3							
38.95		1	37							2					1							1	8	2					
40.30			3	1											1							1	3	4					
41.99		1	36												42							11	3	5					
47.10		1	22																			25	32	1					
50.16		34	10												19				1			4	5	2					
53.03		3	11												9				1		1	4	4	14					
54.33		2	2							11					5								6						
56.73		7	7																			1	11						
58.33		15	26							1						7					2	3	25	1					1
61.30		9	13							1					1						2	3	11						
64.13		2	3																				3						
66.80			8																		2	16	23						
69.80			17					1							1						2	4	18						
74.00			12					18															38						
77.94		7								162				2							7	5	35						
80.71										7						1							84						
82.05		1								1	2	2			3		1	1			2		56						
87.10		1		1				1						1						3	11		8						
88.95		4		5		1	4	3	1	1										4	23				2	2	2	1	
91.77		3		2	1											1	2			1	8								
93.03		2		1				3					1		1							1		1					

Appendix A (continued)

Depth (mbsf)	*Cibicides* sp.6	*Cibicidoides bradyi*	*Cibicidoides kullenbergi*	*Cibicidoides laurisae*	*Cibicidoides mundulus*	*Cibicidoides pachyderma*	*Cibicidoides robertsoniana*	*Cibicidoides* sp.1	*Cibicidoides* sp.2	*Cibicidoides* sp.3	*Cibicidoides* sp.5	*Cibicidoides* sp.6	*Cibicidoides* sp.8	*Cibicidoides* sp.10	*Cibicidoides* sp.11	*Cibicidoides* sp.12	*Cibicidoides* sp.14	*Cibicidoides* sp.15	*Cibicidoides wuellerstorfi* (smooth)	*Cibicidoides wuellerstorfi* (coarse)	*Dentalina communis*	*Dentalina* sp. 10	*Dentalina* sp.3	*Dentalina* sp.4	*Dentalina* sp.5	*Dentalina* sp.6	*Dentalina* sp.7	*Dentalina* sp.8	*Dentalina* sp.9
13.32		1			2		1																						
18.30					27														51				3						
19.85					5												4		36										
22.78		1			1				2	1									2										
24.42					2														33										
28.00			1		2														45				1						
29.61			1		22														28				2						
33.94					10														11										
37.45					24														25				1						
38.95					4	5		1								1			14										
40.30		1			4															3									
41.99					19											1			5	17									
47.10					44				1											40			1						
50.16			1		13															22			2						
53.03			2												1					36			3						
54.33		20			1															2									
56.73					12			1												30	5		1						
58.33	1		1		5															20	1		3			1			
61.30					5															2			3						
64.13		2																3					2						
66.80			3		9									2	2								6						
69.80			2	1	3			1			2									5			3						
74.00			1		16						1												6						
77.94				4	18			1	2		1	2	2							3		2	1						
80.71			1		24			1	1		1									2									
82.05			4	8	50				2											1			3						1
87.10			2	3	4						2	1								1			3						
88.95				7	15			2	1											5		4	3			1		2	1
91.77				23	32			1	2														4	1	3	1	1		
93.03	5	1	3	6	9			2															1			1			

Appendix A (continued)

Depth (mbsf)	*Dentalina* sp.11	*Dentalina* sp.12	*Dentalina* sp.13	*Dentalina* sp.14	*Dentalina* sp.16	*Diocibicides* sp.1?	*Dorothia brevis*	*Duquepsamina* sp.1	*Eggerella bradyi*	*Ehrenbergina carinata*	*Ehrenbergina* sp.1	*Epistominella exigua*	*Fissurina marginata*	*Fissurina* sp.1	*Fissurina* sp.3	*Fissurina* sp.4	*Fissurina* sp.5	*Fissurina* sp.6	*Fissurina* sp.7	*Fissurina* sp.8	*Fissurina* sp.9	*Fissurina* sp.10	*Fissurina* sp.11	*Fissurina* sp.12	*Fissurina* sp.14	*Fissurina* sp.15	*Fissurina* sp.16	*Fissurina* sp.16?	*Fissurina* sp.17
13.32									8			6	2	1			1												
18.30	1								6	70			5	1	2	1	1	1											
19.85									5	24			3	1			1	1											
22.78									4	2		7																	
24.42									9	24		4	3														1		
28.00	1								6				2			1	7	1											
29.61		1							7				2	1	4		2				1								
33.94									2				2	2			1												
37.45					1								6		3														
38.95									6		4		3	1				1										2	
40.30									1			3																	
41.99									6				2	4	1	1	1											1	1
47.10					3		3		6				1					2									1	4	
50.16	1								3				1	1													1		
53.03		2					3						4	2															
54.33												8																	
56.73							2						3													2			
58.33							2						9					2											
61.30		1			3				1				3												1				
64.13												1		1			2									1			
66.80					3								6																
69.80														1			1												
74.00				2					1				1	2							2								
77.94		1	3						1																				
80.71		2							2				2	1															
82.05		2				1		1					1																
87.10	1	2				2			1				1				1				1								
88.95						2		1							1						1	2	1	1					
91.77																			1	1	1								
93.03									2																				

Appendix A (continued)

Depth (mbsf)	*Fissurina* sp.18	*Fissurina* sp.49	*Florilus clavatus*	*Gaudryina pyramidata*	*Gaudryina* sp.	*Gavelinopsis lobatulus*	*Globobulimina* sp.	*Globocassidulina minuta*	*Globocassidulina subglobosa*	*Globulina gibba*	*Globulina* sp.1	*Globulina* sp.2	*Globulina* sp.3	*Globulina* sp.4	*Guttulina austriacea*	*Guttulina ovata*	*Gyrodinoides lamarckianus*	*Gyrodinoides* sp.1	*Gyrodinoides* sp.1?	*Gyrodinoides* sp.3	*Gyroidinoides soldanii*	*Hanzawaia laurisae*	*Heronallenia pulvinulinoides*	*Heronallenia* sp.	*Karreriella bradyi*	*Karreriella* sp.1	*Karreriella* sp.2	*Lagena alticostata*	*Lagena* cf. *L.striata*
13.32	1			5		35			8									1			1		1					
18.30			3					5	56								5				8				6			3	
19.85			3			1		4	46								2				9				1			2	
22.78						28			4												4				2				
24.42						9		3	33								1				6		1		4			1	2
28.00								16	31	2					1		9				4	5		1	8			3	1
29.61								25	43	1	1						1				5		1		8			1	
33.94						7		9	74	2						1					5							1	
37.45						4		7	48												3		2		7			1	5
38.95								7	16												10		2		5			5	2
40.30						1		3	8												1		2					1	1
41.99								2	22	1							4			1	8			3	7			3	1
47.10			5					1	18	2									1		13			3	8			2	1
50.16			2					1	24	1											13			1				2	
53.03			4						25	1											4		3	3					1
54.33			1	1				2	4									1			1		1						
56.73				6					22		2										11		4		3			1	
58.33				9		34		8	64	2							1				13			3	6			2	
61.30				1				5	27					2		2				1	4			2	1				1
64.13						7			14												1			2					1
66.80				5			1		41				1							3	10			1				2	7
69.80			3	1			1	2	42			1					1				6			1					1
74.00			2	1				6	26			1				1					10		2	3					
77.94			1	2					16								1				9			6	1		1		1
80.71				1				1	7								2				10		3		3				
82.05			4	2	2				7		1								1		10			3					
87.10		5	3		1			6	41	1											8			11					
88.95			3	1				1	52												6			6	1				
91.77									63												10			3		1			1
93.03									13												1			1					

Appendix A (continued)

Depth (mbsf)	*Lagena* sp.1	*Lagena* sp.2	*Lagena* sp. 4	*Lagena* sp. 5	*Lagena* sp. 9	*Lagena* sp.7	*Lagena* sp.8	*Lagena* sp.10	*Lagena* sp.11	*Lagena* sp.12	*Lagena* sp.13	*Lagena* sp.15	*Lagena* sp.17	*Lagena* sp.18	*Lagena* sp.19	*Lagena* sp.20	*Lagena striata*	*Laminononion tumidum*	*Laticarinina pauperata*	*Lenticulina convergens*	*Lenticulina cultrata*	*Lenticulina gibba*	*Lenticulina* sp.1	*Lenticulina* sp.2	*Lenticulina* sp.3	*Lenticulina* sp.4	*Lenticulina* sp.5	*Lenticulina* sp.6	*Lenticulina* sp.7
13.32		2	1												1				1			1							
18.30	5								2									1	7	1		2							
19.85	1	1							2							1			8		1								
22.78									4										2			1							
24.42									1								2		4		3		2						
28.00	2			1					1										10	3	1								
29.61				2												1		1	5		1		1						
33.94	1								3									1	3		1		1						
37.45	2								1			2					1	2	13	1									
38.95							2		1							2			5	2	1								
40.30									1										1										
41.99	1								3							1			5		3								
47.10	2			2					1			1					2		9	2	4	2		1					
50.16	1								5										3	5	2					1		2	
53.03									2										1	3	3		4						
54.33																	1		1										
56.73									1								1		4	1	9		1						2
58.33	1												1	1	3	2		3	7	13	17	1	2					1	
61.30	1		3	1					2									2		3	8	4	2						
64.13																		2		1		1							
66.80				1								1					7	9		7	22	1		1					
69.80						1				1							2			4	9		4						
74.00						1		2									1			8	14		5						
77.94			1			1						1							8	3	9	5	2				2		
80.71	1			1				1	2		1							1	2	10	4	1	1						
82.05							2										1	2	6	9	26								
87.10									2	1								1	7	6	8	3	3						
88.95	5	1			1		2	1									2	1	7	17	14		5	2					
91.77	1		1	1	1	1											5		6	16	17	6	4	6	1	1			
93.03						1														3		2							

Appendix A (continued)

Depth (mbsf)	*Lenticulina* sp.8	*Lobatulus lobatulus*	*Marsonella* sp.1	*Marsonella* sp.2	*Martinottiella communis*	*Martinottiella scabra*	*Melonis barleeanus*	*Nodosaria* sp.1	*Nodosaria* sp.2	*Nodosaria* sp.3	*Nodosaria* sp.5	*Nodosaria* sp.6	*Nodosaria* sp.7 ?	*Nodosaria* sp.8	*Nodosaria* sp.9	*Nodosaria* sp.13	*Nodosaria* sp.14	*Nodosaria* sp.18	*Nonionella iridea*	*Nonionella* sp.	*Nuttalides umbonifera*	*Favulina hexagona*	*Oolina* sp.1	*Oolina* sp.2	*Oolina squamosa*	*Ordorsalis* sp.1?	*Oridorsalis umbonatus*	*Orthomorphina ambigua*	*Orthomorphina jedlitschkai*
13.32							3																		1		4		
18.30						1	1									2		1							1		20	5	
19.85							1									1										1	11		
22.78																													
24.42						2								1								1					5	3	
28.00																1			1								13	2	2
29.61																											21		2
33.94																				5	1						6		2
37.45																				1							7	2	
38.95																	1		2								18		
40.30															1					2									
41.99						2								2						1	1	1					7	3	
47.10	2					7								1		2	2			2							14	1	
50.16	1															1			2	1		2	1				8	1	
53.03						2	2					1	1				2		1	1		1					6	1	2
54.33																	1		1	4	4						2		
56.73						3	5					1					3		1	4	4					1	18	3	4
58.33		1				13	21										6	1	24	16	37						15	1	3
61.30							1	1											2		23						10		
64.13																	1										1		
66.80			2	4	2		1				1					4	2				8	1					21	1	
69.80																1				7	4						18		
74.00				2													6			11	5						14		
77.94			1	3		2															28						4	1	
80.71																3					50						5	1	
82.05		2	1						3			1									63						15		
87.10		1						1		1		1				3					1						3		
88.95		1								2											1		1	1			6		
91.77		1			1			1	1		2					3					8						8		
93.03																	2				12						2		

Appendix A (continued)

Depth (mbsf)	*Orthomorphina perversa*	*Osangularia culter*	*Osangularia* sp.	*Paracassidulina minuta*	*Parafissurina* sp.	*Planoglabratella* sp.1	*Planoglabratella* sp.2	*Planularia* sp.	*Planulina costata*	*Planulina renzi*	*Planulina* sp.	*Pleurostomella brevis*	*Pleurostomella frons*	*Pleurostomella subnodosa*	*Pleurostomellaacuminata*	*Pleurostomella alternans*	*Pleurostomella recens*	*Pleurostomella* sp.2	*Pleurostomella* sp.4	*Pleurostomella* sp.6	*Procerolagena gracilis*	*Pullenia bulloides*	*Pullenia quinqueloba*	*Pullenia* sp.1	*Pullenia* sp.2	*Pullenia subcarinata*	*Pyrgo murhina*	*Quinqueloculina* sp.2	*Quinqueloculina* sp.3
13.32													1										1				1	1	
18.30	11	3											1	1	7	1					3	5	6			2			
19.85	4	1													2						1	1	1			2		1	
22.78	1	1																											
24.42	5	1														1					3	11	2						
28.00	9	4		6									1		6	1					1	1				3		1	
29.61	7	4											2		1	2					1	7	2			1			
33.94	8											1	2		9					1	1	5	3			1			
37.45	3	3										3	2		13	2					3	2	2						
38.95	6														6			1			4	12	1			3			
40.30										1																			
41.99	7	1		11											3						1	17	3						
47.10	7	1		4								1	1		9	1					4	22	3						
50.16		5													8	1				1	3	13	4		1	2			
53.03	1	3		2								1	3		11						3	14	4			2			
54.33	1											1			1	1					1								
56.73	3	3		2			1		5				1		29	2				5	1	13	3			1			
58.33	4	9	1				1		25	3		2	1		7		2	1			3	21	8	2	1	10			
61.30	3	2		6					2	2			4		5	1			1		3	8				6			
64.13				1			1																						3
66.80		7		9					13			1			8	3		1				5	4			3			
69.80	1	3		12					1						8	4		3			3	6	1						
74.00		2		5			1		15	1					4	1					1	4	6			3			
77.94		5		7					5	5					3						2	6	2						
80.71	2	1		1					4						6	2						8	4			2			
82.05	5	15		5					7	4												11	10			1			
87.10	8			2					5	4		2			2						5	7	5						
88.95	5	1		2		1			4	1	1				4			1			1	21	12			2			
91.77	1	5		3	1			1			2	1			1							9	8			7			
93.03		2																				4	1						

Appendix A (continued)

Depth (mbsf)	*Quinqueloculina venusta*	*Rectuvigerina multicostata opima*	*Rectuvigerina striata*	*Saracenaria altifrons*	*Saracenaria arcuata*	*Saracenaria schencki*	*Siphonodosaria lepidula*	*Textularia catenata*	*Sphaeroidina bulloides*	*Spiroloculina depressa*	*Stainforthia complanata*	*Stilostomella bradyi*	*Stilostomella* cf. *S. annulifera*	*Stilostomella modesta*	*Stilostomella* sp.1	*Stilostomella* sp.3	*Stilostomella* sp.5	*Stilostomella* sp.7	*Stilostomella* sp.8	*Siphonodosaria subspinosa*	*Strictocostella matanzana*	*Strictocostella scharbergana*	*Textularia* sp.3	*Textularia* sp.4
13.32											1	1	2							3	1			
18.30							27		1	1	2			5								11		2
19.85	1	1					3		1		3			2						1	4	24		
22.78									1		3									1		3		
24.42							14			5										18	10	18		
28.00							3			2				4					1	18		64		
29.61							4		1											22	3	11	3	
33.94	1						4							3						16	1	25		1
37.45			1											2						9		104		
38.95		1								3				1						8		7		4
40.30														1						1				
41.99		2					1	1	1	1				5						8		21		2
47.10							3	2						1			1	1		86				
50.16		1					1		1					1						16		1		
53.03	1	2		1					1					1						12	16	15		
54.33								2	1											4	1			
56.73	1						18		2					1						1	7	20	1	
58.33		1	5			1	49	3	5					2						25		13	3	
61.30	4		2				24							4						59		9		
64.13							6						1							18				
66.80			9	2	1		31	8	6					2						52		70	2	
69.80			4	2			20		2					9						38		9	1	
74.00			12	1			36		1					3		2				58		6		
77.94			8	5			3	1	4					1						24		1		
80.71	1			3			6		4					9						1		23		
82.05	2				1	2	42	1						1						1		20		
87.10	1		1				27		2					4						5		29		
88.95	3		2				59	1	1					8	1	1				10		21		
91.77				2	3		21		14					1								13		
93.03	1			1			9		1				1	1						1	1	10		

Appendix A (continued)

Depth (mbsf)	*Textularia* sp.5	*Textularia tatumi*	*Trifarina angulosa*	*Trifarina bradyi*	*Trifarina* sp.1	*Trochammina* sp.?	*Undefined (agglutinated) sp.2*	*Undefined (agglutinated) sp.1*	Unknown sp.1	*Uvigerina auberiana*	*Uvigerina hispidocostata*	*Uvigerina peregrina*	*Siphouvigerina hispida*	*Uvigerina* sp.1	*Uvigerina* sp.4	*Uvigerina* sp.5	*Uvigerina* sp.7	*Uvigerina* sp.9	*Uvigerina* sp.10	*Uvigerina* sp.12	*Uvigerina* sp.13	*Uvigerina* sp.14	*Valvulina pennatula*	*Valvulina spinosa*
13.32										3	1													
18.30	4		2							4														
19.85			34			6				5														
22.78			8			1				1														
24.42		2	2			27			1	12											3	1		
28.00			88			1				8										2				
29.61			115			1			1	17			3											
33.94			2						3	3										2				
37.45			6			1				37						5				3				
38.95			5							7														
40.30			3							5														
41.99		1	23							8														1
47.10			68			2							1											2
50.16			21		1					9			3						1					1
53.03			15	1						9			2						3					
54.33																								
56.73		3		35				3		11									2				2	
58.33		6	17	8						7			3						2					3
61.30				2						16		8						1						
64.13										7	1			2										
66.80		14		5				7		13													2	2
69.80		2		17		1	1	2		23		2						2		1				1
74.00		6		25				6		2		3						4					1	
77.94		2				1		7			2	1											1	5
80.71		1						2		3		5					1							
82.05		3					2	6		3	7	2											1	
87.10										2	7					1								2
88.95		3								2	13	5			1									
91.77		1						1			5	1												2
93.03		1	1												1									

Appendix B: Benthic foraminifera species checklist at ODP Site 1168 Hole A.

1168A (core, section, Interval (cm))	Age (Ma)	Depth (mbsf)	*Abditodentrix pseudothalmanni*	*Ammobaculites agglutinans*	*Amphicoryna scalaris*	*Amphicoryna* sp.1	*Anomalinoides alazanensis*	*Anomalinoides* sp.1	*Anomalinoides* sp.1?	*Anomalinoides* sp.2	*Anomalinoides* sp.5	*Anomalinoides* sp.6	*Anomalinoides* sp.6?	*Anomalinoides* sp.9	*Anomalinoides* sp.10	*Anomalinoides* sp.11	*Anomalinoides* sp.12	*Astacolus crepidulus*	*Astrononion pusillum*	*Astrononion umbilicatulum*
8H-1 , 100-104	Early Pliocene	65.30	39		1				6											
9H-3 , 51-55		77.31	66						11											4
10H-2 , 80-84	Late Miocene	85.60	32			1														5
11H-5 , 90-94		99.70	19						1											6
12H-1 , 75-79		103.05	17																	5
13X-1 , 40-44		112.20	28						3		1									2
14X-4 , 45-49		123.45	21						2											2
15X-2 , 76-80		130.36	28					3	10											7
16X-2 , 100-104		140.20	19																	2
17X-3 , 100-104		151.30	6			1			2						1					6
18X-5 , 80-84		163.70	43						2											2
19X-4 , 70-74		171.70	26							1										3
20X-3 , 100-104		180.10	10						9											
21X-1 , 100-104		186.70	7						5									2		11
22X-2 , 45-49		197.35	19							1										7
23X-3 , 74-78	Mid-Miocene	208.74	12																	2
24X-6 , 57-61		222.67	24	1			1											1		7
25X-2 , 41-45		226.11	3																	4
25X-5, 44-48		230.64																		6
26X-2 , 73-77		236.03	2																2	6
26X-6, 75-79		242.05																		1
27X-4 , 73-77		248.63							1							2		1		8
28X-3 , 75-79		256.67	2															2		10
29X-2 , 96-100		265.06	1																	1
30X-3 , 85.5-89.5	Early Miocene	276.06												2	1				4	
31X-5 , 86-90		288.66			1	1														3
32X-4 , 80-84		296.70	5	1																
33X-3 , 90-94		304.60	4		2													2		
34X-1 , 95-99		310.95																		
35X-1 , 65-69		320.25							1	1							1		7	
36X-6 , 62.5-66.5		337.33	2									1	2							2
37X-6 , 75-79		347.05	2								1	1								
38X-3 , 60-64		352.00	3									4						1		
39X-4 , 105-109		363.55	7						1											
40X-2 , 89-93		369.99	3					4										1		1
41X-5 , 67-71		383.97	8																3	
42X-3 , 70-74		390.60	2	2				1												3
45X-6, 52-56		423.72	1																	6
47X-6, 45-49		442.85																		2
49X-3, 52-56	Late Oligocene	457.62	4																	5
50X5, 52-56		470.22	1																	
52X-4, 70-74		488.10	2																	4

Appendix B (continued)

Depth (mbsf)	*Astrononion* sp.B	*Astrononion* sp.C	*Astrononion* sp.D	*Bathysiphon* sp.B	*Bolivina albatrossi*	*Bolivina compacta*	*Bolivina decussata*	*Bolivina dilatata*	*Bolivina huneri*	*Bolivina reticulata*	*Bolivina striatula*	*Bolivina* sp.1?	*Bolivina* sp.2	*Bolivina* sp.3	*Bolivina* sp.3?	*Bolivina* sp.8	*Bolivina* sp.9	*Bolivina* sp.13	*Bolivina* sp.14	*Bolivina* sp.15	*Bolivina* sp.17	*Bolivina* sp.19	*Bolivina* sp.20	*Bolivina* sp.21	*Bolivina* sp.22	*Bolivina* sp.23	*Bolivina* sp.25	*Bolivina* sp.26
65.30	1							8			1			2						1								
77.31		7		1				21		1	31						2											
85.60			1					7			8																	
99.70			1	1				6			1			1						1								
103.05											1																	
112.20	8					1		6	3		2																1	
123.45	2		2					1			4																	
130.36					1					6																		
140.20								1		1	3																	
151.30								5	4	3				1	1											1		
163.70														9														
171.70	1	1			1			20		2	1			1														
180.10						3		1	2	1				14												1		
186.70					2			31			5			1						1								
197.35											1			16						1								
208.74			1					2		1	1			18			2											
222.67														18					3	1								
226.11	3				3			33			2																	
230.64					3			3						5			3											
236.03			1					1	1					5														
242.05		1												2														
248.63	2	1			1					9				2						1								
256.67					1					2	7																	
265.06								2		1																		
276.06						2			3	7																		
288.66								10	7																			
296.70				1	1	1				1							2											
304.60	4	1						1		3	4		6	2														
310.95	1	7						3	3	1				1														1
320.25								17			6																	
337.33	2	8			1			10				1						1							1			
347.05					1	1		20		1				48		1												
352.00				1	2			40		1										1				1				
363.55					2	2		67				5									1		1					
369.99								24		3			1															
383.97	1						1	21		1		6	2	1							2	1						
390.60				1	13			30					1	3														
423.72		3	2		4	20				6			1							2								
442.85		3				9		9						2		1			1									
457.62	1		2	2				9					1	2														
470.22								4																				
488.10						14		1									1											

Appendix B (continued)

Depth (mbsf)	*Bolivina* sp.27	*Bolivina* sp.28	*Bolivina* sp.30	*Bolivina* sp.31	*Bolivina* sp.32	*Bolivinellina pseudopunctata*	*Bolivinopsis cubensis*	*Bulimina truncana*	*Bulimina* cf. *B.elongata*	*Bulimina falconensis*	*Bulimina marginata*	*Bulimina striata*	*Bulimina* sp.?	*Bulimina* sp.4	*Bulimina* sp.5	*Bulimina* sp.7	*Bulimina* sp.8	*Bulimina* sp.9	*Burseolina pacifica*	*Burseolina* cf. *Pacifica*	*Cancris* sp.A	*Cassidulina* sp.4	*Cassidulinoides bradyi*	*Cibicides* sp.1	*Cibicides* sp.4	*Cibicides* sp.5	*Cibicides* sp.7	*Cibicides* sp.11	*Cibicidoides bradyi*
65.30						3		3												3			3						5
77.31						5		6															6						7
85.60						10		5												1									8
99.70						6																							10
103.05						2		3														1	2						2
112.20			1			16		7			2									7			3						8
123.45						4	1					1											4						6
130.36						3		4			2	2											1				1		
140.20						5		1				1											6				1		5
151.30								1				1								2			1						2
163.70								5			1												2						2
171.70			1					3									1												7
180.10								5			1		1			1				1	1								7
186.70		1				1		2				3								3	3		4				2		
197.35					1			5															6						1
208.74								6				1																	2
222.67								5																					1
226.11								2												1			5	1					5
230.64								2																					1
236.03								2												4									12
242.05																													7
248.63								8			1																		8
256.67			2					7				2										2							13
265.06								4				1																	8
276.06											2	2		1					5	3				2		1	7		5
288.66							1	5	7								1			1			3				1		31
296.70								10	8	3	1	6												1			6	1	13
304.60	3							13	12	1		1												2					10
310.95								6		2					1														17
320.25								1	5	3					1			1							1		2		29
337.33								7		4	2	2					1								1		1		9
347.05								7	7	4	3																2		4
352.00			1				2	2	10	5	1						2					1		1	1		18		3
363.55									3	8												1					18		17
369.99							11	5	9		1	1					2							3			1		12
383.97								6	29								2												3
390.60							6	9	20			1											2	2			11		
423.72										1														1			4		2
442.85		2																						1					1
457.62	1						1		14	4		1					1		2								5		3
470.22									12	1	1	2					2												
488.10				2					5	5							4										3		

Appendix B (continued)

Depth (mbsf)	*Cibicidoides crebbsi*	*Cibicidoides eocaenus?*	*Cibicidoides mundulus*	*Cibicidoides pachyderma*	*Cibicidoides pseudoungeriana*	*Cibicidoides robertsoniana*	*Cibicidoides wuellerstorfi* (coarse)	*Cibicidoides wuellerstorfi?*	*Cibicidoides wuellerstorfi* (smooth)	*Cibicidoides* sp.1	*Cibicidoides* sp.3	*Cibicidoides* sp.6	*Cibicidoides* sp.7	*Cibicidoides* sp.9	*Cibicidoides* sp.13	*Cibicidoides* sp.16	*Cibicidoides* sp.17	*Cibicidoides* sp.18	*Cibicidoides* sp.19	*Cibicidoides* sp.20	*Cibicidoides* sp.21	*Cibicidoides* sp.22	*Cibicidoides* sp.23	*Cibicidoides* sp.24	*Cibicidoides* sp.25	*Cibicidoides* sp.26	*Dentalina filiformis*	*Dentalina* sp.1	*Dentalina* sp.13
65.30			1	3			1		1	1						4										3			
77.31			1	3			19			3																		1	
85.60			3						6										1										
99.70				5			1			4		2																	
103.05	2		4	5			8		1	4															1	1			
112.20			6	3			1		1			5											2					1	
123.45				4	1	1	5			1		4																	
130.36	1				4		11		3	3																1			
140.20				5			3																					1	
151.30	1		1	5			2					4				2			3										
163.70			7	2			3			2				1	3														
171.70			10	4			3		1			3																	
180.10			1				3			2		3							3					3					
186.70			4	11					2	1																4			
197.35	1		7		2		1			4			3		4														
208.74				2	5	1	6		1	1																			
222.67	1	1	2		1		2					3	4		12														
226.11		1	2	4			5			3		2				2		1				1							1
230.64			8				4																						
236.03			3	2		1			2	2										3		2			3		1		
242.05		3	2			1			1	2		2																	
248.63			5	1	4		3		1	4								1				1							
256.67			9						2	2																			1
265.06			3			1		3	2							1			2			2							
276.06			5	2			1			1												12						2	
288.66	1		6			2	2			1	1	5										3							
296.70	1		19						5			1													1				
304.60			6	4		2	10		2			1					2												
310.95			4						3			6										5							
320.25												2						1	4	1		10	7			1			
337.33	1		4		3	1						6	3						4	19	1								
347.05	4		8						4	3	1																		
352.00			5				6						1					3	1							2			
363.55			13	1		2	9												7							2			
369.99			21				2	3								1			20										
383.97	3						2					6	3				4	4										1	
390.60			2						6	5																			
423.72			10	1					9			1							2										
442.85			8						4	2																4			
457.62				5						2			1					2			1					2			
470.22			1	1								4							2							1			
488.10																		5	2								1		

Appendix B (continued)

Depth (mbsf)	*Dentalina* sp.15	*Dentalina* sp.17	*Dentalina* sp.18	*Dentalina* sp.19	*Dentalina* sp.20	*Discorbinella deflata*	*Discorbinella* sp.?	*Discorbis* sp.A	*Dorothia brevis*	*Eggerella bradyi*	*Ehrenbergina carinata*	*Ehrenbergina* sp.1	*Ehrenbergina* sp.2	*Ellipsoidina ellipsoides*	*Elphidium* sp.	*Epistominella exigua*	*Eubuliminella exilis*	*Favulina hexagona*	*Fissurina laevigata*	*Fissurina marginata*	*Fissurina* sp.1	*Fissurina* sp.1?	*Fissurina* sp.2?	*Fissurina* sp.4	*Fissurina* sp.5	*Fissurina* sp.8	*Fissurina* sp.12	*Fissurina* sp.13	*Fissurina* sp.13?
65.30										1			1			20	10			2						1	5		
77.31						1										29	4				2								
85.60										3						14	3		1					1				2	
99.70									1	3			3			41			1									1	
103.05												6				10	8			1				1				3	
112.20						1				4	1					20	15			1									1
123.45										2	2					30	12		1		1								
130.36										1		7				12	20		2		2					2	1		
140.20										3		2		1		13	64							1					
151.30			1							1						32	48		1		2								
163.70		1								5						12	44		1			4			1			1	1
171.70						1			1	2						13	20		1	1									
180.10										1		1			1	10	74				1			2					
186.70					1		1			5						6	42				1								
197.35	1	1								6						18	17	1	1	1	2								
208.74												2				12	67		1		1								
222.67										6						5	82				2					1			
226.11				1		1				3						26	47				1			1					1
230.64										2						5	19									1			
236.03										1					3	10	24				1	2	1				1		
242.05										1						9	8												
248.63									1	4						16	28				1			1		1			
256.67										2						9	31			1	1			1					
265.06										2		2			1	15	19				2								1
276.06						1				1					4	14	14		1										
288.66										5						37													
296.70										1						43													2
304.60							1			3	1					30			3		3								
310.95								2								110				1	2								
320.25									2	6						43													
337.33										1						97	2												
347.05																49												1	
352.00										3						13				1									
363.55										2						12													
369.99										3					1	14		1						1					1
383.97										2	1				4	40				1	3								
390.60										5						50				1	1								
423.72																10		1	3		3								
442.85																20					3								
457.62			1				1									26										2			
470.22										2						24													
488.10										1						18													

Appendix B (continued)

Depth (mbsf)	*Fissurina* sp.19	*Fissurina* sp.20	*Fissurina* sp.21	*Fissurina* sp.22	*Fissurina* sp.23	*Fissurina* sp.24	*Fissurina* sp.25	*Fissurina* sp.26	*Fissurina* sp.27	*Fissurina* sp.28	*Fissurina* sp.29	*Fissurina* sp.30	*Fissurina* sp.31	*Fissurina* sp.32	*Fissurina* sp.33	*Fissurina* sp.34	*Fissurina* sp.35	*Fissurina* sp.36	*Fissurina* sp.39	*Fissurina* sp.41	*Fissurina* sp.43	*Fissurina* sp.44	*Fissurina* sp.45	*Fissurina* sp.46	*Fissurina* sp.47	*Fissurina* sp.48	*Fissurina* sp.49	*Fissurina* sp.50	*Fissurina* sp.52
65.30		1	1																										
77.31																													
85.60						1																							
99.70																													
103.05	1																								1				
112.20				1		1	2	1	1	1										1						1			
123.45																	1	1								1			
130.36																								1		1			
140.20																										2			
151.30																													
163.70																													
171.70																													
180.10					1																								
186.70				1											1	1													
197.35																													
208.74																						2							
222.67																					1		1	1					
226.11																										1			
230.64									1																				
236.03																			2										
242.05																													
248.63																					1								
256.67																					2	1					1		
265.06					1					1				1							1								
276.06																													
288.66																										1			
296.70																													
304.60												2	1								1								
310.95											1												1						
320.25																													
337.33				1																								1	
347.05																													
352.00																													
363.55																													
369.99																													
383.97																													
390.60																				1									
423.72																				5						1			
442.85																	1					1							1
457.62																													
470.22																													
488.10																													

Appendix B (continued)

Depth (mbsf)	*Floresina* sp.1	*Fursenkoina* sp.B	*Fursenkoina* sp.D	*Fursenkoina* sp.E	*Fursenkoina texturata*	*Glandulina leavigata*	*Globocassidulina minuta*	*Globocassidulina subglobosa*	*Globocassidulina* sp.2	*Globulina gibba*	*Glomospira charoides*	*Guttulina austriacea*	*Gyroidinoides soldanii*	*Gyrodinoides* sp.1	*Gyrodinoides* sp.2	*Gyrodinoides* sp.4	*Gyroidinoides* sp.5	*Hanzawaia* sp.A	*Hanzawaia* sp.B	*Hanzawaia* sp.C	*Hanzawaia* sp.D	*Heronallenia lingulata*	*Heronallenia pulvinulinoides*	*Heronallenia* sp.B	*Karreriella bradyi*	*Lagena* cf. *L. striata*	*Lagena spiralis*	*Lagena* sp.?	*Lagena* sp.3
65.30					2		6	13					7	3	2														
77.31				5	6		6	18					7	7															
85.60				1	1		3	22					7	2											2	1			
99.70					4		4	21					7	10						3									
103.05					2		2	24					9		10							2							
112.20	1				9		18	31				1	13	4	11														1
123.45					14			48					8	5	1										1				
130.36				1	7		7	42					8	5	12														
140.20					27		2	18				2	5	3											1	1			
151.30							6	29					5	1										2					
163.70			2		3	1	1	16					6	2	1										7				
171.70								26				1	7	7		3						2							
180.10		1						23				1	6	4											2				
186.70					1		2	29					6	4		2		1	1				1	1	3				
197.35					1		5	33				2	4		3			1											1
208.74					2		1	10					3	8								1							
222.67				1	1		6	27				1	7	1	4				1			1		2	5				
226.11					1		1	24					6	1								1	1	2	1				
230.64				1			1	16					7	1	3									1					
236.03							2	28					6	6						2									
242.05						1		16							4								2						
248.63								59					15	14			1					2				1			
256.67							7	39				2	8		7							1							
265.06					15			43					8	13								1		1	1				
276.06				3	1		6	18	1			1	12	3						1		1				1			
288.66					9			27	1				5	5	2			1				2							
296.70					1		7	26	1			1	7	4	25										2				
304.60							13	25		1			14	5							1	2		1		1			1
310.95							16	25					7		11		2					1		2					
320.25							4	15					7	3								1			2				
337.33							5	24			2				5		2					2		1	1				
347.05								37					5		6							1							
352.00							5	37					1		3							2		1				1	
363.55							2	50					7		3							2			2				
369.99							4	20					10																
383.97							3	25					3																
390.60							4	25				1	3		7							4							
423.72					1		4	28							5			6			3		2			1	1		
442.85							3	19				1	2		1						1	1		1					
457.62					1		2	5					1		2							1	2						
470.22								6						1	2														
488.10							9	13							7			1				1		1					

Appendix B (continued)

Depth (mbsf)	*Lagena* sp.4	*Lagena* sp.11	*Lagena* sp.13	*Lagena* sp.21	*Lagena* sp.22	*Lagena* sp.23	*Lagena* sp.24	*Lagena* sp.25	*Lagena* sp.26	*Laminononion tumidum*	*Laticarinina pauperata*	*Lenticulina calcar*	*Lenticulina convergens*	*Lenticulina gibba*	*Lenticulina limbosus*	*Martinotella scabra*	*Melonis barleeanus*	*Melonis* sp.2	*Melonis* sp.?	*Nodosaria franki*	*Nodosaria* sp.2?	*Nodosaria* sp.7	*Nodosaria* sp.8	*Nodosaria* sp.10	*Nodosaria* sp.11	*Nodosaria* sp.16	*Nodosaria* sp.17	*Nodosaria* sp.21	*Nodosaria* sp.22
65.30		5								1				1			3		1		1							1	
77.31		4												1			4					1			2				
85.60		1								3				1			4												
99.70																	1					1							
103.05	1	3		1						5	1						6								1			1	
112.20	1													1			15												
123.45		3									1			2			10												
130.36				1						1				2											2			1	
140.20	1																												
151.30		2									1					1	3												
163.70		1	2							1							2												
171.70														3			4												
180.10			1						2				1			1	3												
186.70		1							1		1						3												2
197.35		2		1							1			1			1					1							
208.74		1			1						1						3								1			1	
222.67		3								4	1						3												
226.11											1						5												
230.64	1										1			1				5					1						
236.03								1		1	1			2		1													
242.05											1			2			2											1	
248.63	1													1			3												
256.67	1	1									1			3											1				
265.06								1			1			4	1		1										1	1	
276.06														3			3										1		
288.66														2		2	4												
296.70														1			1	2						1		1			
304.60														5	2		4												
310.95	1																2												
320.25					2						2						5												
337.33		1												1			3												
347.05											1			1			4						1						
352.00							1										8						1					2	
363.55						1					1				1		5								1				
369.99														2	3		2					1	1						
383.97		1										1					1												
390.60		2															2												
423.72		1								1				1			11											1	
442.85		1			1									1			5											2	
457.62		1																									1		
470.22																	7			1						11			
488.10	1													3															

Appendix B (continued)

Depth (mbsf)	*Nodosaria* sp.26	*Nodosaria* sp.27	*Nodosaria* sp.28	*Nodosaria* sp.29	*Nodosaria* sp.30	*Nonion commune*	*Nonion micra*	*Nonionella turgida*	Nonion sp.1?	*Nonion* sp.2	*Nonion* sp.4	*Nonionella* sp.2?	*Nonionella* sp.4	*Nonionella* sp.5	*Nonionella* sp.6	*Nonionella* sp.7	*Nuttalides umbonifera*	*Oolina* sp.2?	*Oolina* sp.4	*Oridorsalis* sp.3	*Oridorsalis* sp.4	*Oridorsalis umbonatus*	*Orthomorphina ambigua*	*Orthomorphina perversa*	*Orthomorphina jedlitschkai*	*Osangularia culter*	*Parafissurina lateralis*	*Planulina renzi*	*Planulina* sp.
65.30						2																41		2		3	1		
77.31						1											5					20				5	2		1
85.60						1																5			1		1		
99.70								1							1			1				12				1			
103.05						2				2												27				7	2		
112.20																1	46					17			2		1		
123.45																	7					19		1					
130.36																	7					6		2		4			
140.20			2			2											2					1	1	1		2			
151.30									1								4					16				1			
163.70																	80					3					2		
171.70		1															11					8		1					
180.10																	5					2	1	1			1		
186.70									1								32	2				10		1			1		1
197.35									2								10						3				1		
208.74									1								26					9					2		
222.67									2													9					2		
226.11		1															4				4	15							
230.64																	15				2	5					1		
236.03									1								46					11							
242.05								1			2						28				1	4				2			
248.63									1								8					15		2		5			
256.67							3										25	1	1			6	1			9	1		
265.06													2				5					9				7			
276.06							2										13	1				8				3			
288.66						3											4					9				2			
296.70																	1					19		1					
304.60																	15					3				8			
310.95																	5					9				1	3		
320.25																	2	1			1	8		3					
337.33							1										1			2	1	2							
347.05																	1					8							
352.00																						17	1	1					
363.55																						3							
369.99																	14					12				3			
383.97							2										2				3	13				1			
390.60	1											1					9					9		1			1		
423.72																			1			3					1	4	
442.85						1																2	1						
457.62				2										1					1			2		1			1		
470.22					1												3	1				1							
488.10		1															4					2					1		

Appendix B (continued)

Depth (mbsf)	*Planulinoides biconcavus*	*Pleurostomella subnodosa*	*Pleurostomella acuminata*	*Pleurostomella alternans*	*Pleurostomella bolivinoides*	*Pleurostomella brevis*	*Pleurostomella* sp.1	*Pleurostomella* sp.5	*Pleurostomella* sp.7	*Pleurostomella* p.8	*Pleurostomella* p.9	*Pleurostomella* p.10	*Pleurostomella* sp.11	*Paracassidulina minuta*	*Procerolagena gracilis*	*Polymorphina* sp.A	*Polymorphina* sp.B	*Hyalinonetrion gracillimum*	*Pullenia bulloides*	*Pullenia quinqueloba*	*Pullenia* cf. *P. quinqueloba*	*Pullenia quinqueloba* ?	*Pullenia subcarinata*	*Pyrgo murrhina*	*Pyrgo* sp.1	*Pyrgo* sp.2	*Pyrgo* sp.3	*Quadrimorphina laevigata*	*Quinqueloculina* sp.
65.30		1	2	3		3								3					3	3				9	1	1	1		
77.31	1		1	1										24	1				3	2			2	4					
85.60			1				1							6										2	2			1	
99.70														2					1					2					
103.05			2	4	1				1					2					2	7				4					
112.20			2	1			1							7					5	9				6		3			
123.45		1	2	4															2	3				5					
130.36			2	3	6	2									1				2	1			3		1				
140.20			1			1								2	1				2				2						
151.30			2	2						1				2						3			2						
163.70		1	3	4		1					1			1	1	3			6	7			1	1					
171.70		4	3	2			1			1				6				2	5	1			2						
180.10		1	2								2			5	1				1	3									
186.70	1	1	1			2					1			10				1	1	3				1					
197.35		1	10	1	1	2				1				7					6	2			5						
208.74			3											1	1			1		2			1						
222.67			4			5								8					5	3									
226.11	1	1	2	1		2								2				2	11			3							
230.64			2	3						1				2				1		1									1
236.03			2										1	1					3	3									
242.05														1		1			1										
248.63	1		3			4								2					5				1						
256.67			2			2		1		1	1			2			1			2			2	1					1
265.06			2			4									1				3	2			2	2					1
276.06																			3	3									
288.66	1			1						1									1	2									
296.70					2	2				1	1								2	1		1	2						
304.60			5	1		2								8		1			2	3			1						
310.95			4	3	1													2	2	1									
320.25		1	9	1										3	2			5		10	2								
337.33		2	3	1			1												1	2	1								
347.05			1		1	1	1				1	1		3				2	2				2						
352.00	1					2												1	1	1									
363.55					1						3			1						3									
369.99																			1	4			2						
383.97			2	1	1									17		1			1	6			3					1	
390.60			2	2	1									2					3	2			16						
423.72														2	1	1			1	3									
442.85			3		3									1															
457.62			6			1												1	1										
470.22			1			1												5	1										
488.10						1																	2						

Appendix B (continued)

Depth (mbsf)	*Quinqueloculina* sp.2?	*Quinqueloculina venusta*	*Rectuvigerina multicostata opima*	*Rectuvigerina striata*	*Rosalina* sp.A	*Rosalina* sp.B	*Sigmoilopsis schlumbergeri*	*Siphonia tenucarinata*	*Siphonodosaria lepidula*	*Siphouvigerina hispida*	*Sphaeroidina bulloides*	*Spiroloculina depressa*	*Spiroloculina* sp.1	*Spiroloculina* sp.2	*Stainforthia concava*	*Stilostomella abyssorum*	*Stilostomella* cf. *S. annulifera*	*Stilostomella modesta*	*Stilostomella* sp.4	*Stilostomella* sp.4?	*Stilostomella* sp.7	*Stilostomella* sp.8	*Stilostomella* sp.9	*Stilostomella* sp.13	*Stilostomella* sp.14	*Stilostomella* sp.16	*Stilostomella* sp.17	*Siphonodosaria subspinosa*	*Textularia catenata*
65.30		2							12	7	1				6		2		1									1	
77.31		18				1			14	25	2			1		2	3		1								1	1	
85.60		10					1		4	24	1				2		3							1	2				
99.70		14							1	12	3			6	2	1	2		9						1			2	
103.05		6				1	2		19	9							18		2									2	2
112.20	1	1				1			1		2			1			22		6	8					2			4	
123.45		11				1					3			2			22		4									1	
130.36									5			2					32		1				1					10	1
140.20		1									1			2			5		2						1			1	
151.30		1							1	1	2						7		4						1			4	2
163.70		5								1	1	2					10											12	2
171.70						6			3					2			3		2		1				2	1			3
180.10		1						1	2	2	2			1			3		2									1	
186.70		4				12			1					2		1	9	1	3						1			5	
197.35		3							2					1			6		5									9	
208.74						3		1	1			2		1			3								3				
222.67														1			14		5									2	1
226.11		1				1			1							1	6		1				1						
230.64		1				9		1	2			1					7	1	5									1	
236.03								1	4		10						6		1									3	
242.05						5			5			1																	
248.63						4		3	4		1						1		1									3	
256.67								2	4	7		4		1			2					1						
265.06		2	4			1			4			2						1					1						
276.06		1						1	6		3			1			7	1	1										
288.66									4		2	1				3	1											4	
296.70									4		1						2											2	
304.60				1				1	2	1	3	3				2	1		6				3					3	
310.95						1			5	2	2			1		3	2	1										2	
320.25									5			1				2			2				1						
337.33									6		5							1											1
347.05		1			1				2	4	3						4											3	
352.00									7		5	1					1							1				2	
363.55									4		3							2					2					1	
369.99									21								3												
383.97								3	9			2				1	1											1	
390.60		2							3	1	2	3	1						1									3	
423.72		2					1	2	1								3												
442.85											1								2									2	
457.62									1		1						2						1					2	1
470.22		1							1	2						3			1									3	
488.10						1		1	2		2					1			1										

Appendix B (continued)

Depth (mbsf)	*Textularia* sp.1	*Textularia* sp.3	*Textularia* sp.4	*Textularia tatumi*	*Trifarina angulosa*	*Trifarina bradyi*	*Triloculina* sp.1	*Triloculina* sp.2	*Triloculina* sp.3	Undefined sp. (agglutinated)	Unknown sp.3	*Uvigerina basicordata*	*Uvigerina laevis*	*Uvigerina peregrina*	*Uvigerina spinicostata*	*Uvigerina* sp.	*Uvigerina* sp.3	*Uvigerina* sp.6	*Uvigerina* sp.8	*Uvigerina* sp.11	*Uvigerina* sp.11?	*Uvigerina* sp.15	*Valvulina spinosa*	*Valvulineria* sp.A
65.30					8		4							31										
77.31						2	2	1						29	1		4					2		
85.60					9			1				1		23					10					
99.70					2	1								15										
103.05					11	1	1							74			2					2		
112.20		1			2						1			26			3		3					1
123.45					3	1								34				2	1					
130.36					4	4								19	3				1					
140.20	1					1								9										
151.30					1	6								4										
163.70			1										1	40	3									
171.70	1					1								7							2			
180.10					12	1								5				1						
186.70						3								3				1	1		1			
197.35					4	1	3							22					4					
208.74					4	2								25	6							3		
222.67														5										
226.11					1									6										
230.64																								1
236.03									1	1														
242.05														2										
248.63								1						4										
256.67								4			1			8								2		
265.06					2			1						16										
276.06														11					2					
288.66				2										13					3				4	
296.70	1							1			2			14								2		
304.60					4			2				1		12					2			1	1	2
310.95				1	2						1			5						2				
320.25		1				1	1							8										
337.33		1			2	1	1															3		
347.05											1			2			1							
352.00					1							1		2		1			9					
363.55							1							9		1		1						
369.99						2	1					1												
383.97					2	4								4			1							
390.60						1	1				1			1			6							
423.72											1													
442.85						2								1									1	
457.62						3								2	1							2		
470.22														1										
488.10								1						3			1							

Appendix C: Benthic foraminifera species checklist at ODP Site 1139 Hole A.

1139A (core, section, interval (cm))	Age (Ma)	Depth (mbsf)	*Abditodentrix pseudothalmanni*	*Ammodiscus* sp.	*Amphicoryna scalaris*	*Anomalinoides* sp.1?	*Anomalinoides* sp.2	*Anomalinoides* sp.3	*Anomalinoides* sp.14	*Anomalinoides* sp.15	*Astacolus crepidulus*	*Astrononion* sp.A	*Astrononion umbilicatulum*	*Bathysiphon* sp.A	*Bolivina variabilis*	*Bolivina dilatata*	*Bolivina reticulata*	*Bolivina striatula*	*Bolivina* sp.1
3R-1 , 30-34	L. Moicene	19.30	6										8				2		
3R-2 , 100-104	Mid-Miocene	21.50	12			1							9				1	2	
3R-4 , 32-36		23.82	2				8			1			15				9		
4R-1, 40-44		28.90	13			1							6				2		
4R-2 , 105-109		31.05	17										8				12		
4R-4 , 75-79	Early Miocene	33.75	5										5						
5R-1 , 121-125		39.21	9		1				4		1		67	1	2			4	
6R-1 , 71-75		48.21											6						
7R-1 , 111-115		58.11	3										1	5					
7R-3, 45-49		60.45	3			1							5						3
8R-1 , 45-49		66.95	17					1					7		4				
9R-4 , 105-109		80.39	2										11	1	2				
10R-2 , 45-49		87.45	9	1									2	1					
11R-1, 35-39		95.45	2										16	1					
12R-2 , 71-75		106.91	16										14	1					
12R-5, 90-94		111.60	17										1			3			
13R-5 , 80-84		121.20	13										25						
14R-4 , 65-69		129.15	1			3					1		9	3					
15R-2, 95-99		135.95				4							3	1		1			
15R-4 , 41-45		138.41	2			1							6	3	1				
16R-2 , 55-59		145.25	1			2							24	2	1				
17R-3 , 91-95	Late Oligocene	156.71	1			4	1						15						
18R-1 , 96-100		163.46	1			6							8		2				
19R-2, 60.5-64.5		174.21	13			1	1					1	69		14				3
20R-4, 40-44		186.60	2				1				1		1		8			18	2

Appendix C (continued)

Depth (mbsf)	*Bolivina* sp.3	*Bolivina* sp.4	*Bolivina* sp.18	*Bolivina* sp.29	*Bolivina* sp.33	*Bolivina* sp.34	*Bolivinopsis compta*	*Brizalina alata*	*Brizalina subaenariensis var. mexicana*	*Bulimina cf. B. elongata*	*Bulimina gibba*	*Bulimina marginata*	*Bulimina striata*	*Bulimina truncana*	*Bulimina* sp.1	*Bulimina* sp.2	*Bulimina* sp.7	*Bulimina* sp.8	*Bulimina* sp.9	*Bulimina tuxpamensis*	*Burseolina cf. Pacifica*	*Paracassidulina minuta*	*Cassidulina* sp.2	*Cassidulinoides bradyi*	*Cibicides* sp.8	*Cibicides* sp.9	*Cibicides sp.1*	*Cibicidoides bradyi*	*Cibicidoides cicatricosus*
19.30		2								1		1					1						4		1	1		2	
21.50	5	6		1					2	1	2	1										3				1			
23.82	1								1	1				18							15							4	2
28.90	3										1		3	3								1		1	1			6	1
31.05							2			5		1	2	1								2		1				2	
33.75	6									2			2	1									2					5	3
39.21							1		5	4	1		23	71								6	2					4	5
48.21							1			82	12		6	1						1								4	
58.11	3						1			11	19		3	4		1	1			4							1	9	
60.45			1							2	24		2	1										1				9	
66.95	3						1			14	19		4							3								12	
80.39	1									13	4		12	14		2								2				6	
87.45							2				56		1	3															
95.45	3										29		3	4							1								
106.91	1			1						6	31		1	6		1													
111.60	1							1			13																	5	
121.20		1						16			6		21	9		2													
129.15	1							3		5			7	4				1								1			
135.95	1							3					4	1											2			21	
138.41	4							7					1	9		1													
145.25	1			1						5			7						47										
156.71											82		14		1						3								
163.46	4	2								35	26		12						1			7			3				
174.21	1						2				1		9								1	9		3					
186.60	6			5	1	1				43			1															3	

Appendix C (continued)

Depth (mbsf)	*Cibicidoides crebbsi*	*Cibicidoides laurisae*	*Cibicidoides laurisae ?*	*Cibicidoides mundulus*	*Cibicidoides pachyderma*	*Cibicidoides robertsoniana*	*Cibicidoides* sp.1	*Cibicidoides* sp. 2	*Cibicidoides* sp.3	*Cibicidoides* sp.4	*Cibicidoides wuellerstorfi* (coarse)	*Cibicidoides wuellerstorfi* (smooth)	*Dentalina* sp.	*Dentalina* sp.1	*Dentalina* sp. 2	*Dentalina* sp.12	*Dentalina* sp.13	*Dentalina* sp.15	*Discorbinella deflata*	*Dorothia brevis*	*Eggerella bradyi*	*Ehrenbergina* sp.1	*Ellipsoidina ellipsoides*	*Epistominella exigua*	*Fissurina* sp.1	*Fissurina* sp.2	*Fissurina* sp.5	*Fissurina* sp.6	*Fissurina* sp.7
19.30			2	5																	1			3				1	1
21.50			4	1															2					1				1	
23.82				32			6	2	1		14	57	1				1			3					1			1	
28.90			2	1							2									2	1			41					
31.05				16				1	1		1	19									1	1	1	16					
33.75					5						1													19					1
39.21	7			51	18	5	2		3	2	2	72								7	1	5		1	1			4	
48.21				8	1		1													1	1			1					
58.11		2		28	9				3			1		1			1				5			5					
60.45				2	4											2				1	2			1					
66.95				22	1	1		2				1		1						3	2			5	1				1
80.39				16																	3								
87.45				11			1	2												3	2			11				2	1
95.45				18													2			6	6		2	1	2		1		1
106.91		1		4																				5					
111.60	5			3			1							1						2				3					
121.20				1		2								1						1					1				
129.15				9		7								1							15			3		1		2	1
135.95	9			2		1	1																	4					
138.41			1	5									2			1				1				4	1				
145.25				11														2			1			1				1	
156.71				15										1	1					1	2			1	1		1		
163.46				15																3	3			1	2				
174.21				29										1							11			1	2	1			
186.60			2	6			3																	17					

Appendix C (continued)

Depth (mbsf)	*Fissurina* sp.8	*Fissurina* sp.9?	*Fissurina* sp.12	*Fissurina* sp.37	*Fissurina* sp.38	*Fissurina* sp.39	*Fissurina sp.4*	*Fissurina* sp.41	*Fissurina* sp.42	*Fissurina* sp.49	*Fissurina* sp.51	*Frondicularia* sp.	*Fursenkoina complanata*	*Fursenkoina texturata*	*Fursenkoina* sp.A	*Fursenkoina* sp.B	*Fursenkoina* sp.C	*Gavelinopsis lobatulus*	*Glandulina* sp.?	*Globocassidulina minuta*	*Globocassidulina* sp.1	*Globocassidulina subglobosa*	*Globulina gibba*	*Glomospira charoides*	*Guttulina austriaca*	*Guttulina ovata*	*Gyrodinoides* sp.1	*Gyrodinoides* sp.2	*Gyroidinoides soldanii*
19.30									1											1	1	12					3		6
21.50					1						1							3				5							2
23.82			1				1							1	1		1		2			5	1		2		2	7	36
28.90																		4				28					3	6	4
31.05					1													2		2		4	1				1	5	4
33.75														1				7				21					4	2	5
39.21																		5			1	43			3			23	2
48.21								1													1	3			1		1	2	
58.11						1		1								1					2	2					1	6	11
60.45							1														1					1	2	5	2
66.95			1	1		1		1			2										4	1				1	5	5	12
80.39			2				1	2												1	7	3					1	2	4
87.45											1				4						4						2	2	5
95.45											2										5	1			1		4	8	7
106.91												1			1						5						11		3
111.60											1		2			1					2	2					5	4	2
121.20						4	1														2	1	1		1	1	1	5	1
129.15	1	1													3						2	21		1		2		8	8
135.95											1				1						6	4						2	3
138.41											1					1					11	2				4	1	3	3
145.25																1					5		1			1	2	2	2
156.71				1	1															2	2	9	1		2	1	5		1
163.46										1	1				5					16	7	1					6	1	8
174.21											1			1		4				8	2	14				1	6	8	14
186.60											1										2	7					6	4	6

Appendix C (continued)

Depth (mbsf)	*Heronallenia* sp.A	*Hyalinonetrion gracillimum*	*Karreriella bradyi*	*Lagena gibbera*	*Lagena alticostata*	*Lagena* sp.4	*Lagena* sp.6	*Lagena* sp.9	*Lagena* sp.11	*Lagena* sp.12?	*Lagena* sp.14	*Lagena* sp.16	*Lagena* sp.22	*Laminononion tumidum*	*Laticarinina pauperata*	*Lenticulina convergens*	*Lenticulina gibba*	*Lenticulina cultrata*	*Lenticulina* sp.1	*Lenticulina* sp.2	*Lenticulina* sp.3	*Lenticulina* sp.4	*Martinotella communis*	*Martinotella scabra*	*Martinotella* sp.	*Melonis barleeanus*	*Melonis* sp.1	*Melonis* sp.2	*Melonis* sp.3
19.30					2	1			2					2			1					1						1	
21.50		1																								2			
23.82									1						1									6		9			
28.90					1																								
31.05									2				1		1	1										6			
33.75		1	1															1								1			
39.21		2	1			1			2		3	2			1	1	3	3		1	1		4			1		16	
48.21		1	1												1			1										1	
58.11	1	1						1			2				2		2		1							5		1	
60.45						2		1																				2	
66.95								2							1	1										1			
80.39		2	1														1									2			
87.45		2					1	2									1									3			
95.45													1		2		1							1		9		1	
106.91	1		1																				2						
111.60	1	1													1								3			2		1	
121.20		9						1	1								2									1			1
129.15		4	4					3			1			1			4						1			2			
135.95		2						1					1													2			
138.41		7	1		1	1		2									1									4			
145.25		1															1						3		1	9			
156.71		6		1		1		1	1			2					3						2			4			
163.46															3		2		1							1		3	
174.21	1		2					2			1				1		2									6	1		
186.60						1			1	1																1			

Appendix C (continued)

Depth (mbsf)	*Melonis* sp.4	*Nodosaria* sp.1	*Nodosaria* sp.2?	*Nodosaria* sp.4	*Nodosaria* sp.8	*Nodosaria* sp.12	*Nodosaria* sp.13	*Nodosaria* sp.14	*Nodosaria* sp.15	*Nodosaria* sp.17	*Nodosaria* sp.19	*Nodosaria sp.2*	*Nodosaria* sp.21	*Nodosaria* sp.23	*Nodosaria* sp.24	*Nodosaria* sp.25	*Nodosaria* sp.27	*Nonion micra*	*Nonion* sp.1	*Nonion* sp.1?	*Nonion* sp.3	*Nonionella turgida*	*Nonionella basiloba*	*Nonionella* sp.1	*Nonionella* sp.3	*Nonionella* sp.2	*Nuttalides umbonifera*	*Oolina* sp.3	*Oolina* sp.4
19.30																			2								1		
21.50										1																	1		
23.82							1						1	2													61		
28.90																								1			2		
31.05																				1							5		
33.75																								1			2		
39.21					1		2	1	1		1	1			2			5									9		
48.21																											1		
58.11							1													7							7	1	
60.45																			1	1					1		1		
66.95																			1					1			2		
80.39							3									2			2					1			1		
87.45															1		1							1			1		
95.45							2																				2		
106.91							1																				1		
111.60																			2										
121.20	2																				1		1					1	
129.15						1													5				2				4		
135.95						1								1					1								2		
138.41		1																	1			4	3				2		
145.25				1				1											1										
156.71							2											1			3		3	2				6	
163.46																											2		2
174.21		3	2																2	1						2			
186.60						1						1						1						1			2		

Appendix C (continued)

Depth (mbsf)	*Oridorsalis* sp.1	*Oridorsalis* sp.2	*Oridorsalis umbonatus*	*Orthomorphina ambigua*	*Orthomorphina perversa*	*Orthomorphina jedlitschkai*	*Orthomorphina* sp.	*Osangularia culter*	*Planulina karsteni* ?	*Planulina renzi*	*Pleurostomella subnodosa*	*Pleurostomella acuminata*	*Pleurostomella alternans*	*Pleurostomella brevis*	*Pleurostomella incrassata*	*Pleurostomella tenuis*	*Pleurostomella* sp.3	*Polymorphina* sp.A	*Proxiforns badenensis*	*Pullenia bulloides*	*Pullenia quinqueloba*	*Pyrgo fornasinii*	*Quadrimorphina leavigata*	*Quinqueloculina* sp.?	*Quinqueloculina* sp.1	*Quinqueloculina* sp.1?	*Quinqueloculina venusta*	*Rectuvigerina multicostata opima*	*Recurvoides* sp.?
19.30			7					1				2								3				2	4				
21.50			6		1				7			1		1		1									6				
23.82			3		2			1	2		1	5	1	2		8				6	8						1	6	
28.90			7		1			5				1				1				2	2								
31.05			2					9				5	1			2				4	3								
33.75			3					2				2									1				3				
39.21			2		5			16	33			16	4	3						28	9		1					21	
48.21			2									1		1						2	1		2						
58.11			21		5			11				13		1			1			4	6	1					1		
60.45			1					1												1	2				1				
66.95			32		1			42				8	2		1					3	8				1				
80.39			12		1			1				6		1						2			1						
87.45			7		2			1						2	1			2		1	2		8						
95.45			7	1	2			8				8		2	1					7									
106.91			24		1			2				3								1			1						
111.60		1	6		2							3		1							1								
121.20			5		2							7		3				2		1	2		2				2		
129.15			25		1			8				5	1	4			2				1		1			2			
135.95			4					5				2									2		1						
138.41			7					3					1	5	1				1		5		2						
145.25			8			1	1	2				4	2	2						4	1		1						1
156.71	16		4									1	1							4	8		2						
163.46			5					14		1		1	1				2			2	4								
174.21			2		5			11				6					1				1		2						
186.60			4					1				4	1							2	1								

Appendix C (continued)

Depth (mbsf)	*Saracenaria altifrons*	*Textularia catenata*	*Siphouvigerina hispida*	*Sphaeroidina bulloides*	*Spiroloculina depressa*	*Stainforthia concava*	*Stilostomella cf. S. annulifera*	*Siphonodosaria lepidula*	*Stilostomella modesta*	*Stilostomella modesta?*	*Stilostomella sp.2*	*Stilostomella sp.6*	*Stilostomella sp.1*	*Stilostomella sp.11*	*Stilostomella sp.12*	*Siphonodosaria subspinosa*	*Strictocostella matanzana*	*Textularia sp.1*	*Textularia sp.2*	*Textularia tatumi*	*Trifarina angulosa*	*Trifarina bradyi*	*Triloculina sp.1*	*Unknown sp.2*	*Unknown sp.3*	*Unknown* sp.4 (agglutinated)	*Uvigerina basicordata*	*Uvigerina peregrina*	*Uvigerina sp.2*	*Uvigerina sp.3*	*Uvigerina sp.16*	*Valvulineria californica*	*Valvulineria sp.*
19.30			1			1	12	6								1	1				8										2	
21.50							6	8								1	11				5											
23.82			17	1	3		11	13	3			1			3		6					4						19			1		3
28.90					1		2	4									2				15			2				2	7				1
31.05		1	2	1	2		19	5	3							3	17				22	2								23			1
33.75			3	2			4															3					3					
39.21	2		74	9	3		41	29	8							13	7		1			13			1			26		3			
48.21			4	15			2	39									64										3	6					
58.11		1	45	13	1		13	36								22	2	1		1					2	1		2		6			
60.45			6	2			5	9								1	5							2				1					
66.95			17	44	2		5	24																	2		2	13		1			
80.39			5	11			22	14		1			3			1	38					1	2		2	1	1	15		3			
87.45			2	12			36	6						1		3	5					1			2			11					
95.45		2		22	2		43	46			3					1	26					1			1		7	63					
106.91			2	7			18	12								1	3										6	86					
111.60				4			9	5																1		1	1	3				5	
121.20				11			11	29		1							4						1				2	6					
129.15			1	1			12	25		1						2	31						1			8		5	1	1			
135.95				1			3	7									1										1	5				6	
138.41				4			83	21		1						9	18						1	1			2					1	
145.25			3	6			16	11								2	2									2		15	1	1			
156.71				1			39	18								3	13						1				1	29		1			
163.46			1	8			16									6	25							3				8					
174.21			5	3	3		18	2								3	28					3	4	11			6	2		2			
186.60			1	5			1	2								1	6							8		1		2			2		1

Appendix D: The most abundance species of each clusters at the studied Sites 752A, 1168A and 1139A.

Clusters	ODP Holes		
	752A	**1168A**	**1139A**
A	*Bolivina* cf. *reticulata*, *Globocassidulina subglobosa*, *Bolivinellina* cf. *B. translucens*, *Oridorsalis umbonatus*, *Cibicidoides wuellerstorfi* (smooth) and *Ehrenbergina carinata*.	*Abdetodentrix peudothalmanni*, *Astrononion umbilicatulum*, *Bolivina dilatata*, *Epistominella exigua*, *Globocassidulina subglobosa*, *Oridorsalis umbonatus*, *Uvigerina peregrina*, *Melonis barleeanus*, *Siphouvigerina hispida*, *Stilostomella* cf. *S. annulifera* and *Eubuliminella exilis*	*Abdetodentrix peudothalmanni*, *Astrononion umbilicatulum*, *Epistominella exigua*, *Globocassidulina subglobosa*, *Oridorsalis umbonatus*, *Stilostomella* cf. *S. annulifera* and *Trifarina angulosa*.
B	*Bolivina* cf. *reticulata*, *Globocassidulina subglobosa*, *Strictocostella scharbergana*, *Siphonodosaria subspinosa*, *Bolivina viennensis*, *Cibicidoides mundulus*, *Oridorsalis umbonatus*, *Abdetodentrix peudothalmanni*, *Trifarina angulosa*, *Cibicidoides wuellerstorfi* (smooth) and *Uvigerina auberiana*.	*Abdetodentrix peudothalmanni*, *Astrononion umbilicatulum*, *Bolivina dilatata*, *Epistominella exigua*, *Globocassidulina subglobosa*, *Nuttalides umbonifera*, *Oridorsalis umbonatus*, *Uvigerina peregrina*, *Bolivina* sp.3, *Stilostomella* cf. *S. annulifera* and *Eubuliminella exilis*.	*Abdetodentrix peudothalmanni*, *Astrononion umbilicatulum*, *Epistominella exigua*, *Globocassidulina subglobosa*, *Cibicidoides mundulus*, *Stilostomella* cf. *S. annulifera*, *Strictocostella matanzana*, *Osangularia culter*, *Bulimina truncana*, *Cibicidoides wuellerstorfi* (smooth and coarse types), *Gavelinopsis lobatulus*, *Bolivina reticulata* and *Trifarina angulosa*.
C	*Bolivina* cf. *B. reticulata*, *Globocassidulina subglobosa*, *Strictocostella scharbergana*, *Siphonodosaria subspinosa*, *Bolivina viennensis*, *Cibicidoides mundulus*, *Burseolina* cf. *pacifica*, *Abdetodentrix peudothalmanni*, *Trifarina angulosa*, *Pullenia bulloides*, *Cibicidoides wuellerstorfi* (coarse), *Uvigerina auberiana*, and *Burseolina pacifica*.	*Astrononion umbilicatulum*, *Epistominella exigua*, *Globocassidulina subglobosa*, *Nuttalides umbonifera*, *Oridorsalis umbonatus*, *Uvigerina peregrina* and *Eubuliminella exilis*.	*Astrononion umbilicatulum*, *Bulimina* cf. *B. elongata*, *Bulimina striata*, *Cibicidoides bradyi*, *Cibicidoides mundulus*, *Gyrodinoides soldanii*, *Oridorsalis umbonatus*, *Sphaeroidina bulloides*, *Siphouvigerina hispida*, *Stilostomella* cf. *S. annulifera*, *Siphonodosaria lepidula*, *Siphonodosaria subspinosa*, *Strictocostella matanzana*, *Uvigerina peregrina*, *Bulimina gibba* and *Laticarinina pauperata*.

Appendix D (continued)

Clusters	ODP Holes		
	752A	1168A	1139A
D	*Bolivina* cf. *reticulata*, *Globocassidulina subglobosa*, *Strictocostella scharbergana*, *Siphonodosaria subspinosa*, *Bolivina viennensis*, *Siphonodosaria lepidula*, *Cibicidoides mundulus*, *Burseolina* cf. *pacifica*, *Abdetodentrix peudothalmanni*, *Pullenia bulloides*, *Cibicidoides wuellerstorfi* (coarse), *Nuttalides umbonifera*, *Uvigerina auberiana*, *Bolivina reticulata, Trifarina bradyi, Pleurostomella acuminata and Planulina costata.*	*Bolivina dilatata*, *Epistominella exigua*, *Globocassidulina subglobosa*, *Uvigerina peregrina*, *Cibicidoides mundulus*, *Bolivina* sp.3, *Cibicidoides bradyi*, and *Bulimina truncana*.	*Abdetodentrix peudothalmanni*, *Astrononion umbilicatulum*, *Epistominella exigua*, *Globocassidulina subglobosa*, *Oridorsalis umbonatus*, *Stilostomella* cf. *S. annulifera*, *Siphonodosaria lepidula*, *Cibicidoides mundulus*, *Gyrodinoides soldanii*, *Gyrodinoides* sp.1, *Pleurostomella acuminata*, *Sphaeroidina bulloides*, *Strictocostella matanzana*, *Uvigerina peregrina*, *Bulimina gibba*, *Orthomorphina perversa*, *Osangularia culter*, and *Bulimina truncana*.
E	*Globocassidulina subglobosa*, *Strictocostella scharbergana*, *Siphonodosaria subspinosa*, *Bolivina viennensis*, *Siphonodosaria lepidula*, *Cibicidoides mundulus*, *Burseolina* cf. *pacifica*, *Abdetodentrix peudothalmanni*, *Nuttalides umbonifera*, *Uvigerina auberiana*, *Bolivina reticulata*, *Trifarina bradyi*, *Lenticulina cultrata*, *Pleurostomella acuminata* and *Planulina costata*.	*Bolivina dilatata*, *Bulimina* cf. *B. elongata*, *Epistominella exigua*, *Globocassidulina subglobosa*, *Oridorsalis umbonatus*, *Cibicidoides mundulus*, *Cibicidoides bradyi*, and *Bulimina truncana*.	*Astrononion umbilicatulum*, *Bulimina striata*, *Cibicidoides mundulus*, *Epistominella exigua*, *Globocassidulina subglobosa*, *Oridorsalis umbonatus*, *Stilostomella* cf. *S. annulifera*, *Siphonodosaria lepidula*, *Gyrodinoides soldanii*, *Gyrodinoides* sp.1, *Pullenia quinqueloba*, *Strictocostella matanzana*, *Uvigerina peregrina*, *Bulimina gibba*, *Eggerella bradyi*, and *Osangularia culter*.
F	*Globocassidulina subglobosa*, *Strictocostella scharbergana*, *Siphonodosaria lepidula*, *Cibicidoides mundulus*, *Burseolina* cf. *pacifica*, *Abdetodentrix peudothalmanni*, *Nuttalides umbonifera*, *Bolivina huneri*, *Pullenia bulloides*, *Lenticulina cultrata*, and *Planulina costata*.	*Bolivina dilatata*, *Bulimina* cf. *B. elongata*, *Epistominella exigua*, *Globocassidulina subglobosa*, and *Melonis barleeanus*.	

Appendix E: Diversity indices and age (Ma) of thirty samples at the Hole 752A. Diversities are calculated by past software (PAST 3.25) (Hammer et al., 2001).

752A Core, section	Dominance_D	Shannon_H	Taxa_S	Evenness_e^ H/S	Age (Ma) ATNTS2012 in GTS 2012
2H-4	0.10	3.05	42	0.50	4.14
3H-1	0.10	3.01	59	0.34	5.30
3H-2	0.11	2.86	58	0.30	5.61
3H-4	0.14	2.44	30	0.38	6.62
3H-5	0.19	2.60	51	0.26	7.19
4H-1	0.09	3.05	63	0.34	7.96
4H-2	0.17	2.51	55	0.22	8.25
4H-5	0.20	2.45	48	0.24	9.06
5H-1	0.14	2.66	49	0.29	9.71
5H-2	0.16	2.77	52	0.31	9.98
5H-3	0.19	2.29	29	0.34	10.23
5H-4	0.09	3.14	63	0.37	10.55
6H-1	0.07	3.25	71	0.36	11.49
6H-3	0.09	3.18	64	0.37	12.06
6H-5	0.05	3.52	67	0.51	12.59
6H-6	0.11	2.77	36	0.44	12.83
7H-1	0.04	3.68	69	0.57	13.28
7H-2	0.03	3.92	94	0.54	13.56
7H-4	0.06	3.44	67	0.47	14.41
7H-6	0.08	2.90	32	0.57	15.21
8H-1	0.04	3.64	73	0.52	15.98
8H-3	0.04	3.57	70	0.51	16.84
8H-6	0.05	3.48	64	0.51	18.04
9H-2	0.11	3.14	71	0.32	19.16
9H-4	0.09	3.22	64	0.39	19.96
9H-5	0.06	3.39	70	0.42	20.34
10H-2	0.05	3.65	71	0.54	21.78
10H-3	0.04	3.71	90	0.45	22.31
10H-5	0.13	2.99	71	0.28	23.12
10H-6	0.09	3.10	46	0.48	23.48

Appendix F: The data used for calculating Benthic Foraminifera Accumulation Rate (BFAR) and MAR $_{carbonate}$ at the Site 752 Hole A, the Dry Bulk Density and $CaCO_3$ % data derived from the Initial Report (Shipboard Scientific Party, 1989a).

752A Core, section	Depth (mbsf)	Total BF (counted)	Fraction selected	Dry Wt.(gm)	Total BF/gm	Rate of Sedimentation (cm $k.a^{-1}$)	Dry Bulk Density (DBD) (g/cm^3)	$CaCO_3$ %	MAR carbonate	BFAR (Spec.$*cm^{-2}*k.a^{-1}$)	Age (Ma) ATNTS2012 in GTS 2012
2H-4	13.32	132	1/64	5.96	1417	0.43	1.08	94.60	0.44	658	4.14
3H-1	18.30	617	1/8	11.55	427	0.50	0.99	97.40	0.48	212	5.30
3H-2	19.85	517	1/32	9.56	1731	0.29	0.90	97.00	0.25	452	5.61
3H-4	22.78	240	1/64	2.52	6095	0.29	0.91	95.90	0.25	1609	6.62
3H-5	24.42	697	1/16	8.97	1243	0.46	0.95	91.60	0.40	540	7.19
4H-1	28.00	591	1/8	7.72	612	0.54	0.96	96.50	0.50	317	7.96
4H-2	29.61	775	1/16	8.46	1466	0.54	0.94	96.00	0.49	744	8.25
4H-5	33.94	516	1/16	5.99	1378	0.54	0.90	90.80	0.44	674	9.06
5H-1	37.45	734	1/8	15.66	375	0.54	0.90	96.00	0.47	185	9.71
5H-2	38.95	447	1/16	7.55	947	0.54	0.87	97.00	0.46	445	9.98
5H-3	40.30	148	1/64	3.47	2730	0.54	0.92	94.80	0.47	1349	10.23
5H-4	41.99	505	1/8	5.85	691	0.54	0.90	97.00	0.47	336	10.55
6H-1	47.10	636	1/8	11.09	459	0.54	1.04	96.80	0.54	258	11.49
6H-3	50.16	423	1/16	8.90	760	0.54	1.07	96.00	0.55	437	12.06
6H-5	53.03	387	1/8	6.66	465	0.54	1.05	96.00	0.54	264	12.59
6H-6	54.33	164	1/32	2.35	2233	0.54	1.03	96.90	0.54	1242	12.83
7H-1	56.73	412	1/8	6.40	515	0.57	1.03	96.90	0.57	302	13.28
7H-2	58.33	808	1/8	12.38	522	0.35	1.01	96.10	0.34	185	13.56
7H-4	61.30	457	1/16	8.20	892	0.35	0.85	95.10	0.28	265	14.41
7H-6	64.13	132	1/32	2.27	1861	0.35	1.09	96.00	0.37	707	15.21
8H-1	66.80	599	1/8	13.91	345	0.35	1.32	96.00	0.44	159	15.98
8H-3	69.80	407	1/16	9.41	692	0.35	1.13	96.60	0.38	274	16.84
8H-6	74.00	502	1/16	9.19	874	0.35	1.08	94.70	0.36	330	18.04
9H-2	77.94	537	1/16	7.60	1131	0.35	1.16	95.90	0.39	459	19.16
9H-4	80.71	366	1/16	8.25	710	0.35	1.14	96.00	0.38	283	19.96
9H-5	82.05	489	1/16	13.44	582	0.35	1.19	96.50	0.40	241	20.34
10H-2	87.10	310	1/16	5.54	895	0.35	1.21	95.90	0.41	378	21.78
10H-3	88.95	473	1/16	9.51	796	0.35	1.19	91.60	0.38	330	22.31
10H-5	91.77	550	1/32	14.34	1227	0.35	1.13	95.40	0.38	483	23.12
10H-6	93.03	164	1/64	3.72	2822	0.40	0.99	89.90	0.36	1112	23.48

Appendix G: Diversity indices and age (Ma) of forty-two samples at the Hole 1168A. Diversities have calculated by past software (PAST 3.25) (Hammer et al., 2001).

1168A core, section	Taxa_S	Shannon_H	Dominance_D	Evenness_e^H/S	Age (Ma) GTS 2012 in ATNTS2012
8H-1	69	3.53	0.05	0.50	4.23
9H-3	66	3.48	0.05	0.49	5.01
10H-2	56	3.42	0.05	0.55	5.55
11H-5	51	3.31	0.06	0.54	6.46
12H-1	66	3.44	0.06	0.47	6.68
13X-1	82	3.73	0.04	0.51	7.27
14X-4	58	3.34	0.06	0.48	8.00
15X-2	65	3.56	0.05	0.54	8.45
16X-2	53	3.04	0.10	0.39	9.62
17X-3	60	3.30	0.07	0.45	9.82
18X-5	62	3.14	0.08	0.37	10.03
19X-4	61	3.55	0.04	0.57	10.18
20X-3	65	3.25	0.10	0.40	10.32
21X-1	79	3.61	0.05	0.47	10.44
22X-2	65	3.60	0.04	0.56	11.08
23X-3	57	3.16	0.09	0.41	11.83
24X-6	56	3.17	0.09	0.42	12.74
25X-2	63	3.31	0.07	0.43	12.97
25X-5	47	3.37	0.05	0.62	13.26
26X-2	54	3.25	0.07	0.48	13.62
26X-6	34	2.93	0.09	0.55	14.01
27X-4	58	3.29	0.07	0.46	14.44
28X-3	65	3.50	0.05	0.51	14.97
29X-2	61	3.41	0.06	0.50	15.52
30X-3	58	3.64	0.04	0.66	16.24
31X-5	54	3.35	0.06	0.53	17.07
32X-4	58	3.29	0.06	0.46	17.60
33X-3	76	3.83	0.03	0.60	18.11
34X-1	54	2.89	0.15	0.33	18.53
35X-1	55	3.37	0.06	0.53	19.14
36X-6	65	3.06	0.13	0.33	20.26
37X-6	52	3.02	0.09	0.39	20.90
38X-3	60	3.31	0.07	0.45	21.22
39X-4	46	2.95	0.10	0.41	21.84
40X-2	46	3.27	0.05	0.57	21.94
41X-5	58	3.37	0.06	0.50	22.15
42X-3	58	3.34	0.06	0.49	22.25
45X-6	53	3.43	0.05	0.58	22.75
47X-6	44	3.25	0.06	0.58	23.03
49X-3	56	3.51	0.05	0.60	23.25
50X5	35	2.99	0.08	0.57	23.87
52X-4	38	3.16	0.06	0.62	25.20

Appendix H: The data used for calculating Benthic Foraminifera Accumulation Rate (BFAR) and MAR $_{carbonate}$ at the Site 1168 Hole A. The Dry Bulk Density and $CaCO_3$ % data derived from the Initial Report (Shipboard Scientific Party, 2001a).

1168A core, section	Depth (m)	Dry Weight (gm)	Fraction	Total BF/gm	Rate of Sedimentation (cm $k.a^{-1}$)	DBD (Dry Bulk Density g/cm^3)	$CaCO_3$ %	MAR carbonate	BFAR (Spec.$*cm^{-2}*k.a^{-1}$)	Age (Ma) GTS 2012 in ATNTS2012
8H-1	65.30	12.85	1/8	207	1.54	1.23	92.90	1.76	392	4.23
9H-3	77.31	12.73	1/8	299	1.54	1.23	91.50	1.73	565	5.01
10H-2	85.60	13.67	1/16	321	1.54	1.16	89.70	1.60	573	5.55
11H-5	99.70	14.35	1/8	144	1.54	1.25	86.10	1.66	277	6.46
12H-1	103.05	16.74	1/8	178	1.54	1.22	88.80	1.67	335	6.68
13X-1	112.20	13.31	1/16	557	1.54	1.17	88.00	1.59	1003	7.27
14X-4	123.45	12.67	1/16	428	1.54	1.12	93.40	1.61	738	8.00
15X-2	130.36	14.75	1/8	191	0.84	1.11	93.50	0.87	178	8.45
16X-2	140.20	14.00	1/8	139	5.67	1.20	96.10	6.54	949	9.62
17X-3	151.30	14.68	1/8	141	5.67	1.14	95.20	6.15	908	9.82
18X-5	163.70	14.27	1/4	110	5.67	1.15	93.90	6.12	716	10.03
19X-4	171.70	13.46	1/8	157	5.67	1.11	89.30	5.62	983	10.18
20X-3	180.10	14.65	1/8	146	5.67	1.08	94.10	5.76	896	10.32
21X-1	186.70	15.22	1/8	180	1.67	1.14	90.50	1.72	342	10.44
22X-2	197.35	12.96	1/8	183	1.52	1.14	68.40	1.19	318	11.08
23X-3	208.74	12.59	1/8	180	1.52	1.09	91.70	1.52	298	11.83
24X-6	222.67	12.79	1/8	201	1.52	1.11	91.30	1.54	337	12.74
25X-2	226.11	12.73	1/8	175	1.52	1.13	85.70	1.47	300	12.97
25X-5	230.64	4.14	1/2	80	1.52	1.12	98.00	1.67	136	13.26
26X-2	236.03	9.48	1/8	207	1.52	1.28	92.50	1.80	402	13.62
26X-6	242.05	2.12	1/8	464	1.52	1.19	66.60	1.20	840	14.01
27X-4	248.63	7.62	1/4	149	1.52	1.33	90.60	1.83	300	14.44
28X-3	256.67	16.92	1/8	134	1.52	1.36	80.60	1.67	277	14.97
29X-2	265.06	9.41	1/4	104	1.52	1.31	42.90	0.85	206	15.52
30X-3	276.06	10.38	1/8	175	1.52	1.28	70.10	1.36	340	16.24
31X-5	288.66	9.81	1/8	210	1.52	1.36	64.70	1.34	433	17.07
32X-4	296.70	18.49	1/4	60	1.52	1.38	59.10	1.24	125	17.60
33X-3	304.60	8.73	1/4	146	1.52	1.38	38.80	0.81	305	18.11
34X-1	310.95	10.35	1/4	118	1.52	1.38	53.40	1.12	247	18.53

Appendix H (continued)

1168A core, section	Depth (m)	Dry Weight (gm)	Fraction	Total BF/gm	Rate of Sedimentation (cm $k.a^{-1}$)	DBD (Dry Bulk Density g/cm^3)	$CaCO_3$ %	MAR carbonate	BFAR (Spec.$*cm^{-2}*k.a^{-1}$)	Age (Ma) GTS 2012 in ATNTS2012
35X-1	320.25	10.84	1/2	49	1.52	1.44	44.60	0.98	107	19.14
36X-6	337.33	10.50	1/8	219	1.52	1.47	27.10	0.61	489	20.26
37X-6	347.05	14.13	1/2	39	1.52	1.50	41.60	0.95	89	20.90
38X-3	352.00	9.74	1/8	209	1.86	1.57	48.80	1.43	609	21.22
39X-4	363.55	9.85	1/4	118	6.68	1.53	32.10	3.28	1204	21.84
40X-2	369.99	10.57	1/4	97	6.68	1.56	49.40	5.15	1010	21.94
41X-5	383.97	9.60	1/4	115	6.68	1.40	47.60	4.45	1079	22.15
42X-3	390.60	14.44	1/8	167	6.68	1.49	42.30	4.21	1665	22.25
45X-6	423.72	2.56	1/8	600	6.68	1.38	25.90	2.39	5511	22.75
47X-6	442.85	4.23	1/8	253	6.68	1.43	24.70	2.36	2412	23.03
49X-3	457.62	2.17	1/2	138	2.05	1.44	25.30	0.75	408	23.25
50X5	470.22	3.92	1/1	29	1.34	1.35	13.70	0.25	51	23.87
52X-4	488.10	2.24	1/4	229	1.34	1.41	28.90	0.55	432	25.20

Appendix I: Diversity indices and age (Ma) of twenty-five samples at the Hole 1139A. Diversities calculated by past software (PAST 3.25) (Hammer et al., 2001).

1139A Core, section	Dominance_D	Shannon_H	Taxa_S	Evenness_e^H/S	Age (Ma)GTS 2012 (1139A)
3R-1	0.07	3.26	46	0.57	11.25
3R-2	0.05	3.32	40	0.69	11.99
3R-4	0.05	3.48	69	0.47	12.77
4R-1	0.09	3.06	43	0.49	14.49
4R-2	0.04	3.45	55	0.57	15.22
4R-4	0.06	3.14	35	0.66	16.13
5R-1	0.04	3.68	88	0.45	17.98
6R-1	0.15	2.47	39	0.30	18.61
7R-1	0.07	3.34	68	0.41	19.03
7R-3	0.06	3.27	43	0.61	19.14
8R-1	0.06	3.32	58	0.48	19.42
9R-4	0.05	3.41	54	0.56	20.00
10R-2	0.08	3.17	50	0.48	20.30
11R-1	0.06	3.19	52	0.46	20.64
12R-2	0.13	2.67	37	0.39	21.14
12R-5	0.05	3.35	42	0.68	21.34
13R-5	0.06	3.29	50	0.54	21.76
14R-4	0.04	3.58	63	0.57	22.10
15R-2	0.06	3.31	41	0.67	22.39
15R-4	0.11	3.10	55	0.40	22.50
16R-2	0.07	3.22	51	0.49	22.79
17R-3	0.09	3.09	57	0.38	23.18
18R-1	0.05	3.36	48	0.60	23.28
19R-2	0.05	3.54	63	0.55	23.43
20R-4	0.07	3.23	50	0.50	23.60

Appendix J: The data used for calculating Benthic Foraminifera Accumulation Rate (BFAR) and MAR $_{carbonate}$ at the Site 1139 Hole A. The Dry Bulk Density and $CaCO_3$ % data derived from the Initial Report (Shipboard Scientific Party, 2000).

1139A Core, section	Depth (m)	Dry Weight (gm)	Fraction	Total BF	BF/gm	Rate of Sedimentation (cm k.a^{-1})	DBD (gm/cm^3)	$CaCO_3$ %	MAR carbonate	BFAR	Age (Ma) GTS 2012 in ATNTS2012
3R-1	19.30	3.66	1/32	157	1373	0.30	1.03	73.61	0.23	416	11.25
3R-2	21.50	2.33	1/32	136	1868	0.30	1.03	-	-	567	11.99
3R-4	23.82	13.20	1/8	487	294	0.30	0.97	-	-	84	12.77
4R-1	28.90	1.94	1/32	195	3216	0.30	1.01	83.34	0.26	962	14.49
4R-2	31.05	12.90	1/16	283	351	0.30	1.03	-	-	107	15.22
4R-4	33.75	2.06	1/32	139	2159	0.30	1.01	-	-	646	16.13
5R-1	39.21	6.72	1/4	947	564	1.43	0.92	76.32	0.22	743	17.98
6R-1	48.21	7.83	1/8	292	298	2.32	0.80	60.65	0.18	553	18.61
7R-1	58.11	7.01	1/4	550	314	2.32	0.79	51.33	0.16	575	19.03
7R-3	60.45	2.86	1/16	131	733	2.32	0.82	-	-	1393	19.14
8R-1	66.95	6.31	1/4	376	238	2.32	0.91	72.89	0.22	503	19.42
9R-4	80.39	5.50	1/4	298	217	2.32	0.76	32.78	0.43	382	20.00
10R-2	87.45	10.20	1/8	280	219	2.32	0.82	24.94	0.46	417	20.30
11R-1	95.45	6.84	1/4	425	249	2.32	0.88	62.13	1.14	507	20.64
12R-2	106.91	10.40	1/8	282	217	2.32	0.89	28.08	0.53	448	21.14
12R-5	111.60	3.33	1/8	138	332	2.32	0.79	7.46	0.16	607	21.34
13R-5	121.20	5.38	1/2	237	88	2.32	0.69	21.19	0.37	141	21.76
14R-4	129.15	11.50	1/2	305	53	2.32	0.84	19.92	0.38	103	22.10
15R-2	135.95	1.77	1/4	124	280	2.32	0.84	19.92	0.41	546	22.39
15R-4	138.41	4.33	1/2	279	129	2.32	0.78	31.99	0.66	233	22.50
16R-2	145.25	8.00	1/2	243	61	2.95	0.79	31.99	0.59	142	22.79
17R-3	156.71	6.68	1/2	349	104	7.06	0.80	32.61	0.52	590	23.18
18R-1	163.46	10.30	1/16	297	460	7.06	0.79	58.51	1.14	2567	23.28
19R-2	174.21	8.62	1/8	466	432	7.06	1.09	58.22	1.13	3330	23.43
20R-4	186.60	3.49	1/32	200	1834	7.06	0.93	52.78	0.96	11982	23.60

Appendix K: 1) Correlation coefficient (R-value) and Statistically significant value (P-value) calculated from 13 species in each Hole (752A, 1168A & 1139A) and diversity (Shannon_H).

2) Correlation coefficient for 5 species at the study Holes (752A, 1168A & 1139A) calculated from maximum size values and relative abundance of each species.

1)

ODP Holes	Hole 752A		Hole 1168A		Hole 1139A	
Correlation coefficient & Statistical significant	R-value	P-value	R-value	P-value	R-value	P-value
Bolivina cf. *reticulata*	-0.74	2.70E-06				
Astrononion umbilicatulum	0.32	0.09	0.22	0.11	0.24	0.24
Burseolina pacifica	0.18	0.35				
Globocassidulina subglobosa	0.14	0.46	-0.14	0.51	0.04	0.86
Strictocostella scharbergana	0.17	0.37				
Siphonodosaria subspinosa	0.27	0.14	0.05	0.68	0.17	0.42
Gavelinopsis lobatulus	-0.15	0.44				
Trifarina angulosa	-0.22	0.25	0.18	0.38	0.03	0.91
Trifarina bradyi	0.43	0.02	0.13	0.37	0.27	0.2
Nuttalides umbonifera	0.22	0.24	-0.07	0.73	0.23	0.28
Cibicidoides wuellerstorfi (smooth)	-0.39	0.03	0.03	0.83	0.4	0.05
Cibicidoides wuellerstorfi (coarse)	0.35	0.06	0.16	0.26	-0.02	0.93
Bulimina striata	-0.27	0.15			0.06	0.78
Bulimina truncana	-0.01	0.95	0.15	0.32	0.31	0.13
Abditodentrix pseudothalmanni			0.22	0.25	0.02	0.91
Bolivina dilatata			-0.16	0.33		
Stilostomella cf. S. annulifera			0.3	0.04	-0.1	0.65
Epistominella exigua			-0.41	0.01	-0.13	0.45
Sphaeroidina bulloides			-0.15	0.37	-0.16	0.44

2)

Benthic foraminifera	**Correlation coefficient (R- value)**		
	752A	**1168A**	**1139A**
Abditodentrix pseudothalmanni	-0.09	0.83	0.51
Globocassidulina subglobosa	-0.05	-0.19	0.49
Cibicidoides mundulus	0.32	0.29	0.62
Nuttalides umbonifera	0.02	0.80	0.63
Sphaeroidina bulloides	0.08	0.42	0.43

Appendix L: The size (µm) and the number of specimens of *Abditodentrix pseudothalmanni* at ODP Sites 752, 1139 &1168. The mean values and standard deviations have calculated for different sizes at each sample.

752A (core section, interval (cm))	*Abditodentrix pseudothalmanni* (752A)														
	Size	Number	Size	Number	Size	Number	Size	Number	Size	Number	Sum	Mean	STDV	smallest test	largest test
2H-4, 65-70											0				
3H-1, 50-55	175	2	250	1	375	3					6	288	100	175	375
3H-2 ,60-65	250	6	375	1							7	268	47	250	375
3H-4 ,40-45	175	16	200	23	250	10					49	202	27	175	250
3H-5 ,70-75	175	8	250	16	375	6					30	255	69	175	375
4H-1 ,70-75	175	3	200	2	275	1					6	200	39	175	275
4H-2 ,85-90											0				
4H-5 ,70-75	175	13	200	10	250	1	300	1			25	193	28	175	300
5H-1 ,70-75	175	7	200	17	250	6	350	1			31	209	36	175	350
5H-2 ,70-75	175	21	200	11	250	3					35	189	22	175	250
5H-3 ,90-95	125	32	175	12	250	1					45	141	28	125	250
5H-4 ,70-75	175	5	200	8	250	4					17	204	28	175	250
6H-1 ,70-75	150	2	175	8	200	10	250	2	300	1	23	196	33	150	300
6H-3 ,75-80	175	1	200	7	225	2	275	1			11	209	26	175	275
6H-5 ,70-75	150	3	175	5	200	18	225	21	300	1	48	207	26	150	300
6H-6 ,20-25	125	10	150	12	175	4	200	15	250	1	42	167	33	125	250
7H-1 ,65-70	200	6	250	4							10	220	26	200	250
7H-2 ,80-85	250	2									2	250	0	250	250
7H-4 ,70-75	175	1	200	8	225	1					10	200	12	175	225
7H-6 ,100-105	150	5	175	5	200	7	250	2	275	1	20	190	36	150	275
8H-1 ,100-105	200	4									4	200	0	200	200
8H-3 ,100-105	200	3	250	5	300	1					9	239	33	200	300
8H-6 ,70-75	200	9	225	1							10	203	8	200	225
9H-2 ,100-105	150	1	175	1	200	3					5	185	22	150	200
9H-4 ,80-85	175	1	200	1	250	2					4	219	38	175	250
9H-5 ,65-70	175	4	200	3	275	1					8	197	34	175	275
10H-2 ,60-65	175	3	200	5	275	1					9	200	31	175	275
10H-3 ,100-105	150	2	175	2	225	3	250	4			11	211	41	150	250
10H-5 ,80-85											0				
10H-6 ,110-115	150	2	175	1	200	2					5	175	25	150	200

1139A (core, section, interval (cm))	*Abditodentrix pseudothalmanni* (1139A)																		
	Size	No.	Size	No.	Size	No.	Size	No.	Size	No.	Size	No.	Size	No.	Sum	Mean	STDV	smallest test	largest test
3R-1 , 30-34	100	1	150	1	175	2	225	1	275	1					6	183	61	100	275
3R-2 , 100-104	125	2	150	4	175	3	200	1	250	1	300	1			12	177	52	125	300
3R-4 , 32-36	225	1	275	1											2	250	35	225	275
4R-1, 40-44	100	2	125	3	175	4	200	1	225	1	250	1	275	1	13	171	56	100	275
4R-2 , 105-109	175	1	200	3	225	1	275	3	300	8	375	1			17	271	52	175	375
4R-4 , 75-79	150	1	175	1	200	2	250	1							5	195	37	150	250
5R-1 , 121-125	250	5	275	3	300	1									9	264	18	250	300
6R-1 , 71-75															0				
7R-1 , 111-115	175	1	250	1	275	1									3	233	52	175	275
7R-3, 45-49	125	1	200	1	225	1									3	183	52	125	225
8R-1 , 45-49	125	1	150	2	175	2	200	4	225	2	250	6			17	207	41	125	250
9R-4 , 105-109	150	1	200	5	225	7	250	6	325	1					20	228	34	150	325
10R-2 , 45-49	150	2	175	2	200	3	225	1	275	1					9	194	39	150	275
11R-1, 35-39	175	5	200	7	225	4	250	3	325	1					20	213	37	175	325
12R-2 , 71-75	150	5	175	3	200	2	225	3	250	3					16	194	39	150	250
12R-5, 90-94	125	5	150	5	175	1	200	1	225	3	250	1	325	1	17	176	57	125	325
13R-5 , 80-84	150	1	175	4	200	2	225	3	275	2	300	1			13	213	46	150	300
14R-4 , 65-69	175	1													1	175		175	175
15R-2, 95-99															0				
15R-4 , 41-45	200	2													2	200	0	200	200
16R-2 , 55-59	250	1													1	250		250	250
17R-3 , 91-95	250	1													1	250		250	250
18R-1 , 96-100	275	1													1	275		275	275
19R-2, 60.5-64.5	225	4	250	4	275	2	300	1	325	1	375	1			13	265	45	225	375
20R-4, 40-44	200	2													2	200	0	200	200

Appendix L (continued)

1168A (core, section, Interval (cm))	*Abditodentrix pseudothalmanni* (1168A)																				
	Size	No.	Size	No.	Size	No.	Size	No.	Size	No.	Size	No.	Size	No.	Size	No.	Sum	Mean	STD	smallest test	largest test
8H-1 , 100-104	125	3	150	3	200	12	225	8	300	4	350	7	375	1	425	1	39	243	79	125	425
9H-3 , 51-55	150	6	175	25	200	8	250	10	300	7	375	7	400	3			66	232	78	150	400
10H-2 , 80-84	150	3	175	10	225	9	250	2	300	2	325	4	375	2			32	230	67	150	375
11H-5 , 90-94	125	1	150	5	175	6	250	3	300	3	375	1					19	208	70	125	375
12H-1 , 75-79	175	7	200	2	250	4	275	4									17	219	44	175	275
13X-1 , 40-44	125	1	150	4	175	2	200	8	225	3	250	8	350	2			28	216	53	125	350
14X-4 , 45-49	125	2	150	2	175	5	200	4	250	4	300	3	350	1			21	213	63	125	350
15X-2 , 76-80	175	3	200	7	250	6	300	4	350	4	375	3	400	1			28	270	73	175	400
16X-2 , 100-104	150	1	175	3	200	3	250	3	275	6	350	3					19	249	62	150	350
17X-3 , 100-104	175	2	200	1	225	2	250	1									6	208	30	175	250
18X-5 , 80-84	175	13	200	7	250	13	325	4	375	6							43	244	70	175	375
19X-4 , 70-74	175	8	200	5	250	6	300	4	350	3							26	237	61	175	350
20X-3 , 100-104	125	1	150	1	200	4	250	2	275	1	350	1					10	220	64	125	350
21X-1 , 100-104	175	2	200	2	250	2	300	1									7	221	47	175	300
22X-2 , 45-49	150	5	200	7	250	3	275	2	300	2							19	213	52	150	300
23X-3 , 74-78	175	5	250	3	325	2	350	1	400	1							12	252	81	175	400
24X-6 , 57-61	150	3	175	5	200	7	250	3	325	4	400	2					24	232	77	150	400
25X-2 , 41-45	125	1	225	1	300	1											3	217	88	125	300
25X-5, 44-48																	0				
26X-2 , 73-77	275	1	300	1													2	288	18	275	300
26X-6, 75-79																	0				
27X-4 , 73-77																	0				
28X-3 , 75-79	175	1	225	1													2	200	35	175	225
29X-2 , 96-100	200	1															1	200		200	200
30X-3 , 85.5-89.5																	0				
31X-5 , 86-90																	0				
32X-4 , 80-84	125	2	150	2	200	1											5	150	31	125	200
33X-3 , 90-94	200	4															4	200	0	200	200
34X-1 , 95-99																	0				
35X-1 , 65-69																	0				
36X-6 , 62.5-66.5	150	1	175	1													2	163	18	150	175
37X-6 , 75-79	200	2															2	200	0	200	200
38X-3 , 60-64	150	1	175	1	200	1											3	175	25	150	200
39X-4 , 105-109	150	7															7	150	0	150	150
40X-2 , 89-93	150	1	175	2													3	167	14	150	175
41X-5 W, 67-71	125	1	150	4	200	1	225	2									8	172	39	125	225
42X-3 , 70-74	175	2															2	175	0	175	175
45X-6, 52-56	175	1															1	175		175	175
47X-6, 45-49																	0				
49X-3, 52-56	150	1	175	1	225	2											4	194	38	150	225
50X5, 52-56	150	1															1	150		150	150
52X-4, 70-74	150	1	175	1													2	163	18	150	175

Appendix M: The size (µm) and the number of specimens of *Globocassidulina subglobosa* at ODP Sites 752, 1139 &1168. The mean values and standard deviations have calculated for different sizes at each sample.

752A (core section, interval (cm))	*Globocassidulina subglobosa* (752A)																							
	Size	No.	Size	No.	Size	No.	Size	No.	Size	No.	Size	No.	Size	No.	Size	No.	Size	No.	Size	No.	Sum	Mean	STDV	smallest test	largest test
2H-4, 65-70	125	3	175	3	475	2															8	231	152	125	475
3H-1, 50-55	150	30	175	12	200	6	250	8													56	175	35	150	250
3H-2 ,60-65	125	10	150	16	175	3	200	6	225	5	250	4	275	1	300	1					46	176	47	125	300
3H-4 ,40-45	125	3	175	1																	4	138	25	125	175
3H-5 ,70-75	150	16	250	13	450	1	675	3													33	246	152	150	675
4H-1 ,70-75	175	13	200	7	250	7	300	4													31	214	45	175	300
4H-2 ,85-90	150	6	200	8	250	20	375	7	500	2											43	259	86	150	500
4H-5 ,70-75	125	6	175	37	250	17	300	14													74	212	56	125	300
5H-1 ,70-75	150	6	175	16	250	5	300	8	375	7	550	6									48	277	129	150	550
5H-2 ,70-75	100	1	125	9	175	4	250	2													16	152	45	100	250
5H-3 ,90-95	125	8																			8	125	0	125	125
5H-4 ,70-75	125	7	150	4	200	2	250	2	275	3	350	4									22	209	87	125	350
6H-1 ,70-75	125	8	150	3	200	3	300	3	375	1											18	185	80	125	375
6H-3 ,75-80	125	2	175	8	200	6	250	3	300	3	350	2									24	217	63	125	350
6H-5 ,70-75	100	1	125	6	175	6	200	8	275	1	375	1	525	2							25	208	111	100	525
6H-6 ,20-25	100	3	200	1																	4	125	50	100	200
7H-1 ,65-70	150	5	200	2	250	6	300	2	325	4	650	2	675	1							22	297	160	150	675
7H-2 ,80-85	125	2	175	3	200	3	250	3	300	10	375	4	450	9	500	20	550	1	575	9	64	413	132	125	575
7H-4 ,70-75	125	7	175	5	200	6	250	3	275	1	300	2	325	2	450	1					27	210	80	125	450
7H-6 ,100-105	100	1	125	6	150	2	175	2	275	2	500	1									14	182	106	100	500
8H-1 ,100-105	175	11	200	4	225	10	250	5	300	1	325	1	375	3	450	2	500	3	625	1	41	268	115	175	625
8H-3 ,100-105	100	3	125	3	150	8	200	12	250	10	275	2	325	4							42	205	63	100	325
8H-6 ,70-75	125	1	150	6	175	5	200	2	225	4	250	5	300	2	425	1					26	211	65	125	425
9H-2 ,100-105	125	1	150	1	175	5	200	5	250	2	625	1	925	1							16	263	210	125	925
9H-4 ,80-85	125	1	175	1	200	1	250	4													7	214	50	125	250
9H-5 ,65-70	125	1	175	1	200	2	250	3													7	207	47	125	250
10H-2 ,60-65	125	10	150	20	200	9	250	2													41	160	33	125	250
10H-3 ,100-105	125	2	150	5	175	16	200	20	250	7	300	1	400	1							52	197	44	125	400
10H-5 ,80-85	125	2	150	5	200	43	250	9	300	3	325	1									63	208	38	125	325
10H-6 ,110-115	125	1	175	1	200	1	275	10													13	250	50	125	275

1139A (core, section, interval (cm))	*Globocassidulina subglobosa* (1139A)																
	Size	No.	Size	No.	Size	No.	Size	No.	Size	No.	Size	No.	Sum	Mean	STDV	smallest test	largest test
3R-1 , 30-34	100	2	125	4	150	2	175	2	200	1	250	1	12	150	44	100	250
3R-2 , 100-104	100	1	125	3	150	1							5	125	18	100	150
3R-4 , 32-36	175	1	200	2	225	1	300	1					5	220	48	175	300
4R-1, 40-44	100	2	125	19	150	3	175	3	500	1			28	145	72	100	500
4R-2 , 105-109	200	2	225	2									4	213	14	200	225
4R-4 , 75-79	100	3	125	14	150	2	175	2					21	129	20	100	175
5R-1 , 121-125	125	9	150	6	175	2	200	18	250	6	300	2	43	188	48	125	300
6R-1 , 71-75	100	2	200	1									3	133	58	100	200
7R-1 , 111-115	175	1	200	1									2	188	18	175	200
7R-3, 45-49													0				
8R-1 , 45-49	150	1											1	150		150	
9R-4 , 105-109	125	2	150	1									3	133	14	125	150
10R-2 , 45-49													0				
11R-1, 35-39	125	1											1	125		125	
12R-2 , 71-75													0				
12R-5, 90-94	125	1	150	1									2	138	18	125	150
13R-5 , 80-84	150	1											1	150		150	
14R-4 , 65-69	100	5	125	6	150	6	175	2	200	2			21	138	31	100	200
15R-2, 95-99	100	4											4	100	0	100	100
15R-4 , 41-45	125	1	175	1									2	150	35	125	175
16R-2 , 55-59													0				
17R-3 , 91-95	100	1	125	3	150	2	175	3					9	144	27	100	175
18R-1 , 96-100	125	3	150	4	175	2	200	1					10	153	25	125	200
19R-2, 60.5-64.5	100	1	150	4	175	7	200	2					14	166	25	100	200
20R-4, 40-44	100	3	125	3	175	1							7	121	27	100	175

Appendix M (continued)

1168A (core, section, Interval (cm))	*Globocassidulina subglobosa* (1168A)																										
	Size	No.	Size	No.	Size	No.	Size	No.	Size	No.	Size	No.	Size	No.	Size	No.	Size	No.	Size	No.	Size	No.	Sum	Mean	STDV	smallest test	largest test
8H-1 , 100-104	125	5	150	1	175	2	200	1	250	1	375	1	500	1	650	1							13	238	168	125	650
9H-3 , 51-55	100	6	125	7	150	2	175	3															18	128	27	100	175
10H-2 , 80-84	100	5	125	10	175	4	250	1	400	2													22	159	86	100	400
11H-5 , 90-94	100	9	125	7	150	4	375	1															21	131	59	100	375
12H-1 , 75-79	100	6	125	13	200	2	300	1	500	2													24	164	113	100	500
13X-1 , 40-44	100	9	125	6	150	8	175	2	200	1	250	2	300	1	500	1	575	1					31	170	110	100	575
14X-4 , 45-49	100	19	125	13	150	3	175	1	200	6	225	3	250	3									48	141	49	100	250
15X-2 , 76-80	100	2	125	13	150	19	175	4	200	4													42	147	25	100	200
16X-2 , 100-104	125	4	150	6	200	1	250	1	300	3	350	1	500	2									18	228	123	125	500
17X-3 , 100-104	125	11	150	8	200	2	225	2	250	2	325	1	350	1	550	2							29	197	115	125	550
18X-5 , 80-84	100	1	150	3	200	4	250	2	300	2	350	1	500	2	575	1							16	273	141	100	575
19X-4 , 70-74	100	9	125	8	150	4	175	3	200	2													26	132	32	100	200
20X-3 , 100-104	125	6	150	10	200	4	250	2	350	1													23	170	54	125	350
21X-1 , 100-104	100	10	125	7	150	3	175	2	300	1	325	1	400	3	575	2							29	195	143	100	575
22X-2 , 45-49	100	4	125	12	150	4	175	5	200	1	250	1	275	1	350	1	425	4					33	186	104	100	425
23X-3 , 74-78	125	3	150	3	175	2	225	1	250	1													10	165	43	125	250
24X-6 , 57-61	100	4	125	8	150	4	175	3	250	4	300	2	425	2									27	184	92	100	425
25X-2 , 41-45	100	5	125	9	150	3	175	3	200	2	350	1	600	1									24	165	107	100	600
25X-5, 44-48	125	3	150	3	175	2	200	1	250	3	450	2	550	1	750	1							16	270	183	125	750
26X-2 , 73-77	100	5	125	7	150	2	175	14															28	147	31	100	175
26X-6, 75-79	100	6	125	5	150	3	175	1	225	1													16	130	34	100	225
27X-4 , 73-77	100	10	125	21	150	20	175	5	250	3													59	140	34	100	250
28X-3 , 75-79	100	3	125	6	150	17	175	2	200	1	225	4	275	1	450	1	500	1	550	2	600	1	39	204	133	100	600
29X-2 , 96-100	100	10	125	12	150	9	175	10	200	2													43	140	30	100	200
30X-3 , 85.5-89.5	100	2	125	5	150	7	175	1	200	1	250	1	300	1									18	156	50	100	300
31X-5 , 86-90	100	4	125	14	150	4	175	5															27	134	24	100	175
32X-4 , 80-84	100	6	125	6	150	7	175	3	200	3	300	1											26	147	45	100	300
33X-3 , 90-94	100	3	125	5	150	7	175	5	200	4	425	1											25	163	63	100	425
34X-1 , 95-99	100	3	125	4	150	5	175	7	375	3	450	1	500	2									25	214	129	100	500
35X-1 , 65-69	100	4	125	3	175	3	200	3	250	2													15	160	53	100	250
36X-6 , 62.5-66.5	100	4	125	6	150	8	175	2	200	1	250	3											24	152	45	100	250
37X-6 , 75-79	100	2	125	11	150	23	175	1															37	141	16	100	175
38X-3 , 60-64	100	8	125	11	150	14	375	1	425	1	500	2											37	164	104	100	500
39X-4 , 105-109	100	12	125	34	150	2	175	1	600	1													50	131	69	100	600
40X-2 , 89-93	100	6	125	10	150	3	200	1															20	125	24	100	200
41X-5 W, 67-71	100	7	125	10	150	8																	25	126	20	100	150
42X-3 , 70-74	100	2	125	12	150	7	175	4															25	138	22	100	175
45X-6, 52-56	100	12	125	8	150	4	175	4															28	125	27	100	175
47X-6, 45-49	100	5	125	12	150	2																	19	121	15	100	150
49X-3, 52-56	100	3	125	1	400	1																	5	165	132	100	400
50X5, 52-56	100	2	125	1	200	1	300	2															6	188	95	100	300
52X-4, 70-74	100	1	125	6	150	2	175	4															13	142	26	100	175

Appendix N: The size (μm) and the number of specimens of *Cibicidoides mundulus* at ODP Sites 752, 1139 &1168. The mean values and standard deviations have calculated for different sizes at each sample.

752A (core section, interval (cm))	*Cibicidoides mundulus* (752A)																								
	Size	No.	Size	No.	Size	No.	Size	No.	Size	No.	Size	No.	Size	No.	Size	No.	Size	No.	Size	No.	Sum	Mean	STDV	smallest test	largest test
2H-4, 65-70	425	1	525	1																	2	475	71	425	525
3H-1, 50-55	250	1	375	8	350	5	500	8	600	3	675	2									27	450	112	250	675
3H-2 ,60-65	200	2	250	3																	5	230	27	200	250
3H-4 ,40-45	175	1																			1	175		175	175
3H-5 ,70-75	400	1	550	1																	2	475	106	400	550
4H-1 ,70-75	250	1	550	1																	2	400	212	250	550
4H-2 ,85-90	175	1	200	1	225	2	250	2	300	1	325	3	375	3	425	4	450	3	500	2	22	353	99	175	500
4H-5 ,70-75	175	1	200	1	225	1	250	1	300	2	425	2	450	1	500	1					10	325	116	175	500
5H-1 ,70-75	300	3	325	3	375	6	450	5	500	5	550	2									24	416	81	300	550
5H-2 ,70-75	175	1	250	1	500	2															4	356	169	175	500
5H-3 ,90-95	150	1	175	1	350	1	425	1													4	275	134	150	425
5H-4 ,70-75	225	2	250	3	275	1	350	4	425	4	450	5									19	359	87	225	450
6H-1 ,70-75	175	4	225	3	250	10	300	6	375	7	425	5	450	8	500	1					44	330	97	175	500
6H-3 ,75-80	175	1	225	1	250	1	300	1	350	2	375	1	425	2	450	2	500	2			13	367	105	175	500
6H-5 ,70-75																					0				
6H-6 ,20-25	150	1																			1	150		150	150
7H-1 ,65-70	150	1	175	1	250	1	325	1	375	2	425	3	450	2	500	1					12	360	113	150	500
7H-2 ,80-85	250	1	275	1	375	1	450	2													5	360	95	250	450
7H-4 ,70-75	150	1	375	1	425	1	500	2													5	390	144	150	500
7H-6 ,100-105	175	1	200	1	300	1	375	3	400	1	425	1	500	1							0				
8H-1 ,100-105	275	1	450	1	500	1															9	347	105	175	500
8H-3 ,100-105																					3	408	118	275	500
8H-6 ,70-75	175	2	200	2	250	3	300	3	350	2	375	3	400	1							16	289	77	175	400
9H-2 ,100-105	200	1	225	1	250	2	300	1	350	3	375	4	400	1	425	2	450	2	550	1	18	360	89	200	550
9H-4 ,80-85	175	2	200	2	225	3	250	2	300	4	375	2	400	4	450	1	425	2	525	2	24	326	107	175	525
9H-5 ,65-70	175	3	200	4	225	4	250	10	325	7	350	10	375	5	425	4	500	3			50	312	87	175	500
10H-2 ,60-65	150	2	175	1	400	1															4	219	121	150	400
10H-3 ,100-105	175	5	250	1	300	4	350	2	400	3											15	282	89	175	400
10H-5 ,80-85	175	2	200	10	250	4	300	7	325	5	375	2	400	1	600	1					32	276	87	175	600
10H-6 ,110-115	200	2	250	2	300	4	400	1													9	278	62	200	400

1139A (core, section, interval (cm))	*Cibicidoides mundulus* (1139A)																				
	Size	No.	Size	No.	Size	No.	Size	No.	Size	No.	Size	No.	Size	No.	Size	No.	Sum	Mean	STDV	smallest test	largest test
3R-1 , 30-34	150	1	250	1	300	1	375	1	500	1							5	315	132	150	500
3R-2 , 100-104	150	1															1	150		150	150
3R-4 , 32-36	175	1	250	4	300	10	375	5	425	8	500	4					32	358	86	175	500
4R-1, 40-44	150	1															1	150		150	150
4R-2 , 105-109	150	1	175	1	250	3	300	2	325	4	375	1	425	3	500	1	16	320	95	150	500
4R-4 , 75-79																	0				
5R-1 , 121-125	200	2	225	4	250	20	300	15	375	10							51	285	52	200	375
6R-1 , 71-75	200	1	225	1	300	4	400	1	450	1							8	309	82	200	450
7R-1 , 111-115	150	1	175	2	200	4	250	8	325	8	450	3	500	2			28	295	99	150	500
7R-3, 45-49	150	1	375	1													2	263	159	150	375
8R-1 , 45-49	150	5	200	3	250	4	375	5	400	3	500	2					22	292	117	150	500
9R-4 , 105-109	150	2	175	2	200	2	250	2	325	6	375	1	400	1			16	267	83	150	400
10R-2 , 45-49	175	2	200	1	250	1	300	5	325	2							11	268	58	175	325
11R-1, 35-39	175	2	200	2	250	6	325	6	375	2							18	275	64	175	375
12R-2 , 71-75	150	2	300	2													4	225	87	150	300
12R-5, 90-94	150	1	200	1	300	1											3	217	76	150	300
13R-5 , 80-84	125	1	200	2	250	1	300	3	425	2	625	1					10	315	144	125	625
14R-4 , 65-69	175	1	225	2	300	2	375	2	400	2							9	308	85	175	400
15R-2, 95-99	150	1	375	1													2	263	159	150	375
15R-4 , 41-45	150	1	250	1	375	3											5	305	102	150	375
16R-2 , 55-59	175	1	200	1	225	1	250	2	300	1	375	1	400	2	525	2	11	330	124	175	525
17R-3 , 91-95	175	1	225	2	250	4	300	1	375	3	450	4					15	323	98	175	450
18R-1 , 96-100	150	3	225	1	250	4	325	3	375	1	425	1	500	2			15	297	115	150	500
19R-2, 60.5-64.5	200	5	225	3	250	7	275	3	325	4	375	7					29	282	65	200	375
20R-4, 40-44	175	1	250	3	325	1	550	1									6	300	131	175	550

Appendix N (continued)

1168A (core, section, Interval (cm))	*Cibicidoides mundulus* (1168A)																				
	Size	No.	Size	No.	Size	No.	Size	No.	Size	No.	Size	No.	Size	No.	Size	No.	Sum	Mean	STDV	smallest test	largest test
8H-1 , 100-104	450	1															1	450		450	450
9H-3 , 51-55	200	1															1	200		200	200
10H-2 , 80-84	125	1	250	1	575	1											3	317	232	125	575
11H-5 , 90-94																	0				
12H-1 , 75-79	300	2	325	1	375	1											4	325	35	300	375
13X-1 , 40-44	150	2	175	1	225	1	250	1	400	1							6	225	95	150	400
14X-4 , 45-49																	0				
15X-2 , 76-80																	0				
16X-2 , 100-104																	0				
17X-3 , 100-104	175	1															1	175		175	175
18X-5 , 80-84	175	1	325	1	350	2	425	1	550	2							7	389	133	175	550
19X-4 , 70-74	125	4	150	4	225	1	525	1									10	185	123	125	525
20X-3 , 100-104	525	1															1	525		525	525
21X-1 , 100-104	125	1	475	2	550	1											4	406	191	125	550
22X-2 , 45-49	150	1	225	1	400	3	425	1	475	1							7	354	119	150	475
23X-3 , 74-78																	0				
24X-6 , 57-61	250	1	300	1													2	275	35	250	300
25X-2 , 41-45	325	2															2	325	0	325	325
25X-5, 44-48	125	2	150	1	175	2	375	1	600	2							8	291	207	125	600
26X-2 , 73-77	400	1	450	1	500	1											3	450	50	400	500
26X-6, 75-79	150	2															2	150	0	150	150
27X-4 , 73-77	125	2	425	1	500	2											5	335	194	125	500
28X-3 , 75-79	125	1	300	3	350	2	375	2	650	1							9	347	137	125	650
29X-2 , 96-100	150	1	250	1	550	1											3	317	208	150	550
30X-3 , 85.5-89.5	125	2	150	1	325	1	425	1									5	230	137	125	425
31X-5 , 86-90	125	1	250	1	300	2	325	2									6	271	77	125	325
32X-4 , 80-84	125	3	150	2	175	7	325	1	425	1	600	1	700	1	800	3	19	334	262	125	800
33X-3 , 90-94	125	1	150	4	375	1											6	183	94	125	375
34X-1 , 95-99	125	1	200	1	225	2											4	194	47	125	225
35X-1 , 65-69																	0				
36X-6 , 62.5-66.5	150	1	175	3													4	169	13	150	175
37X-6 , 75-79	300	1	325	2	400	2	450	1	675	2							8	444	151	300	675
38X-3 , 60-64	225	2	375	3													5	315	82	225	375
39X-4 , 105-109	125	7	375	5	475	1											13	248	141	125	475
40X-2 , 89-93	125	3	150	2	175	6	225	1	250	2	350	1	375	3	450	3	21	251	118	125	450
41X-5 W, 67-71																	0				
42X-3 , 70-74	150	2															2	150	0	150	150
45X-6, 52-56	125	2	150	2	175	4	200	2									10	165	27	125	200
47X-6, 45-49	125	7	150	1													8	128	9	125	150
49X-3, 52-56																	0				
50X5, 52-56	125	1															1	125		125	125
52X-4, 70-74																	0				

Appendix O: The size (µm) and the number of specimens of *Nuttalides umbonifera* at ODP Sites 752, 1139 &1168. The mean values and standard deviations have calculated for different sizes at each sample.

752A (core section, interval (cm))	*Nuttalides umbonifera* (752A)																		
	Size	No.	Size	No.	Size	No.	Size	No.	Size	No.	Size	No.	Size	No.	Sum	Mean	STDV	smallest test	largest test
2H-4, 65-70															0				
3H-1, 50-55															0				
3H-2 ,60-65															0				
3H-4 ,40-45															0				
3H-5 ,70-75															0				
4H-1 ,70-75															0				
4H-2 ,85-90															0				
4H-5 ,70-75	150	1	175	1	300	1	325	2							5	255	86	150	325
5H-1 ,70-75	300	1													1	300		300	300
5H-2 ,70-75															0				
5H-3 ,90-95	200	1	250	1											2	225	35	200	250
5H-4 ,70-75	250	1													1	250		250	250
6H-1 ,70-75	200	1	250	1											2	225	35	200	250
6H-3 ,75-80															0				
6H-5 ,70-75															0				
6H-6 ,20-25	100	1	125	2	175	1									4	131	31	100	175
7H-1 ,65-70	150	1	250	2	275	1									4	231	55	150	275
7H-2 ,80-85	150	1	200	6	225	9	250	9	275	7	300	3	325	2	37	246	38	150	325
7H-4 ,70-75	150	1	175	5	200	8	225	4	250	4	325	1			23	211	38	150	325
7H-6 ,100-105															0				
8H-1 ,100-105	225	5	250	1	275	1	300	1							8	244	29	225	300
8H-3 ,100-105	200	1	250	1	300	2									4	263	48	200	300
8H-6 ,70-75	225	1	250	3	400	1									5	275	71	225	400
9H-2 ,100-105	200	10	225	15	250	3									28	219	16	200	250
9H-4 ,80-85	175	7	200	19	225	14	250	7	275	3					50	215	27	175	275
9H-5 ,65-70	175	6	200	20	225	19	250	18							63	219	24	175	250
10H-2 ,60-65	175	1													1	175		175	175
10H-3 ,100-105	200	1													1	200		200	200
10H-5 ,80-85	150	1	175	3	200	2	225	2							8	191	27	150	225
10H-6 ,110-115	175	4	200	4	225	3	250	1							12	202	25	175	250

1139A (core, section, interval (cm))	*Nuttalides umbonifera* (1139A)																			
	Size	No.	Size	No.	Size	No.	Size	No.	Size	No.	Size	No.	Size	No.	Size	No.	Sum	Mean	STDV	smallest test	largest test
3R-1 , 30-34	125	1															1	125		125	125
3R-2 , 100-104	200	1															1	200		200	200
3R-4 , 32-36	175	2	250	7	275	1	300	21	350	12	375	2	400	8	425	8	61	332	63	175	425
4R-1, 40-44	150	1	225	1													2	188	53	150	225
4R-2 , 105-109	150	1	175	1	200	1	250	2									5	205	45	150	250
4R-4 , 75-79	150	1	225	1													2	188	53	150	225
5R-1 , 121-125	175	2	200	3	250	4											9	217	33	175	250
6R-1 , 71-75	175	1															1	175		175	175
7R-1 , 111-115	125	1	150	1	175	2	200	1	225	1	250	1					7	186	43	125	250
7R-3, 45-49	125	1															1	125		125	125
8R-1 , 45-49	175	1	200	1													2	188	18	175	200
9R-4 , 105-109	175	1															1	175		175	175
10R-2 , 45-49	125	1															1	125		125	125
11R-1, 35-39	175	1	400	1													2	288	159	175	400
12R-2 , 71-75	125	1															1	125		125	125
12R-5, 90-94																	0				
13R-5 , 80-84																	0				
14R-4 , 65-69	125	1	175	3													4	163	25	125	175
15R-2, 95-99	125	2															2	125	0	125	125
15R-4 , 41-45	125	2															2	125	0	125	125
16R-2 , 55-59																	0				
17R-3 , 91-95																	0				
18R-1 , 96-100	125	1	150	1													2	138	18	125	150
19R-2, 60.5-64.5																	0				
20R-4, 40-44	125	1	150	1													2	138	18	125	150

1168A (core, section, Interval (cm))	*Nuttalides umbonifera* (1168A)																										
	Size	No.	Size	No.	Size	No.	Size	No.	Size	No.	Size	No.	Size	No.	Size	No.	Size	No.	Size	No.	Size	No.	Sum	Mean	STDV	smallest test	largest test
8H-1 , 100-104																							0				
9H-3 , 51-55	150	2	175	2	200	1																	5	170	21	150	200
10H-2 , 80-84																							0				
11H-5 , 90-94																							0				
12H-1 , 75-79																							0				
13X-1 , 40-44	125	4	150	9	175	9	200	14	250	10													46	190	40	125	250
14X-4 , 45-49	150	2	175	3	200	2																	7	175	20	150	200
15X-2 , 76-80	125	1	150	4	200	1	250	1															7	168	43	125	250
16X-2 , 100-104	175	1	375	1																			2	275	141	175	375
17X-3 , 100-104	125	1	250	3																			4	219	63	125	250
18X-5 , 80-84	100	2	175	2	200	3	250	15	300	7	325	20	375	15	400	7	500	6	550	2	750	1	80	335	102	100	750
19X-4 , 70-74	125	3	150	1	200	2	300	2	375	2	400	1											11	243	110	125	400
20X-3 , 100-104	150	1	175	2	200	2																	5	180	21	150	200
21X-1 , 100-104	150	1	175	1	225	3	250	10	325	5	375	8	400	1	450	2	525	1					32	311	86	150	525
22X-2 , 45-49	100	3	125	2	150	2	250	1	375	2													10	185	109	100	375
23X-3 , 74-78	150	3	175	10	200	4	250	2	300	1	325	1	500	2	575	2	600	1					26	264	149	150	600
24X-6 , 57-61																							0				
25X-2 , 41-45	125	2	150	1	325	1																	4	181	97	125	325
25X-5, 44-48	250	5	275	2	325	1	350	1	375	4	450	2											15	325	73	250	450
26X-2 , 73-77	125	2	150	3	175	8	200	3	250	23	300	2	350	3	500	1	550	1					46	242	81	125	550
26X-6, 75-79	125	8	150	2	175	1	200	4	225	3	250	5	300	1	350	1	450	1	500	2			28	225	109	125	500
27X-4 , 73-77	125	2	150	3	175	3																	8	153	21	125	175
28X-3 , 75-79	150	1	175	3	200	2	225	2	250	3	275	1	300	9	375	2	425	2					25	274	75	150	425
29X-2 , 96-100	175	3	200	1	275	1																	5	200	43	175	275
30X-3 , 85.5-89.5	150	2	175	2	200	2	225	1	250	2	300	3	375	1									13	235	69	150	375
31X-5 , 86-90	125	1	150	2	175	1																	4	150	20	125	175
32X-4 , 80-84	125	1																					1	125		125	125
33X-3 , 90-94	100	2	125	3	150	1	175	2	200	4	225	3											15	170	46	100	225
34X-1 , 95-99	125	2	200	2	225	1																	5	175	47	125	225
35X-1 , 65-69	150	1	225	1																			2	188	53	150	225
36X-6 , 62.5-66.5	125	1																					1	125		125	125
37X-6 , 75-79	125	1																					1	125		125	125
38X-3 , 60-64																							0				
39X-4 , 105-109																							0				
40X-2 , 89-93	125	3	150	6	175	5																	14	154	19	125	175
41X-5 W, 67-71	150	1	200	1																			2	175	35	150	200
42X-3 , 70-74	125	2	150	5	175	2																	9	150	18	125	175
45X-6, 52-56																							0				
47X-6, 45-49																							0				
49X-3, 52-56																							0				
50X5, 52-56	150	1	250	2																			3	217	58	150	250
52X-4, 70-74	125	3	250	1																			4	156	63	125	250

Appendix P: The size (µm) and the number of specimens of *Sphaeroidina bulloides* at ODP Sites 752, 1139 &1168. The mean values and standard deviations have calculated for different sizes at each sample.

752A (core section, interval (cm))	*Sphaeroidina bulloides* (752A)																		Sum	Mean	STDV	smallest test	largest test
	Size	No.	Size	No.	Size	No.	Size	No.	Size	No.	Size	No.	Size	No.	Size	No.	Size	No.					
2H-4, 65-70																			0				
3H-1, 50-55	300	1																	1	300		300	300
3H-2 ,60-65	225	1																	1	225		225	225
3H-4 ,40-45	500	1																	1	500		500	500
3H-5 ,70-75																			0				
4H-1 ,70-75																			0				
4H-2 ,85-90	250	1																	1	250		250	250
4H-5 ,70-75																			0				
5H-1 ,70-75																			0				
5H-2 ,70-75																			0				
5H-3 ,90-95																			0				
5H-4 ,70-75	450	1																	1	450		450	450
6H-1 ,70-75																			0				
6H-3 ,75-80	625	1																	1	625		625	625
6H-5 ,70-75	375	1																	1			375	375
6H-6 ,20-25	525	1																	1	525		525	525
7H-1 ,65-70	375	1	450	1															2	413	53	375	450
7H-2 ,80-85	400	1	425	1	450	1	475	1	600	1									5	470	78	400	600
7H-4 ,70-75																			0				
7H-6 ,100-105																			0				
8H-1 ,100-105	175	1	225	1	250	4													6	233	30	175	250
8H-3 ,100-105	325	1	400	1															2	363	53	325	400
8H-6 ,70-75	575	1																	1	575		575	575
9H-2 ,100-105	200	1	250	1	450	1	600	1											4	375	185	200	600
9H-4 ,80-85	175	1	200	1	275	1	325	1											4	244	69	175	325
9H-5 ,65-70																			0				
10H-2 ,60-65	250	1	375	1															2	313	88	250	375
10H-3 ,100-105	250	1																	1	250		250	250
10H-5 ,80-85	200	1	225	1	250	4	275	1	300	2	325	2	350	1	375	1	450	1	14	295	67	200	450
10H-6 ,110-115	425	1																	1	425		425	425

1139A (core, section, interval (cm))	*Sphaeroidina bulloides* (1139A)																				Sum	Mean	STDV	smallest test	largest test
	Size	No.	Size	No.	Size	No.	Size	No.	Size	No.	Size	No.	Size	No.	Size	No.	Size	No.	Size	No.					
3R-1 , 30-34																					0				
3R-2 , 100-104																					0				
3R-4 , 32-36	250	1																			1	250		250	250
4R-1, 40-44																					0				
4R-2 , 105-109	200	1																			1	200		200	200
4R-4 , 75-79	250	1	300	1																	2	275	35	250	300
5R-1 , 121-125	175	1	225	1	275	1	325	1	400	1	500	2	700	2							9	422	193	175	700
6R-1 , 71-75	175	1	200	1	225	1	250	1	375	3	500	8									15	398	127	175	500
7R-1 , 111-115	125	1	175	1	200	1	225	1	250	1	275	2	350	2	375	3	425	1			13	290	92	125	425
7R-3, 45-49	175	1	525	1																	2	350	247	175	525
8R-1 , 45-49	150	3	225	4	250	8	300	6	325	4	375	3	425	6	500	4	525	4	575	2	44	349	121	150	575
9R-4 , 105-109	150	1	225	1	250	2	350	2	375	3	450	2									11	327	96	150	450
10R-2 , 45-49	150	2	175	1	200	1	225	1	250	4	275	1	300	1	375	1					12	238	64	150	375
11R-1, 35-39	175	2	200	4	225	2	250	1	300	2	350	3	400	3	475	3	500	2			22	324	116	175	500
12R-2 , 71-75	125	2	150	2	275	1	300	2													7	204	83	125	300
12R-5, 90-94	125	1	150	1	250	1	325	1													4	213	92	125	325
13R-5 , 80-84	125	1	150	1	200	3	225	2	400	4											11	266	110	125	400
14R-4 , 65-69	175	1	200	4	250	1	275	1	375	1	500	2									10	288	126	175	500
15R-2, 95-99	200	1																			1	200		200	200
15R-4 , 41-45	175	1	400	1	550	2															4	419	177	175	550
16R-2 , 55-59	200	1	225	1	250	2	375	2													6	279	77	200	375
17R-3 , 91-95	225	1																			1	225		225	225
18R-1 , 96-100	175	2	200	1	250	3	300	1	375	1											8	247	67	175	375
19R-2, 60.5-64.5	225	1	250	1	425	1															3	300	109	225	425
20R-4, 40-44	125	2	225	1	250	1	450	1													5	235	133	125	450

1168A (core, section, Interval (cm))	*Sphaeroidina bulloides* (1168A)																
	Size	No.	Size	No.	Size	No.	Size	No.	Size	No.	Size	No.	Sum	Mean	STDV	smallest test	largest test
8H-1 , 100-104	525	1											1	525		525	525
9H-3 , 51-55	125	1	175	1									2	150	35	125	175
10H-2 , 80-84	125	1											1	125		125	125
11H-5 , 90-94	125	2	250	1									3	167	72	125	250
12H-1 , 75-79													0				
13X-1 , 40-44	150	2											2	150	0	150	150
14X-4 , 45-49	250	1	600	1	725	1							3	525	246	250	725
15X-2 , 76-80													0				
16X-2 , 100-104	300	1											1	300		300	300
17X-3 , 100-104	125	1	175	1									2	150	35	125	175
18X-5 , 80-84	275	1											1	275		275	275
19X-4 , 70-74													0				
20X-3 , 100-104	125	1	375	1									2	250	177	125	375
21X-1 , 100-104													0				
22X-2 , 45-49													0				
23X-3 , 74-78													0				
24X-6 , 57-61													0				
25X-2 , 41-45													0				
25X-5, 44-48													0				
26X-2 , 73-77	250	3	300	1	425	1	500	2	625	2	700	1	10	443	174	250	700
26X-6, 75-79													0				
27X-4 , 73-77	250	1											1	250		250	250
28X-3 , 75-79													0				
29X-2 , 96-100													0				
30X-3 , 85.5-89.5	375	1	450	1	600	1							3	475	115	375	600
31X-5 , 86-90	125	1	175	1									2	150	35	125	175
32X-4 , 80-84	125	1											1	125		125	125
33X-3 , 90-94	125	1	250	1	375	1							3	250	125	125	375
34X-1 , 95-99	125	2											2	125	0	125	125
35X-1 , 65-69													0				
36X-6 , 62.5-66.5	125	2	150	1	175	1	200	1					5	155	33	125	200
37X-6 , 75-79	125	2	250	1									3	167	72	125	250
38X-3 , 60-64	125	3	150	2									5	135	14	125	150
39X-4 , 105-109	225	1	275	1	325	1							3	275	50	225	325
40X-2 , 89-93													0				
41X-5 W, 67-71													0				
42X-3 , 70-74	175	2											2	175	0	175	175
45X-6, 52-56													0				
47X-6, 45-49	125	1											1	125		125	125
49X-3, 52-56	200	1											1	200		200	200
50X5, 52-56													0		0		
52X-4, 70-74	150	1	175	1									2	163	18	150	175

Appendix Q: Carbon and Oxygen Isotope data for benthic foraminifera species standardised to *Cibicidoides mundulus* at 752A. The bold values at the bottom are the mean difference (offset) between *C. mundulus* and both *C. wuellerstorfi* and *Planulina costata*.

752A Cores, section	Mean (*C. mun.*) ($\delta^{13}C$)	Mean Corr. (*C.wul.*) ($\delta^{13}C$)	Mean Corr. (*P.cost.*) ($\delta^{13}C$)	Composite mean ($\delta^{13}C$)	St. Dev. (all corrected values)	Mean (*C. mun.*) ($\delta^{18}O$)	Mean Corr. (*C.wul.*) ($\delta^{18}O$)	Mean Corr. (*P.cost.*) ($\delta^{18}O$)	Composite mean ($\delta^{18}O$)	St. Dev. (all corrected values)	Age (Ma)
2H-4	0.72			0.72		2.74			2.74		4.14
3H-1	0.88	0.76		0.82	0.09	2.94	2.73		2.84	0.15	5.30
3H-2	0.84	0.71		0.77	0.09	2.41	2.94		2.67	0.37	5.61
3H-4		0.85		0.85			3.01		3.01		6.62
3H-5	1.08	0.83		0.96	0.18	2.39	2.60		2.49	0.14	7.19
4H-1		1.02		1.02			2.39		2.39		7.96
4H-2	1.27	1.37		1.32	0.07	2.76	2.55		2.66	0.15	8.25
4H-5	1.23	0.99		1.11	0.17	2.73	2.47		2.60	0.19	9.06
5H-1	0.96	1.18		1.07	0.15	2.42	2.51		2.46	0.07	9.71
5H-2	1.34	1.27		1.30	0.05	2.22	2.69		2.45	0.33	9.98
5H-3	1.18	1.34		1.26	0.11	2.20	2.34		2.27	0.10	10.2
5H-4	1.49	1.43		1.46	0.04	2.21	2.63		2.42	0.30	10.5
6H-1	1.55	1.63		1.59	0.05	2.51	2.54		2.53	0.02	11.4
6H-3	1.49	1.44		1.46	0.03	2.42	1.88		2.15	0.38	12.0
6H-5		1.60		1.60			2.26		2.26		12.5
6H-6	1.32	1.65		1.49	0.23	2.18	2.13		2.16	0.03	12.8
7H-1	1.75	1.78	1.76	1.76	0.02	2.02	1.83	2.34	2.06	0.26	13.2
7H-2	2.14	2.18	1.88	2.07	0.16	2.22	1.85	1.90	1.99	0.20	13.5
7H-4	1.60		2.00	1.80	0.28	1.71		1.91	1.81	0.14	14.4
8H-1	1.66		1.77	1.71	0.08	1.35		1.28	1.32	0.05	15.9
8H-3	1.73		1.73	1.73	0.01	1.77		1.74	1.75	0.02	16.8
8H-6	1.25		1.39	1.32	0.10	1.63		1.73	1.68	0.07	18.0
9H-2	1.62			1.62		2.00			2.00		19.1
9H-4	1.42		1.41	1.41	0.01	1.87		1.68	1.77	0.14	19.9
9H-5	1.54		1.27	1.40	0.19	1.94		1.80	1.87	0.10	20.3
10H-2	1.88		1.67	1.78	0.15	1.91		1.86	1.88	0.03	21.7
10H-3	1.61		1.70	1.65	0.06	1.63		1.82	1.73	0.14	22.3
10H-5	1.45			1.45		1.72			1.72		23.1
10H-6	1.23			1.23		1.55			1.55		23.4
Mean Diff.		**-0.21**	**-0.07**				**0.03**	**0.22**			

Appendix R: Carbon Isotope data for benthic foraminifera species (standardised benthic foraminifera Isotope) at 1168A. The bold values at the bottom are the mean difference (offset) between *C. mundulus* and six different species.

1168A Cores, section	**$\delta^{13}C$ (*C. mun.*)**	**Mean Corr (*Oridor. um.*) ($\delta^{13}C$)**	**Mean Corr (*Glob. sub.*) ($\delta^{13}C$)**	**Mean Corr (*Gyro. sol.*) ($\delta^{13}C$)**	**Mean Corr (*Eps. ex.*) ($\delta^{13}C$)**	**Mean Corr (*C. wul.*) ($\delta^{13}C$)**	**Mean Corr (*Nut. um.*) ($\delta^{13}C$)**	***Cibicidoides* sp.11 ($\delta^{13}C$)**	***Cibicidoides* sp. ($\delta^{13}C$)**	**Composite mean ($\delta^{13}C$)**	**St. Dev. (all corrected values)**	**Age (Ma)**
8H-1	-0.02	-0.02								-0.02	0.00	4.23
9H-3	0.43									0.43		5.01
10H-2	0.21									0.21		5.55
11H-5				0.78				0.35		0.57	0.31	6.46
12H-1	0.47									0.47		6.68
13X-1	0.59					0.59				0.59	0.00	7.27
14X-4						0.84				0.84		8.00
15X-2					1.70					1.70		8.45
16X-2					1.46					1.46		9.62
17X-3						0.95				0.95		9.82
18X-5							0.66			0.66		10.03
19X-4							0.56			0.56		10.18
21X-1					1.76		0.88			1.32	0.62	10.44
22X-2	0.91				0.91					0.91	0.00	11.08
23X-3							0.57			0.57		11.83
24X-6	1.15									1.15		12.74
25X-2	1.51									1.51		12.97
25X-5							0.53			0.53		13.26
26X-2							0.81			0.81		13.62
26X-6							0.86			0.86		14.01
27X-4						0.92				0.92		14.44
28X-3	2.49									2.49		14.97
29X-2	1.16									1.16		15.52
30X-3	1.30									1.30		16.24
31X-5	0.80									0.80		17.07
32X-4	0.15			0.15						0.15	0.00	17.60
34X-1	0.55		0.55							0.55	0.00	18.53
36X-6		-1.35								-1.35		20.26
37X-6	-0.10									-0.10		20.90
38X-3	-0.51									-0.51		21.22
39X-4	0.06									0.06		21.84
40X-2	-1.05									-1.05		21.94
41X-5				0.45					0.15	0.30	0.21	22.15
42X-3	0.30						0.30			0.30	0.00	22.25
47X-6	0.69									0.69		23.03
Mean Diff.		**0.90**	**0.76**	**1.22**	**0.97**	**-0.31**	**-0.08**					

Appendix S: Oxygen Isotope data for benthic foraminifera species (standardised benthic foraminifera Isotope) at 1168A. The bold values at the bottom are the mean difference (offset) between *C. mundulus* and six different species.

1168A Cores, section	**$\delta^{18}O$ (*C. mun.*)**	**Mean Corr (*Oridor. um.*) ($\delta^{18}O$)**	**Mean Corr (*Glob. sub.*) ($\delta^{18}O$)**	**Mean Corr (*Gyro. sol.*) ($\delta^{18}O$)**	**Mean Corr (*Eps. ex.*) ($\delta^{18}O$)**	**Mean Corr (*C. wul.*) ($\delta^{18}O$)**	**Mean Corr (*Nut. um.*) ($\delta^{18}O$)**	***Cibicidoides* sp.11 ($\delta^{18}O$)**	***Cibicidoides* sp. ($\delta^{18}O$)**	**Composite mean ($\delta^{18}O$)**	**St Dev (all corrected values)**	**Age (Ma)**
8H-1	3.40	3.40								3.40	0.0	4.23
9H-3	3.09									3.09		5.01
10H-2	3.40									3.40		5.55
11H-5				2.43				2.88		2.66	0.3	6.46
12H-1	3.07									3.07		6.68
13X-1	3.34					3.34				3.34	0.0	7.27
14X-4						3.13				3.13		8.00
15X-2					4.98					4.98		8.45
16X-2					2.73					2.73		9.62
17X-3						3.30				3.30		9.82
18X-5							3.11			3.11		10.03
19X-4							2.55			2.55		10.18
21X-1					3.58		2.96			3.27	0.4	10.44
22X-2	2.72				2.72					2.72	0.0	11.08
23X-3							3.01			3.01		11.83
24X-6	2.95									2.95		12.74
25X-2	4.24									4.24		12.97
25X-5							2.26			2.26		13.26
26X-2							2.43			2.43		13.62
26X-6							1.94			1.94		14.01
27X-4						2.37				2.37		14.44
28X-3	4.48									4.48		14.97
29X-2	1.54									1.54		15.52
30X-3	2.07									2.07		16.24
31X-5	2.15									2.15		17.07
32X-4	1.94			1.94						1.94	0.0	17.60
34X-1	1.88		1.88							1.88	0.0	18.53
36X-6		2.75								2.75		20.26
37X-6	2.21									2.21		20.90
38X-3	1.59									1.59		21.22
39X-4	2.25									2.25		21.84
40X-2	1.49									1.49		21.94
41X-5				1.35					2.55	1.95	0.8	22.15
42X-3	1.78						1.78			1.78	0.0	22.25
47X-6	1.16									1.16		23.03
Mean Diff.		**0.90**	**0.76**	**1.22**	**0.97**	**-0.31**	**-0.08**					

Appendix T: Carbon and Oxygen Isotope data for benthic foraminifera species (standardised benthic foraminifera Isotope) at 1139A. The bold values at the bottom are the mean difference (offset) between *C. mundulus* and *Epistominella exigua*.

1139A Core, section	**Mean $\delta^{13}C$ (*C.mun.*)**	**Mean Corr (*Eps.ex.*) ($\delta^{13}C$)**	***Sph. bull.* ($\delta^{13}C$)**	**Composite mean ($\delta^{13}C$)**	**St. Dev. (all corrected values) ($\delta^{13}C$)**	**Mean $\delta^{18}O$ (*C. mun.*)**	**Mean Corr *Ep.ex.* ($\delta^{18}O$)**	***Sph. bull.* ($\delta^{18}O$)**	**Composite mean ($\delta^{18}O$)**	**St. Dev. (all corrected values) ($\delta^{18}O$)**	**Age (Ma)**
3R-1	0.93			0.93		2.47			2.47		11.25
3R-2	1.41			1.41		2.52			2.52		11.99
3R-4	1.44			1.44		1.52			1.52		12.77
4R-1	1.56	1.47		1.52	0.06	1.70	1.48		1.59	0.1	14.49
4R-2	1.56	1.64		1.60	0.06	1.62	1.84		1.73	0.1	15.22
4R-4		1.69		1.69			1.44		1.44		16.13
5R-1	1.33			1.33		0.85			0.85		17.98
6R-1	0.88			0.88		1.50			1.50		18.61
7R-1	0.62			0.62		1.56			1.56		19.03
7R-3	0.82			0.82		1.77			1.77		19.14
8R-1	0.75			0.75		1.73			1.73		19.42
9R-4	0.47			0.47		1.57			1.57		20.00
10R-2	0.69			0.69		1.54			1.54		20.30
11R-1	0.74			0.74		1.32			1.32		20.64
12R-2	0.85			0.85		1.84			1.84		21.14
12R-5	0.61			0.61		1.52			1.52		21.34
13R-5			0.69	0.69				2.14	2.14		21.76
14R-4			0.28	0.28				1.45	1.45		22.10
15R-2			0.42	0.42				1.55	1.55		22.39
16R-2	0.75			0.75		1.52			1.52		22.79
17R-3	0.88			0.88		1.30			1.30		23.18
18R-1	1.05			1.05		1.17			1.17		23.28
19R-2	1.42			1.42		1.81			1.81		23.43
20R-4	1.25			1.25		1.34			1.34		23.60
Mean Diff.		**0.54**					**-0.18**				

Appendix U: Age and isotope values of Site 754A. The age is determined based on the first and last occurrence of nine nannofossil species (Appx U (1)) which provided by Shipboard Scientific Party (1989b) and revised by ATNTS2012 in GTS2012 (Hilgen et al., 2012) (Appx U(3)). Oxygen and carbon data of 754A provided by Rea et al. (1991) and the data conducted on *Cibicidoides* sp. (Appx U (2)).

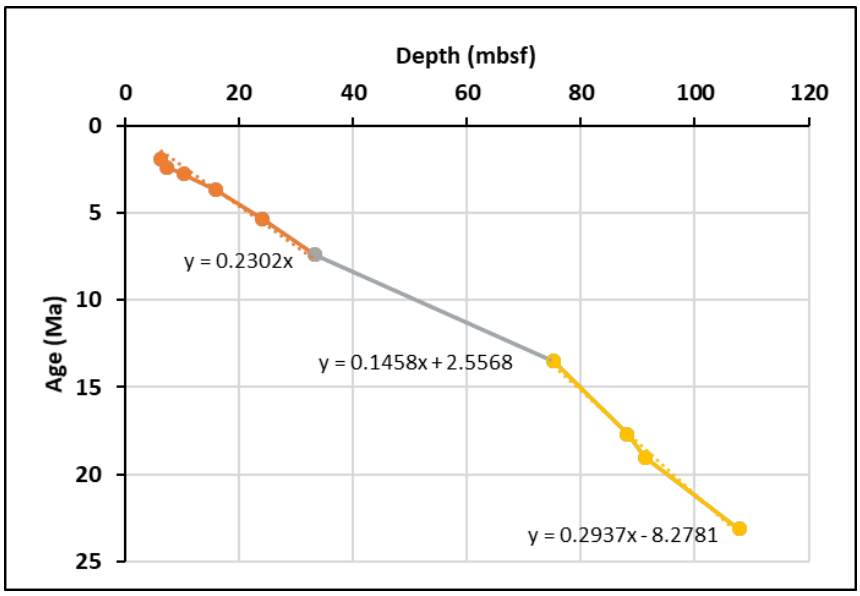
1)

Hole 754A (Events)	Depth (mbsf)				Age (initial report)	Age (ATNTS2012 in GTS2012)
	bottom	top	average	errors		
LO *Discoaster brouweri*	6.60	6.10	6.35	0.25	1.90	1.93
LO *Discoaster pentaradiatus*	8.10	6.60	7.35	0.75	2.20	2.39
LO *Discoaster tamalis*	11.10	9.60	10.35	0.75	2.60	2.80
LO *Reticulofenestra pseudoumbilica*	16.20	15.70	15.95	0.25	3.50	3.70
FO *Ceratolithus acutus*	22.70	25.30	24.00	-1.30	5.00	5.35
FO *Amaurolithus primus*	31.80	34.90	33.35	-1.55	6.50	7.42
LO *Sphenolithus heteromorphus*	77.00	73.50	75.25	1.75	14.40	13.53
FO *Sphenolithus heteromorphus*	86.70	89.70	88.20	-1.50	17.10	17.71
FO *Sphenolithus belemnos*	89.70	92.90	91.30	-1.60	21.50	19.03
LO *Reticulofenestra bisecta*	108.60	107.10	107.85	0.75	23.70	23.13

2)

depth (mbsf)	Age (ATNTS2012 in GTS2012)	$\delta^{18}O$	$\delta^{13}C$	depth (mbsf)	Age (ATNTS2012 in GTS2012)	$\delta^{18}O$	$\delta^{13}C$
17.98	4.14	2.03	0.70	64.58	11.97	1.54	1.63
19.48	4.48	1.77	1.00	66.08	12.19	1.92	1.75
20.98	4.83	1.79	0.70	67.58	12.41	1.69	1.74
22.48	5.17	2.07	0.75	69.08	12.63	1.68	1.81
23.98	5.52	2.21	0.88	70.58	12.85	1.67	1.69
26.08	6.00	2.06	0.87	72.08	13.07	1.58	1.74
27.58	6.35	1.93	0.79	73.58	13.28	1.60	1.83
29.08	6.69	2.07	1.03	74.28	13.39	1.23	1.84
30.58	7.04	1.75	0.87	75.78	13.98	1.24	1.95
32.08	7.38	1.84	1.11	77.28	14.42	0.80	2.00
33.58	7.45	1.81	1.24	78.78	14.86	0.99	2.26
35.68	7.76	1.98	1.34	80.28	15.30	0.87	1.91
37.18	7.98	1.81	1.37	81.78	15.74	1.29	2.41
38.68	8.20	2.04	1.13	83.98	16.39	0.82	1.58
40.18	8.42	1.74	1.48	85.48	16.83	1.23	1.51
41.68	8.63	1.79	1.33	86.98	17.27	0.91	0.93
43.18	8.85	1.78	1.45	88.48	17.71	1.16	1.43
45.28	9.16	2.10	1.17	89.98	18.15	1.02	1.35
46.78	9.38	2.06	0.82	91.48	18.59	0.96	1.50
48.28	9.60	1.86	1.16	93.68	19.24	1.25	1.27
49.78	9.81	1.57	1.10	95.18	19.68	1.23	1.49
51.28	10.03	1.82	1.16	96.68	20.12	1.11	1.38
52.78	10.25	1.85	1.44	98.2	20.56	1.28	1.45
54.88	10.56	1.56	1.34	99.68	21.00	0.88	1.40
56.38	10.78	1.65	1.08	101.18	21.44	0.97	1.50
57.88	11.00	1.77	1.55	103.38	22.08	1.29	1.69
59.38	11.21	1.74	1.48	104.88	22.53	1.20	1.79
60.88	11.43	1.87	1.96	106.38	22.97	1.24	1.40
62.38	11.65	1.62	1.51	107.88	23.41	0.67	1.24
				109.38	23.85	0.79	1.26

3) calculated age by using trendline equations as shown in the graph



Appendix V: The age model and isotope values of 1170A. Chronozones and nannofossil ages have provided by (Stickley et al., 2004) (Appx V (1)) and revised by ATNTS2012 in GTS2012 (Hilgen et al., 2012) (Appx V (3)). The isotope values have supplied by Ennyu and Arthur (2004a) (Appx V (2)).

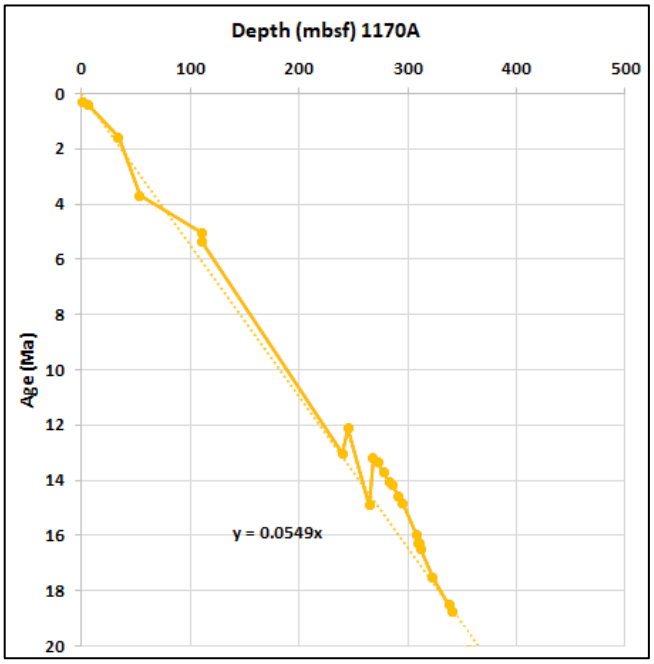
1)

Events	Age (Ma) in ATNTS2012	Mean Depth (mbsf)	Calculated Age
FO *Emiliania huxleyi*	0.29	0.82	0.04
LO *Pseudoemiliania lacunosa*	0.44	6.66	0.35
LO *Calcidiscus macintyrei*	1.60	34.24	1.81
LO *Reticulofenestra pseudoumbilica*	3.70	53.64	2.84
LO *Ceratolithus acutus*	5.04	110.85	5.86
FO *Ceratolithus acutus*	5.35	110.85	5.86
M Termination C5AAn	13.03	240.00	12.70
LO *Cyclicargolithus floridanus*	12.12	245.04	12.96
LO *Helicosphaera ampliaperta*	14.90	264.83	14.01
M Onset C5AAn	13.18	268.50	14.20
M Termination C5ABn	13.36	273.00	14.44
M Termination C5ACn	13.74	278.00	14.71
M Onset C5ACn	14.07	283.00	14.97
M Termination C5ADn	14.16	286.00	15.13
M Onset C5ADn	14.61	292.00	15.45
M Onset C5Bn.1n	14.87	296.00	15.66
M Termination C5Cn.1n	15.97	308.00	16.29
M Onset C5Cn.1n	16.27	310.00	16.40
M Termination C5Cn.2n	16.30	311.00	16.45
M Onset C5Cn.2n	16.47	312.00	16.50
M Onset C5Dn	17.53	323.00	17.09
M Onset C5En	18.52	338.00	17.88
M Termination C6n	18.75	341.00	18.04

2)

Age (Ma) ATNTS2012 in GTS2012	*Cibicidoides mundulus* (1170)		Age (Ma) ATNTS2012 in GTS2012	*Cibicidoides mundulus* (1170)	
	($\delta^{13}C$)	($\delta^{18}O$)		($\delta^{13}C$)	($\delta^{18}O$)
11.93	0.98	2.42	11.93	0.98	2.42
12.46	1.13	2.38	12.46	1.13	2.38
12.85	1.01	2.44	12.85	1.01	2.44
13.46	1.38	2.60	13.46	1.38	2.60
13.63	0.57	2.20	13.63	0.57	2.20
13.71	1.46	3.01	13.71	1.46	3.01
14.23	0.91	2.31	14.23	0.91	2.31
14.51	1.13	2.51	14.51	1.13	2.51
14.76	1.41	2.06	14.76	1.41	2.06
14.96	1.30	2.23	14.96	1.30	2.23
15.04	1.60	2.01	15.04	1.60	2.01
15.21	1.48	1.89	15.21	1.48	1.89
15.29	2.05	2.33	15.29	2.05	2.33
15.37	1.97	2.18	15.37	1.97	2.18
15.45	1.56	2.01	15.45	1.56	2.01
15.49	1.25	1.32	15.49	1.25	1.32
15.57	1.34	1.57	15.57	1.34	1.57
15.65	1.71	1.89	15.65	1.71	1.89
15.73	1.47	1.92	15.73	1.47	1.92
15.82	1.34	1.54	15.82	1.34	1.54

3) calculated age by using trendline equations as shown in the graph

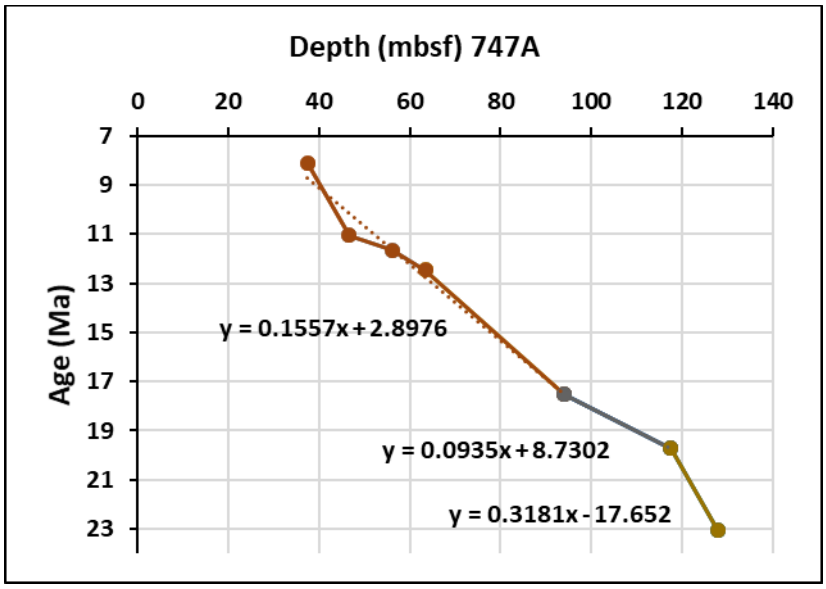


Appendix W: The isotope values and chronozones of the Site 747 Hole A have provided by Wright and Miller (1992), and the Chronozone C6cn2 has provided by Berggren (1992). The age has revised by ATNTS2012 in GTS2012 (Hilgen et al., 2012) (Appx W (1,2)). The isotope values for 747A measured for *Cibicidoides* spp. (Wright and Miller, 1992) (Appx W (3)).

1)

Events	Depth (mbsf)	Age (ATNTS2012 in GTS2012)
base C4n	37.40	8.11
C5n	46.60	11.06
C5r	56.04	11.66
C5An	63.50	12.47
C5Dn	94.10	17.53
C6n	117.50	19.72
C6cn2	127.90	23.03

2) calculated age by using trendline equations as shown in the graph



3)

Depth (mbsf)	($\delta^{18}O$)	($\delta^{13}C$)	Age (ATNTS2012 in GTS2012)	Depth (mbsf)	($\delta^{18}O$)	($\delta^{13}C$)	Age (ATNTS2012 in GTS2012)	Depth (mbsf)	($\delta^{18}O$)	($\delta^{13}C$)	Age (ATNTS2012 in GTS2012)
33.50	2.30	1.03	8.11	69.40	1.74	1.50	13.70	101.51	1.39	0.88	18.22
33.50	2.70	0.65	8.11	70.00	1.73	1.73	13.80	102.90	1.64	0.83	18.35
35.00	2.43	1.34	8.35	70.00	1.79	1.83	13.80	103.01	1.37	0.78	18.36
35.00	2.53	1.24	8.35	70.90	1.50	1.23	13.94	103.60	1.33	0.82	18.42
36.50	2.44	1.02	8.58	71.50	1.40	1.12	14.03	103.90	1.43	0.96	18.44
37.10	2.33	1.18	8.67	71.50	1.55	1.16	14.03	104.40	1.45	0.95	18.49
37.40	2.51	1.28	8.72	73.00	1.47	1.50	14.26	105.00	1.20	0.84	18.55
37.40	2.45	1.30	8.72	73.00	1.69	1.50	14.26	105.90	1.48	0.92	18.63
40.90	2.51	1.04	9.27	73.90	1.48	1.59	14.40	106.50	1.50	0.98	18.69
41.55	2.21	0.96	9.37	74.50	1.29	1.62	14.50	107.40	1.49	1.10	18.77
42.40	2.51	1.11	9.50	75.12	1.17	1.38	14.59	108.00	1.54	1.02	18.83
43.05	2.36	0.89	9.60	75.90	1.18	1.58	14.72	108.90	1.38	0.89	18.91
43.90	2.40	1.00	9.73	76.50	1.11	1.48	14.81	109.50	1.39	0.87	18.97
44.55	2.37	0.87	9.83	77.40	1.13	1.57	14.95	109.50	1.34	1.04	18.97
45.40	2.53	1.06	9.97	78.00	1.03	1.52	15.04	110.40	1.67	1.11	19.05
46.05	2.41	1.07	10.07	78.90	0.93	1.36	15.18	111.00	1.63	1.30	19.11
46.60	2.42	1.06	10.15	79.51	1.30	1.70	15.28	111.00	1.57	0.93	19.11
46.90	2.08	1.03	10.20	79.51	1.44	1.71	15.28	111.90	1.60	1.29	19.19
46.90	2.22	1.06	10.20	80.40	1.12	1.48	15.42	112.50	1.61	0.92	19.25
47.40	2.31	1.08	10.28	81.00	0.85	1.10	15.51	112.50	1.61	0.93	19.25
48.05	2.20	0.91	10.38	81.90	1.02	1.50	15.65	113.10	1.42	1.29	19.31
48.90	2.34	1.09	10.51	82.48	1.20	1.67	15.74	113.10	1.56	0.97	19.31
49.55	2.19	0.99	10.61	83.40	1.26	1.89	15.88	113.40	1.51	1.11	19.33
50.40	2.21	0.83	10.74	84.00	1.48	1.81	15.98	113.90	1.64	1.15	19.38
51.05	2.21	1.00	10.85	84.00	1.35	1.66	15.98	114.51	1.35	0.77	19.44
51.90	2.21	0.91	10.98	84.60	1.12	1.65	16.07	115.40	1.41	0.77	19.52
52.55	1.99	0.54	11.08	84.60	1.15	1.32	16.07	116.01	1.55	0.86	19.58
52.55	2.15	0.68	11.08	84.75	1.06	1.63	16.09	116.90	1.53	0.89	19.66
53.40	2.25	0.75	11.21	84.90	1.46	1.80	16.12	117.51	1.64	0.69	19.73
54.05	2.08	1.15	11.31	84.90	1.39	1.71	16.12	118.40	1.74	1.11	20.01
54.90	2.36	1.47	11.45	85.40	1.05	1.52	16.19	119.01	1.52	0.83	20.21
55.55	2.18	1.38	11.55	86.00	0.97	1.34	16.29	119.01	1.47	0.85	20.21
56.10	2.14	1.13	11.63	86.90	1.11	1.32	16.43	119.90	1.77	1.02	20.49
56.40	2.21	0.99	11.68	87.50	1.10	1.49	16.52	120.50	1.52	1.03	20.68
56.90	2.55	1.44	11.76	88.40	1.16	1.27	16.66	120.50	1.52	0.89	20.68
57.52	2.04	1.45	11.85	89.00	1.12	1.41	16.75	121.40	1.42	0.81	20.97
58.40	2.30	1.33	11.99	89.90	1.13	1.22	16.90	122.00	1.38	0.79	21.16
59.04	2.49	1.45	12.09	90.50	1.09	1.30	16.99	122.60	1.29	0.73	21.35
59.90	2.45	1.40	12.22	92.00	1.59	1.31	17.22	122.90	1.58	0.83	21.44
60.50	2.11	1.20	12.32	92.90	1.60	1.34	17.36	123.40	1.63	1.19	21.60
61.40	2.23	1.09	12.46	93.50	1.36	1.42	17.46	124.02	1.64	1.38	21.80
62.01	2.06	0.94	12.55	93.50	1.52	1.33	17.46	124.90	1.74	1.19	22.08
62.90	2.20	1.14	12.69	94.10	1.71	1.38	17.55	125.52	1.64	1.20	22.28
63.50	2.14	0.93	12.78	94.40	1.44	1.33	17.56	126.40	1.84	1.09	22.56
64.40	2.35	0.95	12.92	94.90	1.26	1.03	17.60	127.02	1.83	1.00	22.75
65.00	1.96	0.84	13.02	95.50	1.58	1.19	17.66	127.02	1.48	1.04	22.75
65.60	2.08	1.29	13.11	96.40	1.65	1.10	17.74	127.90	1.88	1.43	23.03
65.60	2.00	1.13	13.11	97.02	1.32	0.89	17.80	128.52	1.45	1.18	23.23
65.90	2.22	1.04	13.16	97.90	1.43	1.04	17.88	128.52	1.56	1.19	23.23
66.40	1.93	1.08	13.24	98.50	1.46	0.85	17.94	129.40	1.69	1.06	23.51
67.00	1.62	1.01	13.33	99.40	1.43	0.92	18.02	130.01	1.51	1.18	23.70
67.90	1.73	1.20	13.47	100.00	1.32	0.80	18.08	130.01	1.53	1.25	23.70
68.50	1.73	1.26	13.56	100.90	1.39	0.80	18.16				

Appendix X: The sea surface temperature (SST) of the Miocene at 1168A by using alkenones as SST biomarkers. The temperature values have provided by Knee-Robinson (2018).

Age (Ma)	Conte SST
4.23	17.54
5.01	18.97
6.46	19.18
6.68	18.25
7.27	23.23
8.00	20.76
8.45	23.52
9.62	21.80
9.82	24.22
10.03	20.72
10.18	24.03
10.32	21.89
10.44	23.65
11.08	22.59
12.97	25.94
13.62	26.23
14.44	19.47
14.97	17.69
15.52	23.04
16.24	22.60
17.07	24.51
17.60	27.41
18.12	27.19
20.26	25.78
20.90	24.95
21.22	25.84
21.84	26.21
21.94	23.08
22.15	25.58
22.25	19.61